CHARACTERIZATION AND MANIPULATION OF THE WHEAT B GENOME

A Dissertation
Submitted to the Graduate Faculty
of the
North Dakota State University
of Agriculture and Applied Science

By

Wei Zhang

In Partial Fulfillment of the Requirements
for the Degree of
DOCTOR OF PHILOSOPHY

Major Program:
Genomics and Bioinformatics

July 2017

Fargo, North Dakota

North Dakota State University
Graduate School

Title

CHARACTERIZATION AND MANIPULATION OF THE WHEAT B GENOME

By

Wei Zhang

The Supervisory Committee certifies that this ***disquisition*** complies with North Dakota State University's regulations and meets the accepted standards for the degree of

DOCTOR OF PHILOSOPHY

SUPERVISORY COMMITTEE:

Xiwen Cai
Chair

Phillip McClean

Steven Xu

Justin Faris

Approved:

7/28/2017
Date

Phillip McClean
Department Chair

ABSTRACT

Common wheat originated from interspecific hybridization of three diploid ancestors followed by spontaneous chromosome doubling. *Aegilops speltoides* (genome SS) has been controversially considered a possible candidate for the donor of the wheat B genome. However, the relationship of the *Ae. speltoides* S genome with the wheat B genome remains largely obscure. The first aim of this study was to characterize the homology between the wheat B genome and the *Ae. speltoides* S genome. In this study, meiotic pairing for each of the B-S homoeologous pairs was investigated individually. Noticeable homology between chromosomes 1B and 1S was discovered, but not between other homoeologous B-S pairs. An *Ae. speltoides*-originated segment spanning a genomic region of approximately 10.46 Mb was detected on the long arm of wheat chromosome 1B. The *Ae. speltoides*-originated segment on 1BL was found to co-evolve with the rest of the B genome. Evidently, *Ae. speltoides* was involved in the origin of the wheat B genome, but should not be considered an exclusive donor of this genome.

Aegilops speltoides and *Thinopyrum elongatum* (genome EE), two of diploid relatives of wheat, are considered important sources of novel genes for wheat improvement. However, the development of compensating wheat-alien translocations has been limited by laborious cytological analysis. This study aimed to develop an effective procedure of inducing, recovering, and detecting homoeologous recombination in wheat-alien gene introgression lines. Totally, 112 wheat-*Ae. speltoides* 2B-2S and 87 wheat-*Th. elongatum* 2B-2E translocation lines were developed through this procedure. Composite bin maps for chromosome 2B as well as homoeologous chromosomes 2S and 2E were constructed by genotyping the translocations using 90K SNP arrays. In addition, genes for resistance to stem rust, tan spot, and SNB on chromosome 2S were physically mapped and incorporated into the wheat genome. Also, an *Ae.*

speltoides-derived deleterious growth gene was physically mapped to the subtelomeric region of chromosome 2S. In summary, the results of the study led to a large number of 2B-2S and 2B-2E recombinants, physically mapped disease and growth-related genes on chromosome 2S, developed novel molecular markers, and optimized chromosome engineering procedures.

ACKNOWLEDGEMENTS

I would like to acknowledge everyone who has assisted me throughout my doctoral studies over the years. I express my deepest appreciation and thanks to my major advisor, Dr. Xiwen Cai, for his guidance, encouragement, and patience on my project and throughout my Doctoral program.

I would also thank members in my graduate committee members, Drs. Steven Xu, Justin Faris, and Phillip McClean for their patience and assistance.

I also express my sincere thanks to Dr. Shiaoman Chao for her help on 90K SNP genotyping and the training on GenomeStudio. I extend my sincere thanks to Dr. Yuming Long for help on STARP markers, and to Dr. Qijun Zhang for his technical assistance on stem rust inoculation and scoring. Also, I would like to thanks Drs. Zhaohui Liu and Gongjun Shi for their help on tan spot and SNB inoculation and scoring.

I would like to thank previous and current members of the lab, Rachel McArthur, Yadav Gyawali, Guojia Ma, Xianwen Zhu, Somo Ibrahim, Mingyi Zhang, and Shaungfeng Ren for their friendship and collaboration.

I am very grateful to the Department of Plant Sciences, the Program of Genomics and Bioinformatics, North Dakota State University (NDSU) for providing me with this great opportunity to pursue my Ph.D.

I am deeply grateful to my parents for their unconditioned love and support, and my friends for the friendship and encouragement.

TABLE OF CONTENTS

LIST OF TABLES

LIST OF FIGURES

CHAPTER 1. GENERAL INTRODUCTION

Wheat is one of the earliest domesticated crops in the Fertile Crescent of the Middle East and now widely cultivated, and provides 20% of the calories consumed all over the world. Due to rapid population growth in the world, demand for wheat is expected to increase by 40% by 2030 (Dixon et al., 2009). Because of the economic value of wheat and the desire for its genetic improvement, researches concerning the evolution of wheat have been under intense scientific scrutiny.

Common wheat (*Triticum aestivum* L, 2n = 6x = 42, genome AABBDD) originated from spontaneous interspecific hybridization of three diploid ancestors and subsequent chromosome doubling (McFadden and Sears, 1946; Riley and Chapman, 1958; Dvorak et al., 1993; Huang et al., 2002; Cai and Xu, 2007; Jauhar, 2007; Cai et al., 2010). *T. urartu* (2n = 2x = 14, genome AA) and *Aegilops. tauschii* (2n = 2x = 14, genome DD) contributed the A and D genome to common wheat, respectively (Kihara, 1944; McFadden and Sears, 1946; Dvorak et al., 1993; Petersen et al., 2006). The search for the ancestor of the wheat B genome has been performed for nearly a century (Jenkins, 1929). However, the ancestry of the B genome remains controversial even though *Ae. sepltoides* has been proposed to be the most closely related one (Riley and Chapman, 1958; Zohary and Feldman, 1962; Blake et al., 1999).

These two rounds of hybridization combined three subgenomes into a large and complex polyploid genome of common wheat. Meanwhile, this polyploidization process substantially reduced the nucleotide diversity in cultivated germplasms, indicating a severe genetic bottleneck in the evolution of common wheat (Peng et al., 2011; Faris, 2014; Marcussen et al., 2014). The narrowed genetic variability makes wheat vulnerable to various biotic and abiotic stresses. It is estimated that up to 20% of global wheat yields is lost each year due to disease and pests (Oerke,

2006). Thus, genetic improvement for disease resistance is an important endeavour of increasing wheat grain yield. Stem rust, caused by the fungal species *Puccinia graminis* Pers.:Pers. f. sp. *tritici* Eriks. & E. Henn., is one of the major destructive diseases for wheat. Heavy losses of wheat production were caused by the stem rust epidemics that occurred from the 1920s to the 1960s worldwide (Leonard and Szabo, 2005). Tan spot and Septoria nodorum blotch (SNB), caused by the fungi *Pyrenophora tritici-repentis* and *Parastagonospora nodorum* respectively, are two economically significant diseases of wheat in many of the world's wheat-growing regions, especially the Northern Great Plains of the United States (De Wolf et al., 1998; Friesen et al., 2006; Faris et al., 2013; Liu et al., 2015). Both pathogens produce multiple necrotrophic effectors (NE) to cause disease in host plants under a reverse gene-for-gene mechanism (Friesen et al., 2006; Faris et al., 2013; Liu et al., 2015).

Screening wheat germplasm to identify sources of tolerance and resistance for various stresses is essential for long-term wheat breeding. The wild relatives provide a vast and untapped reservoir of genetic variation for resistance to the pathogens as well as other wheat production-threatening stresses. Approximately 20 stem rust resistance genes have been identified from the wild relatives of wheat (Zhang, 2013; Yu et al., 2014). Six of them were from *Aegilops* species, including *Sr32, Sr39,* and *Sr47* from the S genome of *Ae. speltoides* (Faris et al., 2008; Niu et al., 2011; Klindworth et al., 2012; Mago et al., 2013), *Sr38* from the N genome of *Ae. verticosa* (genome DDNN) (Bariana and McIntosh, 1993), *Sr51* from the S^s genome of *Ae. searsii* and *Sr53* from the M genome of *Ae. geniculata* (Liu et al., 2011a and b). Also, high levels of resistance to tan spot and SNB have been identified in the wheat-alien species derivatives (Xu et al., 2004; Friesen et al., 2008; Oliver et al., 2008).

The transfer of resistance genes from wild relatives to modern wheat is often accompanied by unacceptable agronomic traits due to the genes present in the alien chromosome segments referred to as linkage drag. In the past, meiotic homoeologous recombination was employed to minimize linkage drag by reducing the size of the alien chromosome segment transferred to the wheat genome (Qi et al., 2007; Rey et al., 2015; Zhang et al., 2015). Normally, meiotic pairing in wheat is restricted to homologous chromosomes due to the presence of the *Ph1* gene located on the chromosome arm 5BL. The meiotic pairing and recombination between homoeologous chromosomes are generally enhanced in the *Ph1*-deficient genetic stocks such as the substitutions of chromosome 5B by 5D and *ph1b* mutant (Qi et al., 2007; Niu et al., 2011). Using *ph1b* mutant, a large number of small compensating wheat-alien chromosome translocations have been developed and utilized in wheat breeding (Friebe et al., 1996; Qi et al., 2007; Niu et al., 2011; Klindworth et al., 2012).

The first aim of this study was to assess the homology of individual wheat B-genome chromosomes with their homoeologues in the S genome of *Ae. speltoides* and to trace the *Ae. speltoides* genomic components in the wheat B genome. Secondly, this study aimed to develop an effective procedure of inducing, recovering, and detecting meiotic homoeologous recombination for alien gene introgression using the genomics tools currently available in wheat. Thirdly, this study aimed to manipulate wheat chromosome 2B by inducing homoeologous recombination with its homoeologue 2S from *Ae. speltoides* and 2E from *Th. elongatum*, and consequently construct a set of compensating wheat-alien translocations. Lastly, I have characterized the 2B-2S and 2B-2E recombinants developed in this study, and have evaluated their reactions to stem rust, tan spot, and SNB, as well as the linkage drag associated with the recombinants.

References

Bariana HS, McIntosh RA (1993) Cytogenetic studies in wheat. XV. Location of rust resistance genes in VPM1 and their genetic linkage with other disease resistance genes in chromosome 2A. Genome 36:476–482

Blake NK, Lehfeldt BR, Lavin M, Talbert LE (1999) Phylogenetic reconstruction based on low copy DNA sequence data in an allopoyploid: The B genome of wheat. Genome 42:351–360

Cai X, Xu SS (2007) Meiosis-driven genome variation in plants. Curr Genomics 8:151–161

Cai X, Xu SS, Zhu X (2010) Mechanism of haploidy–dependent unreductional meiotic cell division in polyploid wheat. Chromosoma 119:275–285

De Wolf ED, Effertz RJ, Ali S, Francl, LJ (1998) Vistas of tan spot research. Can J Plant Pathol 20:349–370

Dixon J, Braun HJ, Kosina PP, Crouch J (2009) Wheat facts and futures. CIMMMYT, Mexico

Dvorak J, Terlizzi P, Zhang HB, Resta P (1993) The evolution of polyploidy wheats: Identification of the A genome donor species. Genome 36:21–31

Faris JD, Xu SS, Cai X, Friesen TL, Jin Y (2008) Molecular and cytogenetic characterization of a durum wheat–*Aegilops speltoides* chromosome translocation conferring resistance to stem rust. Chromosom Res 16:1097–1105

Faris JD, Liu Z, Xu SS (2013) Genetics of tan spot resistance in wheat. Theor Appl Genet 126:2197–2217

Faris JD (2014) Wheat domestication: key to agricultural revolutions past and future. In: Tuberosa R, Graner A, Frison E (eds) Genomics of plant genetic resources. vol 1. Managing, sequencing and mining genetic resources, Springer, Netherlands, pp 439–464

Friebe B, Jiang J, Raupp WJ, McIntosh RA, Gill BS (1996) Characterization of wheat–alien translocations conferring resistance to diseases and pests: current status. Euphytica 91:59–87

Friesen TL, Stukenbrock EH, Liu ZH, Meinhardt SW, Ling H, Faris JD, Rasmussen JB, Solomon PS, Mcdonald BA, Oliver RP (2006) Emergence of a new disease as a result of interspecific virulence gene transfer. Nat Genet 38:953–956

Friesen TL, Xu SS, Harris MO (2008) Stem rust, tan spot, *Stagonospora nodorum* blotch, and hessian fly resistance in Langdon durum–*Aegilops tauschii* synthetic hexaploid wheat lines. Crop Sci 48:1062–1070

Huang S, Sirikhachornkit A, Su X, Faris J, Gill B, Haselkorn R, Gornicki P (2002) Genes encoding plastid acetyl–CoA carboxylase and 3–phosphoglycerate kinase of the

Triticum/Aegilops complex and the evolutionary history of polyploid wheat. Proc Natl Acad Sci USA 99:8133–8138

Jauhar PP (2007) Meiotic restitution in wheat polyhaploids (amphihaploids), a potent evolutionary force. J Hered 98:188–193.

Kihara H (1944) Discovery of the DD–analyser, one of the ancestors of vulgare wheat. Agric Hortic 19:889–890

Klindworth DL, Niu ZX, Chao SM, Friesen TL, Jin Y, Faris JD, Cai XW, Xu SS (2012) Introgression and characterization of a goatgrass gene for a high level of resistance to Ug99 stem rust in tetraploid wheat. G3 2:665–673

Leonard KJ, Szabo LJ (2005) Stem rust of small grains and grasses caused by *Puccinia graminis*. Mol Plant Pathol 6:99–111

Liu W, Jin Y, Rouse M, Friebe B, Gill B, Pumphrey MO (2011a) Development and characterization of wheat–*Ae. searsii* Robertsonian translocations and a recombinant chromosome conferring resistance to stem rust. Theor Appl Genet 122:1537–1545

Liu W, Rouse M, Friebe B, Jin Y, Gill B, Pumphrey MO (2011b) Discovery and molecular mapping of a new gene conferring resistance to stem rust, *Sr53*, derived from *Aegilops geniculata* and characterization of spontaneous translocation stocks with reduced alien chromatin. Chromosom Res 19:669–682

Liu ZH, El–Basyoni I, Kariyawasam G, Zhang G, Fritz A, Hansen JM, Marais F, Friskop AJ, Chao S, Akhunov E, Baenziger PS (2015) Evaluation and association mapping of resistance to tan spot and Stagonospora nodorum blotch in adapted winter wheat germplasm. Plant Dis 99:1333–1341

Mago R, Verlin D, Zhang P, Bansal U, Bariana H, Jin Y, Ellis J, Hoxha S, Dundas I (2013) Development of wheat–*Aegilops speltoides* recombinants and simple PCR–based markers for *Sr32* and a new stem rust resistance gene on the 2S#1 chromosome. Theor Appl Genet 126:2943–2955

Marcussen T, Sandve SR, Heier L, Spannagl M, Pfeifer M, IWGSC, Jakobesn KS, Wulff BBH, Steuernagel B, Mayer KFX, Olsen OA (2014) Ancient hybridizations among the ancestral genomes of bread wheat. Science 345:1250092–1–4

McFadden ES, Sears ER (1946) The origin of *Triticum speltoides* and its free–threshing hexaploid relatives. J Hered 37:107–116

Molnár–Láng M, Ceoloni C, Doležel Je (2015) Alien introgression in wheat. Cytogenetics, molecular biology, and genomics. Springer Cham, Heidelberg

Niu Z, Klindworth DL, Friesen TL, Chao S, Jin Y, Cai X, Xu SS (2011) Targeted introgression of a wheat stem rust resistance gene by DNA marker–assisted chromosome engineering. Genetics 187:1011–1021

Oerke EC (2006) Crop losses to pests. J Agric Sci 144:31–43

Oliver RE, Cai X, Wang RC, Xu SS, Friesen TL (2008) Resistance to tan spot and Stagonospora nodorum blotch in wheat–alien species derivatives. Plant Dis 92:150–157

Peng JH, Sun D, Nevo E (2011) Domestication evolution, genetics and genomics in wheat. Mol Breeding 28:281–301

Petersen G, Seberg O, Yde M, Berthelsen K (2006) Phylogenetic relationships of *Triticum* and *Aegilops* and evidence for the origin of the A, B, and D genomes of common wheat (*Triticum aestivum*). Mol Phylogenet Evol 39:70–82

Qi LL, Friebe B, Zhang P, Gill BS (2007) Homoeologous recombination, chromosome engineering and crop improvement. Chromosome Res 15:3–19

Rey E, Molnár I, Doležel J (2015) Genomics of wild relatives and alien introgressions. In: Molnár–Láng M, Ceoloni C, Doležel J (eds) Alien introgression in wheat. Springer International Publishing, Switzerland, pp 374–381

Riley R, Unrau J, Chapman V (1958) Evidence on the origin of the B genome of wheat. J Hered 49:90–98

Xu SS, Friesen TL, Mujeeb–Kazi A (2004) Seedling resistance to tan spot and Stagonospora nodorum blotch in synthetic hexaploid wheats. Crop Sci 44:2238–2245

Yu LX, Barbier H, Rouse MN, Singh S, Singh RP, Bhavani S, Huerta–Espino J, Sorrells ME (2014) A consensus map for Ug99 stem rust resistance loci in wheat. Theor Appl Genet 127:1561–1581

Zhang P, Dundas IS, McIntosh RA, Xu SS, Park RF, Gill BS, Friebe B (2015) Wheat–*Aegilops* introgressions. In: Molnár–Láng M, Ceoloni C, Doležel J (eds) Alien introgression in wheat. Springer International Publishing, Switzerland, pp 221–44

Zhang QJ (2013) Development and characterization of wheat germplasm for resistance to stem rust Ug99 in wheat. PhD Dissertation. North Dakota State University, Fargo, North Dakota

Zohary D, Feldman M (1962) Hybridization between amphidiploids and the evolution of polyploids in the wheat (*Aegilops–Triticum*) group. Evolution 16:44–61

CHAPTER 2. LITERATURE REVIEW

Meiosis in eukaryotes

Basic structure of chromosome

Chromatin is a complex of DNA and proteins highly condensed and wrapped that forms chromosomes within the nucleus of dividing eukaryotic cells (Cook, 1995; Bártová et al., 2008). Chromatin exists in two forms, including euchromatin which is less condensed and can be transcribed, as well as heterochromatin which is highly condensed and is typically not transcribed. At the simplest level, chromatin is a double-stranded helical structure of DNA associated with histone proteins. Nucleosome is the basic structural unit of chromatin, which contains four histone proteins (H2A, H2B, H3, and H4) in duplicate and about 146 base pairs of DNA wraped outside of the histone octamer (Bram and Ris, 1971). The histone protein H1 associates with another 20 base pairs, resulting in two full turns of DNA around the octamer, and forming a structure called a chromatosome. The nucleosomes fold up to produce a 30 nm fiber that forms loops averaging 300 nm in length. The 300-nm fibers are compressed and folded into a structure in a diameter of 250 nm. Tight coiling of the 250-nm fiber produces the chromatid of a chromosome (Huberman, 1973; Finch et al., 1977; Cook, 1995; Bártová et al., 2008).

In eukaryotes, a centromere is a chromosomal region responsible for the movement of the replicated chromosomes into the two daughter cells during mitosis and meiosis. The centromeric DNA is normally in a heterochromatin state, which is essential for the recruitment of the cohesin complex that mediates sister chromatid cohesion after DNA replication as well as coordinating sister chromatid separation during anaphase. In the centromere region, the normal histone H3 is replaced with a centromere-specific variant, CENP-A (CENH3). The presence of CENP-A is believed to be important for the assembly of the kinetochore on the centromere (Bram and Ris,

1971; Cook, 1995; Bártová et al., 2008). There is one centromere on each chromosome. On the basis of the location of the centromere, chromosomes are classified into four types: metacentric, submetacentric, acrocentric, and telocentric (Levan et al., 1964).

Meiotic recombination in eukaryotes

Meiosis is a type of cell division for eukaryotic species to generate gametes. It determines the fate of chromosomes and maintains genome integrity. Meanwhile, meiosis gives rise to genetic variability through meiotic recombination and chromosome segregation. Meiotic cell division begins with a diploid cell which has two homologues for each of the chromosomes. The mother cell undergoes one round of DNA replication prior to the two successive rounds of nuclear divisions (Cnudde and Gerats, 2005). The entire meiotic process is split into meiosis I and meiosis II. Meiosis I is a type of cell division unique to germ cells that involves homologous chromosome pairing, recombination, and segregation. Meiosis II is similar to mitosis and generates four haploid daughter cells.

Meiotic homologous recombination is mediated by double-strand DNA breaks (DSBs) and crossing over (CO) and results in the exchange of segments between non-sister chromatids in the synapsed homologous chromosomes (Cnudde and Gerats, 2005; Gaeta and Pires, 2010). Chiasmata generated by crossovers that physically connect two paired homologous chromosomes together, and are resolved later to allow homologous chromosomes to segregate at anaphase I (Cai and Xu, 2007; Gaeta and Pires, 2010). The main factor driving meiotic recombination between DNA sequences is homology. Meiotic recombination may occur along the entire chromosome, but recombination frequencies are not evenly distributed along the chromosomes (Gaut et al., 2007). Hotspots have been found within genes in maize (Civardi et al., 1994; Xu et al., 1995) and in intergenic regions in *Arabidopsis*

thaliana (Kim et al., 2007). Many plants display a propensity for recombination at the distal ends of chromosomes near the telomeric or subtelomeric regions , while lack recombination near the centromere (Drouaud et al., 2006). Meiotic recombination can cause various chromosomal rearrangements, including deletions, duplications, gene conversions, and translocations during meiosis (Cnudde and Gerats, 2005; Cai and Xu, 2007).

Meiosis–driven aneuploidy and polyploidy

Normal chromosome pairing, synapsis, and recombination are prerequisites for accurate segregation of homologous chromosomes at meiosis I. Synapsed homologous chromosomes, referred to bivalent, are held together by the chiasmata until anaphase I. Asynapsis is the complete failure of homologous chromosomes to pair or synapse during the first meiotic division. Desynapsis is a condition where homologous chromosomes pair or synapse normally at the beginning of prophase, but fail to maintain this association in the subsequent stages of meiosis (Cai and Xu, 2007). Both asynapsis and desynapsis lead to univalent which are usually observed at metaphase I. Univalents either get lost or are randomly transmitted to daughter cells, resulting in chromosomally unbalanced gametes and eventually aneuploids such as monosomics, nullisomics, trisomics, and tetrasomics in the offspring. In addition, univalents may undergo misdivision, such as transverse division, to produce telocentric chromosomes or isochromosomes (Koul and Dhar, 1998).

Normal meiotic cell division leads to haploid daughter cells with chromosome number reduced by half. However, chromosomes may fail to segregate in the first or second meiotic cell division, leading to restitution nuclei with unreduced chromosomes in the variant meiotic cell division, such as meiotic restitution. Two types of meiotic restitutions or termed unreduced meiotic cell division (UMCD), have been documented in plants, including first division

restitution (FDR) and second division restitution (SDR). The first and second division restitution result from the failure of chromosome segregation at meiosis I and II, respectively (Harlan and deWet, 1975; Ramanna and Jacobsen, 2003; Silkova et al., 2011). Both FDR and SDR result in unreduced gametes, but their genetic compositions may differ from each other (Cai and Xu, 2007). It has been documented that functioning of the unreduced gametes produced through meiotic restitution may have been a major mechanism for the widespread occurrence of polyploidy in nature (Fukuda and Sakamoto, 1992; Xu and Joppa, 2000; Silkova et al., 2003 and 2011; Jauhar, 2007).

The evolution of wheat

Wheat taxonomy

The wheat group contain 13 diploid and 18 polyploid species (Table 2.1). The genomes of the diploid species are distinct from each other. Based on the genomic divergence, the diploid species were classified into eight groups and their genomes were given the following designations: A (A, and A^m), D, S (S, S^s, S^b, S^l, S^{sh}), M, C, U, N, and T (Eig, 1929; Kihara, 1954; Feldman et al., 1979; Hammer, 1980; Kimber and Tsunewaki, 1988; Slageren, 1994). It is estimated that theses diploid species diverged from one another around 2.5-4.5 MYA (Huang et al., 2002; Dvorak and Akhunov, 2005; Middleton et al., 2014; Gornicki et al., 2014). Two genomes found in polyploid wheats were designated differently, B and G, due to their diploid progenitors are controversial (Dvorak and Zhang, 1990; Rodriguez et al., 2000).

Table 2.1. The classification of *Aegilops* and *Triticum*

Genus	Species[a]	Ploidy	Genome[b]
Amblyopyrum	*muticum*	2x	T
Aegilops	*speltoides*	2x	S
	searsii	2x	S^s
	bicornis	2x	S^b
	longissima	2x	S^l
	sharonensis	2x	S^{sh}
	tauschii	2x	D
	markgrafii	2x	C
	comosa	2x	M
	uniaristata	2x	N
	umbellulta	2x	U
	biunicialis	4x	UM
	geniculata	4x	MU
	neglecta	4x	UM
	columnaris	4x	UM
	triuncialis	4x	UC; CU
	kotschyi	4x	SU
	peregrina	4x	SU
	cylindrica	4x	CD
	crassa	4x	DM
	ventricosa	4x	DN
	recta	6x	UMN
	vavilovii	6x	DMS
	crassa	6x	DDM
	juvenalis	6x	DMU
Triticum	*monococcum*	2x	A^m
	uratu	2x	A
	sinskayae	2x	A^b
	turgidum	4x	BA
	timopheevii	4x	GA
	aestivm	6x	BAD
	zhukovskyi	6x	GAA^m

[a]Species designation according to van Slageren (1994)
[b]Genome designations after Kimber and Tsunewaki (1988); the first genome is the donor of the cytoplasm

Based on the obvious morphological differences, *Amblyopyrum*, *Aegilops*, and *Triticum* were regarded as three separate genera (Eig, 1929; Slageren, 1994). *Amblyopyrum muticum* is considered closer to the *Aegilops* species in Sitopsis than other diploids according to the

cytological and molecular evidence (Badaeva et al., 1996). It might be the closest relative of *Ae. speltoides* (Ohta, 1991; Sallares and Brown, 2004). *Ae. speltoides* contains two forms, *ligustica* and *aucheri*. Based on the structure of the dispersal unit, it was assumed that *aucheri* is a more advanced type than *ligustica* evolutionarily. The *aucheri* type might be derived from the hybridization of *ligusica* type of *Ae. speltoides* with *Ae. longissimi* or *Ae. searsii* (Feldman and Levy, 2015).

The genus *Triticum*, including six wheat species, are classified into three sections including *Monococcon* Dumort., *Dicoccoidea*, and *Triticum* Flaksb. The three sections contain diploid species *T. monococcum* L. and *T. urartu* Tumanian ex Gandilyan, tetraploid species *T. turgidum* L. and *T. timopheevii* (Zhuk.) Zhuk., and hexaploid species *T. aestivum* L. and *T. zhukovskyi* Menabde & Ericzjan (Slageren,1994). Modern wheat mainly consists of tetraploid durum wheat [*T. turgidum* ssp. *durum*, 2n = 4x = 28, AABB)] and hexaploid common wheat (*T. aestivum* L. ssp. *aestivum*, 2n = 6x = 42, AABBDD). However, *T. timopheevii* and *T. zhukovskyi* have never been cultivated as a significant crop and are not considered as economically important wheats. Durum wheat accounts for 4% of wheat production and is mainly used to make pasta and other semolina products. Common wheat accounts for 96% of wheat production and is widely used to make bread, cakes, noodles, and cookies (Gill et al., 2004). Durum wheat is an allotetraploid (2n = 4x = 28) with A and B subgenomes, whereas common wheat is an allohexaploid (2n = 6x = 42) with the A, B, and D subgenomes. Wheat allopolyploidy arose from interspecific hybridization events followed by spontaneous chromosome doubling (Dvorak et al., 1993; Cai and Xu, 2007, Faris, 2014). The allopolyploid wheat species and their diploid ancestors have been used as models for the polyploidization and genome studies in polyploids.

Evolutionary lineages of wheat

The genus *Triticum* originated from the Fertile Crescent of the Middle East, belongs to the Triticeae tribe under the Poaceae family (Faris, 2014). It comprises a polyploid series based on x = 7, containing diploids (2n = 2x = 14), tetraploids (2n = 4x= 28), and hexaploids (2n=6x=42) (Sakamura, 1918; Sax 1922; Faris, 2014). Based on these discoveries, chromosome pairing in the hybrids between the species at different ploidy levels disclosed that the polyploids are allopolyploids formed by interspecific or intergeneric hybridization followed by chromosome doubling (Sax, 1921). It is considered that the major grass subfamily Poaceae including wheat, barley, and oats diverged about 20 million year ago (MYA). The diploid progenitors and close relatives of modern wheat originated from a basic 7-chromosome ancestor, and gave rise to the *Triticum* and *Aegilops* taxa about 3 MYA (Dvorak et al., 1993; Dvorak and Akhunov, 2005; Middleton et al., 2014; Faris, 2014). The divergence of the *Triticum* and *Aegilops* lineages established the basal branches of the wheat group. The *Triticum* groups consisted of the A-genome diploids *T. uratu* and *T. monococcum*. The *Aegilops* progenitor evolved, and gave rise to the *Aegilops* Sitopsis section and *Ae. tauschii* about 2.6 MYA (Dvorak et al., 1993; Dvorak and Akhunov, 2005; Faris, 2014).

Genetic evidence has revealed that polyploid wheat has two evolutionary lineages, both of which involved two amphiploidization events. The origin of tetraploid wheat (*T. turgidum* L. 2n = 4x = 28, genome AABB) and hexaploid wheat (*T. aestivum* L., 2n = 6x = 42, genome AABBDD) comprises one lineage. It began with hybridization occurred about 0.5 MYA between *T. urartu* (2n = 2x = 14, genome AA) and the B genome ancestor, led to *T. turgidum*. Though there remains some controversy, *Ae. speoltoides* is generally considered as the B-genome ancestor (Riley and Chapman, 1958; Zohary and Feldman, 1962; Blake et al., 1999, Huang et al.,

2002; Chalupska et al., 2008; Salse et al., 2008). The hexaploid wheat in this lineage originated from an additional hybridization between *T. turgidum* and *Ae. tauschii* (2n = 2x = 14, genome DD) and followed by spontaneous chromosome doubling 8,000 years ago (Dvorak et al., 1993; Cai and Xu, 2007; Faris, 2014; Marcussen et al., 2014).

The formation of *T. timopheevii* (Zhuk.) Zhuk. (2n = 4x = 28, genome AAGG) and *T. zhukovskyi* Men. & Ericz. (2n = 6x = 42, genome A^mA^mAAGG) comprises the other evolutionary lineage. It began with the hybridization of *T. urartu* and *Ae. speltoides* or a close relative thereof (Sarkar and Stebbins, 1956; Riley et al., 1958), which led to the formation of *T. timopheevii* (2n = 4x = 28, genome AAGG). The hybridization between *T. timopheevii* and domesticated einkorn wheat (*T. monococcum*, 2n=2x=14, genome A^mA^m) led to the hexaploid wheat *T. zhukovskyi* Menabde et Ericzjan (2n=6x=42, genome A^mA^mAAGG) belonging to this lineage. It constitutes an important evolutionary lineage of wheat, but didn't result in the formation of modern cultivars.

Domestication of wheat

The only domesticated diploid wheat is einkorn (*T. monococcum*, 2n=2x=14, A^mA^m). It was domesticated from ssp. *aegilopoides* through the acquisition of a non-brittle rachis about 10,000 years before present (BP) in the Karacadag mountain range of southeast Turkey (Renfrew, 1973, Heun et al., 1997). The other wild diploid *Titticum* species *T. uratu* has never been domesticated even though it played an essential role in wheat evolution.

The domesticated tetraploid wheat is known as the non-brittle rachis form of emmer (*T. turgidum*, 2n=4x=28, AABB). It is believed to have been domesticated about 10,000 BP probably in southeast Turkey (Ozkan et al., 2002, 2005, 2010; Mori et al., 2003; Luo et al., 2007; Dvorak et al., 2011). The hexaploid common wheat was not directly derived from a wild

progenitor through domestication selection but from *T. turgidum* (Dvorak et al., 2011, Peng et al., 2011). Many domesticated plants, including wheat, actually share a set of traits, such as growth habit, flowering time, seed size and dispersal, grain yield, plant height, spike number/plant, and kernel number/spike (Elias et al., 1996; Araki et al., 1999; Campbell et al., 2003; Peng et al., 2003; Meyer and Purugganan, 2013). These shared traits are known as domestication syndrome. The chromosomal regions harboring a cluster of domestication QTL are referred to as domestication syndrome factors (DSFs) (Peng et al., 2003). It would be helpful to study the genetics and genomics of these syndrome traits for wheat breeding of high yield and adaptability.

The trait of non-brittle rachis is one of the most important component characters of wheat domestication syndrome. Spikelet disarticulation caused by a brittle rachis in the wild forms of wheat is important for them to disperse seeds and further propagate (Watanabe and Ikebata, 2000). Domesticated types are characterized by the lack of seed dispersal at maturity. Spikelet-type disarticulation is further sub-divided into wedge-type (W-type) and barrel-type (B-type). The *Br1* gene controls W-type disarticulation in the most *Triticum* and *Aegilops* species; *Br2* controls B-type disarticulation in *Ae. tauschii*. Studies on the transition from wild emmer to cultivated emmer indicated the brittle rachis trait in wild emmer was controlled by two genes designated *Br* locating on the short arms of chromosome 3A ($Br1^{3A}$) and 3B ($Br1^{3B}$), respectively (Watanabe and Ikebata 2000; Nalam et al., 2006). Both genes lead to W-type disarticulation, and mutations at both loci are needed to confer the non-brittle rachis of domesticated emmer.

Glume tenacity is another key trait modified by the domestication process in wheat (Gill et al., 2007). The glumes of wild wheat are tough and hold the kernels tightly, whereas cultivated wheats have soft glumes and are free-threshing. Studies of a spontaneous free-threshing mutant

in domesticated einkorn wheat revealed that a recessive gene (*sog*) on the short arm of chromosome $2A^m$ controls the soft glume trait (Taenzler et al., 2002; Sood et al., 2009). The tenacious glume trait in hexaploid wheat was controlled by the gene $Tg1^{2D}$ on the short arm of chromosome 2D (Kerber and Dyck, 1969; Kerber and Rowland, 1974; Nalam et al., 2007; Sood et al., 2009). One QTL corresponded to the free-threshing mapped to the short arm of chromosome 2B ($Tg1^{2B}$) was considered homoeologous with $Tg1^{2D}$ (Simonetti et al, 1999; Faris et al., 2014).

The early wheat varieties were characterized by hulled seeds which were difficult to be liberated from the chaff. The free-threshing trait allows an easy release of naked kernels of domesticated wheat. The free-threshing varieties represent the final steps of wheat domestication (Peng et al., 2011). The free-threshing trait is governed by two genes, *Q* and *Tg,* and *Tg* is epistatic to *Q*. *Q* is a major domestication gene conferring spike shape and threshability in wheat (Sears, 1954; Kerber and Rowland, 1974; Faris et al., 2003, 2005; Simons et al., 2006; Gill et al., 2007). Both the *tg1*and *Q* alleles are required to confer the free-threshing trait in hexaploid wheat. The *Q* gene in wheat has been cloned and shown to have sequence similarity to the Arabidopsis *APETALA2* gene, and thus is a member of the AP2 family of transcription factors (Faris and Gill, 2002; Faris et al., 2003, 2005; Simons et al., 2006; Gill et al., 2007). The homoeologous *q* loci on chromosome 5B (q^{5B}) and 5D (q^{5D}) are highly similar to the *Q* locus on 5A (Q^{5A}) in hexaploid wheat. The pseudogenization of q^{5B}, and subfunctionalization of q^{5D} were noticed during the evolutionary process of polyploid wheat and both events contributed to the domestication traits (Simons et al., 2006; Zhang et al., 2011).

Gene introgression in wheat

The gene pools for wheat improvement

Wheat has a limited genetic variation due to the allopolyploid origin of its genome. This bottleneck arises because only a few diploid genotypes were involved in the allopolyploid speciation events (Feldman and Levy, 2012; Marcussen et al., 2014). The tribe Tritceae contains more than 300 species. They represent an invaluable gene pool for wheat improvement. They have been considered an important gene source to broaden the genetic variability of the wheat genome. The Triticeae species have been categorized into three gene pools for wheat improvement, i.e. primary, secondary, and tertiary gene pools (Jiang et al., 1994). The strategy used for transferring genes from each pool to wheat depends greatly on the crossiblility and evolutionary distance between the species involved (Cai et al., 2005).

The species in the primary gene pool of common wheat share homologous genomes, including hexaploid landraces, cultivars, and breeding lines. Gene transfer from these species are mainly achieved by hybridization, homologous recombination, backcrossing and selection (Cox, 1991; Dvorak et al., 1993; Friebe et al., 1996; Huang et al., 2002).

The secondary gene pool of common wheat includes the species that have at least one homologous genome in common with *T. aestivum,* such as *T. timopheevii* (AAGG), *T. zhukowskyi* (A^mA^mAAGG). The diploid *Aegilops* species with the S genome, such as *Ae. speltoides*, is placed into the secondary gene pool because it has been considered the progenitor of the wheat B genome (Jiang et al., 1994; Kilian et al., 2007). Gene transfer from these species has been performed by direct crosses and backcrosses with varying levels of homologous or homoeologous recombination (Qi et al., 1997, 2007; Liu et al., 2011a, b).

The species in the tertiary gene pool are more distantly related to wheat, such as *Secale cereale* (genome RR), *Th. elongatum* (genome EE) and *Th. intermedium* (2n = 6x = 42, genome JJJ^sJ^sSS). Their genomes are not homologous to those of wheat, making gene transfer from this gene pool to wheat difficult and complex (Friebe et al., 1996; Rey et al., 2015; Zhang et al., 2015). The strategies of inducing chromosome breakage and homoeologous pairing/recombination have been used in gene transfer from the tertiary gene pool to wheat (Qi et al., 2007; Niu et al., 2011; Zhang et al., 2017). Inducing Robertsonian translocations is another strategy for gene introgression from the tertiary gene pool into wheat (Qi et al., 2011; Friebe et al., 2005; Liu et al., 2011a).

Utilization of molecular markers on alien introgression in wheat

The advent of cytogenetic techniques such as Giemsa C-banding, fluorescence *in situ* hybridization (FISH), and Genomic *in situ* hybridization (GISH) are irreplaceable to analyze chromosome constitutions in the wheat-alien introgression (Gill and Kimber 1974; Schwarzacher et al., 1989, 1992; Friebe et al., 1992; Kruppa et al., 2013; King et al., 2017; Zhang et al., 2017). However, the requirement of the complex microscopy skills and tedious procedures involved in these cytogenetic approaches have limited the utility of these techniques in the large-scale alien gene introgression. The integrated cytogenetics and genomics approach has offered new opportunities to manipulate the chromosomes of wheat and its relatives for gene introgression and wheat improvement (Qi et al., 2007; Niu et al., 2011, 2014; Klindworth et al., 2017).

Various high-resolution and high-throughput genotyping platforms, such as single nucleotide polymorphism (SNP) arrays, have been developed to characterize allelic variation of wheat. The 9K and 90K Illumina iSelect® arrays were mainly developed based on the transcriptomes of modern wheat, making them less useful for genotyping the species from the

secondary and tertiary gene pools (Cavanagh et al., 2013; Wang et al., 2014). The low representation of the wheat wild relatives in the SNP design process may limit the utility of the platforms in the wheat-alien introgression breeding (Wulff and Moscou, 2014). To overcome this problem, Axiom® 35K and 820K SNP arrays have been developed to particularly identify and validate the SNPs polymorphic between hexaploid wheat accessions and their relatives (Winfield et al., 2016).

Recently, the SNP-derived genotyping technologies, such as Kompetitive Allele Specific PCR (KASP) and Semi-Thermal Asymmetric Reverse PCR (STARP) SNP markers, have been developed based on the allele-specific primer extension and fluorescence resonance energy transfer for signal generation (Semagn et al., 2014; Long et al., 2017). They are flexible and have been widely used in various genomic and cytogenetic research projects. These molecular marker techniques have been used in screening wheat–alien hybrids and their back-crossed derivatives to detect recombinants and isolate desired introgressions (Petersen et al., 2015; Danilova et al., 2016; Klindworth et al., 2017; Tan et al., 2017; Zhang et al., 2017).

In order to promote the use of SNP markers on wheat-alien gene introgression, it is important to generate new genomic sequence resources from wild relatives of wheat. The progress on the genome sequencing of common wheat and its relatives, including *Ae. speltoides*, *Ae. sharonensis*, *T. urartu*, and *Ae. tauschii,* will facilitate the use of SNP markers in high-throughput screening of wheat-alien introgressions (Brenchley et al., 2012; Ling et al., 2013; Luo et al., 2013; Mayer et al., 2014; Chapman et al., 2015; https://wheat-urgi.versailles.inra.fr/Seq-Repository/Assemblies).

Homoeologous recombination-based chromosome engineering

Since alien chromosomes usually contain desirable genes as well as undesirable genes for wheat improvement, individual alien chromosome addition and substitution lines are difficult to be utilized directly in wheat breeding. Two principal approaches have been developed to transfer alien chromosome segments to cultivated wheat over the past 60 years (Sear, 1956; Qi et al., 2007; Niu et al., 2011; Rey et al., 2015; Zhang et al., 2015; King et al., 2017). The first approach involves induction of alien chromosome breakage by radiation treatments or gametocidal chromosomes (Jiang et al., 1993). Both methods induce random chromosome breakage and fusion of the broken segments, resulting in random chromosome translocations (Sears, 1956; Masoudi-Nejiad et al., 2002). However, the majority of translocations generated by this approach are often between non-homoeologous chromosomes and involves duplications or deficiencies (Jiang et al., 1994; Qi et al., 2007).

The second approach is inducing meiotic homoeolgous pairing/recombination using the genetic stocks with *Ph1* deletion or harboring *Ph1* supperssors in the genome. In hexaploid wheat, the *Ph1* gene suppresses homoeologous pairing and ensures normal meiotic pairing between homologous chromosomes. The *Ph1*-deficient genetic stocks have been successfully employed for inducing meiotic recombination between wheat chromosomes and their alien homeologues (Jiang et al., 1994; Friebe et al., 1996; Qi et al., 2007, Faris et al., 2008). Particularly, the use of the *ph1b* mutant in combination with molecular markers and GISH has proven efficient for eliminating unwanted alien chromosomal segments and minimizing linkage drag in alien gene introgression. (Niu et al., 2011; Klindworth et al., 2012).

References

Araki E, Miura H, Sawada S (1999) Identification of genetic loci affecting amylose content and agronomic traits on chromosome 4A of wheat. Theor Appl Genet 98:977–984

Badaeva ED, Friebe B, Gill BS (1996) Genome differentiation in *Aegilops*. Distribution of highly repetitive DNA sequences on chromosomes of diploid species. Genome 39:293–306

Bártová E, Krejcí J, Harnicarová A, Galiová G, Kozubek S (2008) Histone modifications and nuclear architecture: a review. J Histochem Cytochem 56:711–721

Blake NK, Lehfeldt BR, Lavin M, Talbert LE (1999) Phylogenetic reconstruction based on low copy DNA sequence data in an allopoyploid: The B genome of wheat. Genome 42:351–360

Bram S, Ris H (1971) On the structure of nucleohistone. J Mol Biol 55:325–336

Brenchley R, Spannag M, Pfeifer M, Barker G, D'Amore R, Allen A, McKenzie N, Kramer M, Kerhornou A, Bolser D, Kay S, Waite D, Trick M, Bancroft I, Gu Y, Huo N, Luo M–C, Sehgal S, Gill B, Kianian S, Anderson O, Kersey P, Dvorak J, McCombie W, Hall A, Mayer K, Edwards K, Bevan W, Hall N (2013) Analysis of the bread wheat genome using whole–genome shotgun sequencing. Nature 491:705–710

Cai X, Chen PD, Xu SS, Oliver RE, Chen X (2005) Utilization of alien genes to enhance Fusarium head blight resistance in wheat-a review. Euphytica 142:309–318

Cai X, Xu SS (2007) Meiosis-driven genome variation in plants. Curr Genomics 8:151–161.

Cai X, Xu SS, Zhu X (2010) Mechanism of haploidy-dependent unreductional meiotic cell division in polyploid wheat. Chromosoma 119:275–285

Campbell B, Baenziger PS, Gill KS, Eskridge KM, Budak H, Erayman M, Dweikat I, Yen Y (2003) Identification of QTLs and environmental interactions associated with agronomic traits on chromosome 3A of wheat. Crop Sci 43:1493–1505

Cavanagh CR, Chao S, Wang S, Huang BE, Stephen S, Kiani S, Forrest K, Saintenac C, Brown–Guedira GL, Akhunova A, See D, Bai G, Pumphrey M, Tomar L, Wong D, Kong S, Reynolds M, da Silva ML, Bockelman H, Talbert L, Anderson JA, Dreisigacker S, Baenziger S, Carter A, Korzun V, Morrell PL, Dubcovsky J, Morell MK, Sorrells ME, Hayden MJ, Akhunov E (2013) Genome–wide comparative diversity uncovers multiple targets of selection for improvement in hexaploid wheat landraces and cultivars. Proc Natl Acad Sci USA 110:8057–8062

Chalupska D, LeeHY, Faris JD et al (2008) Acc homoeoloci and the evolution of the wheat genomes. Proc Natl Acad Sci USA 105:9691–9696

Chapman JA, Mascher M, Buluç A, Barry K, Georganas E, Session A, Strnadova V, Jenkins J, Sehgal S, Oliker L, Schmutz J, Yelick KA, Scholz U, Waugh R, Cnudde F, Gerats T (2005) Meiosis: Inducing variation by reduction. Plant Biol 7:321–341.

Civardi L, Xia Y, Edwards KJ, Schnable PS, Nikolau BJ. 1994. The relationship between genetic and physical distances in the cloned *a1- sh2* interval of the *Zea mays* L. genome. Proc Natl Acad Sci USA 91:8268–8272

Poland JA, Muehlbauer GJ, Stein N, Rokhsar DS (2015) A whole-genome shotgun approach for assembling and anchoring the hexaploid bread wheat genome. Genome Biol 16:26–42

Cook PR (1995) A chromomeric model for nuclear and chromosome structure. J Cell Sci 108:2927–2935

Cox TS (1998) Deepening the wheat gene pool. J Crop Prod Recent Advances 1:1–25

Danilova T V., Zhang G, Liu W, Friebe B, Gill BS (2017) Homoeologous recombination-based transfer and molecular cytogenetic mapping of a wheat streak mosaic virus and *Triticum* mosaic virus resistance gene Wsm3 from *Thinopyrum intermedium* to wheat. Theor Appl Genet 130:549–556

Drouaud J, Camilleri C, Bourguignon PY, Canaguier A, Berard A, Vezon D, Giancola S, Brunel D, Colot V, Prum B Quesneville H, Mezard C (2006) Variation in crossing–over rates across chromosome 4 of *Arabidopsis thaliana* reveals the presence of meiotic recombination "hot spots". Genome Res 16:106–114

Dvorak J, Zhang HB (1990) Variation in repeated nucleotide sequences sheds light on the phylogeny of the wheat B and G genomes. Proc Natl Acad Sci U S A 87:9640–9644

Dvorak J, Terlizzi P, Zhang HB, Resta P (1993) The evolution of polyploidy wheats: Identification of the A genome donor species. Genome 36:21–31

Dvorak J, Akhunov ED (2005) Tempos of gene locus deletions and duplications and their relationship to recombination rate during diploid and polyploid evolution in the *Aegilops-Triticum* alliance. Genetics 171:323–332

Dvorak J, Luo MC, Akhunov ED (2011) N.I. Vavilov's theory of centers of diversity in light of current understanding of wheat diversity, domestication and evolution. Czech J Genet Plant Breed 24:20–27

Eig A (1929) Amblyopyrum Eig. A new genus separated from the genus *Aegilops*. PZE Inst Agri Natural History Agric Res 2:199–204

Elias EM, Steiger KD, Cantrell RG (1996) Evaluation of lines derived from wild emmer chromosome substitutions II. Agronomic traits. Crop Sci 36:228–233

Faris J, Gill BS (2002) Genomic targeting and high resolution mapping of the domestication gene *Q* in wheat. Genome 45:706–718

Faris JD, Fellers JP, Brooks SA, Gill BS (2003) A bacterial artificial chromosome contig spanning the major domestication locus *Q* in wheat and identification of a candidate gene. Genetics 164:311–321

Faris JD, Simons KJ, Zhang Z, Gill B (2005) The wheat super domestication gene *Q*. Front Wheat Biosci 100:129–148

Faris JD, Xu SS, Cai X, Friesen TL, Jin Y (2008) Molecular and cytogenetic characterization of a durum wheat–*Aegilops speltoides* chromosome translocation conferring resistance to stem rust. Chromosom Res 16:1097–1105

Faris JD (2014) Wheat domestication: key to agricultural revolutions past and future. In: Tuberosa R, Graner A, Frison E (eds) Genomics of plant genetic resources. vol 1. Managing, sequencing and mining genetic resources, Springer, Netherlands, pp 439–464

Feldman M, Strauss I, Vardi A (1979) Chromosome pairing and fertility of F_1 hybrids of *Aegilops longissima* and Ae. *searsii*. Can J Genet Cytol 21:261–272

Feldman M, Levy AA (2012) Genome evolution due to allopolyploidization in wheat. Genetics, 192:763–774

Feldman M, Levy AA (2015) Origin and evolution of wheat and related *Triticeae* Species. In: Molnár-Láng M, Ceoloni C, Doležel J (eds) Alien introgression in wheat. Springer International Publishing, Switzerland, pp 21–76

Friebe B, Zeller FJ, Mukai Y, Forster BP, Bartos P, McIntosh RA (1992) Characterization of rust-resistant wheat- *Agropyron intermedium* derivatives by C-banding, *in situ* hybridization and isozyme analysis. Theor Appl Genet 83:775–782

Finch JT, Lutter LC, Rhodes D, Brown AS, Rushton B, Levitt M, Klug A (1977) Structure of nucleosome core particles of chromatin. Nature 269:29–36

Friebe B, Jiang J, Raupp WJ, McIntosh RA, Gill BS (1996) Characterization of wheat-alien translocations conferring resistance to diseases and pests: current status. Euphytica 91:59–87

Friebe B, Zhang P, Linc G, Gill BS (2005) Robertsonian translocations in wheat arise by centric misdivision of univalents at anaphase I and rejoining of broken centromeres during interkinesis of meiosis II. Cytogenet Genome Res 109:293–297

Fukuda K, Sakamoto S (1992) Cytological studies on unreduced male gamete formation in hybrids between tetraploid emmer wheats and *Ae. squarrosa* L. Japan J Breed 42:255–266

Gaeta RT, Pires JC (2010) Homoeologous recombination in allopolyploids: the polyploid ratchet. New Phytol 186:18–28

Gaut BS, Wright SI, Rizzon C, Dvořák J, Anderson LK (2007) Recombination: an underappreciated factor in the evolution of plant genomes. Nat Rev Genet 8:77–84

Gornicki P, Zhu H, Wang J, Challa GS, Zhang Z, Gill BS, Li W (2014) The chloroplast view of the evolution of polyploid wheat. New Phytol 204:704–714

Gill BS, Kimber G (1974) Giemsa C-banding and the evolution of wheat. Proc Natl Acad Sci USA 71: 4086–4090

Gill BS, Appels R, Botha–Oberholster AM, Buell CR, Bennetzen JL, Chalhoub B, Chumley F, Dvořák J, Iwanaga M, Keller B, Li W, McCombie WR, Ogihara Y, Quetier F, Sasaki T (2004) A workshop report on wheat genome sequencing: international genome research on wheat consortium. Genetics. 168:1087–1096

Gill BS, Li W, Sood S, Kuraparthy V, Friebe Simons KJ, Zhang Z, Faris JD (2007) Genetics and genomics of wheat domestication-driven evolution. Isr J Plant Sci 55:223–229

Harlan J, deWet JMJ (1975) On Ö. Winge and a prayer: The origins of polyploidy. Bot Rev 41:361–390

Heun M, Schaefer-Pregl R, Klawan D et al (1997) Site of einkorn wheat domestication identified by DNA fingerprinting. Science 278:1312–1314

Huang S, Sirikhachornkit A, Su X, Faris J, Gill B, Haselkorn R, Gornicki P (2002) Genes encoding plastid acetyl-CoA carboxylase and 3-phosphoglycerate kinase of the *Triticum*/*Aegilops* complex and the evolutionary history of polyploid wheat. Proc Natl Acad Sci USA 99:8133–8138

Huberman JA (1973) Structure of chromosome fibers and chromosomes. Annu Rev Biochem 42:355–378

Jauhar PP (2007) Meiotic restitution in wheat polyhaploids (amphihaploids), a potent evolutionary force. J Hered 98:188–193

Jiang, J, Friebe B, Gill BS (1994) Recent advances in alien gene transfer in wheat. Euphytica. 73:199–212

Kerber ER, Dyck PL (1969) Inheritance in hexaploid wheat of leaf rust resistance and other characters derived from *Aegilops squarossa*. Can J Genet Cytol 11:639–647

Kerber ER, Rowland GG (1974) Origin of the free threshing character in hexaploid wheat. Can J Genet Cytol 16:145–154

Kihara H (1954) Considerations on the evolution and distribution of *Aegilops* species based on the analyzer-method. Cytologia 19:336–357

Kilian B, Özkan H, Deusch O, Effgen S, Brandolini A, Kohl J, Martin W, Salamini F (2007) Independent wheat B and G genome origins in outcrossing *Aegilops* progenitor haplotypes. Mol Biol Evol 24: 217–227

Kim S, Plagnol V, Hu TT, Toomajian C, Clark RM, Ossowski S, Ecker JR, Weigel D, Nordborg M (2007) Recombination and linkage disequilibrium in *Arabidopsis thaliana*. Nature Genet 39:1151–1155

Kimber G, Tsunewaki K (1988) Genome symbols and plasma types in the wheat group. In: Miller TE, Koebner RMD (eds.), Proceedings of 7th International Wheat Genet Symp, Cambridge, pp 1209–1210

King J, Grewal S, Yang CY, Hubbart S, Scholefield D, Ashling S, Edwards KJ, Allen AM, Burridge A, Bloor C, Davassi A, da Silva GJ, Chalmers K, King IP (2016) A step change in the transfer of interspecific variation into wheat from *Amblyopyrum muticum*. Plant Biotechnol J 15:217–226

Klindworth DL, Niu ZX, Chao SM, Friesen TL, Jin Y, Faris JD, Cai XW, Xu SS (2012) Introgression and characterization of a goatgrass gene for a high level of resistance to Ug99 stem rust in tetraploid wheat. G3 2:665–673

Klindworth DL, Saini J, Long Y, Rouse MN, Faris JD, Jin Y, Xu SS (2017) Physical mapping of DNA markers linked to stem rust resistance gene *Sr47* in durum wheat. Theor Appl Genet 130:1135–1154

Koul AK, Dhar MK (1998) Plant aneuploids: Suggestions for their classification. Euphytica 104:95–106

Kruppa K, Sepsi A, Szakács É, Röder MS, Molnár–Láng M (2013) Characterization of a 5HS-7DS.7DL wheat–barley translocation line and physical mapping of the 7D chromosome using SSR markers. J Appl Genet 54:251–258

Levan A, Fredga K, Sandberg AA (1964) Nomenclature for centromeric position on chromosomes. Hereditas 52:201–220

Ling HQ, Zhao S, Liu D, Wang J, Sun H, Zhang C, Fan H, Li D, Dong L, Tao Y (2013) Draft genome of the wheat A-genome progenitor *Triticum urartu*. Nature 496:87–90

Liu W, Jin Y, Rouse M, Friebe B, Gill B, Pumphrey MO (2011a) Development and characterization of wheat-*Ae. searsii* Robertsonian translocations and a recombinant chromosome conferring resistance to stem rust. Theor Appl Genet 122:1537–1545

Liu W, Rouse M, Friebe B, Jin Y, Gill B, Pumphrey MO (2011b) Discovery and molecular mapping of a new gene conferring resistance to stem rust, *Sr53*, derived from *Aegilops*

geniculata and characterization of spontaneous translocation stocks with reduced alien chromatin. Chromosom Res 19(5):669–682

Long Y, Chao WS, Ma G, Xu SS, Qi, L (2017) An innovative SNP genotyping method adapting to multiple platforms and throughputs. Theor Appl Genet 130:597–607

Luo MC, Yang ZL, You FM, Kawahara T, Waines JG, Dvorak J (2007) The structure of wild and domesticated emmer wheat populations, gene flow between them, and the site of emmer domestication. Theor Appl Genet 114:947–959

Luo MC, Gu YQ, You FM, Deal KR, Ma Y, Hu Y, Huo N, Wang Y, Wang J, Chen S, Jorgensen CM, Zhang Y, McGuire PE, Pasternak S, Stein JC, Ware D, Kramer M, McCombie WR, Kianian SF, Martis MM, Mayer KFX, Sehgal SK, Li W, Gill BS, Bevan MW, Šimková H, Doležel J, Weining S, Lazo GR, Anderson OD, Dvorak J (2013) A 4-gigabase physical map unlocks the structure and evolution of the complex genome of *Aegilops tauschii*, the wheat D-genome progenitor. Proc Natl Acad Sci USA 110:7940–7945

Marcussen T, Sandve SR, Heier L, Spannagl M, Pfeifer M, IWGSC, Jakobesn KS, Wulff BBH, Steuernagel B, Mayer KFX, Olsen OA (2014) Ancient hybridizations among the ancestral genomes of bread wheat. Science 345:1250092–1–4

Masoudi–Nejad A, Nasuda S, McIntosh RA, Endo TR (2002) Transfer of rye chromosome segments to wheat by a gametocidal gene. Chromosome Res 10: 349Y357

Mayer KX, Rogers J, Dole J, Pozniak C, Eversole K, Feuillet C, Gill B, Friebe B, Lukaszewski J, Sourdille P, Endo TR et al (2014) A chromosome-based draft sequence of the hexaploid bread wheat (*Triticum aestivum*) genome. Science 345:1251788

Meyer RS, Purugganan MD (2013) Evolution of crop species: genetics of domestication and diversification. Nature Rev Genet 14:840–852

Mezard C (2006) Meiotic recombination hotspots in plants. Biochem Soc Trans 34:531–534

Middleton CP, Senerchia N, Stein N, Akhunov ED, Keller B, Wicker T, Kilian B (2014) Sequencing of chloroplast genomes from wheat, barley, rye and their relatives provides a detailed insight into the evolution of the Triticeae tribe. PLoS One 9:e85761

Mori N, Ishii T, Ishido T, Hirosawa S, Watatani H, Kawahara T, Nesbitt M, Belay G, Takumi S, Ogihara Y, Nakamura C (2003) Origin of domesticated emmer and common wheat inferred from chloroplast DNA fingerprinting. 10th international wheat genetics symposium. Paestum, pp 25–28

Nalam V, Vales MI, Watson CJW, Kianian SF, Riera-Lizarazu O (2006) Map based analysis of genes affecting the brittle rachis character in tetraploid wheat. Theor Appl Genet 112:373–381

Niu Z, Klindworth DL, Friesen TL, Chao S, Jin Y, Cai X, Xu SS (2011) Targeted introgression of a wheat stem rust resistance gene by DNA marker–assisted chromosome engineering. Genetics 187:1011–1021

Niu Z, Klindworth DL, Yu G, Friesen TL, Chao S, Jin Y, Cai X, Ohm JB, Rasmussen JB, Xu SS (2014) Development and characterization of wheat lines carrying stem rust resistance gene *Sr43* derived from *Thinopyrum ponticum*. Theor Appl Genet 127:969–980

Ohta S (1991) Phylogenetic relationship of *Aegilops mutica* Boiss with the diploid species of congeneric *Aegilops–Triticum* complex, based on the new method of genome analysis using its B–chromosomes. Mem Coll Agric Kyoto Univ 137:1–116

Ozkan H, Brandolini A, Schafer–Pregl R, Salamini F (2002) AFLP analysis of a collection of tetraploid wheats indicates the origin of emmer and hard wheat domestication in Southeast Turkey. Mol Biol Evol 19:1797–1801

Ozkan H, Brandolini A, Pozzi C, Effgen S, Wunder J, Salamini F (2005) A reconsideration of the domestication geography of tetraploid wheats. Theor Appl Genet 110:1052–1060

Ozkan H, Willcox G, Graner A, Salamini F, Kilian B (2010) Geographic distribution and domestication of wild emmer wheat (*Triticum dicoccoides*). Genet Resour Crop Evol 58:11–53.

Peng JH, Ronnin Y, Fahima T, Roder MS, Li YC, Nevo E, Korol A (2003) Domestication quantitative trait loci in *Triticum dicoccoides*, the progenitor of wheat. Proc Natl Acad Sci USA 100:2489–2494

Peng JH, Sun D, Nevo E (2011) Domestication evolution, genetics and genomics in wheat. Mol Breeding 28:281–301

Petersen S, Lyerly JH, Worthington ML, Parks WR, Cowger C, Marshall DS, Brown–Guedira G, Murphy JP (2014) Mapping of powdery mildew resistance gene *Pm53* introgressed from *Aegilops speltoides* into soft red winter wheat. Theor Appl Genet 128:303–312

Renfrew JM (1973) Palaeoethnobotany: the prehistoric food plants of the Near East and Europe. Methuen and Go. Ltd, London, pp 1–248

Qi LL, Wang SL, Chen PD, Liu DJ, Friebe B, Gill BS (1997) Molecular cytogenetic analysis of *Leymus recemosus* chromosomes added to wheat. Theor Appl Genet 95:1084–1091

Qi LL, Friebe B, Zhang P, Gill BS (2007) Homoeologous recombination, chromosome engineering and crop improvement. Chromosome Res 15:3–19

Qi LL, Pumphrey MO, Friebe B, Zhang P, Qian C, Bowden RL, Rouse MN, Jin Y, Gill BS (2011) A novel Robertsonian translocation event leads to transfer of a stem rust resistance gene

(*Sr52*) effective against race Ug99 from *Dasypyrum villosum* into bread wheat. Theor Appl Genet 123:159–167

Ramanna MS, Jacobsen E (2003) Relevance of sexual polyploidization for crop improvement: a review. Euphytica 133:3–18

Rey E, Molnár I, Doležel J (2015) Genomics of wild relatives and alien introgressions. In: Molnár–Láng M, Ceoloni C, Doležel J (eds) Alien introgression in wheat. Springer International Publishing, Switzerland, pp 374–381

Riley R, Unrau J, Chapman V (1958) Evidence on the origin of the B genome of wheat. J Hered 49:90–98

Rodriguez S, Maestra B, Perera E, Diez M, Naranjo T (2000) Pairing affinities of the B- and G-genome chromosomes of polyploid wheats with those of *Aegilops speltoides*, Genome 43: 814–819

Sakamura T (1918) Kurze mitteilung über die chromosomenzahalen und die verwandtschaftsver– hältnisse der Triticum Arten. Bot Mag 32:151–154

Sallares R, Brown TA (2004) Phylogenetic analysis of complete 5′ external transcribed spacers of the 18S ribosomal RNA genes of diploid *Aegilops* and related species (Triticeae, Poaceae). Genet Resour Crop Evol 51:701–712

Salse J, Chague V, Bolot S, Magdelenat G, Huneau C, Pont C, Belcram H, Couloux A, Gardais S, Evrard A, Segurens B, Charles M, Ravel C, Samain S, Charmet G, Boudet N, Chalhoub B (2008) New insights into the origin of the B genome of hexaploid wheat: evolutionary relationships at the *SPA* genomic region with the S genome of the diploid relative *Aegilops speltoides*. BMC Genomics 9:555

Sarkar P, Stebbins GL (1956) Morphological evidence concerning the origin of the B genome in wheat. Am J Bot 43:297–304

Sax K (1921) Chromosome relationships in wheat. Science 54:413–415

Sax K (1922) Sterility in wheat hybrids. II. Chromosome behavior in partially sterile hybrids. Genetics 7:513–552

Schwarzacher T, Leitch AR, Bennett MD (1989) In situ localization of parental genomes in a wide hybrid. Ann Bot 64:315–324

Schwarzacher T, Anamthawat–Jonsson K, Harrison GE, Islam AKMR, Jia JZ, King IP, Leitch AR, Miller TE, Reader SM, Rogers WJ, Shi M, Heslop–Harrison JS (1992) Genomic *in situ* hybridization to identify alien chomosomes and chromosome segments in wheat. Theor Appl Genet 84:778–786

Sears ER (1954) The aneuploids of common wheat. Res Bull Missouri Agric Exp Stn 572:1–57

Sears ER (1956) The transfer of leaf rust resistance from *Aegilops umbellulata* to wheat. Brookhaven Symp Biol 9:1–22

Semagn K, Babu R, Hearne S, Olse M (2014) Single nucleotide polymorphism genotyping using Kompetitive Allele Specific PCR (KASP): overview of the technology and its application in crop improvement. Mol Breed 33:1–14

Silkova OG, Shchapova AI, Kravtsova LA (2003) Mechanism of meiotic restitution and their genetic regulation in wheat–rye polyhaploid. Russ J Genet 39:1271–1280

Silkova O, Shchapova A, Shumny V (2011) Meiotic restitution in amphihaploids in the tribe Triticeae. Russ J Genet 47:383–393

Simonetti MC, Bellomo MP, Laghetti G, Perrino P, Simeone R, Blanco A (1999) Quantitative trait loci influencing free-threshing habit in tetraploid wheats. Genet Res Crop Evol 46:267–271

Simons K, Fellers JP, Trik HN, Zhang Z, Tai YS, Gill BS, Faris JD (2006) Molecular characterization of the major wheat domestication gene *Q*. Genetics 172:547–555

Sood S, Kuraparthy V, Bai GH, Gill BS (2009) The major threshability genes soft glume (*sog*) and tenacious glume (*Tg*), of diploid and polyploid wheat, trace their origin to independent mutations at non-orthologous loci. Theor Appl Genet 119:341–351

Taenzler B, Esposti RF, Vaccino P et al (2002) Molecular linkage map of einkorn wheat: mapping of storage–protein and soft–glume genes and bread–making quality QTLs. Genet Res Camb 80:131–143

Tan CT, Assanga A, Zhang G, Rudd JC, Haley SD, Xue Q, Ibrahim A, Bai G, Zhang X, Byrne P, Fuentealba MP, Liu S (2017) Development and validation of KASP markers for wheat streak mosaic virus resistance gene *Wsm2*. Crop Sci 57:1–10

Tanaka M, Kawahara T, Sano J (1979) The origin and the evolution of tetraploid wheats. Wheat Inf Serv 47:7–11

Van Slageren, MW (1994) Wild wheats: a monograph of *Aegilops* L. and *Amblyopyrum* (Jaub. & Spach) Eig (Poaceae). Agriculture University, Wageningen–International Center for Agricultural Reaserch in Dry Areas, Aleppo, Syria

Watanabe N, Ikebata N (2000) The effects of homoeologous group 3 chromosomes on grain color dependent seed dormancy and brittle rachis in tetraploid wheat. Euphytica 115:215–220

Winfield MO, Allen AM, Burridge AJ, Barker GLA, Benbow HR, Wilkinson PA, Coghill J, Waterfall C, Davassi A, Scopes G, Pirani A, WebsteR T, Brew F, Bloor C, King J, West C,

Griffiths S, King I, Bentley AR, Edwards KJ (2016) High–density SNP genotyping array for hexaploid wheat and its secondary and tertiary gene pool. Plant Biotech J 14:1195–1206

Wulff BBH, Moscou MJ (2014) Strategies for transferring resistance into wheat: from wide crosses to GM cassettes. Front Plant Sci 5:692

Xu SJ, Joppa LR (2000) First–division restitution in hybrids of Langdon durum disomic substitution lines with rye and *Aegilops squarrosa*. Plant Breed 119:233–241

Xu SS, Friesen TL, Mujeeb–Kazi A (2004) Seedling resistance to tan spot and Stagonospora nodorum blotch in synthetic hexaploid wheats. Crop Sci 44:2238–2245

Xu XJ, Hsia AP, Zhang L, Nikolau BJ, Schnable PS (1995) Meiotic recombination break points resolve at high rates at the 5′ end of a maize coding sequence. Plant Cell 7:2151–2161

Zhang P, Friebe B, Gill BS (2002) Variation in the distribution of a genome-specific DNA sequence on chromosomes reveals evolutionary relationships in the *Triticum* and *Aegilops* complex. Plant Syst Evol 235:169–179

Zhang P, Dundas IS, McIntosh RA, Xu SS, Park RF, Gill BS, Friebe B (2015) Wheat–Aegilopsintrogressions. In: Molnár–Láng M, Ceoloni C, Doležel J (eds) Alien introgression in wheat. Springer International Publishing, Switzerland, pp 221–44

Zhang QJ (2013) Development and characterization of wheat germplasm for resistance to stem rust Ug99 in wheat. PhD Dissertation. North Dakota State University, Fargo, North Dakota

Zhang W, Cao Y, Zhang M, Zhu X, Ren S, Long Y, Gyawali Y, Chao S, Xu S, Cai X (2017) Meiotic homoeologous recombination-based alien gene introgression in the genomics era of wheat. Crop Sci 57:1189–1198

Zhang ZC, Belcram H, Gornicki P, Charles M, Just J, Huneau C, Magdelenat G, Couloux A, Samain S, Gill BS, Rasmussen JB, Barbe V, Faris JD, Chalhoub B (2011) Duplication and partitioning in evolution and function of homoeologous *Q* loci governing domestication characters in polyploid wheat. Proc Natl Acad Sci USA 108:18737–18742

Zohary D, Feldman M (1962) Hybridization between amphidiploids and the evolution of polyploids in the wheat (*Aegilops–Triticum*) group. Evolution 16:44–61

CHAPTER 3. THE FOOTPRINT OF GOATGRASS IN THE WHEAT B GENOME

Abstract

Wheat is a typical allopolyploid with three homoeologous subgenomes (A, B, and D). The donors of the subgenomes A and D had been identified, but not for the subgenome B. The goatgrass *Aegilops speltoides* (genome SS) has been controversially considered a possible candidate for the donor of the wheat B genome. However, the relationship of the *Ae. speltoides* S genome with the wheat B genome remains largely obscure. The present study assessed the homology of the B and S genomes using an integrative cytogenetic and genomic approach, and revealed the contribution of *Ae. speltoides* to the origin of the wheat B genome. We discovered noticeable homology between wheat chromosome 1B and *Ae. speltoides* chromosome 1S, but not between other chromosomes in the B and S genomes. An *Ae. speltoides*-originated segment spanning a genomic region of approximately 10.46 Mb was detected on the long arm of wheat chromosome 1B (1BL). The *Ae. speltoides*-originated segment on 1BL was found to co-evolve with the rest of the B genome. Evidently, *Ae. speltoides* had been involved in the origin of the wheat B genome, but should not be considered an exclusive donor of this genome. The wheat B genome might have a polyphyletic origin with multiple ancestors involved, including *Ae. speltoides*. These novel findings will facilitate genome studies in wheat and other polyploids.

Introduction

Wheat (*Triticum aestivum*, 2n=6x=42, genome AABBDD), a major food grain source for humans, has been considered a typical allohexaploid originated from the interspecific hybridization involving three diploid ancestors (Sakamura, 1918; Kihara, 1919 and 1954; Kihara et al., 1959; Sax, 1922). This evolutionary theory of allopolyploid has led to successful identification of the ancestors for the wheat subgenomes A and D, but not yet for the subgenome

B. The wheat A and D subgenomes were found to be contributed by *T. urartu* (2n=2x=14, genome AA) and *Aegilops tauschii* (2n=2x=14, genome DD), respectively (Kihara, 1944; McFadden and Sears, 1946; Dvorak et al., 1993). The ancestor of the subgenome B, however, remains controversial even though tremendous research efforts have been made to tackle this evolutionary puzzle of wheat for nearly a century.

Early studies on meiotic pairing, karyotyping, plant morphology, and geographic distribution of wheat-related wild species and their hybrids with wheat species (*Triticum* L.) identified the goatgrass *Ae. speltoides* (2n=2x=14, genome SS) as the closest ancestor of the wheat B genome (Jenkins, 1929; Pathak, 1940; Sarkar and Stebbins, 1956; Riley et al., 1958). Meanwhile, questions had been raised about the meiotic pairing-based assessment of genome homology in these early studies because *Ae. speltoides* was suspected to contain genetic factors with epistatic effect on the wheat diploidization system, now designated *Ph* (pairing homoeologous) gene (Jenkins, 1929; Sarkar and Stebbins, 1956; Riley et al., 1958). The *Ph* gene limits meiotic pairing to homologous chromosomes in wheat and wheat hybrids with its relatives. Also, it had been assumed that the ancestral form of the B genome might have undergone a series of changes since its incorporation into wheat (Jenkins, 1929; Sarkar and Stebbins, 1956).

In a later study, Riley et al. (1961) confirmed the presence of the gene(s) in *Ae. speltoides* that suppresses the effect of the *Ph1* gene located on wheat chromosome 5B. Three genotypes with high, intermediate, and low ability to suppress the *Ph1* activity were identified in *Ae. speltoides* (Dvorak, 1972). On the basis of these findings, Kimber and Athwal (1972) reassessed meiotic pairing in the hybrids and amphiploids involving wheat and *Ae. speltoides* accessions with different levels of suppression for the *Ph1* activity. They determined that the variation of meiotic pairing in the hybrids resulted from the presence of different *Ph1* suppressors in the *Ae.*

speltoides accessions. Also, they found that chromosomes predominantly paired as bivalents in the amphiploid involving polyploid wheat and a low pairing *Ae. speltoides* accession, which was very similar to a normal diploidized allopolyploid. As a result, they concluded that *Ae. speltoides* could not be considered as the ancestor of the wheat B genome. This was also supported by the evidence of chromosome banding patterns (Gill and Kimber, 1974) and protein electrophoretic profiles (Johnson, 1972). More recently, three *Ph1* suppressor gene loci were identified and mapped to chromosome 3S, 5S, and 7S of *Ae. speltoides*, respectively (Dvorak et al., 2006).

In contrast, molecular analyses of both nuclear and extranuclear genomic DNAs suggested that *Ae. speltoides* or a species in the evolutionary lineage of *Ae. speltoides* could be the most likely ancestor of the wheat B genome as well as wheat plasmon (Ogihar and Tsunewaki, 1988; Dvorak and Zhang, 1990; Sasanuma et al., 1996; Wang et al., 1997; Kilian et al., 2007). However, comparative analysis of several gene loci and nearby genomic regions across the *Triticum* and *Aegilops* species did not reveal clear evidence supporting that conclusion (Hang et al., 2002; Salse et al., 2008). The *Ae. speltoides* S genome was considered to be evolutionarily closer to the wheat B genome than to the A and D genomes, but its candidacy as the ancestor of B genome remained undetermined in both studies.

The wheat B genome has significantly higher genetic variability than A and D genome (Chao et al., 1989; Felsenburg et al., 1991; Siedler et al., 1994; Petersen et al., 2006). These findings support the hypothesis that the wheat B genome has diverged from its ancestor through various genomic modifications (Jenkins, 1929; Sarkar and Stebbins, 1956; Blake et al., 1999). In addition, *Ae. speltoides* has significantly higher intraspecific genetic variability than any of the other four *Aegilops* species in the Sitopsis section, which is even comparable to the interspecific variability among the other four *Aegilops* species in the section (Sasanuma et al., 1996). This

appears to support the hypothesis that *Ae. speltoides* might contribute to the origin of the wheat B genome, but the current version of *Ae. speltoides* has diverged from the original ancestor of the B genome (Salse, 2008). Another hypothesis, proposed by Zohary and Feldman (Zohary and Feldman, 1962), states that the wheat B genome is a reconstructed genome resulted from meiotic homoeologous recombination between multiple ancestral genomes of the *Aegilops* species. This evolutionary recombination process was assumed to occur in the hybrids of the tetraploid amphiploids that combined the different ancestral *Aegilops* genomes and a common ancestral A genome of *T. urartu*. In other words, the wheat B genome might have a polyphyletic origin. However, no clear evidence has been reported to prove these hypotheses.

A species with a genome more closely related to the wheat B genome than the S genome of *Ae. speltoides* has not been discovered even though an intensive search for the ancestor of B genome has been performed over nearly a century. It seems inevitable to reason that *Ae. speltoides* may more or less have contributed to the origin and evolution of the wheat B genome according to previous studies. The present study aimed to assess the homology of individual wheat B-genome chromosomes with their homoeologous counterparts in the S genome of *Ae. speltoides* and to trace the *Ae. speltoides* genomic components in the wheat B genome, which could not be done in the previous studies due to the lack of the genomics/cytogenetics tools and resources. In this study, we revealed new insights into the involvement of *Ae. speltoides* in the origin of the wheat B genome using a new integrative cytogenetics and genomics research approach. This will enhance knowledge about the origin and evolution of the polyploid genome and facilitate further studies of the complex polyploid genome in wheat and other species.

Materials and methods

Plant materials

Six “Chinese Spring” (CS) wheat B genome-*Ae. speltoides* disomic substitution lines [DS 1S(1B), DS 2S(2B), DS 4S(4B), DS 5S(5B), DS 6S(6B), and DS 7S(7B)] (Friebe et al., 2011), one substitution line involving chromosome 3S and 3A [DS 3S(3A)], and the CS *ph1b* mutant were the initial genetic stocks used in this research. They were provided by the Wheat Genetics Resource Center at Kansas State University, USA. DS 3S(3A) was included in this study because DS 3S(3B) is not available. In addition, six CS wheat B genome-*Thinopyrum elongatum* (2n=2x=14, genome EE) disomic substitution lines [DS 1E(1B), DS 2E(2B), DS 3E(3B), DS 5E(5B), DS 6E(6B), and DS 7E(7B)] and one substitution line involving chromosome 4E and 4D [DS 4E(4D)] were used as controls to assess B-S genome homology in this study. DS 4E(4B) was not available. They were kindly supplied by J. Dvorak at UC Davis. Each of these disomic substitution lines has a pair of wheat chromosomes replaced by their homoeologous counterparts of *Ae. speltoides* or *Th. elongatum*. The common and durum wheat accessions used in this study were selected from the worldwide diversity panel of the Triticeae Coordinated Agricultural Project (T-CAP). The other wheat species/accessions that contain the B genome were obtained from the U.S. National Plant Germplasm System. A total of 179 accessions under 13 wheat species (*Triticum* L.) were chosen based on their geographic origin and distribution, representing a diverse worldwide collection of the tetraploid and hexaploid wheat species (APPENDIX A). A subset of representative wheat species/accessions (n=88) were selected for single nucleotide polymorphism (SNP) genotyping from the 179 accessions.

Construction of the special genotypes for meiotic pairing analysis

The CS-*Ae. speltoides* and CS-*Th. elongatum* disomic substitution lines were crossed and backcrossed with the CS *ph1b* mutant to construct the special genotypes monosomic for the individual B/A-S or B/D-E homoeologous pairs in the presence and absence of *Ph1*, respectively (Figure 3.1). The chromosome-specific DNA markers (Table 3.1) were employed to assist selection of the double monosomics for each of the homoeologous pairs. The selected individuals were verified for the monosomic condition by genomic *in situ* hybridization (GISH). The *Ph1*-specific DNA markers (Roberts et al., 1999) were used to select the double monosomics with *Ph1* as well as those without *Ph1* (i.e. homozygous for *ph1b* deletion mutant) (Figure 3.1)

Table 3.1. Chromosome-specific molecular markers used in this study

Markers	Location	Primer sequences	Tm (°C)	Amplicon size in CS (bp)	References
Xgwm18	1B	5' TGGCGCCATGATTGCATTATCTTC 3' 5' GGTTGCTGAAGAACCTTATTTAGG 3'	50	186	Roder et al. (1998)
Xwmc474	2B	5' ATGCTATTAAACTAGCATGTGTCG 3' 5' AGTGGAAACATCATTCCTGGTA 3'	60	120	Somers et al. (2004)
Xgpw7805	3A	5' CAGCATGTGCATCACCGT 3' 5' CCTCCGCAGGTCAAGCTC 3'	60	172	Dobrovolskaya et al. (2011)
Xgdm61	4B	5' TTCTTTGCGTGTGTGCGT 3' 5' CGCACTTTTTACTAGGGGTC 3'	60	100	Pestsova et al. (2000)
Xgpw5238	5B	5' AAGGGGCACATGAAATGAAG 3' 5' CCACTACAGGGTTGGGTCC 3'	60	243	Sourdille et al. (2004)
Xwmc397	6B	5' AGTCGTGCACCTCCATTTTG 3' 5' CATTGGACATCGGAGACCTG 3'	63	160	Somers et al. (2004)
Xgpw7518	7B	5' GAACCTAAGCACTGTCGATGG 3' 5' TCTCAGCAATTCAGGCACAC 3'	60	203	Sourdille et al. (2004)

Anthers with meiocytes [pollen mother cells (PMCs)] at metaphase I (MI) were collected for meiotic pairing analysis from the heterozygotes with and without *Ph1* following the procedure of Cai and Jones (1997). A total of over 100 meiocytes at MI from 1-6 plants were observed and analyzed for each of the special genotypes. GISH was used to differentially paint chromosomes of *Ae. speltoides*, *Th. elongatum*, and wheat for meiotic pairing analysis.

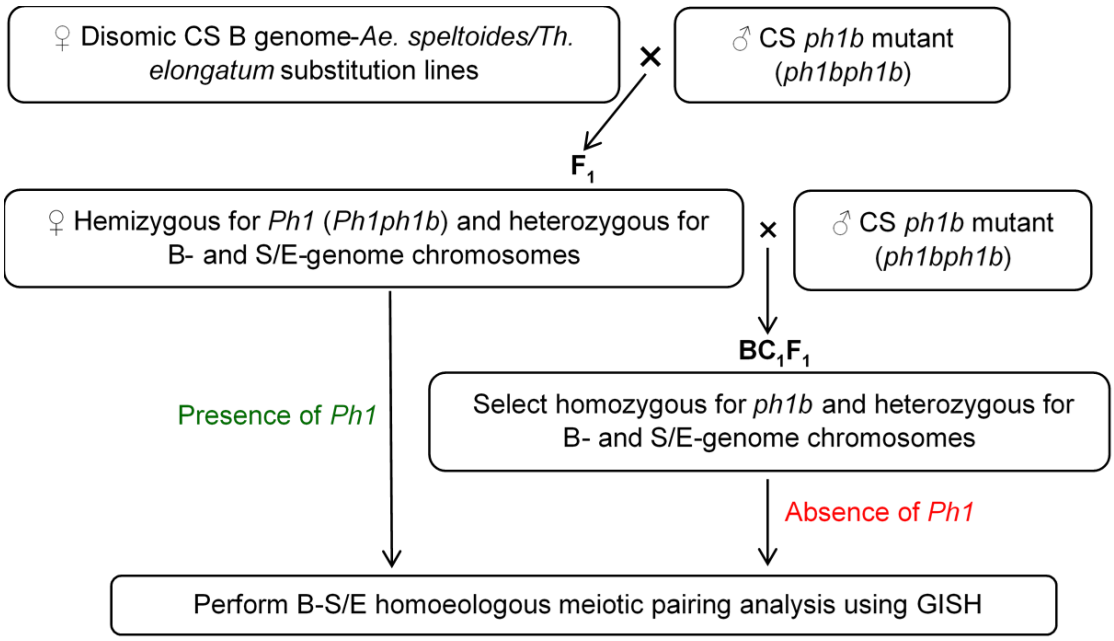

Figure 3.1. Construction of the special genotypes for B/A-S and B/D-E homoeologous meiotic pairing analysis.

DNA marker analysis

DNA samples were prepared as described by Niu et al. (2011). Chromosome-specific DNA markers, including SSRs (simple sequence repeats) and STSs (sequence-tagged sites), were developed and used for the identification of individual B-, S-, and E-genome chromosomes as described by Chen et al. (2007). Two STS markers (*PSR128* and *PSR574*) that tag the *Ph1* allele were used to identify individuals homozygous for the *ph1b* deletion mutant (Roberts et al., 1999). The wheat 90K iSelect SNP arrays were used to perform SNP genotyping assay for CS wheat, the disomic substitution lines, and the 88 representative wheat species/accessions (45 hexaploids and 43 tetraploids) using the Illumina iScan instrument. SNP allele clustering and genotype calling were conducted using the GenomeStudio v2011.1 software (Illumina, Inc.) (Wang et al., 2014). The polymorphisms for each of the homoeologous pairs at the SNP loci were calculated as the percentages of the polymorphic loci out of the total loci genotyped.

Genetic diversity was calculated based on the SNP genotyping data of the 88 representative wheat species/accessions (Nei, 1973) and plotted against the SNP consensus linkage map of wheat chromosome 1B (Wang et al., 2014). The SNP genotype-based cluster dendrogram was developed using the Flapjack software and R package "ape" (Milne et al., 2010; https://cran.r-project.org/).

Fluorescent *in situ* hybridization (FISH)

Fluorescent genomic *in situ* hybridization (GISH) was performed to differentiate wheat B-genome and S/E-genome chromatin from each other as described by Cai et al. (1998). Total genomic DNAs of *Ae. speltoides* and *Th. elongatum* were labeled with biotin-16-dUTP by nick translation as probe DNA for detecting *Ae. speltoides* and *Th. elongatum* chromatin, respectively. Total genomic DNA of CS wheat was used as blocking DNA. *Ae. speltoides*/*Th. elongatum* chromatin was painted with fluorescein isothiocyanate-conjugated avidin (FITC-avidin) as yellow-green and wheat chromatin was counter-stained with propidium iodide (PI) as red. Multicolor FISH was conducted following the procedure of Liu et al. (2006). The clone *pTa71*, a wheat 9 kb rDNA repeating unit that contains the 18S, 5.8S, and 26S rRNA genes and intergenic spacer (Gerlach and Bedbrook, 1979), was supplied by Peng Zhang at The University of Sydney, Australia. It was labeled with dig-11-dUTP and detected by anti-dig-rhodamine as red. This rDNA probe was used to tag the nucleolar organizer region on wheat chromosomes 1B and 6B. Total genomic DNA of *Ae. speltoides* was labeled with biotin-16-dUTP and detected by FITC-avidin as yellow-green. This genomic probe was used to identify *Ae. speltoides* chromatin in the wheat genome. Wheat chromatin was counter-stained with 4',6-diamidino-2-phenylindole (DAPI) as blue. The fluorescence microscopy system BX51 (Olympus, Japan) was used to visualize GISH/FISH-painted chromosomes.

DNA sequence analysis

The IWGSC RefSeq v1.0 (https://wheat-urgi.versailles.inra.fr/) was used to analyze the DNA sequences of chromosome 1B. The contextual sequences of the SNP loci that contain the same alleles at the distal ends of both CS wheat 1BL and *Ae. speltoides* 1SL were aligned to the DNA sequences of chromosome 1B using the program Splign locally (Kapustin et al., 2008). The physical order of the SNP loci was determined based on the DNA sequence alignment.

Results

Homology analysis of the individual B-S homoeologous chromosome pairs

Meiotic pairing has been considered direct cytological evidence for genome homology. It can, however, be influenced by genetic factors in addition to homology, such as the *Ph1* gene in wheat and *Ph1* suppressors in *Ae. speltoides*. To take account of the non-homology factors in the B-S genome homology analysis, we investigated meiotic pairing of individual B-S homoeologous pairs under the same genetic background of CS wheat in the presence and absence of *Ph1*. The CS wheat B genome-*Ae. speltoides* S genome disomic substitution lines dissect the S genome of *Ae. speltoides* into individual chromosomes in the CS wheat background. They were used to construct the double monosomics for the individual B- and S-genome chromosomes. Meanwhile, the *ph1b* deletion mutant of *Ph1* was introduced into the double monosoimcs with assistance of the *Ph1*-specific DNA markers. Thus, we were able to investigate meiotic pairing of individual B-S homoeologous chromosome pairs in the presence as well as absence of *Ph1*. In addition, we investigated meiotic pairing of the individual B-E homoeologous chromosome pairs and used them as controls for B-S genome homology analysis.

Chinese Spring wheat chromosome 1B was found to pair with *Ae. speltoides* chromosome 1S in 67 of the 134 PMCs analyzed (50.00%), while other B/A-S homoeologous

pairs had a relatively low meiotic pairing frequency ranging from 0.00 to 8.63% in the presence of *Ph1* (Figure 3.2). In addition, we noticed that 1B-1S meiotic pairing predominantly involved the long arms of chromosome 1B (1BL) and 1S (1SL). Surprisingly, wheat 1BL was found to contain a small *Ae. speltoides* S genome-derived chromosomal segment at its distal end, where meiotic pairing was mostly initiated (Figure 3.3a). Also, the same *Ae. speltoides*-derived segment was observed on the unpaired 1BL (univalent) (Figure 3.3b). The *Ph1* suppressor genes mapped to *Ae. speltoides* chromosomes 3S, 5S, and 7S (Dvorak et al., 2006). We found that meiotic pairing involving chromosome 5S was noticeably higher than that involving 2S, 3S, 4S, 6S, and 7S in the presence of *Ph1* (Figure 3.2). Thus, there might be a *Ph1* suppressor on this particular *Ae. speltoides* chromosome 5S, but not on chromosomes 3S and 7S involved in this study. In the absence of *Ph1* (i.e. *ph1bph1b*), chromosomes 1B and 1S paired at a frequency of 60%, which was higher than the 1B-1S pairing frequency in the presence of *Ph1* (50%). Meiotic pairing of other homoeologous pairs (2B-2S, 3A-3S, 4B-4S, 5B-5S, 6B-6S, and 7B-7S) was dramatically enhanced by *ph1b* mutant (Figure 3.2). $5B^{ph1b}$-5S also exhibited a high pairing frequency (42.16%), suggesting absence of *Ph1* on *Ae. speltoides* chromosome 5S (Griffiths et al., 2006).

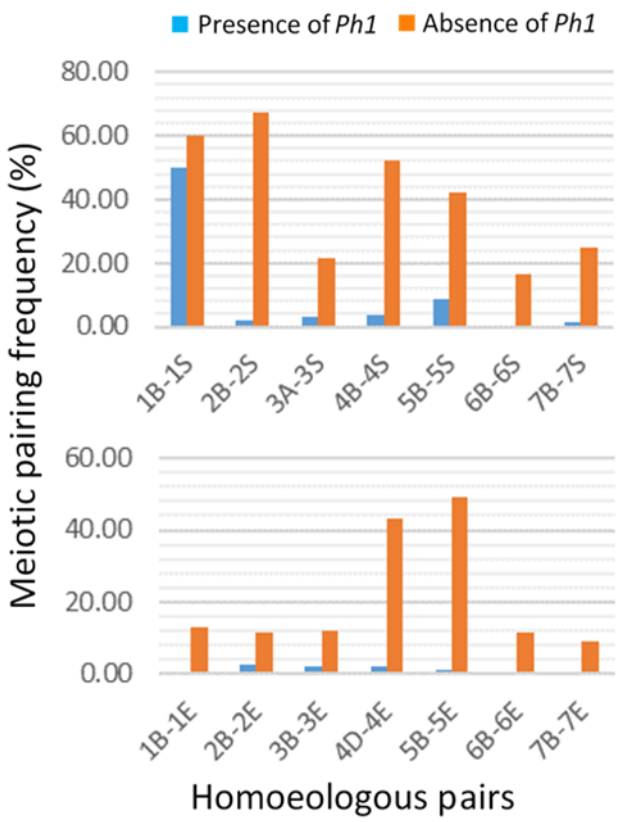

Figure 3.2. Meiotic pairing frequency of B/A-S (*top*) and B/D-E (*bottom*) homoeologous pairs in the presence and absence of *Ph1*.

Meiotic pairing was not observed between CS wheat chromosome 1B and *Th. elongatum* chromosome 1E in the 105 PMCs analyzed under the presence of *Ph1*. The other B/D-E homoeologous chromosome pairs also showed a low meiotic pairing frequency when *Ph1* was present (Figure 3.2). Meiotic pairing of all B/D-E homoeologous chromosome pairs was enhanced by the *ph1b* mutant, but not as extensively as that with B/A-S homoeologous chromosome pairs except 4D-4E and 5B-5E. Apparently, CS wheat chromosome $5B^{ph1b}$ had a high meiotic pairing affinity with *Ae. speltoides* chromosome 5S as well as *Th. elongatum* chromosome 5E (Figure 3.2).

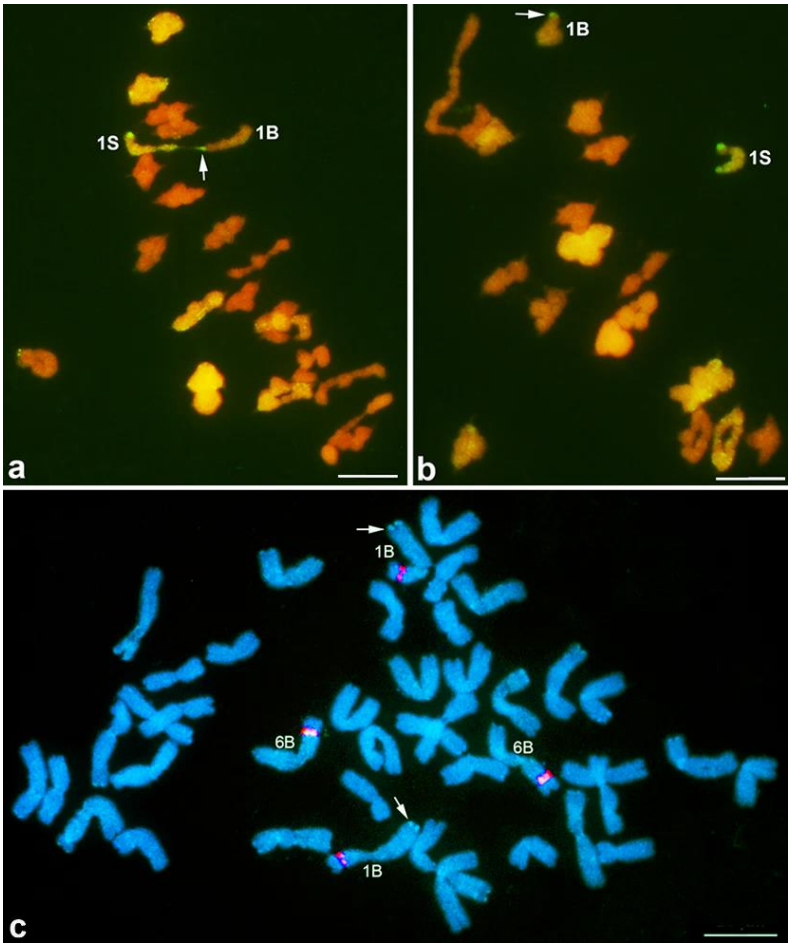

Figure 3.3. GISH/FISH-painted wheat and *Ae. speltoides* chromosomes. **a)** Showing meiotic pairing of CS wheat chromosome 1B with *Ae. speltoides* chromosome 1S as a rod bivalent; **b)** showing unpaired 1B and 1S chromosomes (univalents); and **c)** showing mitotic chromosomes of CS wheat. Arrows point to the *Ae. speltoides*-originated chromosomal segment on 1BL. Wheat and *Ae. speltoides* chromatin was painted as red and yellow-green by GISH, respectively (**a** & **b**). The *Ae. speltoides*-originated chromosomal segment was painted as light blue-green by GISH and the nucleolar organizer regions on 1BS and 6BS were painted as red by FISH. Wheat chromatin was counter-stained as blue by DAPI (**c**). Scale bar = 10 µm.

GISH/FISH analysis of wheat B-genome chromosomes

Meiotic pairing analysis demonstrated a notable homology between CS wheat chromosome 1B and *Ae. speltoides* chromosome 1S (Figure 3.2). Apparently, the *Ae. speltoides*-derived chromosomal segment at the distal end of 1BL contributed to the high 1B-1S pairing. To confirm the *Ae. speltoides* segment on 1BL and determine whether any additional *Ae. speltoides* segments are present on the CS B-genome chromosomes, we performed multicolor FISH/GISH

to the mitotic chromosomes of CS wheat. The CS wheat chromosomes 1B and 6B were tagged by FISH using the rDNA probe *pTa71* and *Ae. speltoides* chromatin was simultaneously painted by *Ae. speltoides* genomic DNA-probed GISH. An *Ae. speltoides* chromosomal segment was clearly detected at the distal end of CS 1BL, but not in other regions of chromosome 1B and other B-genome chromosomes (Figure 3.3c).

To further verify the origin of the distal segment on 1BL, we performed *Th. elongatum* genomic DNA-probed GISH to all three chromosome sets of the CS wheat genome. No *Th. elongatum*-derived GISH signals were observed on any of the CS wheat chromosomes, including 1BL (Figure 3.4A). Thus, the distal chromosomal segment on CS 1BL is *Ae. speltoides* S genome-originated, not a common chromosomal region shared by CS wheat and its relatives.

We surveyed the B genome of 179 representative accessions under 13 wheat species (*Triticum* L.) for the presence of *Ae. speltoides* chromatin by GISH. They were collected from the different geographic regions around the world and represented a diverse collection of the hexaploid and tetraploid wheat species/accessions that contain the B genome. All of these wheat species/accessions were found to contain an *Ae. speltoides* chromosomal segment at the distal end of 1BL as what we observed on 1BL of CS wheat, but not in the other regions of chromosome 1B and other B-genome chromosomes (APPENDIX A and Figure 3.3c). Therefore, the *Ae. speltoides*-derived chromosomal segment is universally present at the distal end of 1BL in the tetraploid and hexaploid wheat species. It has been part of chromosome 1B probably since the incorporation of the B genome into the tetraploid and hexaploid wheat.

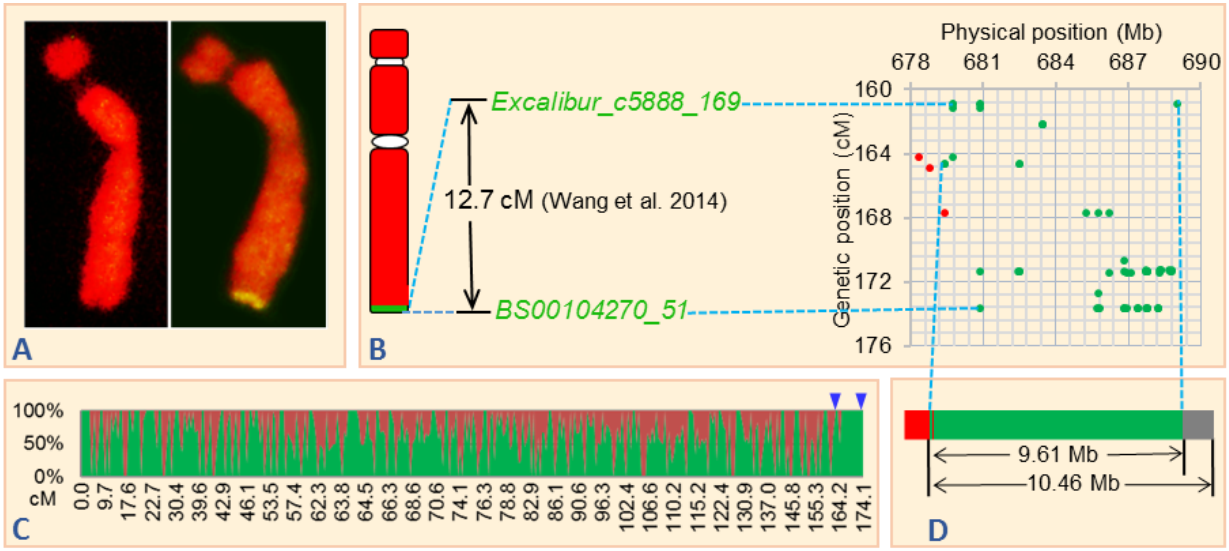

Figure 3.4. Cytogenetic and molecular mapping of the *Ae. speltoides*-originated chromosomal segment on 1BL. (**A)** GISH-painted CS wheat chromosome 1B using *Th. elongatum* genomic DNA as probe (*left*) and *Ae. speltoides* genomic DNA as probe (*right*); wheat chromatin was painted as red and *Ae. speltoides*/*Th. elongatum* chromatin as yellow-green. (**B)** Graphical representation of GISH-painted wheat chromosome 1B using *Ae. speltoides* genomic DNA as probe (*left*); genetic size of the highly monomorphic linkage block harboring 68 SNP loci at the distal ends of 1BL and 1SL (*middle*); and genetic and physical locations of the 68 SNP loci within the region (*right*). Green dots refer to the SNP loci monomorphic between CS wheat 1BL and *Ae. speltoides* 1SL; red dots refer to the polymorphic SNP loci. (**C)** SNP-based comparative graph showing the distribution of polymorphisms between CS wheat chromosome 1B and *Ae. speltoides* chromosome 1S. Red areas refer to polymorphisms and green areas to monomorphisms. Arrow heads demarcate the highly monomorphic linkage block. (**D)** Estimated physical size of the highly monomorphic linkage block harboring the 66 SNP loci and the extended region at the distal end of 1BL. Red, green, and grey bars refer to the polymorphic, monomorphic, and extended genomic regions, respectively.

Comparative analysis of the individual B-S homoeologous pairs

Both CS wheat and CS-*Ae. speltoides* disomic substitution lines were genotyped using wheat 90K iSelect SNP arrays. Our SNP genotyping results indicated that the substitution line originally designated DS 3S(3B) (Friebe et al., 2011) should be DS 3S(3A), which was further confirmed by SSR markers and chromosome C-banding. Thus, DS 3S(3A), instead of DS 3S(3B), was included in the SNP assay in addition to the substitution lines involving other six B-genome chromosomes (1B, 2B, 4B, 5B, 6B, and 7B).

High-throughput genotyping of CS wheat and the CS-*Ae. speltoides* disomic substitution lines at 17,379 SNP loci identified a total of 6,722 SNPs polymorphic in the seven B/A-S homoeologous pairs. The homoeologous pair 2B-2S showed the lowest polymorphism (33.34%) and 7B-7S the highest (43.37%) at the SNP loci surveyed. The polymorphisms of the other five homoeologous pairs ranged from 33.89% (3A-3S) to 41.86% (4B-4S) (Figure 3.5). Plotting of the SNP polymorphisms between CS wheat chromosome 1B and *Ae. speltoides* chromosome 1S against the SNP consensus linkage map of chromosome 1B (Wang et al., 2014) identified a genomic region that shared the same alleles at 65 of the 68 SNP loci within the distal ends of CS wheat 1BL and *Ae. speltoides* 1SL (Figure 3.4C). We did not detect such a monomorphic linkage block in other chromosomal regions of the 1B-1S homoeologous pair and on other B/A-S homoeologous pairs (Figure 3.6).

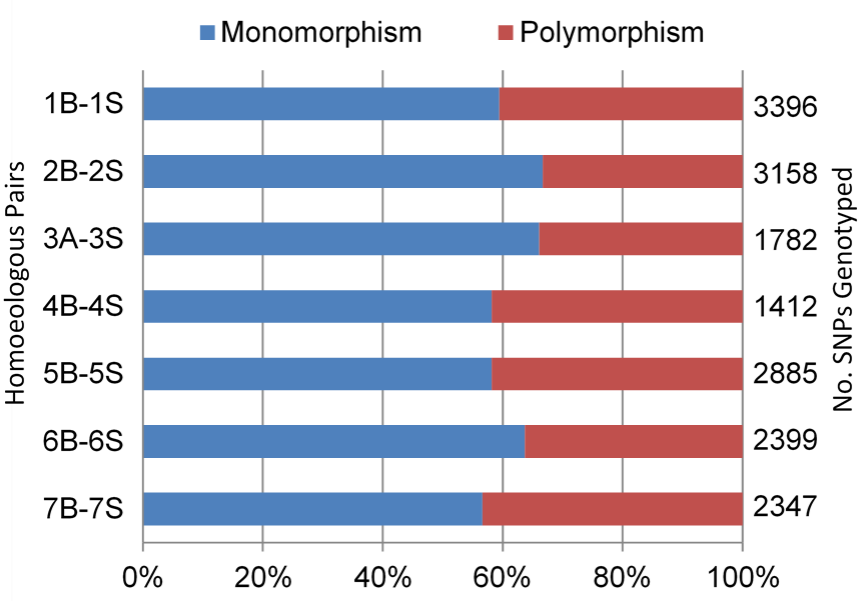

Figure 3.5. Polymorphisms of individual B/A-S homoeologous pairs at the SNP loci mapped on wheat B/A-genome chromosomes.

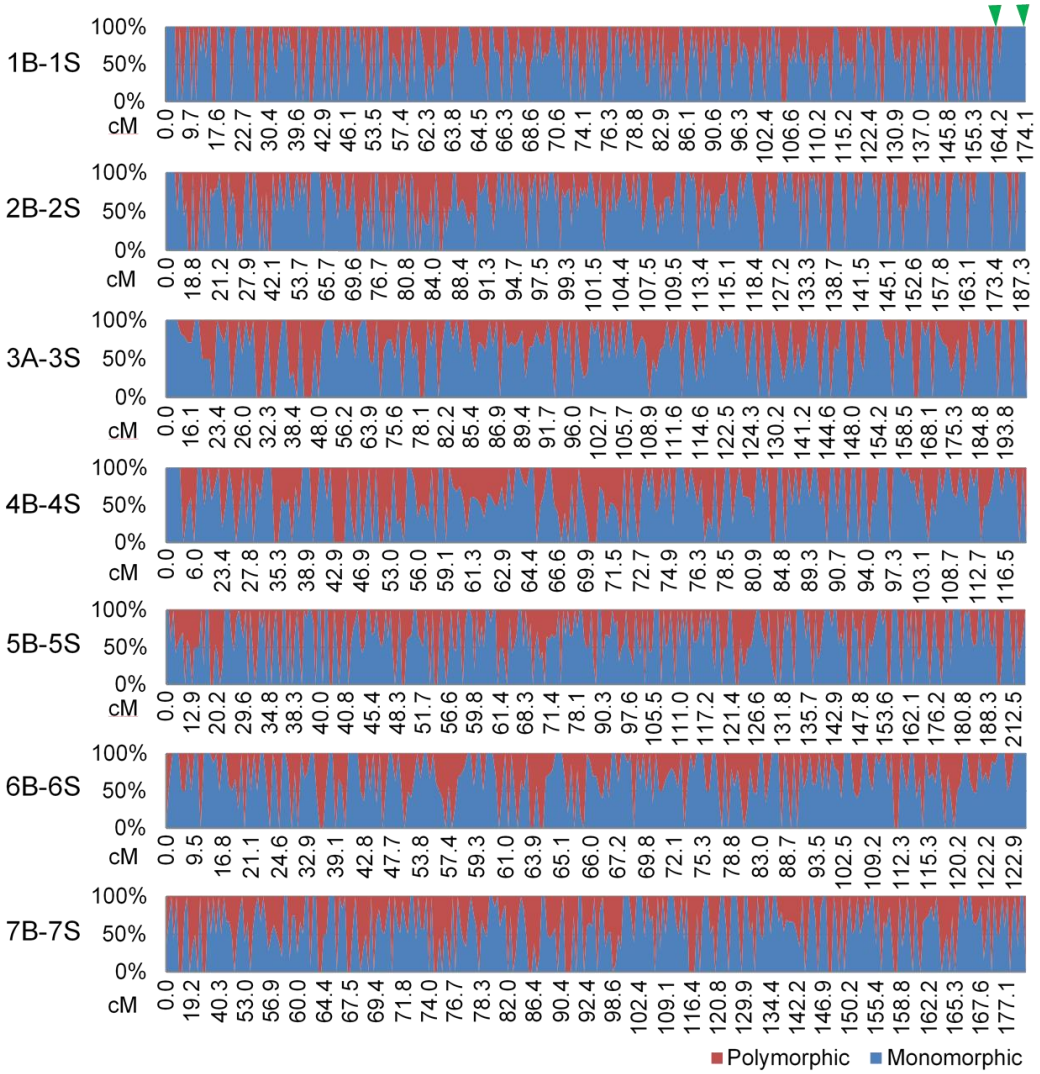

Figure 3.6. Graphical distribution of polymorphisms at the mapped SNP loci between CS wheat chromosome 1B and *Ae. speltoides* chromosome 1S. Red areas refer to polymorphisms and blue areas to monomorphisms. Green arrow heads demarcate the highly monomorphic linkage block.

Genetic and physical characterization of the 1BL distal end

The chromosomal regions at the distal ends of CS wheat 1BL and *Ae. speltoides* 1SL were found to be highly monomorphic at the 68 SNP loci (65 monomorphic/68 SNPs). The three polymorphic SNP loci within the region on 1BL and 1SL were positioned toward the proximal end of the region on the consensus linkage map (Wang et al., 2014). The entire region defined by the 68 SNPs spans a genetic distance of 12.7 cM (Figure 3.4B and APPENDIX B). The contextual sequences of these 68 SNPs were aligned to the DNA sequences of that genomic

region on 1BL available from the IWGSC RefSeq v1.0 (https://wheat-urgi.versailles.inra.fr/Seq-Repository/Assemblies). Two of the three SNP loci polymorphic between 1BL and 1SL, *Tdurum_contig41999_2908* and *Ex_c1058_1537*, were physically assigned to the proximal end of the region. The other polymorphic SNP within the region, *RFL_Contig785_1156*, was distal to the first two polymorphic SNPs. One monomorphic SNP (*RFL_Contig785_1700*) was physically positioned within the interval between *Tdurum_contig41999_2908* and *RFL_Contig785_1156* according to the sequence alignment (Figure 3.4B and APPENDIX B).

The genomic region that spans the 65 SNP loci monomorphic between CS 1BL and *Ae. speltoides* 1SL and one polymorphic SNP (*RFL_Contig785_1156*) was estimated to be 9.61 Mb in length according to the DNA sequence assemblies of 1BL (https://wheat-urgi.versailles.inra.fr/Seq-Repository/Assemblies). The two polymorphic SNP loci (*Tdurum_contig41999_2908* and *Ex_c1058_1537*) at the proximal end of that region were not included in the estimate (Figure 3.4D). In addition, we identified an extended terminal segment of 0.85 Mb distal to the 68 SNP-defined region on 1BL according to the DNA sequence alignment. As a result, the total physical length of the SNP-defined and extended distal genomic region on 1BL was estimated to be 10.46 Mb (Figure 3.4D). The actual physical size of this distal segment on 1BL might be greater than this estimate (10.46 Mb) because the current DNA sequence assemblies (https://wheat-urgi.versailles.inra.fr/Seq-Repository/Assemblies) we used in this study cover 689.9 Mb out of the total length 849 Mb of chromosome 1B (Šafář et al., 2010).

Four hexaploid wheat accessions (Cltr8347, PI429624, PI481728, and CI13113), similar to CS wheat, were found to be highly monomorphic with CS DS1S(1B) at the 68 SNP loci within the distal regions of 1BL and 1SL. They were clustered together with CS wheat and CS DS1S(1B) in the dendrogram (Figure 3.7). Cltr8347, PI429624, and PI481728 are the landraces

from China, Nepal, and Bhutan, respectively. Both CS and Cltr8347 are the landraces collected probably in southwest China (P.D. Chen, personal communication), which is geographically close to the Himalayan region where Nepal and Bhutan are located. CI13113 is a winter wheat germplasm line with CS involved in the pedigree (http://www.arsgrin.gov/npgs/). Thus, these five hexaploid wheat accessions seem to share a similar origin of this particular *Ae. speltoides*-originated genomic region on 1BL. In addition, we found that 11 tetraploid wheat accessions share the same genotypes at the 68 SNP loci on 1BL, making them clustered together in the dendrogram (Figure 3.7). These tetraploid wheat accessions originated from two primary geographical regions, the Mediterranean Basin and South America (APPENDIX A). Overall, the tetraploid wheat accessions showed higher genetic variability than hexaploids in the 68 SNP-defined genomic region on 1BL according to the cluster dendrogram and genetic diversity analysis (Figure 3.7 and 3.8). Four of the 68 SNP loci (46805, 31066, 50867, and 76928) showed no allelic variation at all in the 88 wheat accessions. The other four SNPs (71971, 65270, 71898, and 78965) had very minimal variation in the wheat accessions (APPENDIX B). Apparently, these SNP loci have been very conservative over the evolutionary process of this chromosomal region.

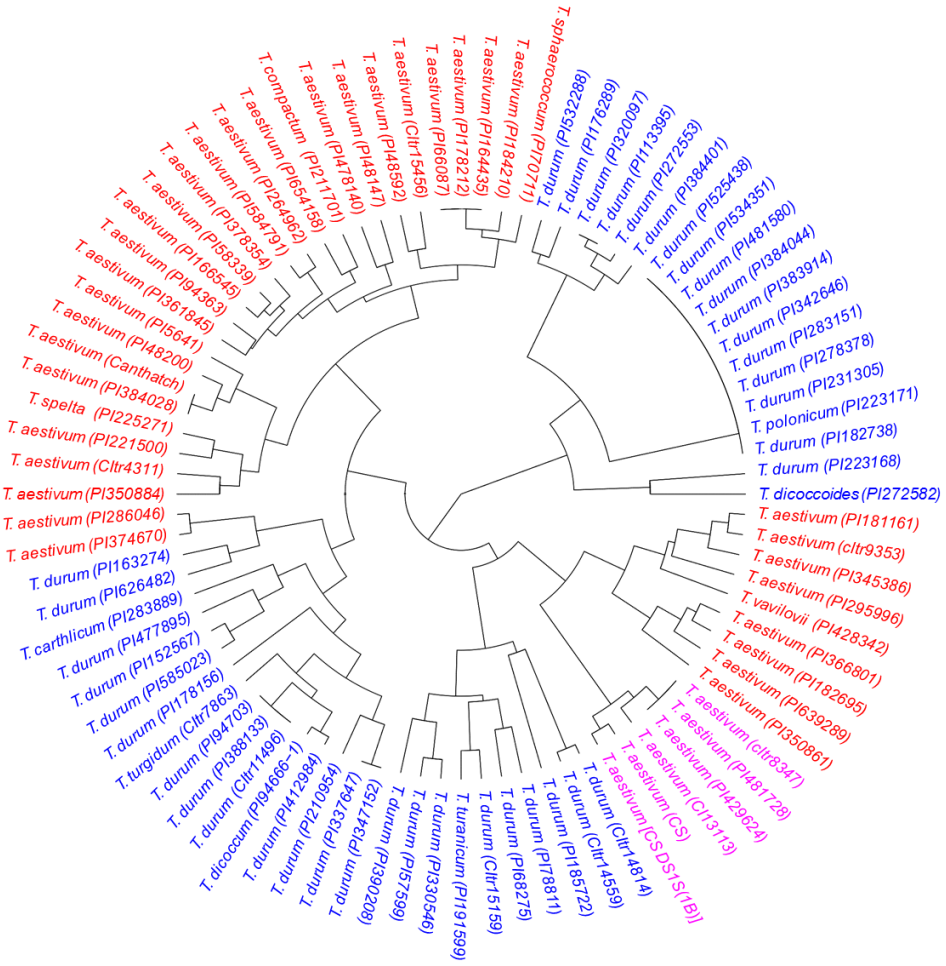

Figure 3.7. Cluster dendrogram of the 88 representative wheat species/accessions constructed based on the genotypes at the 68 SNP loci within the distal end of 1BL.

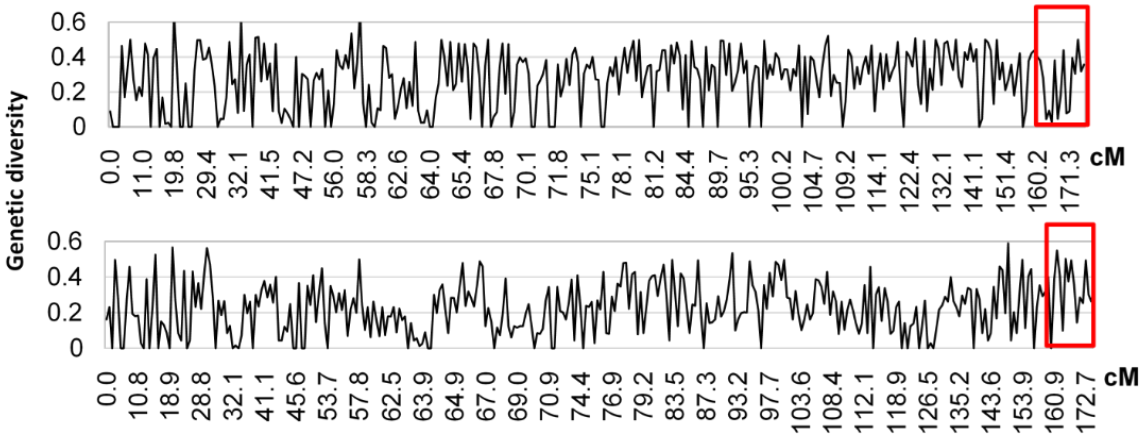

Figure 3.8. Genetic diversity at the SNP loci on chromosome 1B in 45 hexaploid wheat accessions (*top*) and 43 tetraploid wheat accessions (*bottom*). Red rectangles mark the *Ae. speltoides*-originated chromosomal region spanning the 68 SNP loci at the distal end of 1BL. Y-axis indicates genetic diversity defined as the probability of two different alleles randomly selected from the population.

Discussion

Ae. speltoides has been considered the diploid species with a genome most closely related to the wheat B genome according to the previous studies (Jenkins, 1929; Pathak, 1940; Sarkar and Stebbins, 1956; Riley et al., 1958; Dvorak and Zhang, 1990; Sasanuma et al., 1996; Wang et al., 1997; Kilian et al., 2007). However, the relationship of the *Ae. speltoides* S genome with the wheat B genome remains largely obscure. Previous meiotic pairing-based homology analyses had led to inconsistent conclusions about the evolutionary relationship of the B and S genomes due primarily to the influence of the *Ae. speltoides*-derived *Ph1* suppressors on meiotic pairing (Jenkins, 1929; Riley et al., 1958; Kimber and Athwal, 1972). In the present study, we investigated meiotic pairing individually for each of the B/A-S homoeologous pairs in the presence as well as absence of *Ph1*. This allowed us to monitor the effect of *Ph1* and *Ph1* suppressors in meiotic homoeologous pairing and to precisely assess the homology for the individual B/A-S homoeologous pairs.

Substantial meiotic pairing was observed between CS wheat chromosome 1B and *Ae. speltoides* chromosome 1S in the presence of *Ph1* and absence of other S-genome chromosomes. The 1B-1S pairing frequency (50.00%) was significantly higher than any other B/A-S homoeologous pairs (0.00-8.63%). Chromosome 1S does not contain a *Ph1* suppressor gene (Dvorak et al., 2006). Therefore, no *Ph1* suppressor was involved in the 1B-1S meiotic pairing analysis. It was homology that made CS wheat chromosome 1B pair with *Ae. speltoides* chromosome 1S in a relatively high frequency. A small *Ae. speltoides*-derived chromosomal segment was detected at the distal end of CS wheat 1BL by GISH. Also, we found that 1B-1S meiotic pairing occurred mostly on the long arms (i.e. 1BL-1SL) that share the *Ae. speltoides* segment at the distal ends. Therefore, this *Ae. speltoides*-derived segment was the homologous

counterpart on chromosomes 1B and 1S that initiated high meiotic pairing between them. Extremely low meiotic pairing (0 out of 105 PMCs) was observed between CS wheat chromosome 1B and *Th. elongatum* chromosome 1E in the presence of *Ph1*. Also, a *Th. elongatum*-specific segment was not detected on 1B and other B-genome chromosomes of CS wheat by GISH. As a control, these findings further confirmed the *Ae. speltoides* origin of the distal 1BL region in CS wheat.

We detected the *Ae. speltoides*-originated chromosomal segment at the distal end of 1BL in a diverse worldwide collection of tetraploid (including wild and cultivated emmer wheat) and hexaploid wheat (n=179) in addition to CS wheat. Apparently, this *Ae. speltoides*-originated segment on 1BL has been part of the B genome in both tetraploid and hexaploid wheat species probably since the initial incorporation of the B genome into tetraploid wheat. Also, we found that tetraploid wheat had higher genetic diversity than hexaploid wheat within the *Ae. speltoides*-originated genomic region on 1BL, suggesting an evolutionary pattern similar to other genomic regions of polyploid wheat (Doebley et al., 2006). All these new findings consistently support the conclusion that *Ae. speltoides* had been involved in the origin of the wheat B genome. The *Ae. speltoides*-originated chromosomal segment on wheat chromosome 1BL has been retained in the B genome probably throughout the entire evolutionary and domestication process of polyploid wheat.

High-throughput SNP genotyping of individual B/A-S homoeologous pairs and the 88 representative wheat species/accessions identified a sizable highly monomorphic linkage block (12.7 cM) at the distal ends of wheat 1BL and *Ae. speltoides* 1SL. This was surprisingly consistent with the meiotic pairing and GISH results, supporting the *Ae. speltoides* origin of the distal segment on 1BL. The SNP-defined monomorphic genomic region and extended distal end

on 1BL was estimated to be 10.46 Mb in physical size based on the genomic DNA sequence assemblies of chromosome 1B currently available from IWGSC RefSeq v1.0 (https://wheat-urgi.versailles.inra.fr/). This estimate is about 1.2% of the total length of chromosome 1B (849 Mb) (Šafář et al., 2010). The GISH-detected *Ae. speltoides* segment on 1BL appears to span more than 2.0% of the cytogenetic length of chromosome 1B. In addition, the DNA sequence assemblies of the IWGSC RefSeq v1.0 cover approximately 81.3% of the entire chromosome 1B (689.9 Mb out of 849 Mb) (Šafář et al., 2010). Thus, the monomorphic linkage block is probably a portion of the *Ae. speltoides*-originated chromosomal segment on 1BL. The actual physical size of the *Ae. speltoides*-originated distal segment on 1BL might be greater than the estimate of 10.46 Mb.

Relatively low meiotic pairing was observed with each of other B/A-S homoeologous pairs in the presence of *Ph1*. In addition, we did not detect any *Ae. speltoides*-originated chromosomal segments in the other regions of chromosome 1B and on other B-genome chromosomes by GISH. Are there additional *Ae. speltoides*-originated chromosomal segments that are too small to leverage meiotic pairing and undetectable by GISH in the wheat B genome? We observed small monomorphic linkage blocks at multiple locations in other regions of chromosome 1B and on other B-genome chromosomes, but none was comparable in size to the one at the distal end of 1BL. Also, a clear association of those monomorphic linkage blocks with meiotic pairing could not be established in this study. Thus, we were unable to determine whether those B-genome chromosomal regions originated from *Ae. speltoides*. Further studies, such as genome-wide sequence comparative analysis, are needed to uncover the evolutionary relationship of those genomic regions with *Ae. speltoides*.

In summary, we conclude that *Ae. speltoides* had been involved in the origin and evolution of the wheat B genome. The current form of *Ae. speltoides* should not be considered an exclusive donor of the B genome. *Ae. speltoides* is probably one of the diploid ancestors involved in the evolutionary lineage of the B genome as stated in the theory of polyphyletic origin (Zohary and Feldman, 1962). The wheat B genome might be a genome reconstructed from the homoeologous meiotic recombination between multiple ancestral genomes of *Aegilops* species, including *Ae. speltoides*. Further studies of *Aegilops* species, especially those in the Sitopsis section, may reveal additional insights into the origin and evolution of the wheat B genome.

References

Blake NK, Lehfeldt BR, Lavin M, Talbert LE (1999) Phylogenetic reconstruction based on low copy DNA sequence data in an allopoyploid: The B genome of wheat. Genome 42:351–360

Cai X, Jones S (1997) Direct evidence for high level of autosyndetic pairing in hybrids of *Thinopyrum intermedium* and *Th. ponticum* with *Triticum aestivum*. Theor Appl Genet 95:568–572

Cai X, Jones S, Murray T (1998) Molecular cytogenetic characterization of *Thinopyrum* and wheat–*Thinopyrum* translocated chromosomes in a wheat *Thinopyrum* amphiploid. Chromosome Res 6:183–189

Chao S, Sharp PJ, Worland AJ, Koebner RMD, Gale MD (1989) RFLP-based genetic maps of homoeologous group 7 chromosomes. Theor Appl Genet 78:495–504

Chen X, Faris JD, Hu J, Stack RW, Adhikari T, Elias EM, Kianian SF, Cai X (2007) Saturation and comparative mapping of a major Fusarium head blight resistance QTL in tetraploid wheat. Mol Breed 19:113–124

Dobrovolskaya O., Boeuf C, Salse J, Pont C, Sourdille P, Bernard M, Salina, E (2011) Microsatellite mapping of *Ae. speltoides* and map-based comparative analysis of the S, G, and B genomes of Triticeae species. Theor Appl Genet 123:1145–1157

Doebley JF, Gaut BS, Smith BD (2006) The molecular genetics of crop domestication. Cell 127:1309–1321

Dvorak J (1972) Genetic variability in *Aegilops speltoides* affecting homoeologous pairing in wheat. Can J Genet Cytol 14:371–380

Dvorak J, Zhang HB (1990) Variation in repeated nucleotide sequences sheds light on the phylogeny of the wheat B and G genomes. Proc Natl Acad Sci USA 87:9640–9644

Dvorak J, Diterlizzi P, Zhang HB, Resta P (1993) The Evolution of polyploid wheats – identification of the A–genome donor species. Genome 36:21–31

Dvorak J, Deal KR, Luo MC (2006) Discovery and mapping of wheat *Ph1* suppressors. Genetics 174:17–27

Felsenburg T, Levy AA, Galili G, Feldman M (1991) Polymorphism of high molecular weight glutenins in wild tetraploid wheat: spatial and temporal variation in a native site. Isr J Bot 40:451–479

Friebe B, Qi L, Liu C, Gill B (2011) Genetic compensation abilities of *Aegilops speltoides* chromosomes for homoeologous B-genome chromosomes of polyploid wheat in disomic S(B) chromosome substitution lines. Cytogenet Genome Res 134:144–150

Gerlach WL, Bedbrook JR (1979) Cloning and characterization of ribosomal RNA genes from wheat and barley. Nucleic Acids Res 7:1869–1885

Gill BS, Kimber G (1974) Giemsa C–banding and the evolution of wheat. Proc Natl Acad Sci USA 71:4086–4090

Griffiths S, Sharp R, Foote TN, Bertin I, Wanous M, Reader S, Colas I, Moore G (2006) Molecular characterization of *Ph1* as a major chromosome pairing locus in polyploid wheat. Nature 439:749–752

Huang S, Sirikhachornkit A, Su X, Faris J, Gill B, Haselkorn R, Gornicki P (2002) Genes encoding plastid acetyl-CoA carboxylase and 3-phosphoglycerate kinase of the *Triticum/Aegilops* complex and the evolutionary history of polyploid wheat. Proc Natl Acad Sci USA 99:8133–8138

Jenkins JA (1929) Chromosome homologies in wheat and *Aegilops*. Am J Bot 16:238–245

Johnson BL (1972) Protein electrophoretic profiles and the origin of the B genome of wheat. Proc Natl Acad Sci USA 69:1398–1402

Kapustin Y, Souvorov A, Tatusova T, Lipman D (2008) Splign: algorithms for computing spliced alignments with identification of paralogs. Biol Direct 3:20

Kihara H (1919) Ueber cytologische Studien bei einigen Getreidearten. Spezies-Bastarde des Weizen und Weizenroggen-Bastard. Bot Mag 33:17–38

Kihara H (1944) Discovery of the DD-analyser, one of the ancestors of vulgare wheat. Agric Hortic 19:889–890

Kihara H (1954) Considerations on the evolution and distribution of A*egilops* species based on the analyzer-method. Cytologia 19:336–357

Kihara H, Yamashita K, Tanaka M (1959) Genomes of 6x species of *Aegilops*. Wheat Inf Serv 8:3–5

Kilian B, Özkan H, Deusch O, Effgen S, Brandolini A, Kohl J, Martin W, Salamini F (2007) Independent wheat B and G genome origins in outcrossing *Aegilops* progenitor haplotypes. Mol Biol Evol 24: 217–227

Kimber G, Athwal RS (1972) A reassessment of the course of evolution in wheat. Proc Natl Acad Sci USA 69:912–915

Liu Z, Yue W, Dong YS, Zhang XY (2006) Identification and preliminary analysis of several centromere-associated bacterial artificial chromosome clones from a diploid wheat library. J Integr Plant Biol 48:348–358

McFadden ES, Sears ER (1946) The origin of *Triticum speltoides* and its free-threshing hexaploid relatives. J Hered 37:107–116

Milne I, Shaw P, Stephen G, Bayer M, Cardle L, Thomas WTB, Flavell AJ, Marshall D (2010) Flapjack – graphical genotype visualization. Bioinformatics 26:3133–3134

Nei M (1973) Analysis of gene diversity in subdivided populations. Proc Natl Acad Sci USA 70, 3321–3323

Niu Z, Klindworth DL, Friesen TL, Chao S, Jin Y, Cai X, Xu SS (2011) Targeted introgression of a wheat stem rust resistance gene by DNA marker-assisted chromosome engineering. Genetics 187:1011–1021

Ogihara T, Tsunewaki K (1988) Diversity and evolution of chloroplast DNA in *Triticum* and *Aegilops* as revealed by restriction fragment analysis. Theor Appl Genet 76, 321–332

Pathak GN (1940) Studies in the cytology of cereals. J Genet 39:437–467

Pestsova E, Ganal M, Roder M (2000) Isolation and mapping of microsatellite markers specific for the D genome of bread wheat. Genome 43:689–697

Petersen G, Seberg O, Yde M, Berthelsen K (2006) Phylogenetic relationships of *Triticum* and *Aegilops* and evidence for the origin of the A, B, and D genomes of common wheat (*Triticum aestivum).* Mol Phylogenet Evol 39:70–82

Riley R, Unrau J, Chapman V (1958) Evidence on the origin of the B genome of wheat. J Hered 49:90–98

Riley R, Kimber G, Chapman V (1961) Origin of genetic control of diploid-like behavior of polyploid wheat. J Hered 52:22–25

Röder MS, Korzun V, Wendehake K, Plaschke J, Tixier MH, Leroy P, Ganal, MW (1998) A microsatellite map of wheat. Genetics 149:2007–2023

Roberts MA, Reader SM, Dalgliesh C, Miller TE, Foote TN, Fish LJ, Snape JW, Moore G (1999) Induction and characterization of *Ph1* wheat mutants. Genetics 153:1909–1918

Šafář J, Šimková H, Kubaláková M, Číhalíková J, Suchánková P, Bartoš J, Doležel J (2010) Development of chromosome-specific BAC resources for genomics of bread wheat. Cytogenet Genome Res 129:211–223

Sakamura T (1918) Kurze Mitteilung über die Chromosomenzahlen und die Verwandtschaftsverhältnisse der *Triticum*-Arten. Bot Mag 32:150–153

Salse J, Chague V, Bolot S, Magdelenat G, Huneau C, Pont C, Belcram H, Couloux A, Gardais S, Evrard A, Segurens B, Charles M, Ravel C, Samain S, Charmet G, Boudet N, Chalhoub B (2008) New insights into the origin of the B genome of hexaploid wheat: evolutionary relationships at the SPA genomic region with the S genome of the diploid relative *Aegilops speltoides*. BMC Genomics 9:555

Sarkar P, Stebbins GL (1956) Morphological evidence concerning the origin of the B genome in wheat. Am J Bot 43:297–304

Sasanuma T, Miyashita NT, Tsunewaki K (1996) Wheat phylogeny determined by RFLP analysis of nuclear DNA. 3. Intra- and interspecific variations of five *Aegilops* Sitopsis species. Theor Appl Genet 92:928–934

Sax K (1922) Sterility in wheat hybrids. II. Chromosome behavior in partially sterile hybrids. Genetics 7:513–552

Siedler H, Messmer MM, Schachermayr GM, Winzeler H, Winzeler M, Keller B (1994) Genetic diversity in European wheat and spelt breeding material based on RFLP data. Theor Appl Genet 88:994–1003

Somers D, Isaac P, Edwards K (2004) A high-density microsatellite consensus map for bread wheat (*Triticum aestivum* L.). Theor Appl Genet 109:1105–1114

Sourdille P, Gandon B, Chiquet V, Nicot N, Somers D, Murigneux A, Bernard M (2004) Wheat genoplante SSR mapping data release: a new set of markers and comprehensive genetic and physical mapping data. http://wheat.pw.usda.gov/ggpages/SSRclub/GeneticPhysical/

Wang GZ, Miyashita NT, Tsunewaki K (1997) Plasmon analyses of Triticum (wheat) and Aegilops: PCR–single–strand conformational polymorphism (PCR–SSCP) analyses of organellar DNAs. Proc Natl Acad Sci USA 94:14570–14577

Wang S, Wong D, Forrest K, Allen A, Huang BE, Maccaferri M, Salvi S, Milner SG, Cattivelli L, Mastrangelo AM, Whan A, Stephen S, Barker G, Wieseke R, Plieske J, International Wheat Genome Sequencing Consortium, Lillemo M, Mather D, Appels R, Dolferus R, Brown–Guedira G, Korol A, Akhunova AR, Feuillet C, Salse J, Morgante M, Pozniak C, Luo MC, Dvorak J, Morell M, Dubcovsky J, Ganal M, Tuberosa R, Lawley C, Mikoulitch I, Cavanagh C, Edwards KJ, Hayden M, Akhunov E (2014) Characterization of polyploid wheat genomic diversity using a high–density 90,000 single nucleotide polymorphism array. Plant Biotechnol J 12:787–796

Zohary D, Feldman M (1962) Hybridization between amphidiploids and the evolution of polyploids in the wheat (*Aegilops–Triticum*) group. Evolution 16:44–61

CHAPTER 4. MEIOTIC HOMOEOLOGOUS RECOMBINATION-BASED CHROMOSOME ENGINEERING IN THE GENOMICS ERA OF WHEAT

Abstract

Wheat, a major food crop worldwide, is an allopolyploid originated from spontaneous hybridization of three diploid species. The nature of origin and evolution had led to a narrow genetic basis in wheat. However, wheat has numerous wild relatives usable for expanding the genetic variability of its genome by inducing meiotic homoeologous recombination. Traditionally, laborious cytological analyses have been employed to detect homoeologous recombination. This has limited the progress of alien gene introgression in wheat improvement. In this study, the genotypes homozygous for *ph1b* and double monosomic for wheat chromosome 2B and its homoeologue 2S in *Aegilops speltoides* or 2E in *Thinopyrum elongatum* were constructed to enhance 2B-2S and 2B-2E meiotic pairing and recombination. Backcross populations were developed to recover the recombination events. Multiple techniques, including fluorescent genomic *in situ* hybridization (GISH), wheat 90K SNP assay, and SNP-derived STARP markers were employed to detect and delineate the 2B-2S and 2B-2E recombinants. Totally, 112 2B-2S and 87 2B-2E recombinant lines were developed in this study. Evidently, this integrated GISH and high-throughput genotyping approach enhances the recovery and detection of meiotic homoeologous recombination. The SNP marker-assisted chromosome engineering strategy developed in this study will boost the utilization of alien genes in wheat improvement.

Introduction

Wheat is one of the major food crops in the US and worldwide. However, wheat production has been continually challenged by various threats and pressures, such as climate variability and change, new disease pathogens and pests, and a constantly growing food demand.

There is a constant need to strengthen the defense of wheat against various new threats and improve wheat production. The genetic gain for wheat production has declined, due primarily to the draining of the gene pool usable in wheat breeding (Graybosch and Peterson, 2010). The limited genetic variability of the wheat genome has increasingly become a bottleneck for wheat improvement. There is an urgent need to enrich the gene pool of wheat and expand genetic variability of the wheat genome.

Common wheat (*Triticum aestivum*, 2n=6x=42, genome AABBDD) is an allohexaploid with three distinct, but genetically related subgenomes (i.e. A, B, and D). Homoeologous chromosomes in the three subgenomes can genetically compensate for each other. The genomic nature of allohexaploidy makes common wheat tolerate various chromosome modifications, providing tremendous genetic flexibility for wheat improvement by chromosome manipulation (Morris and Sears, 1967). Over the years, a variety of studies have demonstrated that the wheat genome can be artificially reshaped and enriched in terms of genomic structure and gene content through chromosome engineering (Sears, 1972, 1983; Zeller, 1973; Zeller and Hsam, 1983; Shepherd and Islam, 1988; Gale and Miller, 1987; Friebe et al., 1996; Cox, 1998; Xu et al., 2005; Qi et al., 2007, 2008; Niu et al., 2011; Klindworth et al., 2012; McArthur et al., 2012).

Chromosome engineering is the process of modifying ploidy, chromosome structure, and/or chromosome number of an organism for the purpose of genetic improvement. This technology has been used to incorporate favorable genes from wild species into the wheat genome for germplasm and variety development. Alien genes can be introduced into wheat from wild species through chromosome addition, substitution, and translocation. Alien chromosome addition and substitution, which introduce one or more entire alien chromosomes into the wheat genome, usually contain desirable genes as well as undesirable genes on the alien chromosomes.

It is generally difficult to utilize those lines directly in wheat breeding. Chromosome translocation, which can integrate alien chromosome segments containing the gene of interest into the wheat genome, has been the most effective approach for alien gene introgression (Sears, 1983; Jiang et al., 1994; Friebe et al., 1996; Cai et al., 2005; Chen et al., 2005; Xu et al., 2005; Kuraparthy et al., 2007; Faris et al., 2008; Niu et al., 2011; Klindworth et al., 2012). Small compensating wheat-alien chromosome translocations are less likely to contain undesirable genes and are more breeder-friendly for variety development than alien chromosome addition and substitution lines (Sears, 1972, 1983; Zeller, 1973; Zeller and Hsam, 1983; Shepherd and Islam, 1988; Friebe et al., 1996; Qi et al., 2007, 2008; Niu et al., 2011; Klindworth et al., 2012). The compensating translocations generally result from meiotic recombination between wheat chromosomes and their homoeologous counterparts from wild species.

The *Ph1* gene on wheat chromosome 5B limits meiotic pairing/recombination to homologous chromosomes and prevents homoeologous chromosomes from pairing/recombination to each other (Riley and Chapman, 1958). It ensures the integrity of the wheat genome, but also limits the introduction of genetic variability from wild species into wheat by meiotic homoeologous recombination. Genetic stocks involving the *ph1* mutant, *Ph1* inhibitor gene, chromosome 5D(5B) substitution in durum wheat, and chromosome 5D(5B) nulli-tetrasomics in bread wheat have been used to inactivate *Ph1* activity and promote meiotic pairing/recombination between homoeologous chromosomes for alien gene introgression in wheat (Riley et al., 1959; Chapman and Riley, 1970; Chen et al., 1994; Qi et al., 2007 and 2008; Niu et al., 2011; Klindworth et al., 2012). Out of these genetic stocks, the *ph1b* mutant resulting from a large deletion on the long arm of chromosome 5B (5BL) (Sears, 1977; Gill et al., 1993)

has been widely utilized to induce meiotic homoeologous pairing/recombination for alien gene introgression in wheat.

Meiotic homoeologous pairing/recombination can be enhanced by inactivating *Ph1* activity, but usually remains at a low frequency. Thus, a large recombination population is generally required to recover the homoeologous recombinants of interest. Screening such a large recombination population for the recombinants of interest is always a challenge for any cytological techniques, including genomic *in situ* hybridization (GISH). Recent advances in genomics, especially high-throughput genotyping technologies, have opened new opportunities to improve the efficacy of homoeologous recombinant production and alien gene introgression (King et al., 2017; Klindworth et al., 2017). This study aimed to develop an effective procedure of inducing, recovering, and detecting meiotic homoeologous recombination for alien gene introgression using the genomics tools and resources currently available in wheat.

Materials and methods

Plant materials

Chinese Spring (CS) wheat-*Aegilops speltoides* (2n=2x=14, genome SS) disomic substitution line 2S(2B) [DS 2S(2B)] (Friebe et al., 2011) and CS *ph1b* mutant were supplied by the Wheat Genetics Resource Center at Kansas State University. The CS-*Thinopyrum elongatum* (2n=2x=14, genome EE) disomic substitution line 2E(2B) [DS 2E(2B)] was provided by J. Dvorak at UC Davis.

Fluorescent genomic *in situ* hybridization (GISH)

Root tips at about 2 cM long and anthers with the meiocytes at metaphase I and anaphase I were collected and fixed in acetic-acid alcohol (1:3). Chromosome preparation and GISH were performed as described by Cai et al. (1998). The total genomic DNA of *Ae. speltoides* and *Th.*

elongatum were used as probe DNA and labeled with biotin-16-dUTP by nick translation. The genomic DNA of CS wheat was used as blocking DNA. It was prepared by shearing CS total genomic DNA in 0.4 M NaOH in boiling water for 40 to 50 min. Hybridization signals were detected with fluorescein isothiocyanate-conjugated avidin (FITC-avidin) and wheat chromatin was counter-stained with 4'-6-Diamidino- 2-phenylindole (DAPI). *Ae. speltoides/Th. elongatum* chromatin (painted yellow-green) and wheat chromatin (painted red) were differentiated from each other under a fluorescence microscope (BX51, Olympus).

Molecular marker analyses

Simple sequence repeat (SSR) and sequence-tagged site (STS): Two STS markers (*PSR128* and *PSR574*) that tag *Ph1* allele were used to identify individuals homozygous for *ph1b* deletion (Roberts et al., 1999). The chromosome 3A-specific STS marker *Xwgc1079* (unpublished, X. Cai et al.) was employed as an internal control for the PCR of *PSR128* and *PSR574* that had no amplicon with *ph1b* deletion. Two chromosome-specific SSR markers, *Xwmc474* and *Xgwm455*, were used to identify *Ae. speltoides* chromosome 2S and *Th. elongatum* chromosome 2E, respectively. DNA extraction was performed as described by Niu et al. (2011). PCR was run at an annealing temperature required by the markers. PCR products were separated in a non-denatured polyacrylamide gel system (Chen et al., 2007).

Single nucleotide polymorphism (SNP): Wheat 90K SNP genotyping assay was performed on the Illumina BeadStation and iScan instruments according to the manufacturer's protocols (Illumina). SNP allele clustering and genotype calling were done using the GenomeStudio v2011.1 software (Illumina) as described by Wang et al. (2014).

Semi-Thermal Asymmetric Reverse PCR (STARP): Wheat SNPs mapped within the critical chromosome regions were converted to STARP markers following the procedure of Long

et al. (2017) and Qi et al. (2015). Three primers were designed from the contextual sequence of a target SNP, including two-tailed forward allele-specific primers (AS-primers F1 and F2) and one common reverse primer. Two universal priming-element-adjustable primers (PEA1 and PEA2) attached with the fluorescence tag FAM and HEX at 5′ terminus, respectively, were used to run PCR. An additional 4-base oligonucleotide (5′-AGAG-3′) was inserted in PEA2 to produce length polymorphism between two alleles after amplification. PCR was run in 10 µl of volume containing 1× NH_4^+ buffer [10 × NH_4^+ buffer containing 160 mM $(NH_4)_2SO_4$], 670 mM Tris-HCl (pH 8.3), 0.8 M Betaine (Sigma-Aldrich, MO, USA), 0.04% BSA, 1.5 mM $MgCl_2$, 50 µM each dNTP, 200 nM common reverse primer, 200 nM for each of the PEA primers, and 40 nM for each of the AS primers, 1 U of *Taq* polymerase, and 20 ng of genomic DNA. Thermal cycling was set with initial denaturation at 94 °C for 3 minutes, followed by 6 cycles of 2-step touchdown PCR (94 °C for 20 seconds, 56 °C for 2 min, decreasing 1 °C per cycle). After that, additional 36 cycles of 2-step PCR (94 °C for 20 seconds, 62 °C for 30 seconds) were run. Finally, PCR was completed with 2-min extension at 62 °C. The fluorescence intensity of PCR products incorporated into dual-labeled PEA primers was measured in CFX384TM Real-Time PCR machine at 33 °C. For size separation of the PCR products, both PEA primers were labeled with IRDye® 700 fluorophore at 5′ end. The PCR products were diluted 30 times and sorted in an IR2 4300/4200 DNA Analyzer with denaturing polyacrylamide gel electrophoresis (LI-COR, Lincoln, NE, USA).

Results

Induction and recovery of meiotic homoeologous recombination

The disomic CS wheat-*Ae. speltoides* and CS wheat-*Th. elongatum* substitution lines DS 2S(2B) and DS 2E(2B) were verified by GISH (Figure 4.1). The verified DS 2S(2B) and DS 2E(2B) were used as the source materials of *Ae. speltoides* chromosome 2S and *Th. elongatum* chromosome 2E in this study. These two alien chromosomes under group 2 were introduced into the CS wheat background without *Ph1* (i.e. *ph1bph1b*) as a double-monosomic condition, i.e. 2S+2B and 2E+2B, respectively. This was done by crossing and backcrossing each of these two substitution lines [DS 2S(2B) and DS 2E(2B)] with CS *ph1b* mutant (*ph1bph1b*) to develop a BC_1F_1 population segregating for *Ph1*/*ph1b* as well as chromosome 2B/2S or 2B/2E (Figure 4.2).

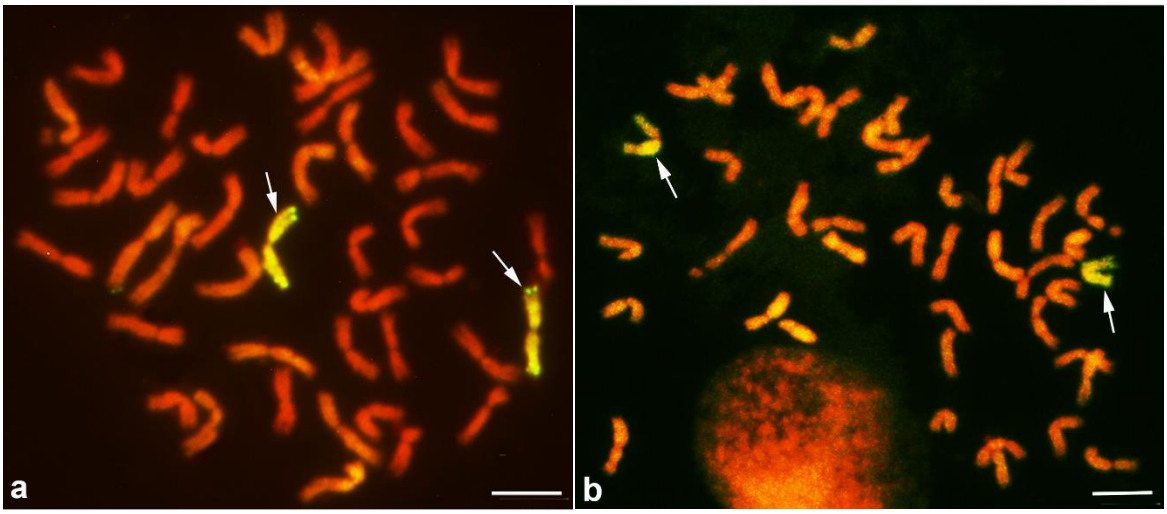

Figure 4.1. GISH patterns of mitotic chromosomes in (a) DS 2S(2B) and (b) DS 2E(2B). *Ae. speltoides* chromosome 2S and *Th. elongatum* chromosome 2E were painted in yellow-green and wheat chromosomes in red. Arrows point to chromosome 2S and 2E, respectively. Scale bar =10 μm.

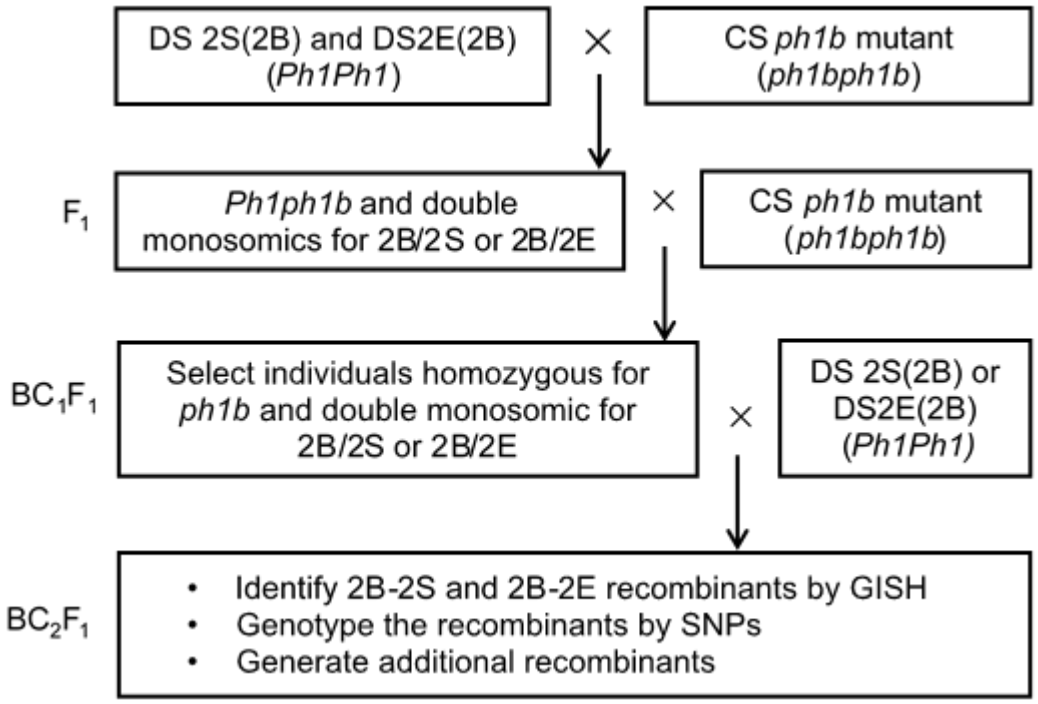

Figure 4.2. Scheme for hybridization procedure to produce meiotic homoeologous recombinants. CS: Chinese Spring; DS 2S(2B): CS wheat -*Ae*. *speltoides* disomic substitution line 2S(2B); DS 2E(2B): CS-*Th. elongatum* disomic substitution line 2E(2B).

Approximately 25% individuals in each of the BC_1F_1 populations were expected to be homozygous for *ph1b* and monosomic for 2B/2S or 2B/2E (i.e. *ph1bph1b*+2B+2S or *ph1bph1b*+2B+2E) if the gametes with different genotypes and chromosome constitutions had an equal transmission rate. A total of 74 individuals from the 2B/2S BC_1F_1 population and 97 from the 2B/2E population were screened for the *ph1b* homozygotes using the *Ph1*-specific molecular marker *PSR128* or *PSR574* (Roberts et al., 1999). Thirty-nine individuals homozygous for *ph1b* were selected from the 2B/2S population and 43 from the 2B/2E population. Meanwhile, we identified a co-dominant SSR marker (*Xwmc474*) specific for the 2B-2S homoeologous pair and another one (*Xgwm455*) for 2B-2E. The selected *ph1b* homozygotes were further screened for 2B/2S and 2B/2E double monosomics using these two chromosome-specific markers (i.e. *Xwmc474* and *Xgwm455*). Nine 2B/2S and sixteen 2B/2E double monosomic individuals were

selected from the *ph1b* homozygotes using *Xwmc474* and *Xgwm455*, respectively, as illustrated in Figure 4.3. Segregation of the homoeologous pair 2B-2E fitted in a 1:1 segregation ratio, while 2B-2S did not. Overall, chromosome 2B had a higher transmission rate than chromosome 2E and 2S (Table 4.1). The 2B/2S and 2B/2E double monosomics were further confirmed by GISH of meiotic chromosomes. Meiotic homoeologous pairing was observed between chromosomes 2B and 2S and between 2B and 2E in the homozygous *ph1b* background (Figure 4.4).

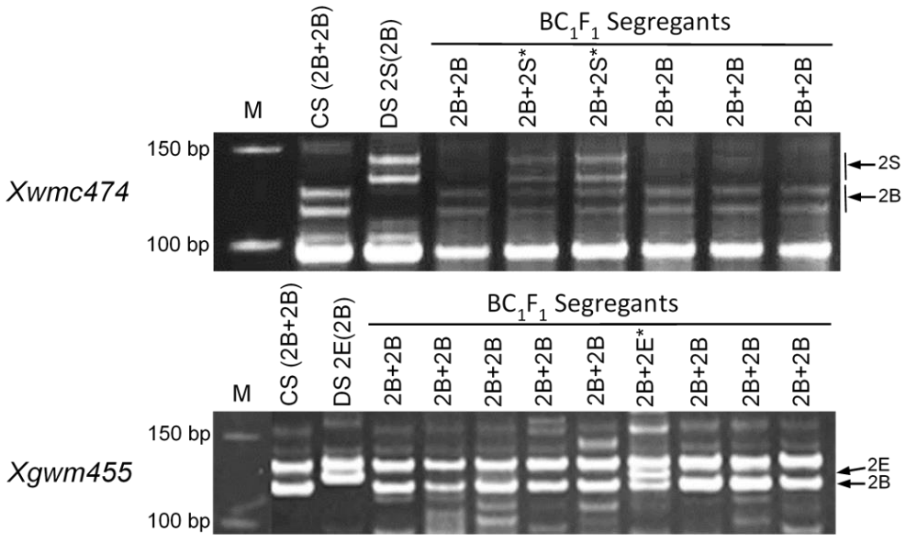

Figure 4.3. Selection of the double monosomics 2B/2S by the SSR marker *Xwmc474* (top) and the double monosomics 2B/2E by the SSR marker *Xgwm455* (bottom). "M" refers to size marker and "*" indicates the double monosomic individuals selected.

Table 4.1. Segregation of 2B-2S and 2B-2S homoeologous pairs in the BC_1F_1 populations

Homoeologous group	No. of BC_1F_1 plants screened	*ph1bph1b*			
		2B+2B	2B+2S or 2B+2E	$\chi 2$ (1:1)	Probability
2S-2B	74	30	9	11.31	0.001
2E-2B	97	27	16	2.81	0.093

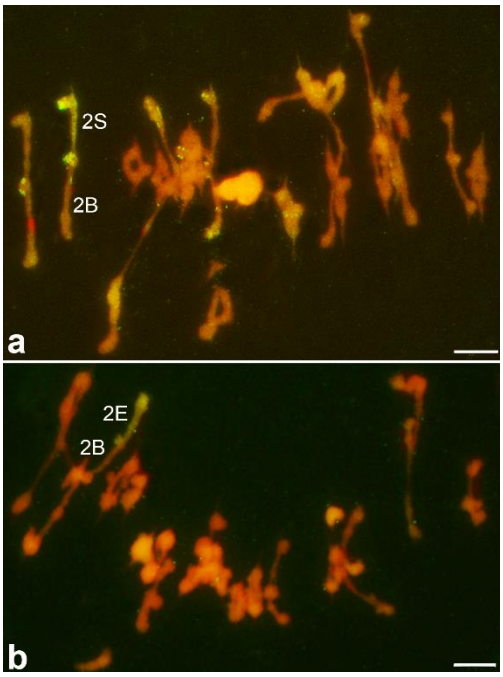

Figure 4.4. Fluorescent genomic *in situ* hybridization (GISH) patterns of meiotic chromosomes showing 2B–2S and 2B–2E homoeologous pairing (rod bivalent). (**a**) the BC_1F_1 individual heterozygous for chromosomes 2B/2S and homozygous for *ph1b*, and (**b**) the BC_1F_1 individual heterozygous for chromosomes 2B/2E and homozygous for *ph1b*. *Ae. speltoides* chromosome 2S and *Th. elongatum* chromosome 2E were painted in yellow-green and wheat chromosomes in red. Scale bar =10 μm

Preliminary screening and genotyping of recombinants

The plants identified as homozygous for *ph1b* and monosomic for 2B/2S or 2B/2E were crossed with their respective substitution line DS 2S(2B) or DS 2E(2B) to recover the gametes that contained 2B-2S or 2B-2E recombinant chromosomes. From those crosses, two large BC_2F_1 populations (n>1,000) was constructed to recover the recombinants for each of these two homoeologous pairs (Figure 4.2). As expected, each of these two populations contained two major classes of individuals according to their compositions for chromosome 2B, 2S, and 2E. One class contained a 2B-2S or 2B-2E recombinant chromosome in addition to a complete chromosome 2S or 2E from the substitution line parent. The other class contained non-recombinant chromosomes with three different chromosome combinations in each population, including 2B+2B, 2B+2S, and 2S+2S for the 2B/2S population and 2B+2B, 2B+2E, and 2E+2E

for the 2B/2E population. We performed a preliminary screening of these two populations by GISH to select 2B-2S and 2B-2E recombinants for investigating molecular marker-assisted detection of homoeologous recombination.

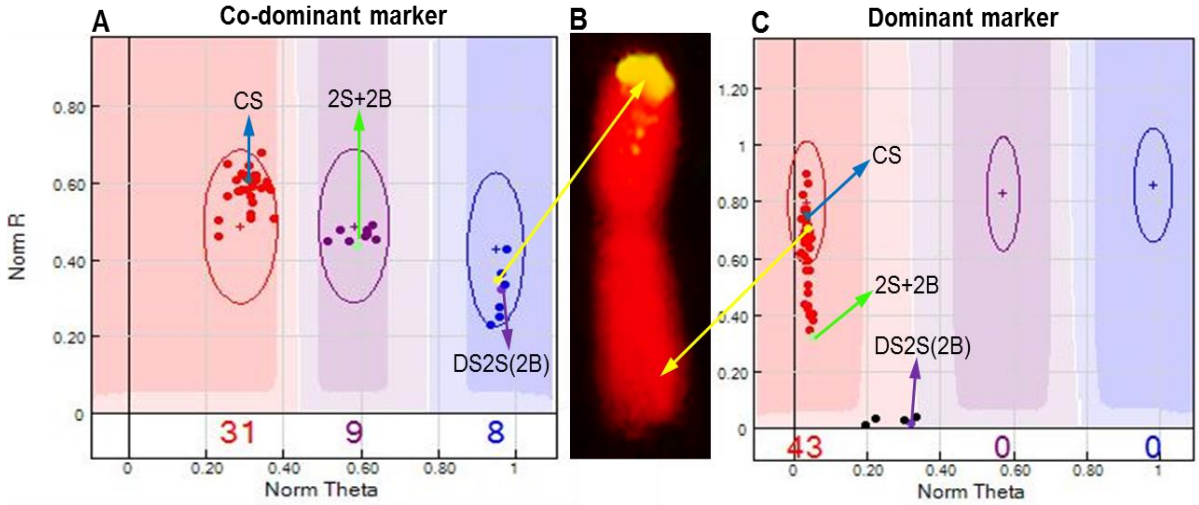

Figure 4.5. Genotyping of the 2B-2S recombinant R3 (2SS-2BS·2BL) via wheat 90K SNP arrays. **(A)** co-dominant SNP (*Kukri_c30847_344*) mapped on chromosome 2BS (Wang et al., 2014); **(B)** GISH pattern of R3; **(C)** dominant SNP (*BS00067828_51*) mapped on chromosome 2BL (Wang et al., 2014). Clusters were generated by GenomeStudio v2011.1 software (Illumina, Inc.).

Homoeologous 2B-2S and 2B-2E recombinants were identified from these two recovery populations by GISH. Two 2B-2S recombinants (2SS-2BS·2BL) designated R1 and R3 and two 2B-2E recombinants designated R2 (2BS-2ES·2EL) and R4 (2ES-2BS·2BL) were used to investigate the utility of molecular markers in the detection of homoeologous recombinants in this study (Figure 4.5B, 4.6B and 4.6C). These four recombinants along with CS, DS 2B(2S), DS 2B(2E), 2B/2S double monosoimcs (2B+2S), 2B/2E double monosoimcs (2B+2E), and several other recombinants were genotyped using wheat 90K iSelect SNP arrays. A total of 3,158 SNP loci were surveyed for polymorphisms among chromosomes 2B, 2S, and 2E. Both dominant and co-dominant SNPs were identified for the 2B-2S and 2B-2E homoeologous pairs as illustrated in Figure 4.5. Co-dominance was observed at the SNP locus *Kukri_c30847_344* mapped to the distal end of 2BS on chromosome 2B and 2S (Figure 4.5A). Dominance was observed at the

SNP locus *BS00067828_51* mapped to the distal end of 2BL on chromosome 2B and 2S with a null allele on 2SL (Figure 4.5C). As expected, we detected null alleles at some of the SNP loci on chromosome 2S and 2E because the 90K SNP arrays were developed from the transcriptomes of modern wheat accessions.

Development and validation of the STARP markers for recombinant screening

A subset of polymorphic SNPs (n=8-10) locating in the distal and centromeric regions of chromosome 2B, respectively, were selected to develop STARP markers for recombinant detection according to the wheat 90K SNP linkage map (Wang et al., 2014). A clear co-dominant SNP without homoeoallelic interference from chromosome 2A and 2D was directly converted to STARP marker. Many of the SNPs on chromosome 2B, however, were influenced by the homoeoalleles on 2A and/or 2D, leading to complicated clusters in the SNP assay. Under this circumstance, we performed comparative analysis of the DNA sequences flanking the selected SNP loci on chromosome 2B, 2A, 2D, 2S, and 2E to identify new nearby SNP loci that were polymorphic between 2B and 2S/2E as well as between 2B/2S/2E and 2A/2D. The contextual sequences of the selected SNPs in the critical regions of chromosome 2B were used as BLAST queries to search for extended genomic sequences flanking the SNP loci on 2B as well as their collinear regions on chromosome 2A, 2D, 2S, and 2E from the publicly available genome sequences of wheat, *Ae. speltoides (*https://urgi.versailles.inra.fr), and *Th. Elongatum* (http://blast.ncbi.nlm.nih.gov). The SNPs locating in the telomeric and centromeric regions of chromosome 2B were converted to STARP markers to detect the recombinants involving these chromosomal regions (Figure 4.6A; Table 4.2).

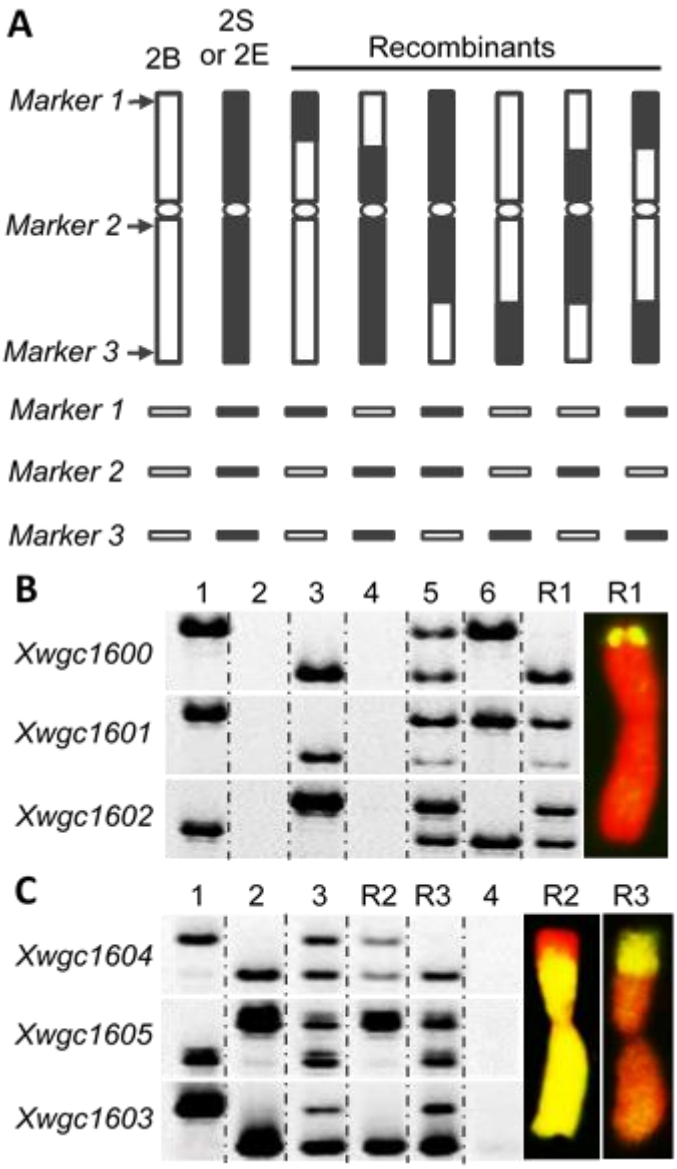

Figure 4.6. Application of STARP markers on the detection of 2B-2S and 2B-2E homoeologous recombination. **(A)** Chromosome ideogram showing homoeologous recombination and locations of the STARP markers (top) and expected haplotypes of the chromosomes at the marker loci (bottom). Blank bars refer to chromosome 2B and its segments in the recombinants, and filled bars to chromosome 2S or 2E and their segments in the recombinants. **(B)** *Left:* Genotypes of CS (*lane 1*), negative control (H_2O) (*lane 2*), DS 2S(2B) (*lane 3*), DS 2E(2B) (*lane 4*), 2B/2S double monosomics (2B+2S) (*lane 5*), 2B/2E double monosomics (2B+2E) (*lane 6*), Recombinant R1 (2SS-2BS·2BL) (*lane R1*) at the three marker loci. *Right:* GISH patterns of recombinant chromosome R1 (2SS-2BS·2BL). **(C)** *Left:* Genotypes of CS (*lane 1*), DS 2E(2B) (*lane 2*), 2B/2E double monosomics (2B+2E) (*lane 3*); Recombinant R2 (2BS-2ES·2EL) (*lane R1*), Recombinant R3 (2ES-2BS·2BL) (*lane R2*), and negative control (H_2O) (*lane 4*) at the three marker loci. *Right:* GISH patterns of the recombinant chromosomes R2 (2BS-2ES·2EL) and R3 (2ES-2BS·2BL). Segments of chromosome 2B were painted in red, while segments from chromosome 2S and 2E were painted in yellow-green.

Table 4.2. SNP-derived STARP markers developed in this study

Marker designation	SNP alleles	SNP position (bp) [a]	Allele-specific forward primers [b]	Reverse primer	Band Size (bp) [c]
Xwgc1600	[C/A]	2BS (7,433,618)	[Tail2]- 5' CCAATTCAGACTGCCTATTTC 3' [Tail1]- 5' CCAATTCAGACTGCCTCCTAA 3'	5' CACAGGATGATCACCACCAAGA 3'	96/100
Xwgc1601	[A/G]	2BL (409,344,640)	[Tail1]- 5' ATACAACCCGTTCCCATTTA 3' [Tail2]- 5' ATACAACCCGTTCCCACCTG 3'	5' TCTGATGCGGTCCAGTTAGTAAC 3'	105/109
Xwgc1602	[T/G]	2BL (769,307,648)	[Tail1]- 5' CTGTTCATGCAATTGATTTCT 3' [Tail2]- 5' CTGTTCATGCAATTGATCCCG 3'	5' GCAGCCTCTACGAATTTTCTACA 3'	82/78
Xwgc1604	[C/G]	2BS(8,593,069)	[Tail1]- 5'TTCTCATCAGCGCCCAAC 3' [Tail2]- 5' TTCTCATCAGCGCCACAG 3'	5' TTACCGAGCTTGGGCATGC 3'	95/99
Xwgc1605	[A/T]	2BL(410,063,189)	[Tail2]- 5' GGGACGTACACTTGATTCA 3' [Tail1]- 5' GGGACGTACACTGGACCCT 3'	5' ACCGCTGAACTGCTCCTCA 3'	77/73
Xwgc1603	[A/T]	2BL (794,886,435)	[Tail1]- 5'AGTGCGCCACCGACCTT 3' [Tail2]- 5'AATGCGCCACAGATATA 3'	5' CCGTTGCAAATGGCCTGATT 3'	67/71

[a] SNP position on IWGSC Reference Sequence v1.0 assembly (IWGSC RefSeq v1.0).
[b] [Tail1] = GCAACAGGAACCAGCTATGAC; [Tail2] = GACGCAAGTGAGCAGTATGAC.
[c] Expected size of PCR products amplified on CS, DS 2S(2B) and DS 2E(2B).

Three STARP markers (*Xwgc1600*, *Xwgc1601*, and *Xwgc1602*) locating in the distal region of 2BS, centromeric region on 2BL, and distal region of 2BL, respectively, have been developed following the procedure described above. These three markers were co-dominant between chromosome 2B and 2S, and clearly delineated the distal and centromeric regions of chromosome 2B, 2S and recombinant chromosome R1 (Table 4.2 and Figure 4.6B). GISH using *Ae. speltoides* genomic DNA as probe was performed on the recombinants. The GISH results were consistent with molecular marker data. However, these three markers were dominant between 2B and 2E, which makes them less useful to detect the 2B-2E recombinants. Thus, three more STARP markers (*Xwgc1603*, *Xwgc1604*, and *Xwgc1605*) co-dominant between 2B and 2E were developed (Table 4.2 and Figure 4.6C). Recombinant chromosomes R2 and R3 were used to validate these three STARP markers. Both recombinants showed diagnostic genotypes at these three marker loci, allowing for the detection of the homoeologous recombination between chromosome 2B and 2E (Figure 4.6C). Additional SNP-derived STARP markers tagging other chromosomal regions would improve the efficacy of the markers in the recombinant detection.

We also validated the newly-developed STARP markers by measuring fluorescence signals as described by Long et al. (2017). The parental and heterozygous genotypes were selected and their DNAs were used as templates. The PCR and signals detection were performed using CFX384 Touch™ Real-Time PCR System. Two of the six STARP markers, *Xwgc1603* and *Xwgc1605*, worked well with parental and heterozygous genotypes plotted into three distinct groups (Figure 4.7). However, the other four STARP markers didn't show distinct clusters on the dot plot of fluorescence intensity. Thus, the bi-allelic discrimination by fluorescence signals is an effective approach for recombinant recovery only if diagnostic markers are available.

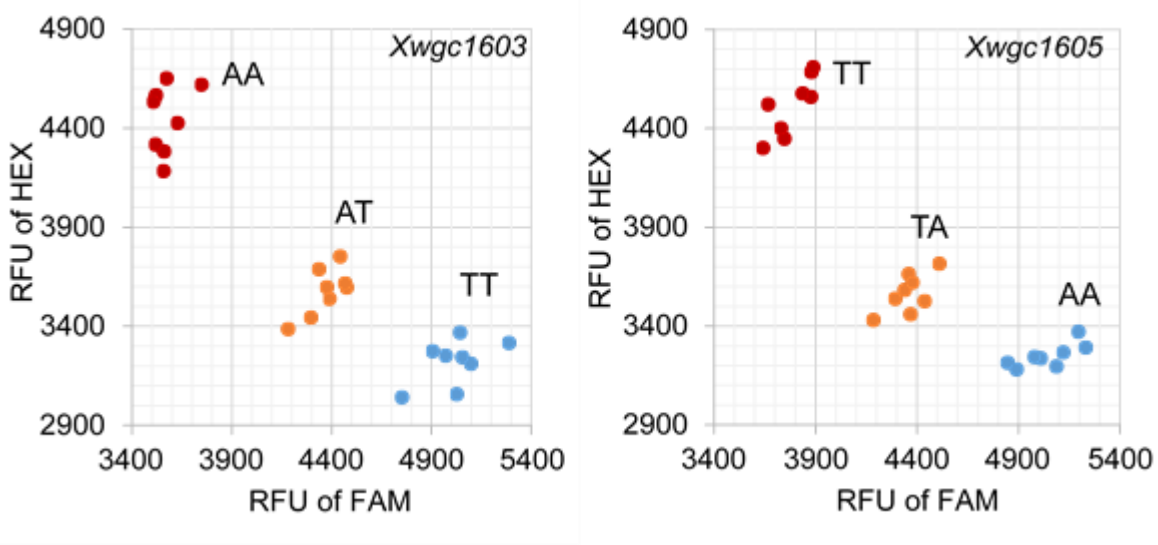

Figure 4.7. Validation of STARP markers (left: *Xwgc1603*; right: *Xwgc1605*) by measuring fluorescence signals. The "AA" and "TT" clusters represent the homozygous *Th. elongatum* 2E and CS 2B alleles, respectively; "TA" and "AT" clusters represent heterozygotes. RFU is relative fluorescence unit.

GISH and STARP marker-mediated detection of meiotic homoeologous recombinants

A total of 859 individuals from the 2B/2S BC_2F_1 population have been screened using the GISH and STARP marker-mediated approach. Of these individuals, 97 (11.3%) were detected harboring reciprocal 2B-2S translocations attributed to homoeologous pairing and crossing over between chromosome 2B and 2S (Table 4.3). Five of them were identified to have two translocated chromosomes with small 2S segments in the distal region (APPENDIX C). This might result from the double crossover of chromosome 2S with chromosome 2B and 2A or 2D involved in a trivalent or other multivalent pairing configuration. Two individuals (0.2%) were found to contain telosomes. Meanwhile, the 2B/2E BC_2F_1 population were screened for 2B-2E homoeologous recombinants. Sixty 2B-2E recombinants (7.6%) were recovered from the 788 BC_2F_1 individuals in the population (Table 4.3 and APPENDIX C). Misdivision (i.e. transverse division of chromosomes) products were observed in 39 out of the 788 BC_2F_1 individuals screened (5.0%), including 2.2% telocentics and 2.8% Robertsonian translocations (Table 4.3).

The meiotic recombination frequency of the 2B-2S homoeologous pair was much higher than that of 2B-2E, suggesting higher homology of *Ae. speltoides* chromosome 2S with wheat chromosome 2B than *Th. elongatum* chromosome 2E with 2B.

Table 4.3. Chromosome constitutions of the 2B-2S and 2B-2E BC_2F_1 individuals

BC_2F_1 populations	No. plants screened	Double monosomics (i.e. 2B+2S or 2B+2E)	Homozygotes for 2S or 2E (i.e. 2S+2S or 2E+2E)	Crossover-derived translocations	Misdivision products	
					Telocentrics	Robertsonian translocations
2B-2S	859	458 (53.3%)	302 (35.2%)	97 (11.3%)	2 (0.2%)	-
2B-2E	788	471 (59.8%)	218 (27.7%)	60 (7.6%)	17 (2.2%)	22 (2.8%)

Th. elongatum genomic DNA-probed GISH was performed on the PMCs at anaphase I/telophase I from the double monosomic 2B/2E plants under the homozygous *ph1b* background to investigate misdivision of chromosomes 2B and 2E (Figure 4.8A). The normal segregation of chromosome 2B and 2E was observed at a frequency of 50.9% during the first meiotic division, including 5.2% segregation with visible exchange of chromosome 2E and 2B segments (Figure 4.8B). Meiotic abnormality attributed to univalents was observed at a frequency of 49.1%, including sister chromatid division of chromosome 2B and/or 2E at anaphase I/telophase I. Centromere misdivision was detected with chromosome 2E in 5.2% of the PMCs analyzed (Figure 4.8B). Similar centromere misdivision should occur with chromosome 2B in the double monosomics individuals because of the formation of the 2B-2E Robertsonian translocations in addition to the telosomes of chromosome 2E in the progeny of the BC_2F_1 individuals (Table 4.3). Also, we found that the frequency of telosomes and Robertsonian translocations (5.0%) in the progenies derived from the double-monosomic 2E/2B plants is similar to the frequency of the centromere misdivision (5.2%) observed in the PMCs at anaphase I/telophase I.

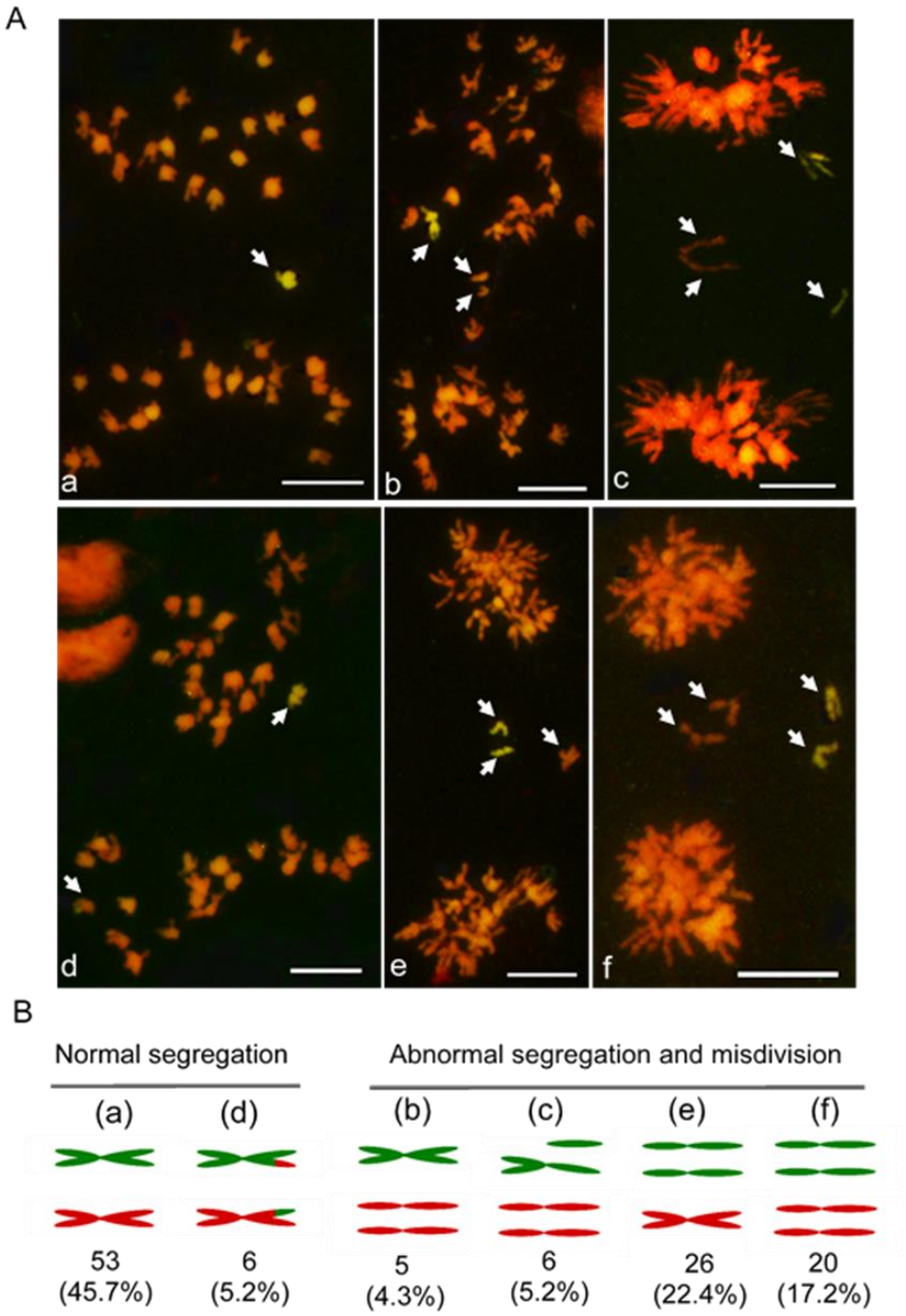

Figure 4.8. Ana-/telophase I segregation of *Th. elongatum* chromosome 2E and CS 2B in double monosomic 2B/2E plants under *ph1b* background. (**A**) Meiotic segregation patterns of *Th. elongatum* chromosome 2E and CS 2B detected by GISH using *Th. elongatum* genomic DNA as probe. Chromosome 2E was detected by green fluorescence and wheat chromosomes were counterstained with PI. The white arrows indicated chromosome 2B or 2E. (**a**) Ana-telophases I showed 2E and 2B undergoing normal chromosome segregation; (**b**) Chromatid segregation of 2B; (**c**) Misdivision of 2E and chromatid segregation of 2B; (**d**) 2E and 2B underwent normal segregation after exchange of chromosome segments; (**e**) Chromatid segregation of 2E; (**f**) Chromatid segregation of both 2B and 2E. (**B**) Frequencies of chromosome 2E (green) and 2B (red) underwent normal and abnormal segregation at ana-/telophase I stage.

Development of the homozygous recombinant lines

The original recombinant lines normally contained a 2B-2S or 2B-2E recombinant chromosome or a telocentic 2S or 2E, a complete chromosome 2S or 2E (from the substitution line parent), and 20 pairs of wheat chromosomes. They were self-pollinated to produce the populations segregating for *Ph1*/*ph1b* and for 2B-2S recombinant/2S chromosome or 2B-2E recombinant/2E chromosome (Figure 4.9A). The segregants homozygous for the recombinant chromosome, but without the *ph1b* deletion were expected to be selected from the segregation populations using molecular markers. The segregating populations were screened first for recombinant homozygotes using the co-dominant STARP markers diagnostic for the recombination (Figure 4.9B and 4.9C). The homozygous recombinants detected by the STARP markers were verified and physically delineated by GISH (Figure 4.9D and 4.9E). Six to thirty-two individuals from each of the self-pollinated populations (BC_2F_2) were analyzed to select homozygous recombinant lines. To date, 1-5 homozygous lines have been obtained for each of the 73 2B-2S and 71 2B-2E recombinants using STARP markers and GISH (APPENDIX D). Meanwhile, we experienced difficulties to obtain homozygous lines in the BC_2F_2 populations for some of the original recombinants due probably to the autosyndetic recombination involving the original recombinant chromosome and other wheat chromosomes. Also, we recovered new meiotic recombination events involving the original recombinant chromosome in the BC_2F_2 populations, leading to new homoeologous recombinants (APPENDIX D).

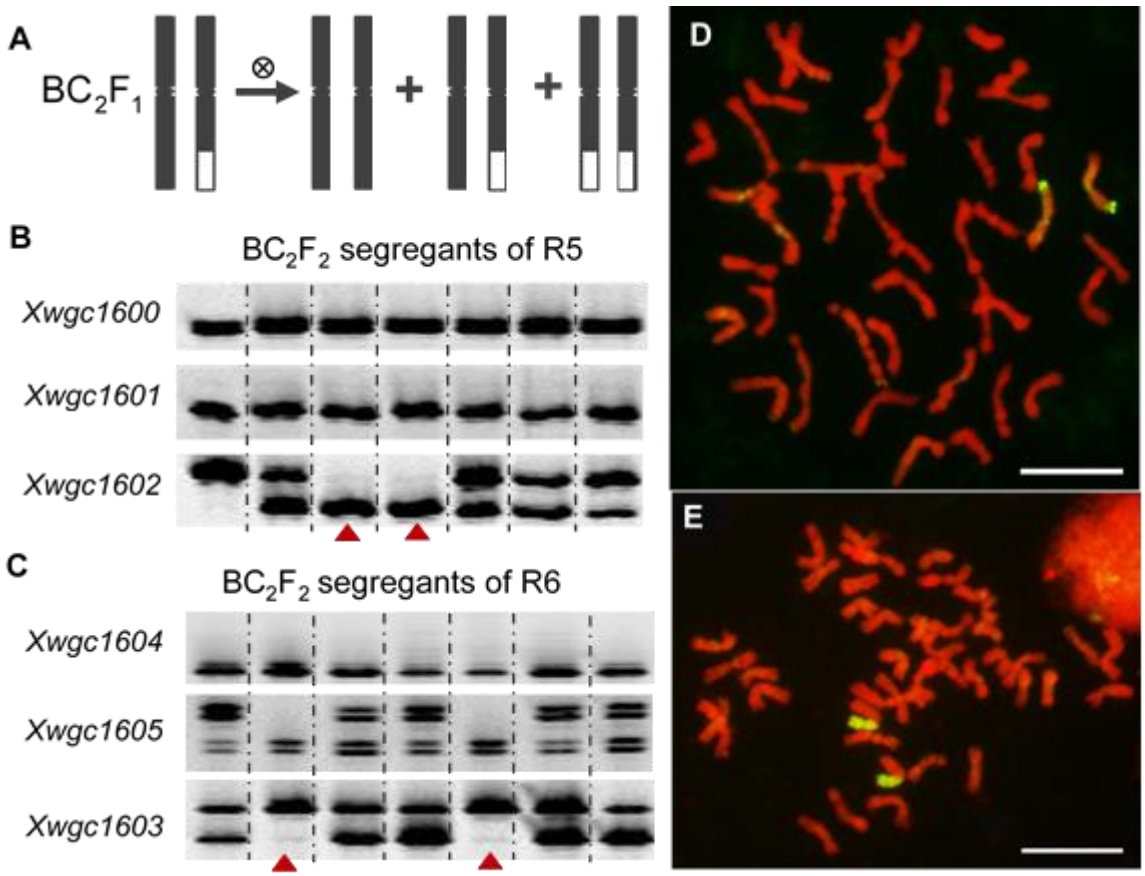

Figure 4.9. Selection of homozygous recombinants by using STARP markers and GISH. **A)** Chromosome ideogram showing chromosome constitution of segregants from self-pollinated recombinant lines. Blank bars refer to chromatin segments from 2B, filled bars refer to chromosome 2S or 2E and their segments in the recombinants. (**B**) Partial gel images showing the three STARP markers on homozygous 2B-2S recombinants screening. The red triangles indicate homozygous lines from the progenies of recombinant R5 (2SS·2SL-2BL). (**B**) Partial gel images showing STARP markers on homozygous 2B-2E recombinants screening. The red triangles indicate homozygous lines from the progenies of recombinant R6 (2ES·2BL). (**D**) and (**E**) showing the GISH image of homozygous recombinant lines (2SS·2SL-2BL) and (2ES·2BL) identified form (B) and (C), respectively. Chromosomes and segments from wheat CS were painted in red, while segments from chromosome 2S and 2E were painted in yellow-green. Scale bar =20 µm.

A total of 112 2B-2S recombinants, one 2SL·2SL isochromosome, and six 2S telosomes were recovered from (Figure 4.10). Sixty-five 2B-2E recombinants, 22 Robertsonian translocations, and 19 telosomes were recovered from the BC_2F_1 and the BC_2F_2 populations (Figure 4.11). The *Ph1*-specific molecular markers *PSR128* or *PSR574* have been used to check the presence of *Ph1* and to eliminate the *ph1b* deletion from the homozygotes selected above

(APPENDIX D). Additional generations are generally needed to obtain homozygous recombinant lines without the *ph1b* deletion because the *Ph1*-specific molecular markers cannot differentiate individuals homozygous for *Ph1* (i.e. *Ph1Ph1*) from hemizygotes (i.e. *Ph1ph1b*).

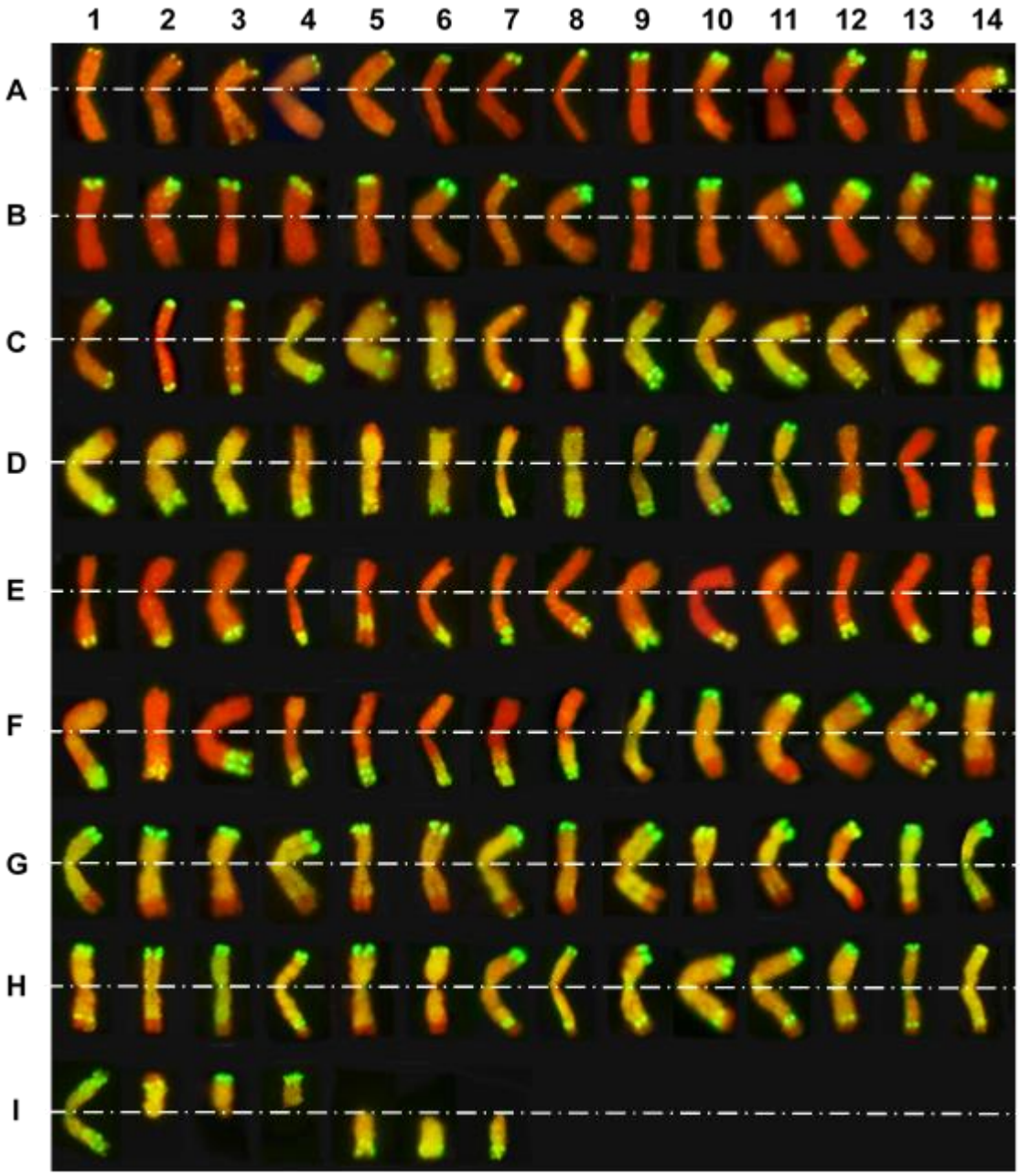

Figure 4.10. GISH-painted 2B-2S recombinant chromosomes, isochromosome, and telosomes in ZW14-203-3 (A1); ZW14-205-7-1 (A2); ZW14-155-2-1 (A3); XWC14-036-40 (A4); XWC14-039-24 (A5); ZW14-117-15 (A6); ZW14-503-2 (A7); ZW14-194-7 (A8); ZW14-510-7 (A9); ZW14-505-1 (A10); ZW14-507-5 (A11); ZW14-188-4-2 (A12); ZW14-167-1-2 (A13); ZW14-173-7-2 (A14); ZW14-010-2 (B1); ZW14-171-4-2 (B2); ZW14-137-7-1 (B3); XWC14-034-40 (B4); ZW14-108-6-2 (B5); ZW14-139-7-1 (B6); ZW14-174-2-2 (B7); ZW14-502-2 (B8); ZW14-095-6 (B9); ZW14-504-5 (B10); ZW14-506-1 (B11); ZW14-184-6 (B12); ZW14-154-3-2 (B13); ZW14-008-5 (B14); ZW14-181-3 (C1); ZW14-166-3-2 (C2); ZW14-197-6 (C3); ZW14-207-2-1 (C4); ZW14-180-5-1 (C5); ZW14-207-2-1 (C6); ZW14-511-7 (C7); ZW14-527-3 (C8); ZW14-525-5 (C9); ZW14-127-8-1 (C10); ZW14-515-8 (C11); ZW14-180-2-1 (C12); ZW14-186-1-2 (C13); ZW14-071-2 (C14); ZW14-007-7 (D1); ZW14-093-8-1 (D2); ZW14-115-7-2 (D3); ZW14-008-5 (D4); XWC14-034-40 (D5); ZW14-142-4-2 (D6); ZW14-141-8-2 (D7); ZW14-149-1-2 (D8); ZW14-134-3-1 (D9); ZW14-519-2 (D10); ZW14-520 (D11); ZW14-001-15 (D12); ZW14-116-5 (D13); ZW14-527-3 (D14); ZW14-512-1 (E1); ZW14-169-5-2 (E2); ZW14-513-6 (E3); ZW14-526-1 (E4); ZW14-162-4 (E5); ZW14-127-8-2 (E6); ZW14-074-2 (E7); ZW14-014-2 (E8); ZW14-117-15 (E9); ZW14-128-1 (E10); ZW14-194-7 (E11); ZW14-121-8 (E12); ZW14-118-1 (E13); XWC14-034-27 (E14); XWC14-039-61 (F1); ZW14-528-5 (F2); ZW14-009-3 (F3); ZW14-077-8-2 (F4); ZW14-527-3 (F5); ZW14-171-4-2 (F6); ZW14-084 (F7); ZW14-201-2 (F8); ZW14-002-1 (F9); ZW14-508-4 (F10); ZW14-527-3 (F11); ZW14-522-4 (F12); ZW14-077-8-1 (F13); ZW14-518-8 (F14); ZW14-111-3-2 (G1); ZW14-521-3 (G2); ZW14-005-8 (G3); ZW14-147-4-1 (G4); ZW14-162-4-2 (G5); ZW14-501-1 (G6); ZW14-523-7 (G7); ZW14-004-1 (G8); ZW14-185-2 (G9); ZW14-011-1 (G10); ZW14-073-1 (G11); ZW14-517-6 (G12); ZW14-512-2 (G13); ZW14-513-6 (G14); ZW14-135-6-2 (H1); ZW14-514-6 (H2); XWC14-034-45 (H3); ZW14-519-3 (H4); ZW14-100-1 (H5); XWC14-039-27 (H6); XWC14-035-20 (H7); ZW14-070-1 (H8); ZW14-013-4 (H9); ZW14-511-7 (H10); ZW14-516-4 (H11); ZW14-524-4 (H12); XWC14-035-17 (H13); XWC14-035-31 (H14); ZW14-175-7-1 (I1); ZW14-089-7-1 (I2); ZW14-106 (I3); ZW14-205-7-1 (I4); ZW14-084-8-2 (I5); ZW14-206 (I6); ZW14-089-7-1 (I7). The segments of chromosome 2B were painted in red and segments of chromosome 2S in yellow-green.

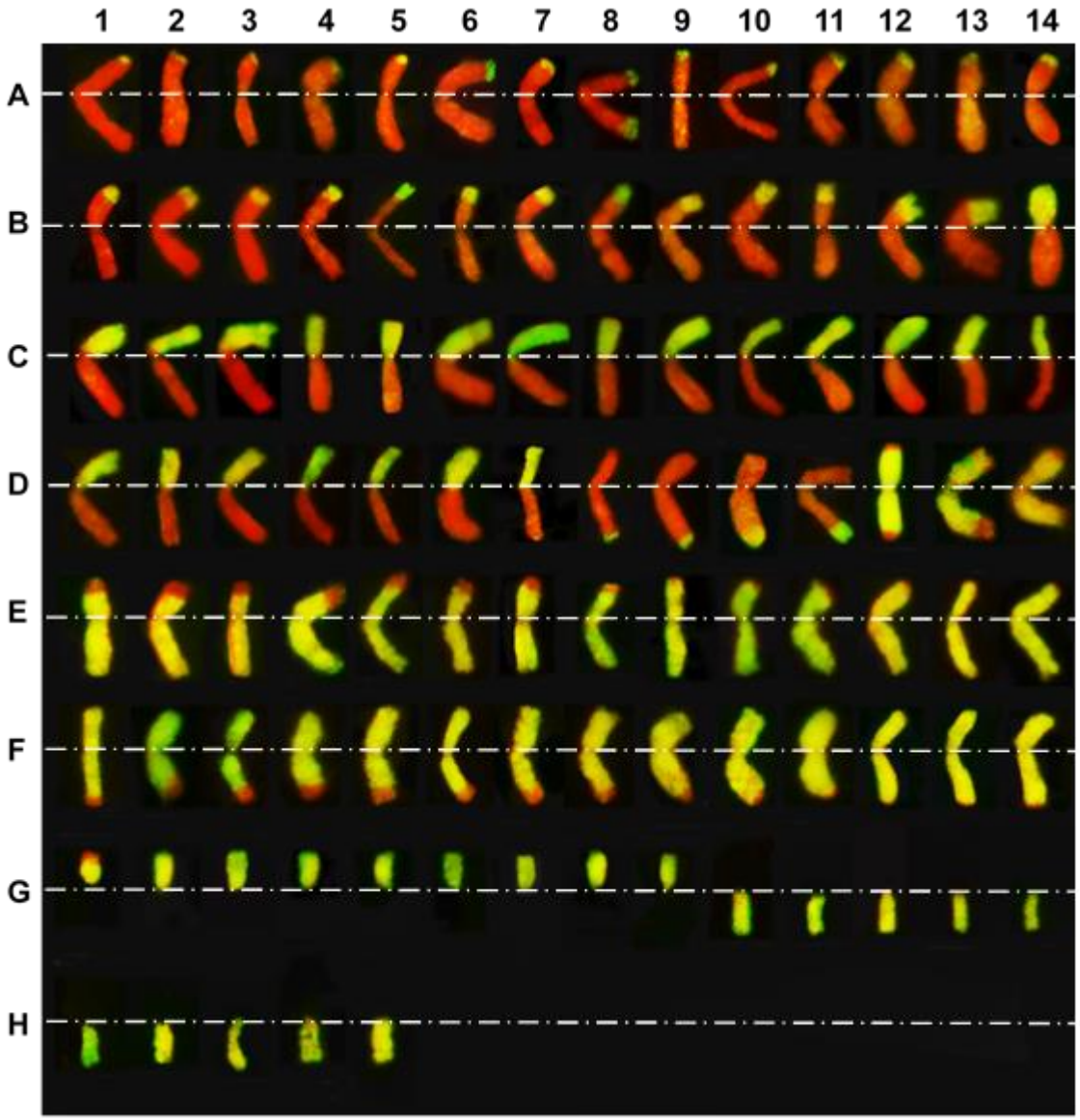
1 2 3 4 5 6 7 8 9 10 11 12 13 14
A
B
C
D
E
F
G
H

Figure 4.11. GISH-painted 2B-2E recombinant chromosomes, Robertsonian translocations, and telosomes in ZW14-410-2 (A1); ZW14-412-4 (A2); ZW14-404-7 (A3); ZW14-280-5 (A4); ZW14-229-2 (A5); ZW14-293-4 (A6); ZW14-407-4 (A7); ZW14-395-4 (A8); ZW14-334-4 (A9); ZW14-399-5 (A10); ZW14-357-8 (A11); ZW14-297-2 (A12); ZW14-328-8 (A13); ZW14-313-8 (A14); ZW14-390-2 (B1); ZW14-392-6 (B2); ZW14-396-7 (B3); ZW14-311-8 (B4); ZW14-401-4 (B5); ZW14-347-4 (B6); ZW14-310-4 (B7); ZW14-406-4 (B8); ZW14-300-6 (B9); ZW14-266-8 (B10); XWC14-131-33 (B11); XWC14-130-3 (B12); ZW14-245-1 (B13); XWC14-131-4 (B14); XWC14-131-2 (C1); ZW14-221 (C2); ZW14-222 (C3); ZW14-224 (C4); ZW14-225 (C5); ZW14-226 (C6); ZW14-227 (C7); ZW14-228 (C8); ZW14-229 (C9); ZW14-230 (C10); ZW14-231 (C11); ZW14-232 (C12); ZW14-233 (C13); ZW14-234-3 (C14); ZW14-235 (D1); ZW14-237 (D2); ZW14-238 (D3); ZW14-239 (D4); ZW14-240 (D5); ZW14-323-1 (D6); ZW14-380 (D7); ZW14-408-4 (D8); ZW14-403-6 (D9); ZW14-391-7 (D10); XWC14-143-59 (D11); ZW14-398-5 (D12); XWC14-132-15 (D13); ZW14-306-2 (D14); ZW14-258-7 (E1); XWC14-132-3 (E2); ZW14-409-6 (E3); XWC14-715-2 (E4); ZW14-402-6 (E5); ZW14-261-4 (E6); ZW14-267-1 (E7); ZW14-257-6 (E8); ZW14-306-2 (E9); ZW14-398-4 (E10); ZW14-270-3 (E11); ZW14-289-3 (E12); ZW14-405-7 (E13); ZW14-394-4 (E14); ZW14-393-1 (F1); ZW14-320-6 (F2); ZW14-253-8 (F3); ZW14-273-6 (F4); ZW14-382-5 (F5); ZW14-243-7 (F6); ZW14-299-5 (F7); ZW14-335-2 (F8); ZW14-272-2 (F9); ZW14-343-2 (F10); ZW14-246-4 (F11); ZW14-308-2 (F12); ZW14-315-1 (F13); ZW14-269-7 (F14); ZW14-214 (G1); ZW14-209 (G2); ZW14-210 (G3); ZW14-211 (G4); ZW14-213 (G5); ZW14-216 (G6); ZW14-218 (G7); ZW14-255-1 (G8); ZW14-301-5 (G9); ZW14-208 (G10); ZW14-212 (G11); ZW14-215 (G12); ZW14-217 (G13); ZW14-242-2 (G14); ZW14-328-4 (H1); ZW14-331 (H2); ZW14-338 (H3); ZW14-381 (H4); ZW14-349 (H5). The segments of chromosome 2B were painted in red and segments of chromosome 2E in yellow-green.

We measured the length of alien segments and detected the breakpoints for all the 2B-2S and 2B-2E recombinant chromosomes that resulted from meiotic homoeologous recombination (APPENDIX E). The telosomes, Robertsonian translocations, and crossover-derived recombinants with too small alien segments to be detected by GISH were not included in the measurement. The size of the alien segment in the recombinant chromosome was calculated as the percentage of the alien segment length over the total length of the recombinant chromosome. The relative size of the 2S segments in the 2B-2S recombinant chromosomes ranged from 3.8% to 95.3%, while the 2E segments ranged from 5.7% to 97.8% among the measured cells (APPENDIX E). Apparently, the recombination breakpoints distributed mostly within the 55% -

95% interval on the distal regions of both chromosomal arms (Figure 4.12). The overall recombination events seemed to occur equally on each chromosome arm without significant difference. The meiotic recombination hot regions for the 2B-2S homoeolgous pair were similar to those of the 2B-2E homoeologous pair even though the wheat B genome has a closer evolutionary relationship with *Ae. speltoides* S genome than with the *Th. elongatum* E genome.

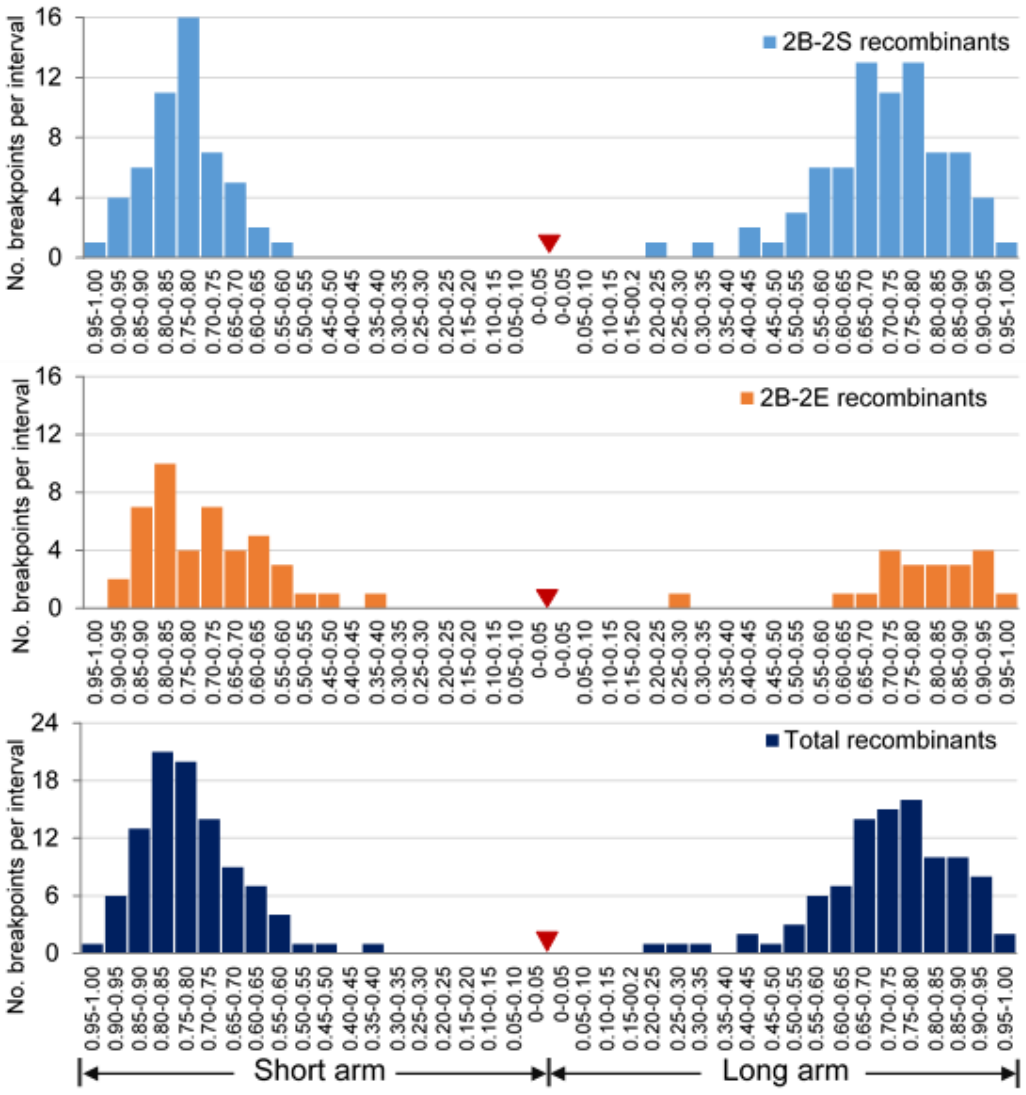

Figure 4.12. Distribution of recombination breakpoints in the 2B-2S and 2B-2E recombinant chromosomes. Each interval on the horizontal axis represents 5% of the physical length on the short and long arm of chromosome 2B. The red triangles indicate the centromeric region of the recombinant chromosomes.

Discussion

Meiotic homoeologous recombination-mediated reciprocal exchange of segments are almost limited to the telomeric and subtelomeric regions of chromosomes at a relatively low frequency in wheat. Accordingly, a large homoeologous recombination population is needed to recover the recombinants of interest for gene introgression from wild species into wheat. Screening such a large population for homoeologous recombinants is laborious using conventional or even modern cytological techniques, such as GISH (Friebe et al., 1991; Lukaszewski et al., 2005; Qi et al., 2007; Wulff and Moscou, 2014). Recent advances in wheat genomics, especially high-throughput genotyping technologies, have provided new opportunities to improve the efficacy of homoeologous recombination detection in alien gene introgression. In this study, we obtained the genotype data at 3,158 SNP loci mapped to wheat chromosome 2B that were polymorphic among wheat chromosome 2B, *Ae. speltoides* chromosome 2S, and *Th. elongatum* chromosome 2E, using the wheat 90K SNP arrays. These genotype data along with the SNP consensus map of wheat chromosome 2B (Wang et al., 2014) provided a useful genomic framework to the development of chromosomal region-specific molecular markers for the detection of meiotic recombination involving these three homoeologous chromosomes.

The multiplexed chip-based SNP assay is high-throughput, but may not be cost-effective and user-friendly for the research project involving small numbers of SNPs and a short data turnaround time (Myakishev et al., 2001; Semagn et al., 2014). For instance, in this study we needed the genotypic data of the SNPs relevant to only 2B-2S and 2B-2E homoeologous pairs for the detection of the meiotic recombination events involving these three homoeologous chromosomes, but not the remaining SNPs on the 90K array. Thus, we developed the uniplex PCR-based STARP markers from the SNPs locating in the critical chromosomal regions to

detect 2B-2S and 2B-2E recombinants. The uniplex STARP markers are more cost-effective and flexible for genotyping small numbers of SNPs than the multiplexed chip-based SNP assay. Also, the STARP marker technology generally has lower error rates and shorter turnaround time than the multiplexed chip-based SNP assay (Semagn et al., 2014, Long et al., 2017). Evidently, the uniplex STARP marker system in combination with high-throughput multiplexed chip-based SNP assay provides an effective approach to detect homoeologous recombinants from large recombination populations.

Bread wheat is an allohexaploid with three homoeologous subgenomes (A, B, and D). Generally, there are three homoeoalleles at a majority of the molecular marker loci in wheat. Homoeoalleles in the polyploid genome of wheat often complicate marker analysis especially for the SNP assay. This has limited the application of the fluorescence-based bi-allelic discrimination technique in the allopolyploid genome (Myakishev et al., 2001; Syvänen, 2001; Semagn et al., 2014; Klindworth et al., 2017; Long et al., 2017). In this study, we designed six STARP markers locating in the distal ends and centromeric region of chromosome 2B to detect the 2B-2S and 2B-2E recombination. Only two of them worked well on the platform of bi-allelic discrimination by fluorescence signals. But, all of the six STARP markers were diagnostic for the three homoeologous chromosomes in the size-based DNA analysis system (e.g. LI-COR DNA Analyzer). Thus, the length polymorphism-based DNA analyzer was used as the primary technique for the STARP marker analysis in this study. Additional STARP markers can be developed from the SNPs spanning other chromosomal regions for the detection of the homoeologous recombination potentially along the entire chromosomes. This procedure extends the application of SNPs in marker-assisted selection and improves the efficacy of SNPs in the

detection of meiotic homoeologous recombination for alien gene introgression in the polyploid genome of wheat.

The wheat 90K SNP arrays were developed primarily from the transcriptomes of modern wheat accessions. Wild relatives of wheat, such as *Ae. speltoides* and *Th. elongatum*, were not included in the wheat SNP discovery process (Wang et al., 2014). As a result, *Ae. speltoides* chromosome 2S and *Th. elongatum* chromosome 2E often exhibited null alleles at some of the wheat chromosome 2B-derived SNP loci. Those dominant SNPs cannot be used to detect the alien segments tagged by the null alleles under the heterozygous condition. To overcome this problem associated with those dominant SNPs, we recovered the homoeologous recombinant gametes by backcrossing the individuals that underwent meiotic 2B-2S and 2B-2E recombination to the disomic substitution lines DS 2S(2B) and DS 2E(2B), respectively. This allowed the use of dominant markers to detect the null allele present on the alien segment of the recombinant along with the respective alien chromosome (i.e. 2S or 2E). In addition, the alien chromosomes 2S and 2E introduced into the recombinant recovery populations served as internal controls for GISH analysis of the recombinants especially for those with small alien segments. Therefore, this backcross strategy makes the dominant markers with null alleles on the alien segments usable in the detection of homoeologous recombination and facilitates GISH analysis of the recombinants.

Generally, the *ph1b* mutant can induce allosyndetic pairing/recombination between wheat chromosomes and their alien homoeologues as well as autosyndetic pairing/recombination between wheat homoeologues from the A, B, and D subgenomes (Cai and Jones, 1997). We observed multivalents involving multiple wheat chromosomes in addition to 2B-2S or 2B-2E bivalents under the homozygous *ph1b* condition (data not shown). Thus, the *ph1b* mutant-

generated gametes with an allosyndetic recombinant may contain one or more autosyndetic recombinants. These gametes are generally less competitive in pollination and fertilization than those without homoeologous recombinants, especially in the male parent. As a result, this may limit the recovery of allosyndetic recombinants, especially by self-pollination of the individuals undergoing allosyndetic pairing/recombination. In this study, we recovered the recombinant gametes by pollinating the individuals undergoing 2B-2S and 2B-2E homoeologous pairing/recombination with the disomic substitution lines DS 2S(2B) and DS 2E(2B), respectively. These two disomic substitution lines went through normal meiosis and had a normal seed set similar to the CS wheat parent. In a preliminary study, we observed a higher homoeologous recombinant frequency in the backcross progeny than self-pollinated progeny. Similarly, a high recovery rate of meiotic homoeologous recombinants was obtained from the backcross progeny in an alien introgression study by Niu et al. (2011). Thus, the backcross scheme with the disomic substitution lines can enhance the recovery of homoeologous recombinants in addition to facilitating the detection of homoeologous recombinants.

Chromosome pairing also known as synapsis is a prerequisite for crossover and recombination during prophase I and segregation of paired chromosomes during anaphase I of meiosis. The frequency of compensating wheat-alien recombinants in the progeny of the double monosomic plants depends on the targeted chromosomes and genetic background. Although the *Ae. speltoides* S genome has been considered to a putative donor of the wheat B, meiotic recombination rarely occurs between the homeologous chromosomes of *Ae. speltoides* and wheat. Thus, most of the *Ae. speltoides*-wheat chromosome recombinants were produced by *ph1b*-induced homeologous recombination (Friebe et al., 1996). In this study, a recombinant frequency of 11.3% and 7.6% were observed for the homoeologus pair 2B-2S and 2B-2E,

respectively, in the progeny of the 2B/2S or 2B/2E double monosomic plants under *ph1bph1b* background. The higher homoeologous recombinant frequency of chromosome 2B with 2S than 2E suggests a closer evolutionary relationship of the wheat B genome with the *Ae. speltoides* S genome than the *Th. elongatum* E genome. However, the 2B-2S and 2B-2E recombination events occurred mostly at the similar hot spot in the distal regions of each chromosomal arm.

The occurrence of univalents is probably the most common meiotic event for the monosomic chromosomes. The univalent laggards at meiosis have a tendency to misdivide at the centromere in a transverse instead of lengthwise manner, which gives rise to telocentric and isochromosomes. Chromosome 2E appeared as a univalent in 88.5% of the PMCs in the 2B/2E double monosomic individuals (see chapter 3). About 5.0% of the univalents underwent centric misdivision at anaphase/telophase I. This probably explain why a high frequency of telosomes and Robertsonian translocations were obtained with *Th. elongatum* chromosome 2E in this study.

Centric misdivision followed by the fusion of the divided arms from different chromosomes could results in whole-arm Robertsonian translocations (Friebe et al., 2005; Liu et al., 2011). DNA sequence homology between non-homologous centromeres may provide the structural basis for meiotic chromosome pairing and recombination that also could result in the formation of Robertsonian translocations (Bandyopadhyay et al., 2002; Berend et al., 2003). In this study, a total of 22 compensating Robertsonian translocations lines were identified in the 788 progenies of the double monosomic 2B/2E plants. Meanwhile, we observed a relatively high frequency of centric misdivision of chromosome 2E under the monosomic condition. Most likely, the 2B-2E Robertsonian translocations recovered from the double monosomic population were produced through the misdivision and fusion mechanism. In addition, we found that fused all the 2B-2E Robertsonian translocations exclusively contained the short arm of *Th. elongatum*

chromosome 2E and the long arm of wheat chromosome 2B. This result suggests that the chromosomal arm 2ES might genetically compensate better for 2BS than 2EL for 2BL.

In summary, we developed an effective DNA marker-assisted approach of inducing and detecting meiotic homoeologous recombination in the polyploid genome of wheat using the genomics technologies and resources currently available in wheat. This new approach will facilitate large-scale alien gene introgression for wheat improvement and ultimately increase the genetic gain of wheat production. Our preliminary data showed that chromosome 2S in the DS 2S(2B) line contains genes for resistance to stem rust, tan spot, and Stagonospora nodorum blotch (SNB) diseases, while chromosome 2E in the DS 2E(2B) line contains genes for tolerance to waterlogging (Taeb et al., 1993). Homozygous recombinants without the *ph1b* deletion have been evaluated for resistance/tolerance to these biotic and abiotic stresses as well as other agronomically important traits. The recombinant lines that contain the genes of interest, but not obvious linkage drag will be released as germplasm for variety development in wheat breeding.

References

Bandyopadhyay R, Heller A, Knox–DuBois C, McCaskill C, Berend SA, Page SL, Shaffer LG (2002) Parental origin and timing of *de novo* Robertsonian translocation formation. Am J Hum Genet 71:1456–1462

Berend SA, Page SL, Atkinson W, McCaskill C, Lamb NE, Sherman SL, Shaffer LG (2003) Obligate short-arm exchange in de novo Robertsonian translocation formation influences placement of crossovers in chromosome 21 nondisjunction. Am J Hum Genet 72:488–95

Cai X, Jones S (1997) Direct evidence for high level of autosyndetic pairing in hybrids of Thinopyrum intermedium and Th. ponticum with *Triticum aestivum*. Theor Appl Genet 95:568–572

Cai X, Jones S, Murray T (1998) Molecular cytogenetic characterization of *Thinopyrum* and wheat-*Thinopyrum* translocated chromosomes in a wheat T*hinopyrum* amphiploid. Chromosome Res 6:183–189

Cai X, Chen PD, Xu SS, Oliver RE, Chen X (2005) Utilization of alien genes to enhance Fusarium head blight resistance in wheat-a review. Euphytica 142:309–318

Chapman V, Riley R (1970) Homoeologous meiotic chromosome pairing in *Triticum aestivum* in which chromosome 5B is replaced by an alien homoeologue. Nature 226:376–377

Chen PD, Tsujimoto H, Gill BS (1994) Transfer of *Ph1* genes promoting homoeologous pairing from *Triticum speltoides* to common wheat. Theor Appl Genet 88:97–101

Chen PD, Liu WX, Yuan JH, Wang X, Zhou B, Wang SL, Zhang SZ, Feng YG, Yang BJ, Liu GX, Liu DJ, Qi L, Zhang P, Friebe B, Gill BS (2005) Development and characterization of wheat–*Leymus racemosus* translocation lines with resistance to Fusarium Head Blight. Theor Appl Genet 111(5):941–948

Chen X, Faris JD, Hu J, Stack RW, Adhikari T, Elias EM, Kianian SF, Cai X (2007) Saturation and comparative mapping of a major Fusarium head blight resistance QTL in tetraploid wheat. Mol Breed 19:113–124

Cox TS (1998) Deepening the wheat gene pool. J Crop Prod 1:1–25

Faris JD, Xu SS, Cai X, Friesen TL, Jin Y (2008) Molecular and cytogenetic characterization of a durum wheat-*Aegilops speltoides* chromosome translocation conferring resistance to stem rust. Chromosom Res 16:1097–1105

Friebe B, Mukai Y, Dhaliwal HS, Martin TJ, Gill BS (1991) Identification of alien chromatin specifying resistance to wheat streak mosaic and greenbug in wheat germ plasm by C-banding and *in-situ* hybridization. Theor Appl Genet 81:381–389

Friebe B, Jiang J, Raupp WJ, McIntosh RA, Gill BS (1996) Characterization of wheat–alien translocations conferring resistance to diseases and pests: current status. Euphytica 91:59–87

Friebe B, Zhang P, Linc G, Gill BS (2005) Robertsonian translocations in wheat arise by centric misdivision of univalents at anaphase I and rejoining of broken centromeres during interkinesis of meiosis II. Cytogenet Genome Res 109:293–297

Friebe B, Qi L, Liu C, Gill B (2011) Genetic compensation abilities of *Aegilops speltoides* chromosomes for homoeologous B-genome chromosomes of polyploid wheat in disomic S(B) chromosome substitution lines. Cytogenet Genome Res 134:144–150

Gale MD, Miller TE (1987) The introduction of alien genetic variation into wheat. In: Lupton, FGH (ed). Wheat breeding: Its scientific basis. Chapman and Hall, UK. pp173–210

Gill KS, Gill BS, Endo TR, Mukai Y (1993) Fine physical mapping of *Ph1*, a chromosome pairing regulator gene in polyploid wheat. Genetics 134:1231–1236

Graybosch RA, Peterson CJ (2010) Genetic improvement in winter wheat yields in the Great Plains of North America, 1959–2008. Crop Sci. 50:1882–1890

Jiang J, Friebe B, Gill BS (1994) Recent advances in alien gene transfer in wheat. Euphytica 73:199–212

King J, Grewal S, Yang CY, Hubbart S, Scholefield D, Ashling S, Edwards KJ, Allen AM, Burridge A, Bloor C, Davassi A, da Silva GJ, Chalmers K, King IP (2016) A step change in the transfer of interspecific variation into wheat from *Amblyopyrum muticum*. Plant Biotechnol J 15:217–226

Klindworth DL, Niu ZX, Chao SM, Friesen TL, Jin Y, Faris JD, Cai XW, Xu SS (2012) Introgression and characterization of a goatgrass gene for a high level of resistance to Ug99 stem rust in tetraploid wheat. G3 2:665–673

Klindworth DL, Saini J, Long Y, Rouse MN, Faris JD, Jin Y, Xu SS (2017) Physical mapping of DNA markers linked to stem rust resistance gene *Sr47* in durum wheat. Theor Appl Genet 130:1135–1154

Kuraparthy V, Chhuneja P, Dhaliwal HS, Kaur S, Bowden RL, Gill BS (2007) Characterization and mapping of cryptic alien introgression from *Aegilops geniculata* with new leaf rust and stripe rust resistance genes *Lr57* and *Yr40* in wheat. Theor. Appl. Genet. 114:1379–1389

Liu W, Jin Y, Rouse M, Friebe B, Gill B, Pumphrey MO (2011) Development and characterization of wheat–*Ae. searsii* Robertsonian translocations and a recombinant chromosome conferring resistance to stem rust. Theor Appl Genet 122:1537–1545

Lukaszewski AJ, Lapinski B, Rybka K (2005) Limitations of in situ hybridization with total genomic DNA in routine screening for alien introgressions in wheat. Cytogent Genome Res 109:373–377

Long YM, Chao WS, Ma G, Xu SS, Qi, L (2017) An innovative SNP genotyping method adapting to multiple platforms and throughputs. Theor Appl Genet 130:597–607

McArthur RI, Zhu X, Oliver RE, Klindworth DL, Xu SS Stack RW, Wang RR, Cai X (2012) Homoeology of *Thinopyrum junceum* and *Elymus rectisetus* chromosomes to wheat and disease resistance conferred by the *Thinopyrum* and *Elymus* chromosomes in wheat. Chrom Res 20:699–715

Morris R, Sears ER (1967) The cytogenetics of wheat and its relatives. In: K.S. Quisenberry KS, Reitz LP (eds). Wheat and wheat improvement, Am Soc Agron, Madison WI, pp 19–87.

Myakishev MV, Khripin Y, Hu S, Hamer DH (2001) High–throughput SNP genotyping by allele–specific PCR with universal energy–transfer–labeled primers. Genome Res 11:163–169

Niu Z, Klindworth DL, Friesen TL, Chao S, Jin Y, Cai X, Xu SS (2011) Targeted introgression of a wheat stem rust resistance gene by DNA marker–assisted chromosome engineering. Genetics 187:1011–1021

Qi LL, Friebe B, Zhang P, Gill BS (2007) Homoeologous recombination, chromosome engineering and crop improvement. Chromosome Res 15:3–19

Qi LL, Pumphrey MO, Friebe B, Chen PD, Gill BS (2008) Molecular cytogenetic characterization of alien introgressions with gene *Fhb3* for resistance to Fusarium head blight disease of wheat. Theor Appl Genet 117:1155–1166

Qi LL, Ma GJ, Long YM, Hulke BS, Markell SG (2015) Relocation of a rust resistance gene R 2 and its marker–assisted gene pyramiding in confection sunflower (*Helianthus annuus* L.). Theor Appl Genet 128:477–488

Riley R, Chapman V (1958) Genetic control of cytologically diploid behaviour of hexaploid wheat. Nature 182:713–715

Riley R, Chapman V, Johnson R (1959) Genetic control of chromosome pairing in intergeneric hybrids with wheat. Nature 183:1244–1246

Roberts MA, Reader SM, Dalgliesh C, Miller TE, Foote TN, Fish LJ, Snape JW, Moore G (1999) Induction and characterization of *Ph1* wheat mutants. Genetics 153:1909–1918

Sears ER (1972) Chromosome engineering in wheat. In: Stadler Genet. Symp., Univ of Missouri, Columbia. pp 23–38

Sears ER (1977) An induced mutant with homoeologous pairing in common wheat. Can J Genet Cytol 19:585–593

Sears ER (1983) The transfer to wheat of interstitial segments of alien chromosomes. In: Sakamoto S (eds), Pro 6th Intern Wheat Genet Symp, Kyoto, Japan. pp 5–12

Semagn K, Babu R, Hearne S, Olsen M (2014) Single nucleotide polymorphism genotyping using Kompetitive Allele Specific PCR (KASP): overview of the technology and its application in crop improvement. Mol. Breed.33:1–14

Shepherd KW, Islam AKMR (1988) Fourth compendium of wheat–alien chromosome lines. In: Proc 7th Intern. Wheat Genet Symp, Cambridge, England, pp 1373–1398

Syvänen AC (2001) Accessing genetic variation: genotyping single nucleotide polymorphisms. Nat Rev Genet 2:930–942

Taeb M, Koebner RMD, Forster BP (1993) Genetic variation for waterlogging tolerance in the Triticeae and the chromosomal location of genes conferring waterlogging tolerance in *Thinopyrum elongatum*. Genome 36:825–830

Wang S, Wong D, Forrest K, Allen A, Huang BE, Maccaferri M, Salvi S, Milner SG, Cattivelli L, Mastrangelo AM, Whan A, Stephen S, Barker G, Wieseke R, Plieske J, International Wheat

Genome Sequencing Consortium, Lillemo M, Mather D, Appels R, Dolferus R, Brown–Guedira G, Korol A, Akhunova AR, Feuillet C, Salse J, Morgante M, Pozniak C, Luo MC, Dvorak J, Morell M, Dubcovsky J, Ganal M, Tuberosa R, Lawley C, Mikoulitch I, Cavanagh C, Edwards KJ, Hayden M, Akhunov E (2014) Characterization of polyploid wheat genomic diversity using a high–density 90,000 single nucleotide polymorphism array. Plant Biotechnol J 12:787–796

Wulff BBH, Moscou MJ (2014) Strategies for transferring resistance into wheat: from wide crosses to GM cassettes. Front Plant Sci 5:692

Xu SS, Faris JD, Cai X, Klindworth DL (2005) Molecular cytogenetic characterization and seed storage protein analysis of 1A/1D translocation lines of durum wheat. Chrom Res 13:559–568

Zeller FJ (1973) 1B/1R wheat–rye chromosome substitutions and translocations. Proc 4th Intern Wheat Genet Symp, Columbia, MO, pp 209–221

Zeller FJ, Hsam SLK (1983) Broadening the genetic variability of cultivated wheat by utilizing rye chromatin. In: Sakamoto S (ed). Proc. 6th Intern. Wheat Genet Symp, Kyoto, Japan, pp 161–173

CHAPTER 5. MOLECULAR, CYTOGENETIC, AND PHENOTYPIC CHARACTERIZATION OF THE WHEAT-ALIEN INTROGRESSION LINES

Abstract

The narrow genetic base of modern wheat (2n = 6x = 42, genome AABBDD) makes it vulnerable to climate change, diseases, and insects. Meiotic homoeologous recombination has been employed to transfer genes from wild relatives to wheat. *Aegilops speltoides* (2n=2x=14, genome SS) and *Thinopyrum elongatum* (2n=2x=14, genome EE), two diploid wild relatives of wheat, contain the genes for resistance/tolerance to the multiple biotic and abiotic stresses that threaten wheat production. However, the progress of alien gene introgression in wheat has been limited due to the lack of the high-throughput technology and genomics resources/tools for the production of meiotic homoeologous recombinants. In this study, we genotyped 83 Chinese Spring (CS) wheat -*Ae. speltoides* 2B-2S and 67 CS- *Th. elongatum* 2B-2E recombinant lines using wheat 90K SNP arrays. Meanwhile, we partitioned chromosome 2B, 2S, and 2E into 93, 66, and 46 bins, respectively, based on the SNP genotyping and GISH results of the recombinants. Consequently, a composite bin map was developed for chromosome 2B and its homoeologous 2S and 2E. In addition, a gene for resistance to stem rust and a gene for nontoxin-associated resistance to both tan spot and SNB were identified on the *Ae. speltoides* chromosome 2S. Both disease resistance genes were incorporated into the wheat genome and physically mapped to the distal region on the short arm of chromosome 2S using the 2B-2S recombinant lines. Also, we identified a small chromosomal interval that contains the gene for stunted growth within the subtelomeric region of chromosome 2S. The 2B-2S recombinants that contain the disease resistance genes, but not the gene for stunted growth were developed. They will be released for variety development in wheat breeding. The 2B-2S and 2B-2E recombinants and

associated information will be extremely useful for further engineering of these two pairs of homoeologous chromosomes and chromosome mapping.

Introduction

Wheat (*Triticum aestivum* L., 2n = 6x = 42, genome AABBDD) is one of the most widely cultivated and consumed food crops in the world and provides about 20% of the calories consumed by humans. However, the narrow genetic base makes wheat vulnerable to various environmental and biological threats. One of the feasible approachs to increase the genetic diversity of wheat is to incorporate genes from wild relatives into wheat by chromosome engineering (Friebe et al., 1996; Qi et al., 2007; Rey et al., 2015; Zhang et al., 2015). *Ae. speltoides* (2n=2x=14, genome SS) and *Th. elongatum* (2n=2x=14, genome EE), two wheat-related diploid wild species, contain favorable genes wheat does not have and have been considered as important sources of new genes for wheat improvement.

A large set of common wheat- *Ae. speltoides* cytogenetic materials, including amphiploids, disomic addition and substitution lines, and translocation lines, have been developed (Friebe et al., 2000 and 2011; Liu et al., 2015; Zhang et al., 2015). Many of them exhibited agronomically useful traits, such as resistance to leaf rust (Dvorak, 1977; Dvorak and Knott, 1980; Dubcovsky et al., 1998; Kerber and Dyck, 1990), stem rust (Faris et al., 2008; McIntosh et al., 2008; Marais et al., 2010; Klindworth et al., 2012), greenbug (Dubcovsky et al., 1998), and powdery mildew (Miller et al.,1987; Hsam et al., 2003; Liu et al., 2017).

Th. elongatum has been found to contain desirable genes for many important traits, including stripe rust resistance gene on chromosome 3E (Ma et al., 2000), FHB resistance genes on chromosome 1E and 7E (Oliver et al., 2005; Fu et al., 2012), and the genes for tolerance to waterlogging on chromosomes 2E and 4E (Taeb et al., 1993) and tolerance to salt on

chromosome3E, 4E, and 7E (Dvorak et al., 1988). The wheat-*Th. elongatum* addition, substitution, and translocation lines generally exhibit *Th. elongatum*-derived traits, demonstrating normal expression of the *Th. elongatum* genes under wheat background (Ma et al., 2010; Fu et al., 2012)

Stem rust, caused by the fungal species *Puccinia graminis* Pers.:Pers. f. sp. *tritici* Eriks. & E. Henn., is a destructive disease for wheat. Host resistance is classified as either race-specific or non-race specific. The mechanism of race-specific resistance to stem rust strictly follows the gene-for-gene hypothesis where the recognition of avirulence gene product by a host resistance gene results in an incompatible interaction (Flor, 1956 and 1971; Singh et al., 2011). As with the avirulence genes in the pathogen, most of the host resistance genes to stem rust are dominant (Singh et al., 2011). To date, about 65 stem rust resistance genes have been identified, and approximately 20 of them are derived from wild relatives of wheat. They have been transferred into common wheat from the wild relatives by developing wheat-alien species chromosome translocations through chromosome engineering (Friebe et al., 1996; Gill et al., 2011; Zhang, 2013; Yu et al., 2014; Zhang et al., 2015).

Tan spot and Stagonospora nodorum blotch (SNB), caused by *Pyrenophora tritici-repentis* (anamorph: *Drechslera tritici-repentis*) and *Parastagonospora nodorum* (synonym *Stagonospora nodorum*, teleomorph: *Phaeosphaeria nodorum*), respectively, are two economically significant diseases of wheat in the northern Great Plains of the United States (De Wolf et al., 1998; Singh et al., 2006; McMullen and Adhikari 2009; Liu et al., 2015). These two diseases are major components of the leaf spotting complex and often occur simultaneously (McMullen and Adhikari, 2009). The typical symptoms of tan spot are large, tan-colored lesions often surrounded by chlorotic haloes in susceptible genotypes, or large areas of dead leaf tissue

in highly susceptible genotypes (Faris et al., 2013). Typical SNB disease symptoms include lens-shaped necrotic and chlorotic lesions on susceptible genotypes very similar to that of tan spot. Both pathogens are known to produce necrotrophic effectors (NEs) and undergo an inverse gene-for-gene model (Liu et al., 2004, 2015). The recognition of a specific NE by the corresponding host gene results in compatible interaction, which leads to susceptibility, whereas the lack of NE recognition by the host results in an incompatible interaction and leads to resistance (Friesen et al., 2006; Faris et al., 2013; Liu et al., 2015).

Three NEs have been identified from *P. tritici-repentis* comprising Ptr ToxA, Ptr ToxB, and Ptr ToxC. Each NEs interacts with its corresponding host gene *Tsn1*, *Tsc2*, and *Tsc1*, which reside on wheat chromosome arms 5BL, 2BS, and 1AS, respectively (Faris et al., 1996; Effertz et al., 2001; Friesen and Faris, 2004; Abeysekara et al., 2010). To date, nine host-effector interactions have been identified in the wheat–*P. nodorum* system, including *Tsn1*-SnToxA (Friesen et al., 2006; Liu et al., 2006; Faris et al., 2010), *Snn1*-SnTox1 (Liu et al., 2004a; Reddy et al., 2008), *Snn2*-SnTox2 (Friesen et al., 2007), *Snn3-B1*-SnTox3 (Friesen et al., 2008b), *Snn3-D1*-SnTox3 (Zhang et al., 2011), *Snn4*-SnTox4 (Abeysekara et al., 2009), *Snn5*-SnTox5 (Friesen et al., 2012), *Snn6*-SnTox6 (Gao et al., 2015), and *Snn7*-SnTox7 (Shi et al., 2015). Among them, only two host genes, *Tsn1* corresponding to *P. tritici-repentis* SnToxA and *Snn1* corresponding to *P. nodorum* SnTox1, have been cloned so far (Faris et al., 2010; Shi et al., 2016).

Screening for resistance to tan spot and SNB has been conducted in various wheat germplasm, including synthetic hexaploid wheat (Xu et al., 2004, Friesen et al., 2008a), tetraploid wheat (Chu et al., 2008a, b), hard red spring wheat (Singh et al., 2006; Mergoum et al., 2007), hard red winter wheat (Liu et al., 2015), and wheat-wild grass derivatives (Alam andGustapson, 1988; Oliver et al., 2008). In addition to the susceptibility genes, other qualitative

genes and QTL conferring race non-specific resistance to tan spot and SNB were reported in various wheat lines, which are different from those of the three NE sensitivity loci (Xu et al., 2004; Faris and Friesen, 2005; Friesen et al., 2008; Faris et al., 2013; Patel et al., 2013; Kollers et al., 2014; Liu et al., 2004, 2015; Kariyawasam et al., 2016). This has led to the identification of new sources of resistance to the diseases. Also, these studies indicate the wheat- *P. tritici-repentis* and wheat- *P. nodorum* systems are much more complex than previously thought.

The transfer of the resistance genes from wild relatives to modern wheat is often accompanied by unacceptable agronomic traits due to deleterious genes present in the alien chromosome segment referred to as linkage drag. Homoeologous recombination has been employed to minimize linkage drag by reducing the size of the alien chromosome segment transferred to the wheat genome. Small compensating recombinants with well-delineated molecular and cytological characteristics are invaluable germplasm for wheat breeding (Friebe et al., 1996; Gill et al., 2011; Niu et al., 2011). In this study, we genotyped the CS-*Ae. speltoides* 2B/2S and CS-*Th. elongatum* 2B/2E recombinant lines (developed in Chapter 4) using the wheat 90K SNP arrays, and characterized the recombination breakpoints for each line using molecular markers and GISH. In addition, we evaluated a set of the 2B-2S recombinant lines for reactions to stem rust, *P. nodorum*, and *P. tritici-repentis* to discover novel resistance genes to these pathogens. Also, we detected and physically mapped a deleterious gene for stunted growth on chromosome 2S. All this work will facilitate further engineering of the 2B-2S and 2B-2E homoeologous pairs for gene introgression and genome studies in wheat and its relatives.

Materials and methods

Plant materials

The common wheat landrace 'Chinese Spring' (CS), CS-*Ae. speltoides* disomic substitution line 2S(2B) [DS 2S(2B)], CS-*Th. elongatum* disomic substitution line 2E(2B) [DS 2E(2B)], CS-*Th. elongatum* disomic substitution line 2E(2A) [DS 2E(2A)], CS nullisomic 2B tetrasomic 2D (N2BT2D), CS nullisomic 2D tetrasomic 2A (N2DT2A), as well as 82 2B-2S and 67 2B-2E recombinant lines were genotyped using wheat 90K SNP arrays. A composite bin map was constructed based on the SNP genotyping data and GISH patterns of the recombinants. Seventeen of the 2B-2S recombinants and their parental lines CS and DS 2S(2B) were evaluated for reaction to stem rust. The wheat-*Ae. speltoides* 2B-2S translocation line 'RL6082' (Niu et al., 2011) was used as a check for stem rust evaluation. Twenty of the 2B-2S recombinants as well as their parental lines CS and DS 2S(2B) were evaluated for reaction to *P. tritici-repentis* isolate Asc1 and the *P. nodorum* isolate Sn4. DS 2E(2B), DS 2E(2A), N2BT2D, and N2DT2A were used as controls in the disease evaluation experiment. The wheat accessions 'Br34', 'Salamouni', 'Glenlea', and '6B365' were included as positive check for tan spot and SNB evaluation. A total of 90 2B-2S recombinants and their parental lines were evaluated for morphological characteristics in the greenhouse. All the evaluation experiments were performed with three completely randomized replications.

SNP marker analysis

The selected lines were genotyped with wheat 90K SNP arrays using the Infinium Assay developed by Illumina (Wang et al., 2014). The raw SNP data set was filtered using several criteria (Figure 5.1A). The contig sequences flanking the SNPs were aligned to the the IWGSC Reference Sequence v1.0 assembly of chromosome 2B (RefSeq v1.0) using both Splign and

Position-Specific Iterated BLAST (PSI-BLAST) programs (Altschul et al., 1997; Kapustin et al., 2008; https://wheat-urgi.versailles.inra.fr/). The filtered data set with 1,038 SNPs on chromosome 2B was used for composite bin map construction.

Stem rust resistance evaluation

All selected lines at seedling stage were evaluated in the greenhouse for stem rust resistance against two races including TMLKC and TPMKC as described by Zhang (2013). The infection types (ITs) of the primary leaf on the seedlings were scored at 12-14 days after inoculation using the scoring system developed by Stakman et al. (1962). In this rating system, IT of 0 to 2 were considered resistant, whereas IT of 3 and 4 were considered susceptible. The sympols "-" and "+" indicate small and large pustules, respectively. In the combination ITs, the first digit refers to the predominant IT, and second digit to the secondary IT. For instance, "34" represents the predominant IT of 3 and the secondary IT of 4.

Tan spot resistance evaluation

The selected lines were evaluated for reaction to *P. tritici-repentis* isolate Asc1 as described by Liu et al. (2015). The inoculum preparation and fungal inoculation were done following the procedure of Lamari and Bernier (1989). At 7 days after inoculation, disease was rated on a 1-to-5 scale based on the lesion type shown on the secondary leaf as described by Lamari and Bernier (1989). In this rating system, lesion types of 1.0 and 2.0 were considered resistant, 3.0 was considered moderately resistant to moderately susceptible reaction, 4.0 moderately susceptible, and 5.0 highly susceptible reaction (Lamari and Bernier, 1989). If a line had equal amounts of two reaction types, an intermediate score was given. The readings from three independent inoculation experiments were used to calculate the average.

SNB resistance evaluation

The reaction of the selected lines to *P. nodorum* isolate Sn4 was evaluated as described by Liu et al. (2015). Disease resistance was scored at 7 days after inoculation using a 0 to 5 qualitative lesion-type rating scale, where 0 = highly resistant; 1 = resistant; 2 = moderately resistant; 3 = moderately susceptible; 4 = susceptible; and 5 = highly susceptible (Liu et al., 2004). Plants having equal numbers of two different lesion types were given an intermediate lesion type. The readings from three independent inoculation experiments were used to calculate the average.

Results

Integrative genetic and physical mapping analysis of the SNPs polymorphic for the homoeologous pairs 2B-2S and 2B-2E

A total of 3,158 SNPs mapped to wheat chromosome 2B according to the SNP consensus genetic map of Wang et al. (2014). Of these mapped SNPs, 900 were polymorphic for the homoeologous pair 2B-2S and 977 polymorphic for 2B-2E (Table 5.1). A little less polymorphism for 2B-2S than 2B-2E might result from the closer relationship of the wheat B genome with the *Ae. speltoides* S genome than with the *Th. elongatum* E genome. A total of the 1,069 polymorphic SNPs were physically aligned to chromosome 2B with a single unambiguous hit by searching against the RefSeq v1.0 of chromosome 2B (https://wheat-urgi.versailles.inra.fr/) via BLASTn (Figure 5.1A and Table 5.1). The current size of chromosome 2B in the RefSeq v1.0 is 802 Mb, which covers 86.4% of the entire chromosome 2B (Šafář et al., 2010; https://wheat-urgi.versailles.inra.fr/). Based on the BLASTn results, the 1,069 SNPs were physically positioned to chromosome 2B and plotted against the consensus linkage map of chromosome 2B (Figure 5.1C, APPENDIX F, and Wang et al., 2014). The 1,069

polymorphic SNPs distributed as an "S" curve with an average chromosome-wide recombination ratio of 0.23 cM/Mb. However, the recombination ratio in the centromeric region (209.1-559.4 Mb) was as low as 0.02 cM/Mb, indicating rare homologous recombination within this region. Of the 1,069 SNPs, 663 were polymorphic for both 2B-2S and 2B-2E, 165 polymorphic only for 2B-2S, and 241 polymorphic only for 2B-2E (Figure 5.1B). These polymorphic SNP markers with unambiguous physical positions were used to characterize the 2B-2S and 2B-2E recombinant chromosomes and to construct the composite bin maps.

Table 5.1. SNPs polymorphic for the homoeologous pair 2B-2S and 2B-2E

Homoeologous pairs	Polymorphic SNPs			
	Single hit[a]	No hit	Multiple hits	Total
2B-2S	828	17	55	900
2B-2E	904	17	56	977
Total	1,069	17	63	1,149

[a]BLASTn hit of the contextual sequence flanking the SNP against the IWGSC Reference Sequence v1.0 assembly of chromosome 2B (RefSeq v1.0, https://wheat-urgi.versailles.inra.fr/).

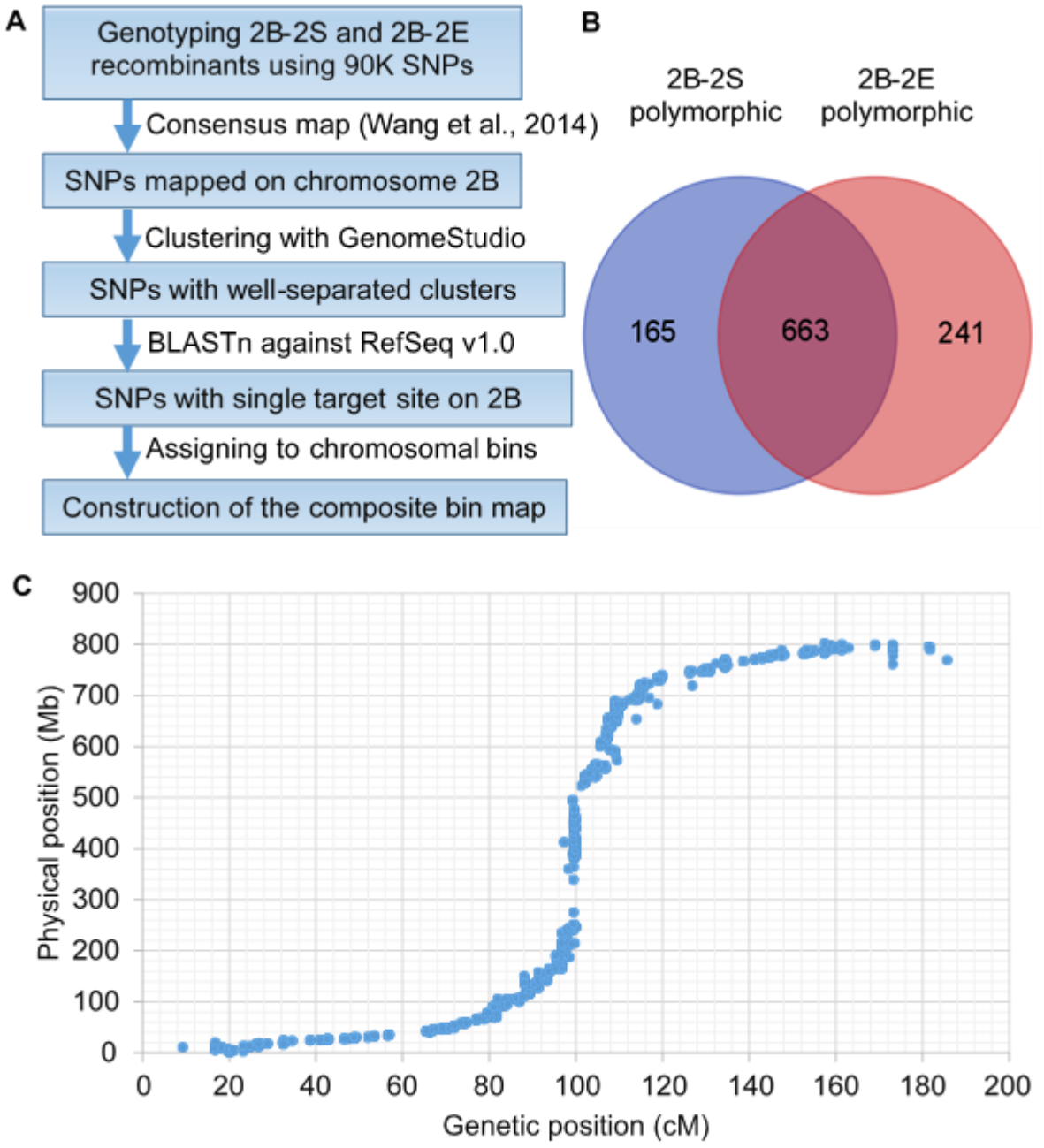

Figure 5.1. Integrative genetic and physical mapping of the SNPs polymorphic for the homoeologous pairs 2B-2S and 2B-2E. (A) Flowchart showing SNP assay and chromosome mapping procedures; (B) Polymorphic SNPs having unique BLASTn hit; (C) Dot plot showing the genetic and physical map positions of the polymorphic SNPs on chromosome 2B.

Construction of the composite bin maps for chromosomes 2B, 2S, and 2E

Some of the 2B-2S and 2B-2E recombinants had the similar compositions of chromosomal segments according to the SNP genotyping and GISH results. Only one of the recombinants with a similar composition was selected for bin map construction. Based on the SNPs genotypes and GISH patterns, we have identified 65 unique breakpoints from the 71 2B-2S recombinants, and 45 unique breakpoints from the 49 2B-2E recombinants (Figure 5.2). Currently, the reference genome sequences of *Ae. speltoides* and *Th. elongatum* are not available. Thus, we performed comparative genomic analysis to assign the polymorphic SNPs to the *Ae. speltoides* 2S and *Th. elongatum* 2E chromosomal segments in the recombinants. This effort was facilitated by the recently released RefSeq v1.0 of common wheat. Consequently, 828 SNPs were assigned to 66 chromosomal bins using the 71 2B-2S recombinants and 904 SNPs to 46 chromsomal bins using the 49 2B-2E recombinants (Figure 5.2). The integrative analysis of the SNP genotyping data for the 2B-2S and 2B-2E recombinants generated a composite bin map of chromosome 2B that composed of 93 bins with 50 on the short arm and 43 on the long arm (Figure 5.3 and APPENDIX F). Totally, 1,037 SNPs were assigned to the composite bin map of chromosome 2B with a density ranging from 1 to 141 SNPs/bin. According to the physical position of the SNPs within a bin, the physical size of the bins was estimated from 0.01 to 157 Mb. The large bins distributed mainly near the centromeric region, indicating rare meiotic homoeologous recombination along that region.

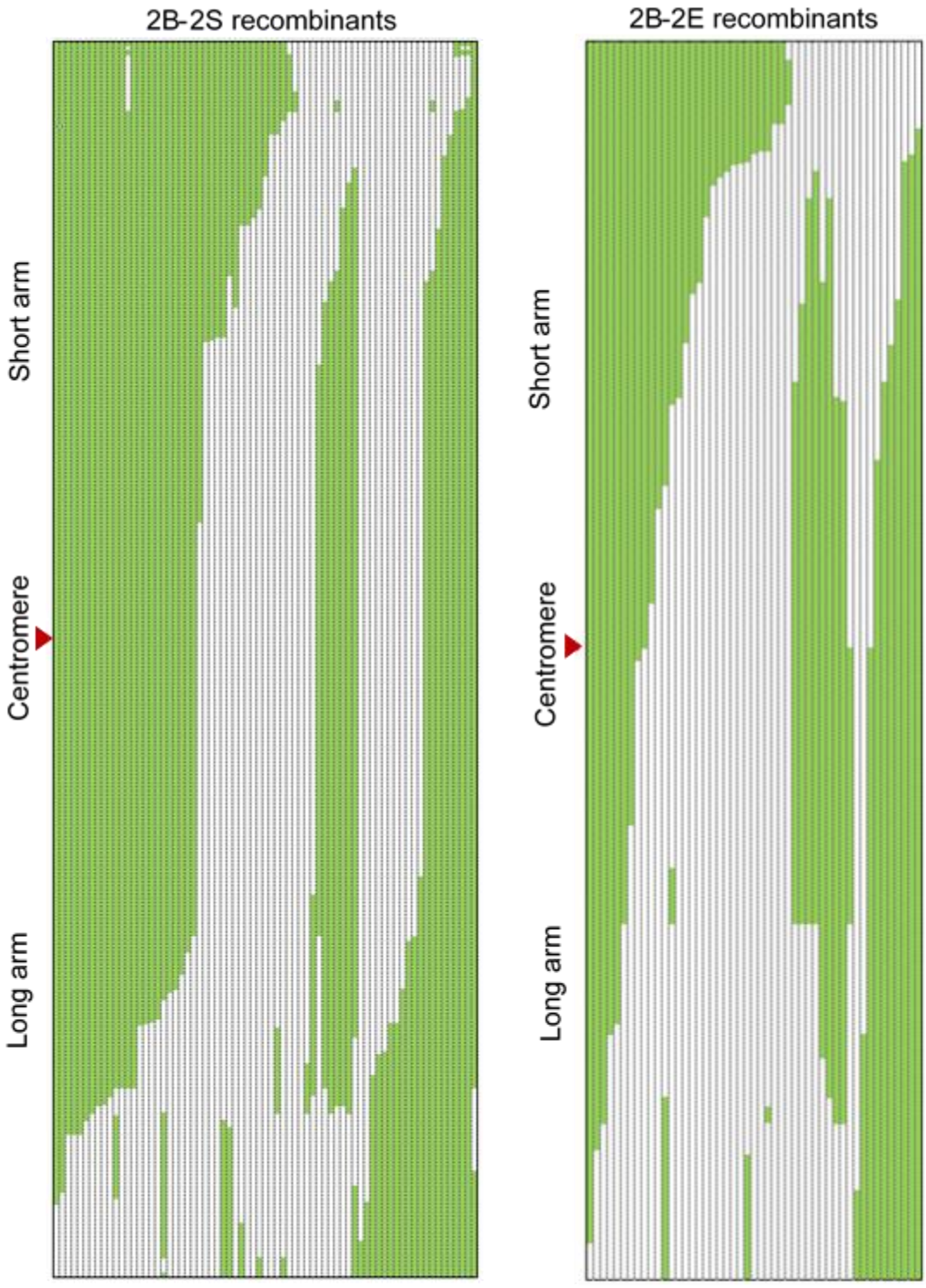

Figure 5.2. SNP-based graphical physical maps of the 2B-2S and 2B-2E recombinants. The left shows the SNP genotypes of the 71 2B-2S recombinants, while the right shows the SNP genotypes of the 49 2B-2E recombinants. The SNP markers are ordered according to their physical positions in the wheat RefSeq v1.0. Green regions indicate the 2S or 2E segments and open regions indicate 2B segments. Red triangles point to the centromeric region.

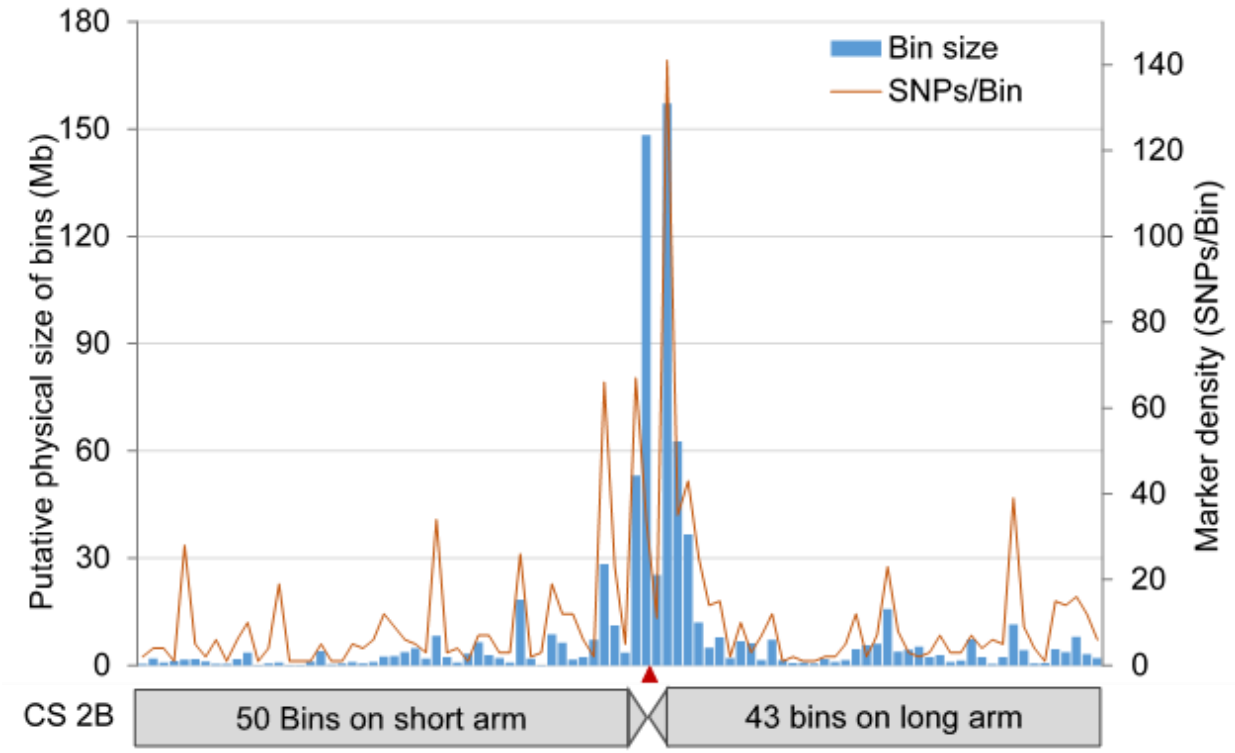

Figure 5.3. SNP distribution across the composite bin map of chromosome 2B. The blue bars indicate the physical size of chromosomal bins and the red curve line indicates the number of SNPs within a chromosomal bin (SNPs/bin).

Physical mapping of the stem rust resistance gene on *Ae. speltoides* chromosome 2S

Both CS DS 2S(2B) and RL6082 showed high levels of resistance to the stem races TPMKC and TMLKC, while CS was susceptible to both races (Figure 5.4 and Table 5.2). In addition, 17 2B-2S recombinants were inoculated with TPMKC and TMLKC. Five of them showed susceptible reactions similar to CS (ZW14-108, ZW14-155, ZW14-166, ZW14-167, and ZW14-169), while 12 of them showed different levels of resistance (Table 5.2). All the resistant 2B-2S recombinant lines shared a common segment from the distal region on the short arm of chromosome 2S, while the susceptible recombinant lines did not contain that chromosomal segment (Figure 5.5 and Table 5.2). This result indicated that the distal segment of the chromosomal arm 2SS should contain the gene for stem rust resistance. According to the recombination breakpoints revealed in the SNP composite bin map, the stem rust resistance gene

was delimited to a 2S segment flanked by the SNP markers *IWB6117* and *IWB39654* (Table 5.3). This chromosome 2S-derived segment was estimated to contain 15.7 Mb DNA within the linkage block of 6.1 cM based on the collinear analysis of CS chromosome 2B and *Ae. speltoides* chromosome 2S (Table 5.3 and Figure 5.10). It is unknown if the stem rust resistance gene identified in this study is different from those previously reported on *Ae. speltoides* chromosome 2S (*Sr32*, *Sr39* and *Sr47*) (Faris et al., 2008; Niu et al., 2011; Klindworth et al., 2012; Mago et al., 2013). Thus, this stem rust resistance gene is temporarily designated *SrAes8t*.

Table 5.2. Reactions of the 2B-2S recombinants and their parental lines to the stem rust races TMLKC and TPMKC

Line	Chromosome 2B and 2S	Infection type					
		TMLKC			TPMKC		
		Rep1	Rep2	Rep3	Rep1	Rep2	Rep3
CS	2B	4	4	4	34	34	34
RL6082	2BS-2SS·2SL	2	12-	2-	12-	12-	12-
DS 2S (2B)	2S	1	2-	1	2-	2-	21
ZW14-108	2SS-2BS·2BL	4	34	4	4	4	4
ZW14-111	2SS·2SL-2BL	22+	2	2	2	2	2
ZW14-115	2BS-2SS·2SL	1-1	1	12-	2-1	1-	1-
ZW14-134	2BS-2SS·2SL	1	1-1	1-1	1-	1	1
ZW14-135	2BS·2BL-2SL	1+	1	1	1	1	12-
ZW14-139	2SS-2BS·2BL	2+	2+	2	2	2+	2
ZW14-141	2BS-2SS·2SL	1-	1-	1-1	1	1-	1-
ZW14-142	2BS-2SS·2SL	1	1	1-1	1	1-1	1-1
ZW14-149	2BS-2SS·2SL	1-1	1-1	1	1	1-1	1
ZW14-154	2SS-2BS·2BL	12-	2	22+	22+	22+	22+
ZW14-155	2SS-2BS·2BL-2SL	4	4	4	4	4	4
ZW14-166	2SS-2BS·2BL-2SL	4	4	4	4	4	4
ZW14-167	2SS-2BS·2BL	4	4	4	3	4	4
ZW14-169	2BS·2BL-2SL	4	4	4	34	4	4
ZW14-174	2SS-2BS·2BL	22+	2	22+	22+	2-2	2
ZW14-180	2SS-2BS-2SS·2SL	1	1	1	1-1	1-1	1-1
ZW14-186	2BS-2SS·2SL	12-	1	1	12-	1-1	1-1

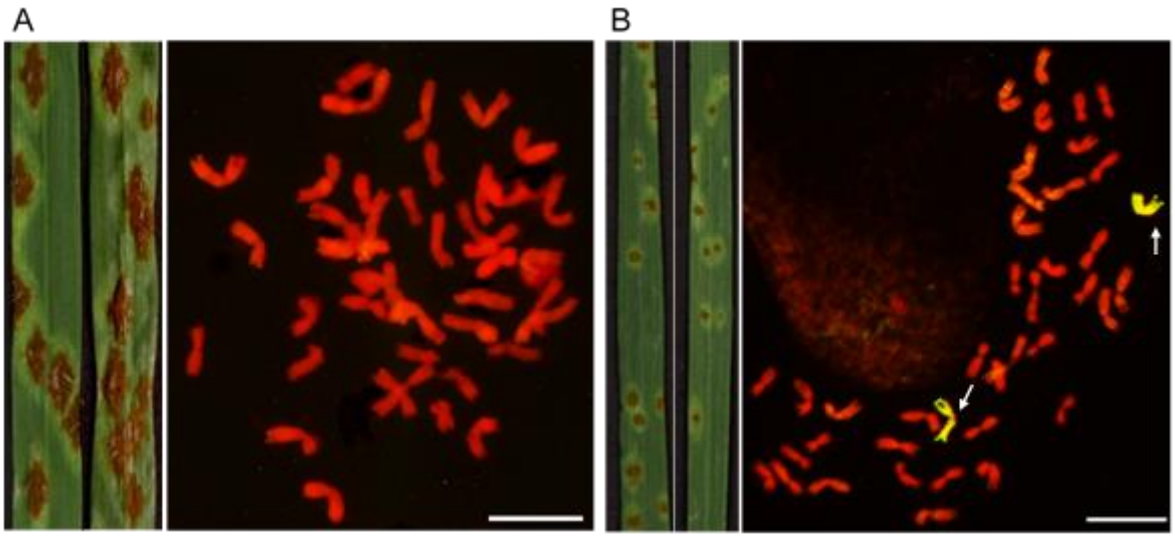

Figure 5.4. The reactions of CS and CS DS 2S(2B) to stem rust. (A) Reactions of CS to the race TPMKC (left leaf) and TMLKC (right leaf) and GISH-painted CS chromosomes; (B) Reactions of CS DS 2S(2B) to the race TPMKC (left leaf) and TMLKC (right leaf) and GISH-painted chromosomes of DS 2S(2B). Wheat chromosomes were painted in red and *Ae. speltoides* chromosome 2S in yellow-green. Arrows point to chromosome 2S. Scale bar =20 μm.

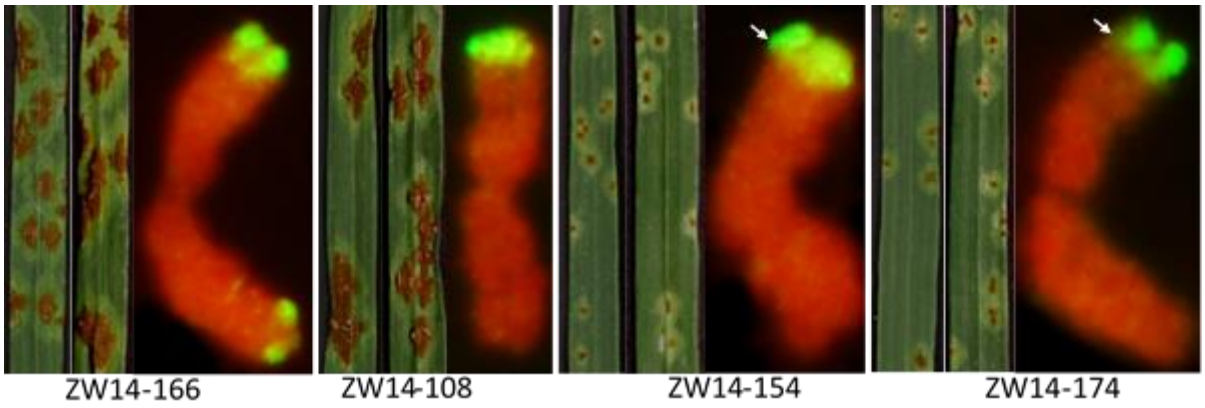

Figure 5.5. Reactions of the four 2B-2S recombinants to TPMKC (left leaf) and TMLKC (right leaf) and their GISH-painted 2B-2S recombinant chromosomes. Segments of chromosome 2B were painted in red, while segments from chromosome 2S were painted in yellow-green. Arrows point to the region containing the stem rust resistance gene on chromosome 2S.

Table 5.3. Physical positions of the SNPs flanking the stem rust resistance gene on chromosome 2S

SNPs	Genetic position (cM)[a]	Bin location[b]	BLASTn[c]		Genotypes of recombinants[d]					
			SNP position (bp)	E value	DS 2S(2B)	CS	ZW14-108	ZW14-166	ZW14-154	ZW14-174
IWB31987	56.86609	28	35,284,630	1E-41	2S	-	2S	2S	2S	2S
IWB31986	56.86609	28	35,367,964	4E-46	2S	-	2S	2S	2S	2S
IWB9207	71.9994	31	50,290,471	4E-46	2S	-	-	2S	2S	2S
IWB46832	71.9994	31	51,890,777	2E-23	2S	-	-	2S	2S	2S
IWB6117	71.9994	32	52,669,992	4E-40	2S	-	-	-	2S	2S
IWB35959	71.9994	32	52,872,937	1E-47	2S	-	-	-	2S	2S
IWB43273	74.46912	34	56,784,859	4E-46	2S	-	-	-	2S	2S
IWB2702	73.74879	34	57,651,518	3E-22	2S	-	-	-	2S	2S
IWB73971	78.99384	37	68,220,786	4E-46	2S	-	-	-	2S	2S
IWB39654	78.11446	37	68,363,434	4E-46	2S	-	-	-	2S	2S
IWB32008	80.77441	38	69,043,295	8E-32	2S	-	-	-	-	2S
IWB21394	79.49277	38	69,344,059	4E-46	2S	-	-	-	-	2S

[a]SNP genetic position in the consensus genetic map of Wang et al. (2014).
[b]Bin location of the SNPs in the composite bin map.
[c]BLASTn against the IWGSC Reference Sequence v1.0 assembly (IWGSC RefSeq v1.0).
[d]The genotype "2S" indicates the presence of the allele from *Ae. speltoides* chromosome 2S, while "-" indicates the absence of the *Ae. speltoides* allele.

Identification of the gene for nontoxin-associated resistance to tan spot and SNB

Chinese Spring (CS), CS DS 2B(2S), CS DS 2E(2B), CS N2BT2D, and four wheat differential lines were evaluated for resistance to *P. nodorum* isolate Sn4 and *P. tritici-repentis* isolate Asc1. The differentials Br34 and Salamouni were resistant to Sn4 and Asc1, while Glenlea and 6B365 were susceptible and showed large necrotic lesions and extensive chlorosis (Figure 5.6). These differentials were used as resistant and susceptible checks in the disease evaluation experiments. Chinese Spring was susceptible to both Asc1 and Sn4, while CS DS 2S(2B) showed significant resistance to both isolates. Both CS N2BT2D and CS DS 2E(2B) showed similar susceptible phenotypes as CS (Table 5.4). Thus, the absence of chromosome 2B in CS did not affect the reaction of CS to both isolates. In addition, no host gene corresponding to Asc1-produced toxins and Sn4-produced toxins has been identified on wheat chromosome 2B. Thus, the *Ae. speltoides* chromosome 2S in CS DS 2S(2B) probably contains the gene for nontoxin-associated resistance to tan spot and SNB.

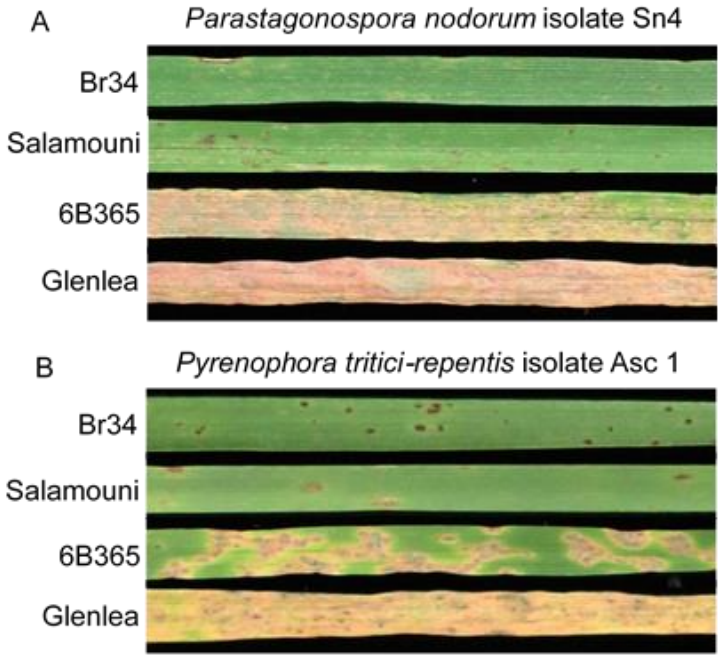

Figure 5.6. Reactions of the resistant and susceptible checks to *Parastagonospora nodorum* isolate Sn4 (A) and *Pyrenophora tritici-repentis* isolate Asc1 (B).

Table 5.4. Reactions of the 2B-2S recombinants to *P. nodorum* isolate Sn4 and *P. tritici-repentis* isolate Asc1

Genotypes	Chromosomes 2A, 2B, 2D, 2S, and 2E	Reaction to pathogens[a]	
		Sn4	Asc1
BR34	2A+2B+2D	0.5	1.5
Salamouni	2A+2B+2D	2	1.5
6B365	2A+2B+2D	3.5	5
Glenlea	2A+2B+2D	5	4.5
CS	2A+2B+2D	3.7	4
CS DS 2S(2B)	2A+2D+2S	1	1
CS N2BT2D	2A+2D	3.5	3.8
CS N2DT2A	2A+2B	4.8	3.5
CS DS 2E(2B)	2A+2D+2E	3.5	3.7
CS DS 2E(2A)	2B+2D+2E	4.3	4.2
ZW14-108-6	2SS-2BS·2BL+2A+2D	1	1
ZW14-111-5	2SS·2SL-2BL+2A+2D	1	1
ZW14-115-7	2BS-2SS·2SL+2A+2D	3.2	3.5
ZW14-135-6	2BS·2BL-2SL+2A+2D	1	1
ZW14-141-8	2BS-2SS·2SL+2A+2D	3.5	3.8
ZW14-142-3	2BS-2SS·2SL+2A+2D	1.7	1.8
ZW14-149-1	2BS-2SS·2SL+2A+2D	3.7	3.5
ZW14-154-3	2SS-2BS·2BL+2A+2D	1.5	1.3
ZW14-166-3	2SS-2BS·2BL-2SL+2A+2D	1	1
ZW14-167-2	2SS-2BS·2BL+2A+2D	1	1.2
ZW14-169-3	2BS·2BL-2SL+2A+2D	3.5	3.5
ZW14-171-4	2SS-2BS·2BL+2A+2D	1	1.5
ZW14-174-2	2SS-2BS·2BL+2A+2D	1.2	1
ZW14-180-2	2SS-2BS-2SS·2SL+2A+2D	3.7	3.2
ZW14-186-1	2BS-2SS·2SL+2A+2D	3.7	3.3
ZW14-162-4	2SS·2SL-2BL+2A+2D	1	1.5
ZW14-173-7	2SS-2BS·2BL+2A+2D	1.5	1.7
ZW14-188-4	2SS-2BS·2BL+2A+2D	1	1.2
ZW14-207-2-1	2SS-2BS·2BL+2A+2D	3.5	3.5
ZW14-505-2	2SS-2BS·2BL+2A+2D	1.5	1.7

[a] Average disease scores of three replications

A total of 20 2B-2S recombinants carrying different segments of chromosome 2S were evaluated for resistance to the isolates Sn4 and Asc1. Seven of them showed similar susceptible reactions to both isolates as CS. The remains 13 recombinants were all resistant to Sn4 (IT 1.0-1.7) and Asc1(IT 1.0-1.8) (Table 5.4). These 13 2B-2S recombinants shared a small subtelomeric

segment on the short arm of chromosome 2S. On the other hand, the recombinants without that chromosomal segment were susceptible to both isolates (Figure 5.7 and Table 5.4). Thus, the subtelomeric segment on the short arm of chromosome 2S should contain the gene(s) for resistance to tan spot and SNB. Apparently, this is a novel *Ae. speltoides*-derived gene conditioning nontoxin-associated resistance to both tan spot and SNB, designated *TsrAes1*/*SnbAes1*. It may confer broad spectrum resistance to tan spot and SNB. Based on the recombination breakpoints revealed in the composite bin map, *TsrAes1*/*SnbAes1* was physically positioned the chromosome 2S segment flanked by the SNP markers *IWB7915* and *IWB60877* (Table 5.5). This chromosome 2S segment was estimated to contain 1.3Mb DNA in a very small linkage block (Table 5.5 and Figure 5.10).

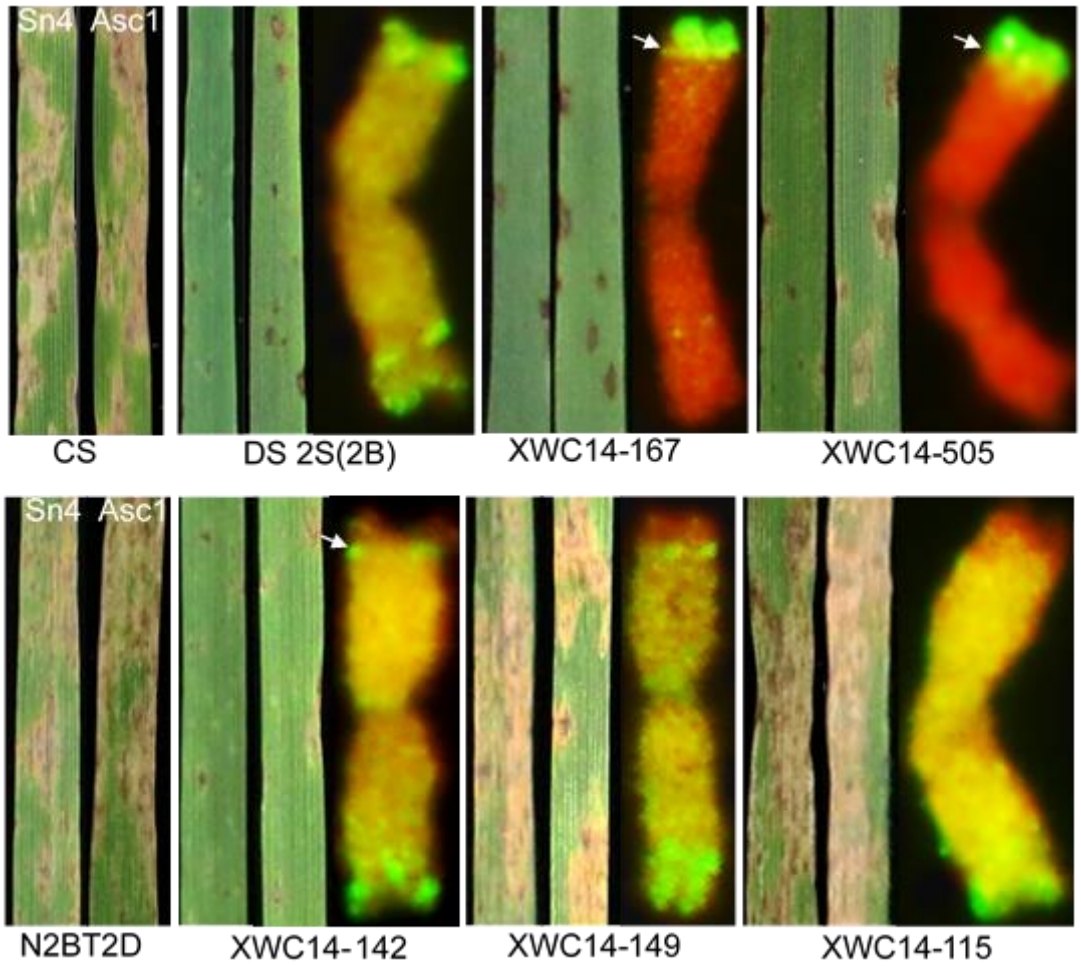

Figure 5.7. Evaluation of seedling reaction of the 2B-2S recombinants to *P. nodorum* isolate Sn4 and *P. tritici-repentis* isolate Asc1. The leaves tissue on left shows reaction to Sn4, while the right one show reaction to Asc1, respectively. Segments of chromosome 2B were painted in red, while segments from chromosome 2S were painted in yellow-green.

Table 5.5. Physical positions of the SNPs flanking the gene for resistance to tan spot and SNB

SNPs	Genetic position (cM)[a]	Bin location[b]	BLASTn[c]		Genotypes of recombinants[d]						
			SNP position (bp)	E value	DS 2S(2B)	CS	ZW14-149	ZW14-115	ZW14-142	ZW14-505	ZW14-167
IWB24314	26.47784	12	14,047,984	2E-41	2S	-	-	-	-	2S	2S
IWB542	26.99237	13	16,813,662	2E-35	2S	-	-	-	-	2S	2S
IWB7915	32.16258	14	16,857,574	4E-46	2S	-	-	-	2S	2S	2S
IWB72375	26.10676	14	16,871,376	8E-29	2S	-	-	-	2S	2S	2S
IWB76943	26.10676	14	16,895,902	1E-100	2S	-	-	-	2S	2S	2S
IWB32197	32.16258	15	17,783,253	1E-41	2S	-	-	-	2S	2S	2S
IWB60877	27.19818	16	18,176,463	9E-44	2S	-	-	-	2S	2S	2S
IWB26232	27.19818	17	18,263,048	1E-24	2S	-	-	2S	2S	-	2S
IWB26233	27.19818	17	18,263,074	9E-41	2S	-	-	2S	2S	-	2S
IWB26231	27.19818	18	18,263,358	4E-46	2S	-	-	2S	2S	-	2S

[a]Wang et al. (2014).

[b]Bin location of the SNPs in the composite bin map.

[c]BLASTn against the IWGSC Reference Sequence v1.0 assembly (IWGSC RefSeq v1.0).

[d]The genotype "2S" indicates the presence of the allele from *Ae. speltoides* chromosome 2S, while "-" indicates the absence of the *Ae. speltoides* allele.

Physical mapping of the gene conferring stunted growth

Chinese Spring DS 2S(2B) exhibited stunted growth similar to its *Ae. speltoide* parent, while CS, CS N2BT2D, and CS 2B/2S double monosomics grew normally (Figure 5.8A). The stunted plants had much shorter stature and narrower leaves than CS, but were fertile (Figure 5.8A). These findings indicate that *Ae. speltoides* chromosome 2S contains the gene for stunted growth.

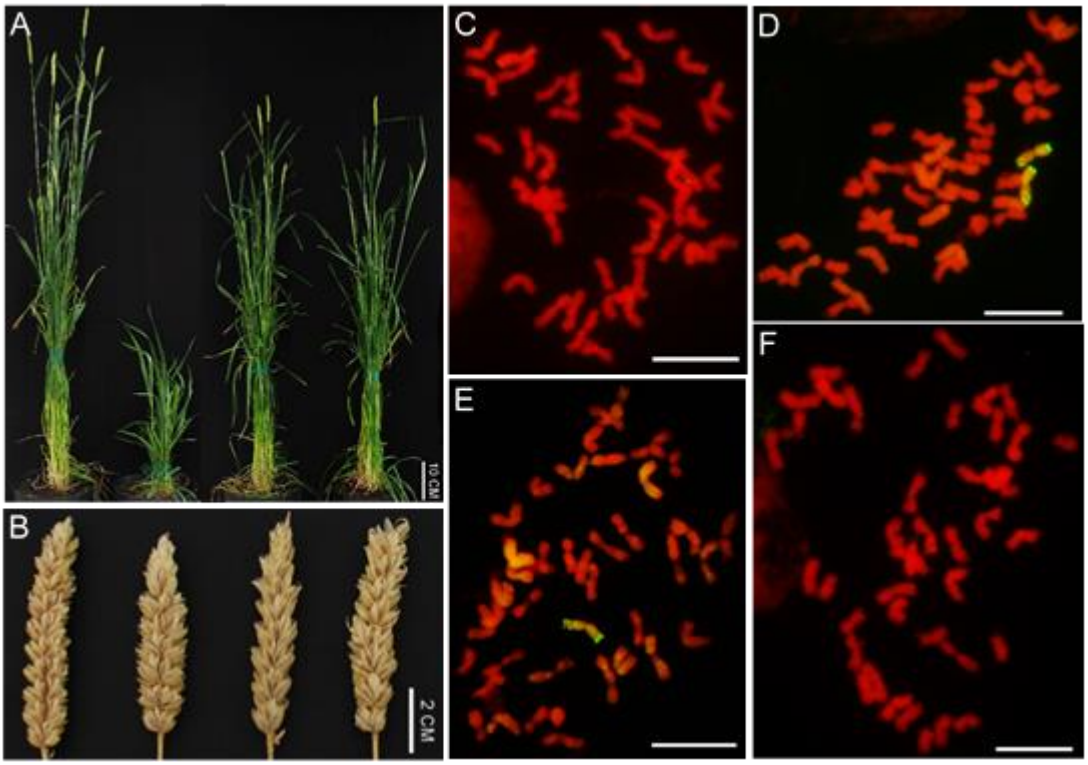

Figure 5.8. Morphological phenotypes and chromosome constitutions of Chinese Spring (CS), CS DS 2S(2B), CS N2BT2D and CS 2B/2S double monosomics. Whole plant (A) and spike (B) morphology of CS, CS DS 2S(2B), CS N2BT2D and CS 2B/2S double monosomics (left to right); and GISH-painted chromosomes of of CS (C), CS DS 2S(2B) (D), CS N2BT2D (E), and CS 2B/2S double monosomics (F). Wheat chromosomes were painted in red, and *Ae. speltoides* chromosome 2S in yellow-green. Scale bar =20 μm.

Totally, 98 2B-2S recombinants were phenotyped for plant growth and morphology in the greenhouse. Fifty-four of them showed stunted growth with short stems and narrow leaves similar to CS DS 2S(2B). The rest 44 recombinants grew normally as CS. The GISH analysis

indicated that all the stunted lines carried a common subtelomeric segment from the short arm of chromosome 2S (Figure 5.9 and APPENDIX G). Interestingly, we found that the recombinant line ZW14-521 seemed to contain the entire short arm of chromosome 2S according to the GISH results, but grew normally. Further analysis of the SNP genotyping data for this recombinant chromosome identified a tiny chromosome 2B segment at the terminal end of its short arm (2BS-2SS·2SL-2BL). Apparently, it was too small to be detected by GISH (Figure 5.9). According to the SNP-derived composite bin map, the gene for stunted growth was physically positioned to the chromosome segment of 2.0 Mb flanked by the SNP markers *IWB59257* and *IWB47291* (Table 5.6 and Figure 5.10). This *Ae. speltoides*-derived gene for stunted growth is novel and designated *SgAes1*.

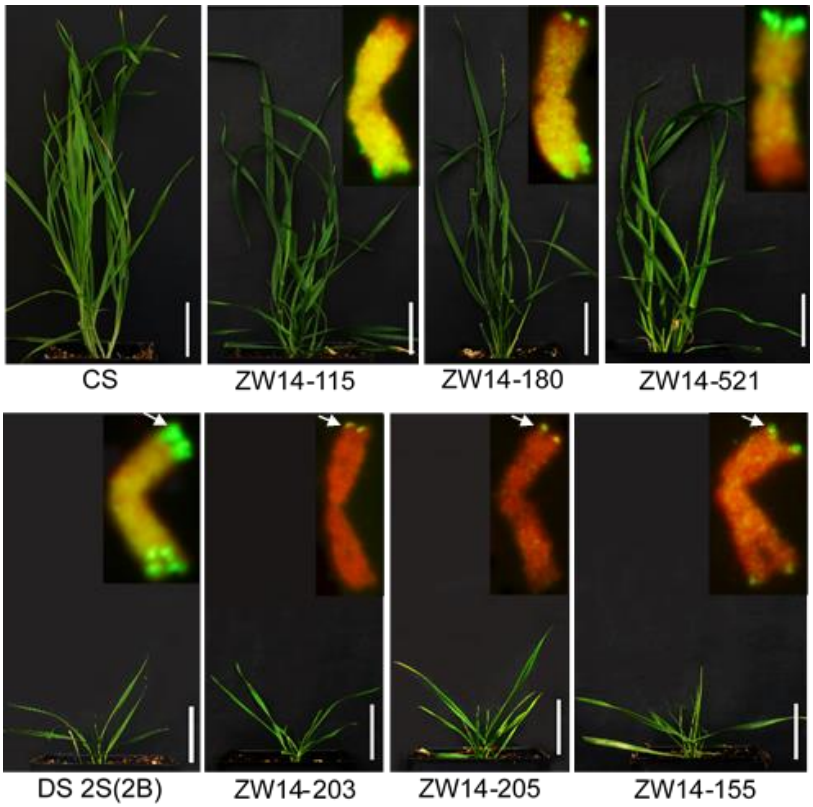

Figure 5.9. Morphological and cytogenetic characteristics of six 2B-2S recombinants and their parental lines. Plant images were captured at 35 days after germination in the greenhouse. Scale bar = 5 centimeter. Segments of chromosome 2B were painted in red and segments of chromosome 2S in yellow-green. Arrows point to the chromosome 2S segment containing the gene for stunted growth.

Table 5.6. Physical positions of the SNPs flanking the gene for stunted growth on chromosome 2S

SNPs	Genetic position (cM)[a]	Bin location[b]	BLASTn[c]		Genotype recombinants[d]							
			SNP position (bp)	e value	DS 2S(2B)	CS	ZW14-115	ZW14-521	ZW14-180	ZW14-205	ZW14-203	ZW14-155
IWB35667	16.87959	6	7,455,359	1E-81	2S	-	-	-	-	-	2S	2S
IWB36143	16.87959	6	7,579,493	3E-19	2S	-	-	-	-	-	2S	2S
IWB59257	18.86909	7	7,909,473	4E-46	2S	-	-	-	-	2S	2S	2S
IWB10720	16.87959	7	8,567,347	4E-46	2S	-	-	-	-	2S	2S	2S
IWB75048	17.93047	8	9,740,995	1E-24	2S	-	-	-	-	2S	2S	2S
IWB47291	16.87959	8	9,871,592	6E-39	2S	-	-	-	-	2S	2S	2S
IWB12069	16.87959	9	10,781,807	4E-46	2S	-	-	-	2S	2S	2S	2S
IWB46236	17.93047	9	10,784,126	4E-38	2S	-	-	-	2S	2S	2S	2S
IWB66351	16.87959	9	11,077,615	2E-41	2S	-	-	-	2S	2S	2S	2S
IWB54334	18.18617	10	11,083,846	4E-46	2S	-	-	-	2S	2S	2S	2S
IWB48525	23.89897	11	11,389,793	7E-43	2S	-	-	2S	-	-	-	2S
IWB3937	25.10889	11	11,390,405	4E-46	2S	-	-	2S	-	-	-	2S

[a] Wang et al. (2014)

[b]SNP-derived composite bin map

[c]BLASTn against the IWGSC Reference Sequence v1.0 assembly (IWGSC RefSeq v1.0).

[d]The genotype "2S" indicates the presence of the allele from *Ae. speltoides* chromosome 2S, while "-" indicates the absence of the *Ae. speltoides* allele.

All the three *Ae. speltoides*-derived genes (*SgAes1*, *TsrAes1*/*SnbAes1*, and *SrAes8t*) identified in this study reside within the distal region of proximately 60.5 Mb on chromosome 2S (Figure 5.10). They were independently incorporated into wheat chromosome 2B by meiotic recombination. The 2B-2S recombinants involving these genes will be useful for variety development in wheat breeding as well as further studies of the genes.

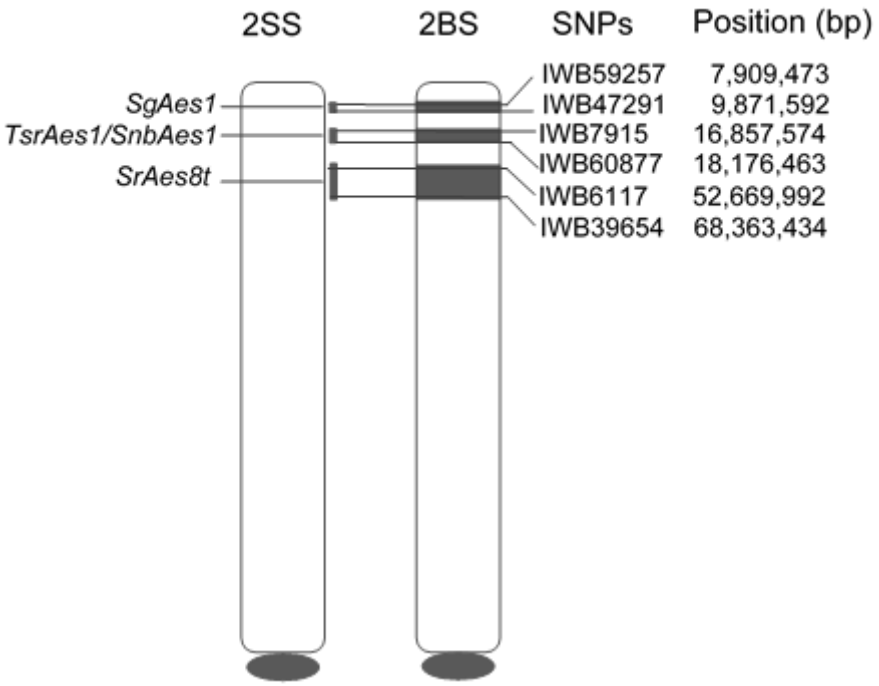

Figure 5.10. Schematic illustration of the chromosome region harboring the three genes identified on *Ae. speltoides* chromosome 2S and its sytenic region on CS chromosome 2B.

Discussion

Common wheat (*T. aestivum*) has a large (17 Gb) and complex genome with more than 80% repetitive DNA sequences (Marcussen et al., 2014; Chapman et al., 2015). It has been a big challenge to physically map and sequence such a large and complex genome. Recent advances in DNA sequencing and related technologies have led to the accomplishment of a quality reference genome sequence for CS wheat (Paux et al., 2008; Breen et al., 2013; Breen et al., 2013; Philippe et al., 2013; Raats et al., 2013; Marcussen et al., 2014; Poursarebani et al., 2014; Kobayashi et al., 2015; Akpinar et al., 2015; Cviková et al., 2015; Chapman et al., 2015;

http://www.wheatgenome.org/). This has tremendously facilitated genome studies in wheat and its relatives. In this study, we identified a total of 1,069 SNPs polymorphic specifically for the homoeologous pairs 2B-2S and 2B-2E from the 90K SNP assay of CS, CS DS2S(2B), and CS DS2E(2B). The polymorphic SNPs were physically aligned to the RefSeq v1.0 of wheat chromosome 2B to determine the physical locations of the SNPs. These SNP markers were used for delineating the GISH-painted 2B-2S and 2B-2E recombinant chromosomes. As a result, wheat chromosome 2B was partitioned into 93 bins based on the SNP genotyping data and GISH patterns of the recombinants. Meanwhile, 1,037 SNPs were assigned to the chromosomal bins, constructing a physical framework of chromosome 2B. This physical framework can be further improved by generating additional bins and new SNP markers for the chromosome. It would be extremely useful for mapping and characterizing such a large and complex genome of wheat, especially for filling the sequence gaps assocated with the complex regions of the wheat genome.

It has been a challenging task to map and clone a wild speices-derived gene incorporated into the wheat genome due to the lack of the genomics resources in the wild species and rare meiotic recombination between alien and wheat chromosomes. In this study, the SNP/GISH-based bin maps of the homoeologous pair 2B-2S and 2B-2E provide a new approach for mapping and cloning of the genes on these two alien chromosomes. The three *Ae. speltoides*-derived genes (*SgAes1*, *TsrAes1*/*SnbAes1*, and *SrAes8t*) targeted in this study were assigned to the specific bins on chromosome 2S by phenotyping the 2B-2S recombinants. The SNPs flanking the chromosomal bins in the critical recombinants were used to anchor the genomic regions harboring the genes. As a result, *SrAes8t*, *TsrAes1*/*SnbAes1*, and *SgAes1* were delimited to a chromosomal interval of 15.7 Mb, 1.3 Mb, 2.0 Mb, respectively. *SrAes8t* mapped proximal to *SgAes1* and *TsrAes1*/*SnbAes1* and resided within the genomic region with lower meiotic

recombination frequecncy than the distal region harboring *SgAes1* and *TsrAes1*/*SnbAes1*. This is probably why *SrAes8t* was delimited into a significantly larger interval than *SgAes1*and *TsrAes1*/*SnbAes1*. In addition, SNP-derived PCR markers, such as semi-thermal asymmetric reverse PCR (STARP), can be developed from the SNPs closely linked to the genes targeted. Evidently, this is an effective approach for mapping and cloning of the alien genes useful in wheat improvement.

Five stem rust resistance genes, including *Sr32*, *Sr39*, *Sr47*, *SrAes1t*, and *SrAes7t*, have been identified from different *Ae. speltoides* accessions, and incorporated into the wheat genome through meiotic homoeologous recombination (Faris et al., 2008; Niu et al., 2011; Klindworth et al., 2012; Mago et al., 2013). *Sr32*, *Sr39*, and *SrAes7t* were located on the short arm, *Sr47* and *SrAes1t* on the long arm of chromosome 2S. It was reported that *SrAes7t* might be the same gene as *Sr39* (Klindworth et al., 2012; Mago et al., 2013). The stem rust resistance gene *SrAes8t* identified on chromosome 2S in this study mapped within the same region as *Sr32* and *Sr39* (Niu et al., 2011; Klindworth et al., 2012; Mago et al., 2013). The line carrying *SrAes8t* [DS 2S(2B)] showed a different infection type (IT) from the line carrying *Sr32* (U5926-2-8), but a similar IT as the line carrying *Sr39* (RWG1) (Zhang, 2013). However, DS 2S(2B) had a different haplotype from RWG1 at the *Sr39*-linked marker loci *Xrwgs27* and *XSr39#22*. Thus, *SrAes8t* might be different from *Sr39* (Zhang, 2013). This needs to be verified by additional studies.

Both tan spot and SNB resistance follows an inverse gene-for-gene model. However, qualitative genes and QTL conferring non-race specific resistance to tan spot were reported in various wheat lines (Faris et al., 2013; Patel et al., 2013; Kollers et al., 2014; Liu et al., 2015; Kariyawasam et al., 2016). This is also the case with the SNB system (Xu et al., 2004; Friesen et al., 2007 and 2008a; Oliver et al., 2008; Liu et al., 2006, 2015). In this study, resistance to both

tan spot and SNB was achieved by transferring chromosomal segments from *Ae. speltoides* to wheat. CS DS 2S(2B) showed significant resistance to both isolates of Asc1 and Sn4, while CS N2BT2D exhibited susceptible reactions similar to CS. These results indicated the mechanism underlying the *Ae. speltoides*-derived resistance might be beyond the reverse gene-for-gene manner. In addition, the host genes *Tsn1* and *Tsc1* corresponding to Asc1-produced toxins mapped to chromosome arms 5BL and 1AS, and none of the genes mediating recognition of Sn4-produced toxins (SnToxA, SnTox1, SnTox2, and SnTox3) resides on chromosome 2B (Faris et al., 1996; Effertz et al., 2001; Friesen and Faris, 2004, Liu et al., 2009). Thus, insensitivity to Asc1- and Sn4-produced toxins does not necessarily imply resistance to isolates Asc1 and Sn4. Apparently, the *Ae. speltoides*-derived resistance identified in this study showed epistatic effects to NE-host interaction mediated susceptibility in both tan spot and SNB systems. It might be a type of nontoxin-associated resistance.

CS DS 2S(2B) exhibited stunted growth, but CS N2BT2D grew normally as CS. Thus, the abnormal stunted growth with CS DS 2S(2B) should be conditioned by *Ae. speltoides* chromosome 2S, not result from the absence of wheat chromosome 2B. In addition, CS 2B/2S double monosomics showed normal growth as CS, suggesting the gene (*SgAes1*) for stunted growth on chromosome 2S is recessive to the one for normal growth on chromosome 2B. The 2B-2S recombinants that contain the disease resistance genes *SrAes8t* and *TsrAes1*/*SnbAes1*, but not *SgAes1* have been developed. They are useful germplasm for variety development in wheat breeding.

References

Abeysekara NS, Friesen TL, Keller B, Faris JD (2009) Identification and characterization of a novel host-toxin interaction in the wheat–Stagonospora nodorum pathosystem. Theor Appl Genet 120:117–126

Abeysekara NS, Friesen TL, Liu ZH, McClean PE, Faris JD (2010) Marker development and saturation mapping of the tan spot Ptr ToxB sensitivity locus *Tsc2* in hexaploid wheat. Plant Genome 3:179–189

Akpinar BA, Magni F, Yuce M, Lucas SJ, Šimková H, Šafář J, Vautrin S, Bergès H, Cattonaro F, Doležel J, Budak (2015) The physical map of wheat chromosome 5DS revealed gene duplications and small rearrangements. BMC Genomics 16:453

Alam KB, Gustapson JP (1988) Tan spot resistance screening of *Aegilops* species. Plant Breed 100:112–118

Altschul SF, Madden TL, Schäffer AA, Zhang J, Zhang Z, Miller W, Lipman DJ (1997) Gapped BLAST and PSI-BLAST: a new generation of protein database search programs, Nucleic Acids Res 25:3389–3402

Breen J, Wicker T, Shatalina M, Frenkel Z, Bertin I, Phillippe R et al. (2013) A physical map of the short arm of wheat chromosome 1A. PLoS One.;11:e80272

Chapman JA., Mascher M, Buluc A, Barry K, Georganas E, Session A et al. (2015) A whole genome shotgun approach for assembling and anchoring the hexaploid bread wheat genome. Genome Biology 16:26–42

Chu CG, Friesen TL, Faris JD, Xu SS (2008a) Evaluation of seedling resistance to tan spot and Stagonospora nodorum blotch in tetraploid wheat. Crop Sci 48:1107–1116

Chu CG, Xu SS, Faris JD, Nevo E, Friesen TL (2008b). Seedling resistance to tan spot and Stagonospora nodorum leaf blotch in wild emmer wheat (*Triticum dicoccoides*). Plant Dis 92:1229–1236

Cviková K, Cattonaro F, Alaux M, Stein N, Mayer KFX, Doležel J et al. (2015) High-throughput physical map anchoring via BAC-pool sequencing. BMC Plant Biol 15:99

De Wolf ED, Effertz RJ, Ali S, Francl, LJ (1998) Vistas of tan spot research. Can J Plant Pathol 20:349–370

Dubcovsky J, Lukaszewski AJ, Echaide M, Antonelli EF, Porter DR (1998) Molecular characterization of two *Triticum speltoides* interstitial translocations carrying leaf rust and greenbug resistance genes. Crop Sci 38:1655–1660

Dvorak J (1977) Transfer of leaf rust resistance from *Aegilops speltoides* to *Triticum aestivum*. Can J Genet Cytol 19:133–141

Dvorak J, Knott DR (1980) Chromosome location of two leaf rust resistance genes transferred from *T. speltoides* to *T. aestivum*. Can J Genet Cytol 22:281–289

Effertz RJ, Anderson JA, Francl LJ (2001) Restriction fragment length polymorphism mapping of resistance to two races of *Pyrenophora tritici–repentis* in adult and seedling wheat. Phytopathology 91:572–578

Faris JD, Anderson JA, Francl LJ, Jordahl JG (1996) Chromosomal location of a gene conditioning insensitivity in wheat to a necrosis-inducing culture filtrate from *Pyrenophora tritici– repentis*. Phytopathology 86:459–463

Faris JD, Friesen TL (2005) Identification of quantitative trait loci for race-nonspecific resistance to tan spot of wheat. Theor Appl Genet 111:386–392

Faris JD, Xu SS, Cai X, Friesen TL, Jin Y (2008) Molecular and cytogenetic characterization of a durum wheat-*Aegilops speltoides* chromosome translocation conferring resistance to stem rust. Chromosome Res 16:1097–1105

Faris JD, Zhang Z, Lu HJ, Lu SW, Reddy L, Cloutier S, Fellers JP, Meinhardt SW, Rasmussen JB, Xu SS, Oliver RP, Simons KJ, Friesen TL (2010) A unique wheat disease resistance-like gene governs effector-triggered susceptibility to necrotrophic pathogens. Proc Natl Acad Sci USA 107:13544–13549

Faris JD, Liu Z, Xu SS (2013) Genetics of tan spot resistance in wheat. Theor Appl Genet 126:2197–2217

Flor HH (1956) The complimentary genetics systems in flax and flax rust. Adv Genet 8:29–54

Flor HH (1971) Current status of the gene-for-gene concept. Annu Rev Phytopathol 9:275–296

Friebe B, Jiang J, Raupp WJ, McIntosh RA, Gill BS (1996) Characterization of wheat–alien translocations conferring resistance to diseases and pests: current status. Euphytica 91:59–87

Friebe B, Qi LL, Nasuda S, Zhang P, Tuleen NA, Gill BS (2000) Development of a complete set of *Triticum aestivum-Aegilops speltoides* chromosome addition lines. Theor Appl Genet 101:51–58

Friebe B, Qi LL, Liu C, Gill BS (2011) Genetic compensation abilities of *Aegilops speltoides* chromosomes for homoeologous B-genome chromosomes of polyploid wheat in disomic S(B) chromosome substitution lines. Cytogenet Genome Res 134:144–150

Friesen TL, Stukenbrock EH, Liu ZH, Meinhardt SW, Ling H, Faris JD, Rasmussen JB, Solomon PS, Mcdonald BA, Oliver RP (2006) Emergence of a new disease as a result of interspecific virulence gene transfer. Nat Genet 38:953–956

Friesen TL, Faris JD (2004) Molecular mapping of resistance to *Pyrenophora tritici–repentis* race 5 and sensitivity to Ptr ToxB in wheat. Theor Appl Genet 109:464–471

Friesen TL, Meinhardt SW, Faris JD (2007) The Stagonospora nodorum - wheat pathosystem involves multiple proteinaceous host-selective toxins and corresponding host sensitivity genes that interact in an inverse gen-for-gene manner. Plant J 51:681–692

Friesen TL, Xu SS, Harris MO (2008a) Stem rust, tan spot, Stagonospora nodorum blotch, and hessian fly resistance in Langdon durum-*Aegilops tauschii* synthetic hexaploid wheat lines. Crop Sci 48:1062–1070

Friesen TL, Zhang ZC, Solomon PS, Oliver RP, Faris JD (2008b) Characterization of the interaction of a novel Stagonospora nodorum host–selective toxin with a wheat susceptibility gene. Plant Physiol 146:682–693

Friesen T, Chu C, Xu SS, Faris J (2012) SnTox5–Snn5: a novel Stagonospora nodorum effector–wheat gene interaction and its relationship with the SnToxA-*Tsn1* and SnTox3-*Snn3*-B1 interactions. Mol Plant Pathol 13:1101–1109

Fu S, Lv Z, Qi B, Guo X, Li J, Liu B, Han F (2012) Molecular cytogenetic characterization of wheat-*Thinopyrum elongatum* addition, substitution and translocation lines with a novel source of resistance to wheat Fusarium head blight. J Genet Genomics 39:103–110

Gao Y, Faris JD, Liu ZH, Xu SS, Friesen TL (2015) Identification and characterization of the SnTox6–*Snn6* interaction in the wheat–Stagonospora nodorum pathosystem. Mol Plant Microbe Interact 28:615–625

Gill BS, Friebe BR, White FF (2011) Alien introgressions represent a rich source of genes for crop improvement. Proc Natl Acad Sci USA 108:7657–7658

Kapustin Y, Souvorov A, Tatusova T, Lipman D (2008) Splign: algorithms for computing spliced alignments with identification of paralogs. Biol Direct 3:20

Kariyawasam GK, Carter AH, Rasmussen JB, Faris JD, Xu SS, Mergoum M, Liu ZH (2016) Genetic relationships between race-nonspecific and race-specific interactions in the wheat-*Pyrenophora tritici-repentis* pathosystem. Theor Appl Genet 129:897–908

Kerber ER, Dyck PL (1990) Transfer to hexaploid wheat of linked genes for adult plant leaf rust and seedling stem rust resistance from an amphiploid of *Aegilops speltoides* x *Triticum monococcum.* Genome 33:530–537

Klindworth DL, Niu Z, Chao S, Friesen TL, Jin Y, Faris JD, Cai X, Xu SS (2012) Introgression and characterization of a goatgrass gene for a high level of resistance to Ug99 stem rust in tetraploid wheat. G3 2:665–673

Kollers S, Rodemann B, Ling J, Korzun V, Ebmeyer E, Argillier O, Hinze M, Plieske J, Kulosa D, Ganal MW, Röder MS (2014) Genome-wide association mapping of tan spot resistance (*Pyr–enophora tritici–repentis*) in European winter wheat. Mol Breed 34:363–371

Lamari L, Bernier CC (1989) Evaluation of wheat lines and cultivars to tan spot (*Pyrenophora tritici–repentis*) based on lesion type. Can J Plant Pathol 11:49–56

Liu W, Koo D, Bernd Friebe B, Gill BS (2016) A set of *Triticum aestivum-Aegilops speltoides* Robertsonian translocation lines. Theor Appl Genet 129: 2359–2368

Liu W, Koo D–H, Xia Q, Li C, Bai F, Song Y, Friebe B, Gill BS (2017) Homoeologous recombination-based transfer and molecular cytogenetic mapping of powdery mildew-resistant gene *Pm57* from *Aegilops searsii* into wheat. Theor Appl Genet 130: 841–848

Liu ZH, Friesen TL, Rasmussen JB, Ali S, Meinhardt SW, Faris JD (2004) Quantitative trait loci analysis and mapping of seedling resistance to Stagonospora nodorum leaf blotch in wheat. Phytopathology 94:1061–1067

Liu ZH, Faris JD, Oliver RP, Tan K, Solomon PS, Mcdonald MC, Mcdonald BA, Nunez A, Lu S, Rasmussen JB, Friesen TL (2009) SnTox3 acts in effector triggered susceptibility to induce disease on wheat carrying the *Snn3* gene. PLoS Pathog 5:1–15

Liu ZH, El–Basyoni I, Kariyawasam G, Zhang G, Fritz A, Hansen JM, Marais F, Friskop AJ, Chao S, Akhunov E, Baenziger PS (2015) Evaluation and association mapping of resistance to tan spot and Stagonospora nodorum blotch in adapted winter wheat germplasm. Plant Dis 99:1333–1341

Ma JX, Zhou RH, Dong YS, Jia JZ (2000) Control and inheritance of resistance to yellow rust in *Triticum aestivum-Lophopyrum elongatum* chromosome substitution lines. Euphytica 111:57–60

Mago R, Verlin D, Zhang P, Bansal U, Bariana H, Jin Y, Ellis J, Hoxha S, Dundas I (2013) Development of wheat-*Aegilops speltoides* recombinants and simple PCR-based markers for *Sr32* and a new stem rust resistance gene on the 2S#1 chromosome. Theor Appl Genet 126:2943–2955

Marais GF, Bekker TA, Eksteen A, McCallum B, Fetch T, Marais AS (2010) Attempts to remove gametocidal genes co-transferred to common wheat with rust resistance from Aegilops speltoides. Euphytica 171:71–85

Marcussen T, Sandve SR, Heier L, Spannagl M, Pfeifer M, IWGSC, Jakobesn KS, Wulff BBH, Steuernagel B, Mayer KFX, Olsen OA (2014) Ancient hybridizations among the ancestral genomes of bread wheat. Science 345:1250092–1–4

McIntosh, R.A., Y. Yamazaki, J. Dubcovsky, J. Rogers, C. Morris, D.J. Somers, R. Appels, and K.M. Devos. 2008. Catalogue of gene symbols for wheat. Available from http://wheat.pw.usda.gov/GG2/Triticum/wgc/2008/ (accessed 20 Aug. 2009; verifi ed 4 May 2010). USDA, Beltsville, MD

McMullen MD, Adhikari T (2009) Fungal Leaf Spot Diseases of Wheat: tan spot, stagonospora nodorum blotch and septoria tritici blotch. North Dakota State University Extension Service. PP1249

Mergoum M, Singh PK, Ali S, Elias EM, Anderson JA, Glover KD, Adhikari TB (2007) Reaction of elite wheat genotypes from the northern Great Plains of North America to Septoria diseases. Plant Dis 91:1310–1315

Oliver RE, Cai X, Xu SS, Chen X, Stack RW (2005) Wheat-alien species derivatives: a novel source of resistance to Fusarium head blight in wheat. Crop Sci 45:1353–1360

Oliver RE, Cai X, Wang RC, Xu SS, Friesen TL (2008) Resistance to tan spot and Stagonospora nodorum blotch in wheat-alien species derivatives. Plant Dis 92:150–157

Patel JS, Mamidi S, Bonman JM, Adhikari TB (2013) Identification of QTL in spring wheat associated with resistance to a novel isolate of *Pyrenophora tritici-repentis*. Crop Sci 53:842–852

Paux E, Sourdille P, Salse J, Saintenac C, Choulet F, Leroy P et al. (2008) A physical map of the 1–gigabase bread wheat chromosome 3B. Science 322:101–4.

Philippe R, Paux E, Bertin I, Sourdille P, Choulet F, Laugier C et al. (2013) A high density physical map of chromosome 1BL advances evolutionary studies, map-based cloning and sequencing in wheat. Genome Biol 14:R64

Poursarebani N, Nussbaumer T, Šimková H, Šafář J, Witsenboer H, van Oeveren J et al. (2014) Whole genome profiling (WGP™) and shotgun sequencing delivers an anchored, gene decorated, physical map assembly of bread wheat chromosome 6A. Plant J 79:334–47

Qi LL, Friebe B, Zhang P, Gill BS (2007) Homoeologous recombination, chromosome engineering and crop improvement. Chromosome Res 15:3–19

Raats D, Frenkel Z, Krugman T, Dodek I, Sela H, Šimková H et al. (2013) The physical map of wheat chromosome 1BS provides insights into its gene space organization and evolution. Genome Biol 14:R138

Reddy L, Friesen TL, Meinhardt SW, Chao S, Faris JD (2008) Genomic analysis of the *Snn1* locus on wheat chromosome arm 1BS and the identification of candidate genes. Plant Genome 1:55–66

Rey E, Molnár I, Doležel J (2015) Genomics of wild relatives and alien introgressions. In: Molnár-Láng M, Ceoloni C, Doležel J (eds) Alien introgression in wheat. Springer International Publishing, Switzerland, pp 374–381

Shi G, Friesen TL, Saini J, Xu SS, Rasmussen JB, Faris JD (2015) The wheat gene confers susceptibility on recognition of the necrotrophic effector SnTox7. Plant Genome 8:1–10

Shi G, Zhang Z, Friesen TL, Raats D, Fahima T, Brueggeman RS, Lu S, Trick HN, Liu Z, Chao W, Frenkel Z, Xu SS, Rasmussen JB, Faris JD (2016) The hijacking of a receptor kinase-driven pathway by a wheat fungal pathogen leads to disease. Sci Adv 2:e1600822

Singh PK, Mergoum M, Ali S, Adhikari TB, Elias EM, Anderson JA, Glover KD, Berzonsky, WA (2006) Evaluation of elite wheat germplasm for resistance to tan spot. Plant Dis 90:1320–1325

Singh RP, Hodson DP, Huerta–Espino J, Jin Y, Bhavani S, Njau P, Herrera-Foessel S, Singh PK, Singh S, Govindan V (2011) The Emergence of Ug99 races of the stem rust fungus is a threat to world wheat production. Annu Rev Phytopathol 49:465–481

Stakman EC, Stewart DM, Loegering WQ (1962) Identification of physiologic races of *Puccinia graminis* var. *tritici*. US Dept Agric ARS–E6/7

Taeb M, Koebner RMD, Forster BP (1993) Genetic variation for waterlogging tolerance in the Triticeae and the chromosomal location of genes conferring waterlogging tolerance in Thinopyrum elongatum. Genome 36, 825–830

Wang S, Wong D, Forrest K, Allen A, Huang BE, Maccaferri M, Salvi S, Milner SG, Cattivelli L, Mastrangelo AM, Whan A, Stephen S, Barker G, Wieseke R, Plieske J, International Wheat Genome Sequencing Consortium, Lillemo M, Mather D, Appels R, Dolferus R, Brown–Guedira G, Korol A, Akhunova AR, Feuillet C, Salse J, Morgante M, Pozniak C, Luo MC, Dvorak J, Morell M, Dubcovsky J, Ganal M, Tuberosa R, Lawley C, Mikoulitch I, Cavanagh C, Edwards KJ, Hayden M, Akhunov E (2014) Characterization of polyploid wheat genomic diversity using a high–density 90,000 single nucleotide polymorphism array. Plant Biotechnol J 12:787–796

Xu SS, Friesen TL, Mujeeb-Kazi A (2004) Seedling resistance to tan spot and Stagonospora nodorum blotch in synthetic hexaploid wheats. Crop Sci 44:2238–2245

Yu LX, Barbier H, Rouse MN, Singh S, Singh RP, Bhavani S, Huerta-Espino J, Sorrells ME (2014) A consensus map for Ug99 stem rust resistance loci in wheat. Theor Appl Genet 127:1561–1581

Zhang P, Dundas IS, McIntosh RA, Xu SS, Park RF, Gill BS, Friebe B (2015) Wheat-*Aegilops* introgressions. In: Molnár-Láng M, Ceoloni C, Doležel J (eds) Alien introgression in wheat. Springer International Publishing, Switzerland, pp 221–44.

Zhang QJ (2013) Development and characterization of wheat germplasm for resistance to stem rust Ug99 in wheat. PhD Dissertation. North Dakota State University, Fargo, North Dakota

Zhang Z, Friesen TL, Xu SS, Shi GJ, Liu Z, Rasmussen JB, Faris JD (2011) Two putatively homoeologous wheat genes mediate recognition of SnTox3 to confer effectortriggered susceptibility to Stagonospora nodorum. Plant J 65:27–38

APPENDIX A. WHEAT ACCESSIONS SURVEYED FOR AE. SPELTOIDES CHROMATIN BY GISH

GRIN ID	Species	Genome	Origin	Source	*Ae. speltoides* segment on 1BL
PI 366801	*T. aestivum*	AABBDD	Afghanistan	T-CAP	+
PI 221500	*T. aestivum*	AABBDD	Afghanistan	T-CAP	+
PI 48592	*T. aestivum*	AABBDD	Algeria	T-CAP	+
PI 94363	*T. aestivum*	AABBDD	Armenia	T-CAP	+
CATALINA	*T. aestivum*	AABBDD	Australia	T-CAP	+
CASCADES	*T. aestivum*	AABBDD	Australia	T-CAP	+
PI 350861	*T. aestivum*	AABBDD	Austria	T-CAP	+
PI 181161	*T. aestivum*	AABBDD	Belgium	T-CAP	+
PI 481728	*T. aestivum*	AABBDD	Bhutan	T-CAP	+
PI 374670	*T. aestivum*	AABBDD	Bosnia	T-CAP	+
PI 184141	*T. aestivum*	AABBDD	Bosnia	T-CAP	+
Canthatch	*T. aestivum*	AABBDD	Canada	T-CAP	+
cltr 8347	*T. aestivum*	AABBDD	China	T-CAP	+
PI 264962	*T. aestivum*	AABBDD	Croatia	T-CAP	+
PI 584791	*T. aestivum*	AABBDD	Czech Republic	T-CAP	+
PI 361845	*T. aestivum*	AABBDD	Denmark	T-CAP	+
Cltr 14974	*T. aestivum*	AABBDD	Egypt	T-CAP	+
Zobel	*T. aestivum*	AABBDD	Europe	T-CAP	+
PI 295996	*T. aestivum*	AABBDD	Finland	T-CAP	+
PI 48200	*T. aestivum*	AABBDD	France	T-CAP	+
PI 572656	*T. aestivum*	AABBDD	Georgia	T-CAP	+
PI 286046	*T. aestivum*	AABBDD	Germany	T-CAP	+
PI 265018	*T. aestivum*	AABBDD	Greece	T-CAP	+
PI 254410	*T. aestivum*	AABBDD	Hungary	T-CAP	+
PI 164435	*T. aestivum*	AABBDD	India	T-CAP	+
CItr 4311	*T. aestivum*	AABBDD	Iran	T-CAP	+
PI 626491	*T. aestivum*	AABBDD	Iran	T-CAP	+
PI 178212	*T. aestivum*	AABBDD	Iraq	T-CAP	+
PI 384028	*T. aestivum*	AABBDD	Israel	T-CAP	+
PI 66087	*T. aestivum*	AABBDD	Italy	T-CAP	+
PI 266147	*T. aestivum*	AABBDD	Italy	T-CAP	+
PI 81046	*T. aestivum*	AABBDD	Japan	T-CAP	+
PI 639289	*T. aestivum*	AABBDD	Kazakhstan	T-CAP	+
PI 378354	*T. aestivum*	AABBDD	Macedonia	T-CAP	+
CM1_74	*T. aestivum*	AABBDD	Mexico	T-CAP	+
CM2_75	*T. aestivum*	AABBDD	Mexico	T-CAP	+
PI 362698	*T. aestivum*	AABBDD	Montenegro	T-CAP	+

GRIN ID	Species	Genome	Origin	Source	*Ae. speltoides* segment on 1BL
PI 345386	*T. aestivum*	AABBDD	Montenegro	T-CAP	+
PI 429624	*T. aestivum*	AABBDD	Nepal	T-CAP	+
PI 572818	*T. aestivum*	AABBDD	Pakistan	T-CAP	+
PI 478140	*T. aestivum*	AABBDD	Pakistan	T-CAP	+
PI 58339	*T. aestivum*	AABBDD	Russian Federation	T-CAP	+
PI 184210	*T. aestivum*	AABBDD	Serbia	T-CAP	+
PI 48147	*T. aestivum*	AABBDD	Spain	T-CAP	+
cltr 9353	*T. aestivum*	AABBDD	Sweden	T-CAP	+
PI 350884	*T. aestivum*	AABBDD	Switzerland	T-CAP	+
PI 182695	*T. aestivum*	AABBDD	Syria	T-CAP	+
PI 654230	*T. aestivum*	AABBDD	Tajikistan	T-CAP	+
PI 654158	*T. aestivum*	AABBDD	Tajikistan	T-CAP	+
Cltr 15456	*T. aestivum*	AABBDD	Tunisia	T-CAP	+
PI 166727	*T. aestivum*	AABBDD	Turkey	T-CAP	+
PI 166545	*T. aestivum*	AABBDD	Turkey	T-CAP	+
PI 5641	*T. aestivum*	AABBDD	Ukraine	T-CAP	+
98S0127-06	*T. aestivum*	AABBDD	USA	T-CAP	+
Baisanyuehuang	*T. aestivum*	AABBDD	USA	T-CAP	+
Chadinghongmai	*T. aestivum*	AABBDD	USA	T-CAP	+
Cardinal	*T. aestivum*	AABBDD	USA	T-CAP	+
CI13113	*T. aestivum*	AABBDD	USA	T-CAP	+
ALSEN	*T. aestivum*	AABBDD	USA	T-CAP	+
98X371-3C	*T. aestivum*	AABBDD	USA	T-CAP	+
ARS970184-1C	*T. aestivum*	AABBDD	USA	T-CAP	+
PI 211701	*T. compactum*	AABBDD	Turkey	NSGC	+
PI 278541	*T. compactum*	AABBDD	Syria	NSGC	+
PI 366118	*T. compactum*	AABBDD	Egypt	NSGC	+
PI 565431	*T. compactum*	AABBDD	USA	NSGC	+
PI 665048	*T. compactum*	AABBDD	USA	NSGC	+
PI 355509	*T. macha*	AABBDD	Former Soviet Union	NSGC	+
PI 428179	*T. macha*	AABBDD	Iran	NSGC	+
PI 542466	*T. macha*	AABBDD	USA	NSGC	+
CItr 17764	*T. spelta*	AABBDD	USA	NSGC	+
PI 191392	*T. spelta*	AABBDD	Ethiopia	NSGC	+
PI 225271	*T. spelta*	AABBDD	Iran	NSGC	+
PI 225295	*T. spelta*	AABBDD	Iran	NSGC	+
PI 355649	*T. spelta*	AABBDD	Germany	NSGC	+

GRIN ID	Species	Genome	Origin	Source	*Ae. speltoides* segment on 1BL
PI 355697	*T. spelta*	AABBDD	Belgium	NSGC	+
PI 367199	*T. spelta*	AABBDD	Afghanistan	NSGC	+
PI 367202	*T. spelta*	AABBDD	Afghanistan	NSGC	+
PI 378480	*T. spelta*	AABBDD	Macedonia	NSGC	+
PI 469032	*T. spelta*	AABBDD	Spain	NSGC	+
PI 70711	*T. sphaerococcum*	AABBDD	Iraq	NSGC	+
PI 83402	*T. sphaerococcum*	AABBDD	China	NSGC	+
PI 168685	*T. sphaerococcum*	AABBDD	USA	NSGC	+
PI 277141	*T. sphaerococcum*	AABBDD	Germany	NSGC	+
PI 277165	*T. sphaerococcum*	AABBDD	Pakistan	NSGC	+
PI 428342	*T. vavilovii*	AABBDD	Sweden	NSGC	+
Israel-A	*T. dicoccoides*	AABB	Israel	NSGC	+
PI 272582	*T. dicoccoides*	AABB	Hungary	NSGC	+
PI 481521	*T. dicoccoides*	AABB	Israel	NSGC	+
PI 272564	*T. polonicum*	AABB	Hungary	NSGC	+
PI 223171	*T. polonicum*	AABB	Jordan	NSGC	+
PI 94666-1	*T. dicoccum*	AABB	Russian Federation	NSGC	+
CItr 14133-1	*T. dicoccum*	AABB	USA	NSGC	+
PI 283889	*T. carthlicum*	AABB	Iran	NSGC	+
PI 94751	*T. carthlicum*	AABB	Georgia	NSGC	+
CItr 7863	*T. turgidum*	AABB	Ethiopia	NSGC	+
CItr 8115	*T. turgidum*	AABB	China	NSGC	+
PI 192641	*T. turanicum*	AABB	Morocco	NSGC	+
PI 191599	*T. turanicum*	AABB	Morocco	NSGC	+
PI 383914	*T. durum*	AABB	Argentina	T-CAP	+
PI 390208	*T. durum*	AABB	Bulgaria	T-CAP	+
PI 519544	*T. durum*	AABB	Mexico	T-CAP	+
PI 384044	*T. durum*	AABB	Israel	T-CAP	+
PI 519811	*T. durum*	AABB	Italy	T-CAP	+
CItr 14559	*T. durum*	AABB	Canada	T-CAP	+
PI 320097	*T. durum*	AABB	Mexico	T-CAP	+
PI 519453	*T. durum*	AABB	Peru	T-CAP	+
PI 420647	*T. durum*	AABB	Uzbekistan	T-CAP	+
PI 274672	*T. durum*	AABB	Russian Federation	T-CAP	+
PI 138971	*T. durum*	AABB	Algeria	T-CAP	+
PI 68275	*T. durum*	AABB	Azerbaijan	T-CAP	+
PI 282911	*T. durum*	AABB	Argentina	T-CAP	+

GRIN ID	Species	Genome	Origin	Source	*Ae. speltoides* segment on 1BL
PI 412984	*T. durum*	AABB	South Africa	T-CAP	+
PI 230366	*T. durum*	AABB	Chile	T-CAP	+
PI 57599	*T. durum*	AABB	Ukraine	T-CAP	+
PI 163274	*T. durum*	AABB	Ecuador	T-CAP	+
PI 182668	*T. durum*	AABB	Lebanon	T-CAP	+
PI 330546	*T. durum*	AABB	United Kingdom	T-CAP	+
PI 94758	*T. durum*	AABB	Ethiopia	T-CAP	+
CItr 15159	*T. durum*	AABB	France	T-CAP	+
CItr 11496	*T. durum*	AABB	China	T-CAP	+
PI 283854	*T. durum*	AABB	India	T-CAP	+
CItr 12818	*T. durum*	AABB	Israel	T-CAP	+
PI 283151	*T. durum*	AABB	Jordan	T-CAP	+
PI 342646	*T. durum*	AABB	Lebanon	T-CAP	+
PI 278380	*T. durum*	AABB	Malta	T-CAP	+
PI 532288	*T. durum*	AABB	Oman	T-CAP	+
PI 272553	*T. durum*	AABB	Hungary	T-CAP	+
PI 190937	*T. durum*	AABB	Portugal	T-CAP	+
PI 210912	*T. durum*	AABB	Pakistan	T-CAP	+
PI 231305	*T. durum*	AABB	Chile	T-CAP	+
PI 585023	*T. durum*	AABB	Saudi Arabia	T-CAP	+
PI 221409	*T. durum*	AABB	Serbia	T-CAP	+
PI 182113	*T. durum*	AABB	Pakistan	T-CAP	+
PI 384401	*T. durum*	AABB	Nigeria	T-CAP	+
PI 324850	*T. durum*	AABB	India	T-CAP	+
PI 525438	*T. durum*	AABB	Morocco	T-CAP	+
PI 51210	*T. durum*	AABB	Tunisia	T-CAP	+
PI 152567	*T. durum*	AABB	Yemen	T-CAP	+
PI 178156	*T. durum*	AABB	Adana Turkey	T-CAP	+
PI 337647	*T. durum*	AABB	Afghanistan	T-CAP	+
PI 470868	*T. durum*	AABB	Algeria	T-CAP	+
PI 94703	*T. durum*	AABB	Ancient Palestine	T-CAP	+
PI 253964	*T. durum*	AABB	Iraq	T-CAP	+
CItr 14810	*T. durum*	AABB	Eritrea	T-CAP	+
PI 347152	*T. durum*	AABB	Afghanistan	T-CAP	+
PI 185722	*T. durum*	AABB	Portugal	T-CAP	+
PI 477895	*T. durum*	AABB	Peru	T-CAP	+
PI 210954	*T. durum*	AABB	Cyprus	T-CAP	+

GRIN ID	Species	Genome	Origin	Source	*Ae. speltoides* segment on 1BL
PI 113395	*T. durum*	AABB	Egypt	T-CAP	+
PI 182738	*T. durum*	AABB	Lebanon	T-CAP	+
CItr 14814	*T. durum*	AABB	Eritrea	T-CAP	+
PI 626482	*T. durum*	AABB	Iran	T-CAP	+
PI 387346	*T. durum*	AABB	Ethiopia	T-CAP	+
PI 78811	*T. durum*	AABB	Georgia	T-CAP	+
PI 469013	*T. durum*	AABB	Greece	T-CAP	+
PI 210381	*T. durum*	AABB	Iran	T-CAP	+
PI 481580	*T. durum*	AABB	Iraq	T-CAP	+
PI 292034	*T. durum*	AABB	Israel	T-CAP	+
PI 223168	*T. durum*	AABB	Jordan	T-CAP	+
PI 91956	*T. durum*	AABB	Peru	T-CAP	+
PI 621474	*T. durum*	AABB	Iran	T-CAP	+
PI 405907	*T. durum*	AABB	Macedonia	T-CAP	+
PI 176289	*T. durum*	AABB	India	T-CAP	+
PI 278378	*T. durum*	AABB	Malta	T-CAP	+
PI 153727	*T. durum*	AABB	North Africa	T-CAP	+
PI 270001	*T. durum*	AABB	Pakistan	T-CAP	+
PI 477867	*T. durum*	AABB	Peru	T-CAP	+
PI 204033	*T. durum*	AABB	Portugal	T-CAP	+
PI 41353	*T. durum*	AABB	India	T-CAP	+
PI 388133	*T. durum*	AABB	Pakistan	T-CAP	+
PI 191357	*T. durum*	AABB	Russian Federation	T-CAP	+
PI 183269	*T. durum*	AABB	Saudi Arabia	T-CAP	+
PI 195695	*T. durum*	AABB	Ethiopia	T-CAP	+
CItr 15408	*T. durum*	AABB	Tunisia	T-CAP	+
PI 384244	*T. durum*	AABB	Ethiopia	T-CAP	+
PI 534351	*T. durum*	AABB	Tunisia	T-CAP	+
PI 166327	*T. durum*	AABB	Turkey	T-CAP	+
PI 623709	*T. durum*	AABB	Iran	T-CAP	+
PI 429317	*T. durum*	AABB	Yemen	T-CAP	+

APPENDIX B. GENOTYPES OF CS AND DS1S(1B) AT THE 68 SNP LOCI WITHIN THE DISTAL ENDS OF 1BL AND 1SL AND GENETIC/PHYSICAL LOCATIONS OF THE SNPS

Index	Name	Chromosome	Genetic position (cM)[a]	Genotype		Physical position (Mb)		
				CS	DS1S (1B)	Start	End	BLASTn Similarity[b]
27844	Excalibur_c5888_169	1B	160.9044	AA	AA	679.749150	679.749251	>98%
27845	Excalibur_c5888_641	1B	160.9044	BB	BB	679.748678	679.748779	>98%
66251	Tdurum_contig10099_454	1B	160.9044	AA	AA	680.867507	680.867718	>98%
74003	Tdurum_contig97527_141	1B	160.9044	AA	AA	680.866533	680.866634	>98%
71971	Tdurum_contig49509_606	1B	160.9044	BB	BB	689.000665	689.000766	>98%
15244	D_contig03023_692	1B	160.9044	BB	BB			No hit
52079	Ra_c4329_599	1B	160.9044	AA	AA			No hit
26024	Excalibur_c39284_949	1B	161.115	AA	AA	679.748594	679.748695	>98%
47439	Kukri_c67939_649	1B	161.115	BB	BB	680.862809	680.862909	>98%
71549	Tdurum_contig44851_927	1B	162.1361	AB	AB	683.470848	683.470949	95%
55986	RAC875_c26801_179	1B	162.1361	AA	AA	683.471605	683.471706	>98%
62169	RAC875_rep_c112737_766	1B	162.1361	AB	AB	683.475012	683.475113	>98%
43736	Kukri_c29537_182	1B	162.1361	AB	AB			No hit
72247	Tdurum_contig52086_524	1B	162.1361	AA	AA			No hit
19632	Ex_c1058_1537	1B	164.2135	BB	AB	678.318048	678.318149	>98%
46805	Kukri_c59535_427	1B	164.2135	AA	AA	679.748212	679.748311	>98%
65272	RFL_Contig785_535	1B	164.6348	BB	BB	679.395912	679.396013	>98%
65271	RFL_Contig785_1700	1B	164.6348	AA	AA	679.394744	679.394845	>98%
56213	RAC875_c28629_189	1B	164.6348	AA	AA	682.470321	682.470413	97%
56212	RAC875_c28629_101	1B	164.6348	BB	BB	682.470400	682.471818	>98%
70716	Tdurum_contig41999_2908	1B	164.8932	NC	BB	678.784344	678.784445	>98%
65270	RFL_Contig785_1156	1B	167.7174	NC	AB	679.395291	679.395392	>98%
20993	Ex_c6112_1248	1B	167.7174	BB	BB	685.277386	685.277485	>98%
49442	Kukri_rep_c110309_129	1B	167.7174	BB	BB	685.740932	685.741033	>98%
29845	Excalibur_rep_c102616_317	1B	167.7174	BB	BB	686.217810	686.217911	>98%
78773	wsnp_Ex_c750_1474351	1B	170.65	BB	BB	686.843885	686.844086	>98%
73820	Tdurum_contig92835_177	1B	171.2276	AA	AA	687.720350	687.720451	>98%
71384	Tdurum_contig42960_865	1B	171.2276	AA	AA	688.284962	688.284863	>98%

Index	Name	Chromosome	Genetic position (cM)[a]	Genotype		Physical position (Mb)		
				CS	DS1S (1B)	Start	End	BLASTn Similarity[b]
72625	Tdurum_contig58710_411	1B	171.2276	BB	BB	688.352419	688.352520	>98%
72626	Tdurum_contig58710_516	1B	171.2276	BB	BB	688.352524	688.352625	>98%
70859	Tdurum_contig42108_958	1B	171.2595	BB	BB	688.707485	688.707586	>98%
71898	Tdurum_contig4851_653	1B	171.2595	BB	BB	688.768601	688.768702	>98%
27547	Excalibur_c55186_351	1B	171.3137	AA	AA	680.862644	680.862745	>98%
52979	RAC875_c102886_73	1B	171.3137	BB	BB	682.469868	682.469969	>98%
34435	IAAV1732	1B	171.3137	AA	AA	682.472658	682.472814	98%
5319	BobWhite_rep_c62955_567	1B	171.3137	AA	AA	682.485409	682.485510	>98%
68524	Tdurum_contig1631_240	1B	171.3137	AA	AA	686.840546	686.840647	>98%
35036	IAAV5516	1B	171.3137	BB	BB	688.710294	688.710482	>98%
78965	wsnp_Ex_c955_1827719	1B	171.3137	BB	BB	688.768195	688.768555	>98%
75471	wsnp_BE446672B_Ta_2_1	1B	171.3137	AB	AB	687.718493	687.718614	>98%
73765	Tdurum_contig9144_222	1B	171.3137	AA	AA	687.719683	687.719784	>98%
45466	Kukri_c44587_130	1B	171.3137	BB	BB	687.795568	687.795667	>98%
76929	wsnp_Ex_c17990_26770800	1B	171.3137	AA	AA	687.797790	687.797991	>98%
77395	wsnp_Ex_c24777_34031473	1B	171.3137	AA	AA	687.798093	687.799050	>98%
31066	Excalibur_rep_c69522_83	1B	171.4254	AA	AA	686.218458	686.218559	>98%
64714	RFL_Contig4538_657	1B	171.4254	AB	AB	686.930639	686.930740	97%
71870	Tdurum_contig48103_1481	1B	171.4254	BB	BB	687.088535	687.088636	>98%
76772	wsnp_Ex_c1597_3045682	1B	171.4254	BB	BB	688.283056	688.283257	>98%
49490	Kukri_rep_c111174_132	1B	172.6731	BB	BB	685.779916	685.780017	>98%
51530	Ra_c23336_538	1B	173.6241	AB	AB	680.867148	680.867239	>98%
62079	RAC875_rep_c111730_97	1B	173.6241	AA	AA	685.723824	685.723920	97%
50867	Ra_c109187_371	1B	173.6241	BB	BB	685.741261	685.741362	>98%
48380	Kukri_c94613_637	1B	173.6241	BB	BB	685.825245	685.825346	>98%
75712	wsnp_BG274687B_Ta_2_1	1B	173.6241	AA	AA	686.843235	686.843356	>98%
4789	BobWhite_rep_c49533_93	1B	173.6241	AA	AA	686.843506	686.843601	>98%
78771	wsnp_Ex_c750_1474184	1B	173.6241	AB	AB	686.843722	686.843919	>98%

Index	Name	Chromosome	Genetic position (cM)[a]	Genotype		Physical position (Mb)		
				CS	DS1S (1B)	Start	End	BLASTn Similarity[b]
72748	Tdurum_contig60566_269	1B	173.6241	AB	AB	686.932074	686.932175	>98%
73657	Tdurum_contig83965_208	1B	173.6241	AA	AA	687.408084	687.408185	>98%
80095	wsnp_Ku_c13952_22097895	1B	173.6241	BB	BB	687.413495	687.413778	>98%
80094	wsnp_Ku_c13952_22097856	1B	173.6241	BB	BB	687.413534	687.413909	>98%
7641	BS00027006_51	1B	173.6241	BB	BB	687.720366	687.720467	>98%
41609	Kukri_c16608_659	1B	173.6241	BB	BB	687.795937	687.796122	>98%
76928	wsnp_Ex_c17990_26770146	1B	173.6241	AA	AA	687.796990	687.797191	>98%
24349	Excalibur_c25640_110	1B	173.6241	BB	BB	687.802260	687.802361	>98%
72218	Tdurum_contig51922_676	1B	173.6241	AA	AA	688.231105	688.231655	>98%
63988	RFL_Contig2550_679	1B	173.6241	AA	AA	688.231105	688.231655	>98%
9889	BS00066805_51	1B	173.6241	AA	AA			No hit
12221	BS00104270_51	1B	173.6241	AB	AB	688.232218	688.232319	>98%

[a]SNPs consensus genetic map (Wang et al., 2014)

[b]BLASTn against IWGSC Reference Sequence v1.0 assembly of chromosome 1B (IWGSC RefSeq v1.0)

APPENDIX C. THE 2B-2S AND 2B-2E RECOMBINANTS IDENTIFIED FROM BC_2F_1 POPULATIONS

Recombinants	Chromosome constitution	Chromosome number	Pedigree
XWC14-034-5	2BS·2BL-2SL + 2S	42	[♀ (♀ CS DS 2S(2B) × ♂ CS *ph1b* mutant) BC_1F_1 × ♂ CS DS 2S(2B)]F_1
XWC14-034-21	2SS·2SL-2BL + 2S	42	[♀ (♀ CS DS 2S(2B) × ♂ CS *ph1b* mutant) BC_1F_1 × ♂ CS DS 2S(2B)]F_1
XWC14-034-27	2BS·2BL-2SL + 2S	42	[♀ (♀ CS DS 2S(2B) × ♂ CS *ph1b* mutant) BC_1F_1 × ♂ CS DS 2S(2B)]F_1
XWC14-034-30	2SS·2SL-2BL + 2S	42	[♀ (♀ CS DS 2S(2B) × ♂ CS *ph1b* mutant) BC_1F_1 × ♂ CS DS 2S(2B)]F_1
XWC14-034-34	2SS·2SL-2BL + 2S	42	[♀ (♀ CS DS 2S(2B) × ♂ CS *ph1b* mutant) BC_1F_1 × ♂ CS DS 2S(2B)]F_1
XWC14-034-40	2BS-2SS·2SL + 2SS-2BS·2BL + 2S	43	[♀ (♀ CS DS 2S(2B) × ♂ CS *ph1b* mutant) BC_1F_1 × ♂ CS DS 2S(2B)]F_1
XWC14-034-45	2SS·2SL-2BL + 2S	42	[♀ (♀ CS DS 2S(2B) × ♂ CS *ph1b* mutant) BC_1F_1 × ♂ CS DS 2S(2B)]F_1
XWC14-034-52	2BS-2SS·2SL + 2S	42	[♀ (♀ CS DS 2S(2B) × ♂ CS *ph1b* mutant) BC_1F_1 × ♂ CS DS 2S(2B)]F_1
XWC14-034-70	2BS-2SS·2SL + 2S	42	[♀ (♀ CS DS 2S(2B) × ♂ CS *ph1b* mutant) BC_1F_1 × ♂ CS DS 2S(2B)]F_1
XWC14-034-74	2BS·2BL-2SL + 2S	42	[♀ (♀ CS DS 2S(2B) × ♂ CS *ph1b* mutant) BC_1F_1 × ♂ CS DS 2S(2B)]F_1
XWC14-034-76	2SS-2BS·2BL + 2S	42	[♀ (♀ CS DS 2S(2B) × ♂ CS *ph1b* mutant) BC_1F_1 × ♂ CS DS 2S(2B)]F_1
XWC14-034-79	2SS·2SL-2BL + 2S	42	[♀ (♀ CS DS 2S(2B) × ♂ CS *ph1b* mutant) BC_1F_1 × ♂ CS DS 2S(2B)]F_1
XWC14-035-9	2SS·2SL-2BL + 2S	42	[♀ (♀ CS DS 2S(2B) × ♂ CS *ph1b* mutant) BC_1F_1 × ♂ CS DS 2S(2B)]F_1
XWC14-035-10	2BS·2BL-2SL + 2S	42	[♀ (♀ CS DS 2S(2B) × ♂ CS *ph1b* mutant) BC_1F_1 × ♂ CS DS 2S(2B)]F_1
XWC14-035-17	2SS·2SL-2BL + 2S	42	[♀ (♀ CS DS 2S(2B) × ♂ CS *ph1b* mutant) BC_1F_1 × ♂ CS DS 2S(2B)]F_1
XWC14-035-19	2BS-2SS·2SL + 2S	42	[♀ (♀ CS DS 2S(2B) × ♂ CS *ph1b* mutant) BC_1F_1 × ♂ CS DS 2S(2B)]F_1
XWC14-035-20	2SS·2SL-2BL + 2S	42	[♀ (♀ CS DS 2S(2B) × ♂ CS *ph1b* mutant) BC_1F_1 × ♂ CS DS 2S(2B)]F_1
XWC14-035-21	2SS·2SL-2BL + 2S	42	[♀ (♀ CS DS 2S(2B) × ♂ CS *ph1b* mutant) BC_1F_1 × ♂ CS DS 2S(2B)]F_1
XWC14-035-26	2BS-2SS·2SL + 2S	42	[♀ (♀ CS DS 2S(2B) × ♂ CS *ph1b* mutant) BC_1F_1 × ♂ CS DS 2S(2B)]F_1
XWC14-035-31	2SS·2SL-2BL + 2S	42	[♀ (♀ CS DS 2S(2B) × ♂ CS *ph1b* mutant) BC_1F_1 × ♂ CS DS 2S(2B)]F_1
XWC14-035-35	2SS·2SL-2BL + 2S	42	[♀ (♀ CS DS 2S(2B) × ♂ CS *ph1b* mutant) BC_1F_1 × ♂ CS DS 2S(2B)]F_1
XWC14-035-36	2BS·2BL-2SL + 2S	42	[♀ (♀ CS DS 2S(2B) × ♂ CS *ph1b* mutant) BC_1F_1 × ♂ CS DS 2S(2B)]F_1
XWC14-036-12	2BS·2BL-2SL + 2S	42	[♀ (♀ CS DS 2S(2B) × ♂ CS *ph1b* mutant) BC_1F_1 × ♂ CS DS 2S(2B)]F_1
XWC14-037-80	2BS·2BL-2SL + 2S	42	[♀ (♀ CS DS 2S(2B) × ♂ CS *ph1b* mutant) BC_1F_1 × ♂ CS DS 2S(2B)]F_1
XWC14-036-40	2SS-2BS·2BL + 2S	42	[♀ (♀ CS DS 2S(2B) × ♂ CS *ph1b* mutant) BC_1F_1 × ♂ CS DS 2S(2B)]F_1
XWC14-036-51	2BS-2SS·2SL + 2S	42	[♀ (♀ CS DS 2S(2B) × ♂ CS *ph1b* mutant) BC_1F_1 × ♂ CS DS 2S(2B)]F_1
XWC14-037-14	2SS-2BS·2BL + 2S	42	[♀ (♀ CS DS 2S(2B) × ♂ CS *ph1b* mutant) BC_1F_1 × ♂ CS DS 2S(2B)]F_1

Recombinants	Chromosome constitution	Chromosome number	Pedigree
XWC14-037-38	2SS·2SL-T2BL + 2S	42	[♀ (♀ CS DS 2S(2B) × ♂ CS *ph1b* mutant) BC_1F_1 × ♂ CS DS 2S(2B)]F_1
XWC14-037-54	T2SS + 2S	42	[♀ (♀ CS DS 2S(2B) × ♂ CS *ph1b* mutant) BC_1F_1 × ♂ CS DS 2S(2B)]F_1
XWC14-037-61	2SS-2BS·2BL + 2S	42	[♀ (♀ CS DS 2S(2B) × ♂ CS *ph1b* mutant) BC_1F_1 × ♂ CS DS 2S(2B)]F_1
XWC14-037-67	2SS·2SL-2BL + 2S	42	[♀ (♀ CS DS 2S(2B) × ♂ CS *ph1b* mutant) BC_1F_1 × ♂ CS DS 2S(2B)]F_1
XWC14-037-75	2BS-2SS·2SL + 2S	42	[♀ (♀ CS DS 2S(2B) × ♂ CS *ph1b* mutant) BC_1F_1 × ♂ CS DS 2S(2B)]F_1
XWC14-037-79	2BS·2BL-2SL + 2S	42	[♀ (♀ CS DS 2S(2B) × ♂ CS *ph1b* mutant) BC_1F_1 × ♂ CS DS 2S(2B)]F_1
XWC14-037-81	2BS·2BL-2SL + 2SS-2BS·2BL + 2S	43	[♀ (♀ CS DS 2S(2B) × ♂ CS *ph1b* mutant) BC_1F_1 × ♂ CS DS 2S(2B)]F_1
XWC14-037-82	2BS·2BL-2SL + 2S	42	[♀ (♀ CS DS 2S(2B) × ♂ CS *ph1b* mutant) BC_1F_1 × ♂ CS DS 2S(2B)]F_1
XWC14-037-87	2BS·2BL-2SL + 2S	42	[♀ (♀ CS DS 2S(2B) × ♂ CS *ph1b* mutant) BC_1F_1 × ♂ CS DS 2S(2B)]F_1
XWC14-037-96	2BS-2SL·2SL + 2S	42	[♀ (♀ CS DS 2S(2B) × ♂ CS *ph1b* mutant) BC_1F_1 × ♂ CS DS 2S(2B)]F_1
XWC14-038-5	2BS·2BL-2SL + 2S	42	[♀ (♀ CS DS 2S(2B) × ♂ CS *ph1b* mutant) BC_1F_1 × ♂ CS DS 2S(2B)]F_1
XWC14-038-13	2BS-2SS·2SL + 2S	42	[♀ (♀ CS DS 2S(2B) × ♂ CS *ph1b* mutant) BC_1F_1 × ♂ CS DS 2S(2B)]F_1
XWC14-038-14	2BS·2BL-2SL + 2S	42	[♀ (♀ CS DS 2S(2B) × ♂ CS *ph1b* mutant) BC_1F_1 × ♂ CS DS 2S(2B)]F_1
XWC14-038-17	2SS-2BS·2BL + 2S	42	[♀ (♀ CS DS 2S(2B) × ♂ CS *ph1b* mutant) BC_1F_1 × ♂ CS DS 2S(2B)]F_1
XWC14-038-21	2SS-2BS·2BL + 2S	42	[♀ (♀ CS DS 2S(2B) × ♂ CS *ph1b* mutant) BC_1F_1 × ♂ CS DS 2S(2B)]F_1
XWC14-038-28	2BS-2SS·2SL + 2S	42	[♀ (♀ CS DS 2S(2B) × ♂ CS *ph1b* mutant) BC_1F_1 × ♂ CS DS 2S(2B)]F_1
XWC14-038-32	2BS-2SS·2SL + 2S	42	[♀ (♀ CS DS 2S(2B) × ♂ CS *ph1b* mutant) BC_1F_1 × ♂ CS DS 2S(2B)]F_1
XWC14-038-38	2SS·2SL-2BL + 2S	42	[♀ (♀ CS DS 2S(2B) × ♂ CS *ph1b* mutant) BC_1F_1 × ♂ CS DS 2S(2B)]F_1
XWC14-038-41	2BS-2SS·2SL + 2S	42	[♀ (♀ CS DS 2S(2B) × ♂ CS *ph1b* mutant) BC_1F_1 × ♂ CS DS 2S(2B)]F_1
XWC14-038-53	2SS-2BS·2BL + 2S	42	[♀ (♀ CS DS 2S(2B) × ♂ CS *ph1b* mutant) BC_1F_1 × ♂ CS DS 2S(2B)]F_1
XWC14-038-54	2SS-2BS·2BL-2SL + 2S	42	[♀ (♀ CS DS 2S(2B) × ♂ CS *ph1b* mutant) BC_1F_1 × ♂ CS DS 2S(2B)]F_1
XWC14-038-68	2SS·2SL-2BL + 2S	42	[♀ (♀ CS DS 2S(2B) × ♂ CS *ph1b* mutant) BC_1F_1 × ♂ CS DS 2S(2B)]F_1
XWC14-038-74	2SS-2BS·2BL-2SL + 2S	42	[♀ (♀ CS DS 2S(2B) × ♂ CS *ph1b* mutant) BC_1F_1 × ♂ CS DS 2S(2B)]F_1
XWC14-038-76	2SS-2BS·2BL + 2S	42	[♀ (♀ CS DS 2S(2B) × ♂ CS *ph1b* mutant) BC_1F_1 × ♂ CS DS 2S(2B)]F_1
XWC14-038-80	2BS·2BL-2SL + 2S	42	[♀ (♀ CS DS 2S(2B) × ♂ CS *ph1b* mutant) BC_1F_1 × ♂ CS DS 2S(2B)]F_1
XWC14-038-86	2BS·2BL-2SL + 2SS-2BS·2BL + 2S	43	[♀ (♀ CS DS 2S(2B) × ♂ CS *ph1b* mutant) BC_1F_1 × ♂ CS DS 2S(2B)]F_1
XWC14-038-89	2SS-2BS·2BL + 2S	42	[♀ (♀ CS DS 2S(2B) × ♂ CS *ph1b* mutant) BC_1F_1 × ♂ CS DS 2S(2B)]F_1
XWC14-038-92	2SS-2BS·2BL + 2S	42	[♀ (♀ CS DS 2S(2B) × ♂ CS *ph1b* mutant) BC_1F_1 × ♂ CS DS 2S(2B)]F_1

Recombinants	Chromosome constitution	Chromosome number	Pedigree
XWC14-038-93	2BS-2SS·D2SL + 2S	42	[♀ (♀ CS DS 2S(2B) × ♂ CS *ph1b* mutant) BC_1F_1 × ♂ CS DS 2S(2B)]F_1
XWC14-038-100	2SS-2BS-2SS·2SL + 2S	42	[♀ (♀ CS DS 2S(2B) × ♂ CS *ph1b* mutant) BC_1F_1 × ♂ CS DS 2S(2B)]F_1
XWC14-039-1	2SS-2BS·2BL-2SL + 2S	42	[♀ (♀ CS DS 2S(2B) × ♂ CS *ph1b* mutant) BC_1F_1 × ♂ CS DS 2S(2B)]F_1
XWC14-039-6	2SS-2BS·2BL + 2S	42	[♀ (♀ CS DS 2S(2B) × ♂ CS *ph1b* mutant) BC_1F_1 × ♂ CS DS 2S(2B)]F_1
XWC14-039-7	2SS·2SL-2BL + 2S	42	[♀ (♀ CS DS 2S(2B) × ♂ CS *ph1b* mutant) BC_1F_1 × ♂ CS DS 2S(2B)]F_1
XWC14-039-9	2BS-2SS·2SL + 2S	42	[♀ (♀ CS DS 2S(2B) × ♂ CS *ph1b* mutant) BC_1F_1 × ♂ CS DS 2S(2B)]F_1
XWC14-039-16	2SS-2BS·2BL + 2S	42	[♀ (♀ CS DS 2S(2B) × ♂ CS *ph1b* mutant) BC_1F_1 × ♂ CS DS 2S(2B)]F_1
XWC14-039-24	2SS-2BS·2BL + 2S	42	[♀ (♀ CS DS 2S(2B) × ♂ CS *ph1b* mutant) BC_1F_1 × ♂ CS DS 2S(2B)]F_1
XWC14-039-27	2SS·2SL-2BL + 2S	42	[♀ (♀ CS DS 2S(2B) × ♂ CS *ph1b* mutant) BC_1F_1 × ♂ CS DS 2S(2B)]F_1
XWC14-039-32	2BS·2BL-2SL + 2S	42	[♀ (♀ CS DS 2S(2B) × ♂ CS *ph1b* mutant) BC_1F_1 × ♂ CS DS 2S(2B)]F_1
XWC14-039-36	2SS-2BS·2BL-2SL + 2S	42	[♀ (♀ CS DS 2S(2B) × ♂ CS *ph1b* mutant) BC_1F_1 × ♂ CS DS 2S(2B)]F_1
XWC14-039-45	2BS·2BL-2SL + 2S	42	[♀ (♀ CS DS 2S(2B) × ♂ CS *ph1b* mutant) BC_1F_1 × ♂ CS DS 2S(2B)]F_1
XWC14-039-60	2SS-2BS·2BL + 2S	42	[♀ (♀ CS DS 2S(2B) × ♂ CS *ph1b* mutant) BC_1F_1 × ♂ CS DS 2S(2B)]F_1
XWC14-039-61	2BS·2BL-2SL + 2S	42	[♀ (♀ CS DS 2S(2B) × ♂ CS *ph1b* mutant) BC_1F_1 × ♂ CS DS 2S(2B)]F_1
XWC14-039-63	2SS-2BS·2BL + 2S	42	[♀ (♀ CS DS 2S(2B) × ♂ CS *ph1b* mutant) BC_1F_1 × ♂ CS DS 2S(2B)]F_1
XWC14-039-64	T2SL + 2S	42	[♀ (♀ CS DS 2S(2B) × ♂ CS *ph1b* mutant) BC_1F_1 × ♂ CS DS 2S(2B)]F_1
XWC14-038-75	2SS-2BS·2BL + 2S	42	[♀ (♀ CS DS 2S(2B) × ♂ CS *ph1b* mutant) BC_1F_1 × ♂ CS DS 2S(2B)]F_1
XWC14-041-6	2SS·2SL-2BL + 2S	42	[♀ (♀ CS DS 2S(2B) × ♂ CS *ph1b* mutant) BC_1F_1 × ♂ CS DS 2S(2B)]F_1
XWC14-041-10	2SS-2BS·2BL + 2S	42	[♀ (♀ CS DS 2S(2B) × ♂ CS *ph1b* mutant) BC_1F_1 × ♂ CS DS 2S(2B)]F_1
XWC14-041-12	2SS-2BS·2BL + 2S	42	[♀ (♀ CS DS 2S(2B) × ♂ CS *ph1b* mutant) BC_1F_1 × ♂ CS DS 2S(2B)]F_1
XWC14-041-13	2SS-2BS·2BL + 2S	42	[♀ (♀ CS DS 2S(2B) × ♂ CS *ph1b* mutant) BC_1F_1 × ♂ CS DS 2S(2B)]F_1
XWC14-041-15	2SS-2BS·2BL + 2S	42	[♀ (♀ CS DS 2S(2B) × ♂ CS *ph1b* mutant) BC_1F_1 × ♂ CS DS 2S(2B)]F_1
XWC14-041-18	2SS-2BS·2BL + 2S	42	[♀ (♀ CS DS 2S(2B) × ♂ CS *ph1b* mutant) BC_1F_1 × ♂ CS DS 2S(2B)]F_1
XWC14-041-19	2SS-2BS·2BL + 2S	42	[♀ (♀ CS DS 2S(2B) × ♂ CS *ph1b* mutant) BC_1F_1 × ♂ CS DS 2S(2B)]F_1
XWC14-041-37	2SS·2SL-2BL + 2S	42	[♀ (♀ CS DS 2S(2B) × ♂ CS *ph1b* mutant) BC_1F_1 × ♂ CS DS 2S(2B)]F_1
XWC14-041-46	2SS-2BS·2BL + 2S	42	[♀ (♀ CS DS 2S(2B) × ♂ CS *ph1b* mutant) BC_1F_1 × ♂ CS DS 2S(2B)]F_1
XWC14-041-49	2BS-2SS·2SL-2BL + 2S	42	[♀ (♀ CS DS 2S(2B) × ♂ CS *ph1b* mutant) BC_1F_1 × ♂ CS DS 2S(2B)]F_1
XWC14-041-63	2SS·2SL-2BL +2BS·2BL-2SL + 2S	43	[♀ (♀ CS DS 2S(2B) × ♂ CS *ph1b* mutant) BC_1F_1 × ♂ CS DS 2S(2B)]F_1

Recombinants	Chromosome constitution	Chromosome number	Pedigree
XWC14-041-66	2BS·2BL-2SL + 2SS·2SL-2BL + 2S	43	[♀ (♀ CS DS 2S(2B) × ♂ CS *ph1b* mutant) BC_1F_1 × ♂ CS DS 2S(2B)]F_1
XWC14-041-78	2SS·2SL-2BL + 2S	42	[♀ (♀ CS DS 2S(2B) × ♂ CS *ph1b* mutant) BC_1F_1 × ♂ CS DS 2S(2B)]F_1
XWC14-041-83	2SS-2BS-2SS·2SL + 2S	42	[♀ (♀ CS DS 2S(2B) × ♂ CS *ph1b* mutant) BC_1F_1 × ♂ CS DS 2S(2B)]F_1
XWC14-041-84	2SS·2SL-2BL + 2S	42	[♀ (♀ CS DS 2S(2B) × ♂ CS *ph1b* mutant) BC_1F_1 × ♂ CS DS 2S(2B)]F_1
XWC14-041-85	2SS·2SL-2BL + 2S	42	[♀ (♀ CS DS 2S(2B) × ♂ CS *ph1b* mutant) BC_1F_1 × ♂ CS DS 2S(2B)]F_1
XWC14-041-87	2SS·2SL-2BL + 2S	42	[♀ (♀ CS DS 2S(2B) × ♂ CS *ph1b* mutant) BC_1F_1 × ♂ CS DS 2S(2B)]F_1
XWC14-043-16	2BS-2SS·2SL + 2S	42	[♀ (♀ CS DS 2S(2B) × ♂ CS *ph1b* mutant) BC_1F_1 × ♂ CS DS 2S(2B)]F_1
XWC14-043-32	2BS-2SS-2BS·2BL + 2S	42	[♀ (♀ CS DS 2S(2B) × ♂ CS *ph1b* mutant) BC_1F_1 × ♂ CS DS 2S(2B)]F_1
XWC14-043-47	2BS-2SS·2SL-2BL + 2S	42	[♀ (♀ CS DS 2S(2B) × ♂ CS *ph1b* mutant) BC_1F_1 × ♂ CS DS 2S(2B)]F_1
XWC14-043-61	2SS·2SL-2BL + 2S	42	[♀ (♀ CS DS 2S(2B) × ♂ CS *ph1b* mutant) BC_1F_1 × ♂ CS DS 2S(2B)]F_1
XWC14-043-87	2SS·2SL-2BL-2SS + 2S	42	[♀ (♀ CS DS 2S(2B) × ♂ CS *ph1b* mutant) BC_1F_1 × ♂ CS DS 2S(2B)]F_1
XWC14-043-89	2SS·2SL-2BL + 2S	42	[♀ (♀ CS DS 2S(2B) × ♂ CS *ph1b* mutant) BC_1F_1 × ♂ CS DS 2S(2B)]F_1
XWC14-043-95	2BS-2SS·2SL-2BL + 2S	42	[♀ (♀ CS DS 2S(2B) × ♂ CS *ph1b* mutant) BC_1F_1 × ♂ CS DS 2S(2B)]F_1
XWC14-043-96	2BS·2BL-2SL + 2S	42	[♀ (♀ CS DS 2S(2B) × ♂ CS *ph1b* mutant) BC_1F_1 × ♂ CS DS 2S(2B)]F_1
XWC14-043-97	2SS·2SL-2BL-2SL + 2S	42	[♀ (♀ CS DS 2S(2B) × ♂ CS *ph1b* mutant) BC_1F_1 × ♂ CS DS 2S(2B)]F_1
XWC14-043-98	2BS·2BL-2SL + 2S	42	[♀ (♀ CS DS 2S(2B) × ♂ CS *ph1b* mutant) BC_1F_1 × ♂ CS DS 2S(2B)]F_1
XWC14-130-9	T2ES + 2E	42	[♀ (♀ CS DS 2E(2B) × ♂ CS *ph1b* mutant) BC_1F_1 × ♂ CS DS 2E(2B)]F_1
XWC14-130-10	T2ES + 2E	42	[♀ (♀ CS DS 2E(2B) × ♂ CS *ph1b* mutant) BC_1F_1 × ♂ CS DS 2E(2B)]F_1
XWC14-130-11	T2ES + 2E	42	[♀ (♀ CS DS 2E(2B) × ♂ CS *ph1b* mutant) BC_1F_1 × ♂ CS DS 2E(2B)]F_1
XWC14-130-13	T2ES + 2E	42	[♀ (♀ CS DS 2E(2B) × ♂ CS *ph1b* mutant) BC_1F_1 × ♂ CS DS 2E(2B)]F_1
XWC14-130-23	T2ES + 2E	42	[♀ (♀ CS DS 2E(2B) × ♂ CS *ph1b* mutant) BC_1F_1 × ♂ CS DS 2E(2B)]F_1
XWC14-130-24	T2ES + 2E	42	[♀ (♀ CS DS 2E(2B) × ♂ CS *ph1b* mutant) BC_1F_1 × ♂ CS DS 2E(2B)]F_1
XWC14-130-27	T2BS-2ES + 2E	42	[♀ (♀ CS DS 2E(2B) × ♂ CS *ph1b* mutant) BC_1F_1 × ♂ CS DS 2E(2B)]F_1
XWC14-130-29	T2ES + 2E	42	[♀ (♀ CS DS 2E(2B) × ♂ CS *ph1b* mutant) BC_1F_1 × ♂ CS DS 2E(2B)]F_1
XWC14-130-30	T2ES + 2E	42	[♀ (♀ CS DS 2E(2B) × ♂ CS *ph1b* mutant) BC_1F_1 × ♂ CS DS 2E(2B)]F_1
XWC14-130-38	T2ES + 2E	42	[♀ (♀ CS DS 2E(2B) × ♂ CS *ph1b* mutant) BC_1F_1 × ♂ CS DS 2E(2B)]F_1
XWC14-130-39	T2ES + 2E	42	[♀ (♀ CS DS 2E(2B) × ♂ CS *ph1b* mutant) BC_1F_1 × ♂ CS DS 2E(2B)]F_1
XWC14-131-2	2ES·2BL + 2E	42	[♀ (♀ CS DS 2E(2B) × ♂ CS *ph1b* mutant) BC_1F_1 × ♂ CS DS 2E(2B)]F_1

Recombinants	Chromosome constitution	Chromosome number	Pedigree
XWC14-131-4	2ES·2BL + 2E	42	[♀ (♀ CS DS 2E(2B) × ♂ CS *ph1b* mutant) BC_1F_1 × ♂ CS DS 2E(2B)]F_1
XWC14-131-8	2ES·2BL + 2E	42	[♀ (♀ CS DS 2E(2B) × ♂ CS *ph1b* mutant) BC_1F_1 × ♂ CS DS 2E(2B)]F_1
XWC14-131-11	2ES·2BL + 2E	42	[♀ (♀ CS DS 2E(2B) × ♂ CS *ph1b* mutant) BC_1F_1 × ♂ CS DS 2E(2B)]F_1
XWC14-131-13	2ES·2BL + 2E	42	[♀ (♀ CS DS 2E(2B) × ♂ CS *ph1b* mutant) BC_1F_1 × ♂ CS DS 2E(2B)]F_1
XWC14-131-17	2ES·2BL + 2E	42	[♀ (♀ CS DS 2E(2B) × ♂ CS *ph1b* mutant) BC_1F_1 × ♂ CS DS 2E(2B)]F_1
XWC14-131-18	2ES·2BL + 2E	42	[♀ (♀ CS DS 2E(2B) × ♂ CS *ph1b* mutant) BC_1F_1 × ♂ CS DS 2E(2B)]F_1
XWC14-131-19	2ES·2BL + 2E	42	[♀ (♀ CS DS 2E(2B) × ♂ CS *ph1b* mutant) BC_1F_1 × ♂ CS DS 2E(2B)]F_1
XWC14-131-20	2ES·2BL + 2E	42	[♀ (♀ CS DS 2E(2B) × ♂ CS *ph1b* mutant) BC_1F_1 × ♂ CS DS 2E(2B)]F_1
XWC14-131-23	2ES·2BL + 2E	42	[♀ (♀ CS DS 2E(2B) × ♂ CS *ph1b* mutant) BC_1F_1 × ♂ CS DS 2E(2B)]F_1
XWC14-131-25	2ES·2BL + 2E	42	[♀ (♀ CS DS 2E(2B) × ♂ CS *ph1b* mutant) BC_1F_1 × ♂ CS DS 2E(2B)]F_1
XWC14-131-26	2ES·2BL + 2E	42	[♀ (♀ CS DS 2E(2B) × ♂ CS *ph1b* mutant) BC_1F_1 × ♂ CS DS 2E(2B)]F_1
XWC14-131-28	2ES·2BL + 2E	42	[♀ (♀ CS DS 2E(2B) × ♂ CS *ph1b* mutant) BC_1F_1 × ♂ CS DS 2E(2B)]F_1
XWC14-131-29	2ES·2BL + 2E	42	[♀ (♀ CS DS 2E(2B) × ♂ CS *ph1b* mutant) BC_1F_1 × ♂ CS DS 2E(2B)]F_1
XWC14-131-31	2ES·2BL + 2E	42	[♀ (♀ CS DS 2E(2B) × ♂ CS *ph1b* mutant) BC_1F_1 × ♂ CS DS 2E(2B)]F_1
XWC14-131-32	2ES·2BL + 2E	42	[♀ (♀ CS DS 2E(2B) × ♂ CS *ph1b* mutant) BC_1F_1 × ♂ CS DS 2E(2B)]F_1
XWC14-131-33	2ES-2BS·2BL + 2E	42	[♀ (♀ CS DS 2E(2B) × ♂ CS *ph1b* mutant) BC_1F_1 × ♂ CS DS 2E(2B)]F_1
XWC14-131-35	2ES·2BL + 2E	42	[♀ (♀ CS DS 2E(2B) × ♂ CS *ph1b* mutant) BC_1F_1 × ♂ CS DS 2E(2B)]F_1
XWC14-131-36	2ES·2BL + 2E	42	[♀ (♀ CS DS 2E(2B) × ♂ CS *ph1b* mutant) BC_1F_1 × ♂ CS DS 2E(2B)]F_1
XWC14-131-38	2ES·2BL + 2E	42	[♀ (♀ CS DS 2E(2B) × ♂ CS *ph1b* mutant) BC_1F_1 × ♂ CS DS 2E(2B)]F_1
XWC14-131-41	2ES·2BL + 2E	42	[♀ (♀ CS DS 2E(2B) × ♂ CS *ph1b* mutant) BC_1F_1 × ♂ CS DS 2E(2B)]F_1
XWC14-132-3	2BS-2ES·2EL + 2E	42	[♀ (♀ CS DS 2E(2B) × ♂ CS *ph1b* mutant) BC_1F_1 × ♂ CS DS 2E(2B)]F_1
XWC14-132-15	2BS-2ES·2EL-2BL + 2E	42	[♀ (♀ CS DS 2E(2B) × ♂ CS *ph1b* mutant) BC_1F_1 × ♂ CS DS 2E(2B)]F_1
XWC14-132-20	2ES·2EL-2BL + 2E	42	[♀ (♀ CS DS 2E(2B) × ♂ CS *ph1b* mutant) BC_1F_1 × ♂ CS DS 2E(2B)]F_1
XWC14-132-36	2ES-2BS·2BL + 2E	42	[♀ (♀ CS DS 2E(2B) × ♂ CS *ph1b* mutant) BC_1F_1 × ♂ CS DS 2E(2B)]F_1
XWC14-132-54	2ES·2EL-2BL + 2E	42	[♀ (♀ CS DS 2E(2B) × ♂ CS *ph1b* mutant) BC_1F_1 × ♂ CS DS 2E(2B)]F_1
XWC14-132-71	2ES·2EL-2BL + 2E	42	[♀ (♀ CS DS 2E(2B) × ♂ CS *ph1b* mutant) BC_1F_1 × ♂ CS DS 2E(2B)]F_1
XWC14-132-73	T2ES + 2E	42	[♀ (♀ CS DS 2E(2B) × ♂ CS *ph1b* mutant) BC_1F_1 × ♂ CS DS 2E(2B)]F_1
XWC14-132-75	2BS-2ES·2EL + 2E	42	[♀ (♀ CS DS 2E(2B) × ♂ CS *ph1b* mutant) BC_1F_1 × ♂ CS DS 2E(2B)]F_1

Recombinants	Chromosome constitution	Chromosome number	Pedigree
XWC14-132-80	2BS-2ES·2EL + 2E	42	[♀ (♀ CS DS 2E(2B) × ♂ CS *ph1b* mutant) BC_1F_1 × ♂ CS DS 2E(2B)]F_1
XWC14-132-87	2BS-2ES·2EL + 2E	42	[♀ (♀ CS DS 2E(2B) × ♂ CS *ph1b* mutant) BC_1F_1 × ♂ CS DS 2E(2B)]F_1
XWC14-132-99	2ES-2BS·2BL + 2E	42	[♀ (♀ CS DS 2E(2B) × ♂ CS *ph1b* mutant) BC_1F_1 × ♂ CS DS 2E(2B)]F_1
XWC14-132-101	2ES-2BS·2BL + 2E	42	[♀ (♀ CS DS 2E(2B) × ♂ CS *ph1b* mutant) BC_1F_1 × ♂ CS DS 2E(2B)]F_1
XWC14-132-105	2ES·2EL-2BL + 2E	42	[♀ (♀ CS DS 2E(2B) × ♂ CS *ph1b* mutant) BC_1F_1 × ♂ CS DS 2E(2B)]F_1
XWC14-132-108	2BS-2ES·2EL + 2E	42	[♀ (♀ CS DS 2E(2B) × ♂ CS *ph1b* mutant) BC_1F_1 × ♂ CS DS 2E(2B)]F_1
XWC14-132-111	2ES·2EL-2BL + 2E	42	[♀ (♀ CS DS 2E(2B) × ♂ CS *ph1b* mutant) BC_1F_1 × ♂ CS DS 2E(2B)]F_1
XWC14-132-114	2ES·2EL-2BL + 2E	42	[♀ (♀ CS DS 2E(2B) × ♂ CS *ph1b* mutant) BC_1F_1 × ♂ CS DS 2E(2B)]F_1
XWC14-132-127	2ES-2BS·2BL + 2E	42	[♀ (♀ CS DS 2E(2B) × ♂ CS *ph1b* mutant) BC_1F_1 × ♂ CS DS 2E(2B)]F_1
XWC14-133-35	2BS-2ES·2EL + 2E	42	[♀ (♀ CS DS 2E(2B) × ♂ CS *ph1b* mutant) BC_1F_1 × ♂ CS DS 2E(2B)]F_1
XWC14-133-49	2ES-2BS·2BL + 2E	42	[♀ (♀ CS DS 2E(2B) × ♂ CS *ph1b* mutant) BC_1F_1 × ♂ CS DS 2E(2B)]F_1
XWC14-133-55	2ES-2BS·2BL + 2E	42	[♀ (♀ CS DS 2E(2B) × ♂ CS *ph1b* mutant) BC_1F_1 × ♂ CS DS 2E(2B)]F_1
XWC14-133-58	2ES·2EL-2BL + 2E	42	[♀ (♀ CS DS 2E(2B) × ♂ CS *ph1b* mutant) BC_1F_1 × ♂ CS DS 2E(2B)]F_1
XWC14-133-59	2ES-2BS·2BL + 2E	42	[♀ (♀ CS DS 2E(2B) × ♂ CS *ph1b* mutant) BC_1F_1 × ♂ CS DS 2E(2B)]F_1
XWC14-133-60	T2ES + 2E	42	[♀ (♀ CS DS 2E(2B) × ♂ CS *ph1b* mutant) BC_1F_1 × ♂ CS DS 2E(2B)]F_1
XWC14-134-6	2BS-2ES·2EL-2BL + 2E	42	[♀ (♀ CS DS 2E(2B) × ♂ CS *ph1b* mutant) BC_1F_1 × ♂ CS DS 2E(2B)]F_1
XWC14-134-10	2ES·2EL-2BL + 2E	42	[♀ (♀ CS DS 2E(2B) × ♂ CS *ph1b* mutant) BC_1F_1 × ♂ CS DS 2E(2B)]F_1
XWC14-134-13	2ES-2BS·2BL + 2E	42	[♀ (♀ CS DS 2E(2B) × ♂ CS *ph1b* mutant) BC_1F_1 × ♂ CS DS 2E(2B)]F_1
XWC14-134-15	2ES-2BS·2BL + 2E	42	[♀ (♀ CS DS 2E(2B) × ♂ CS *ph1b* mutant) BC_1F_1 × ♂ CS DS 2E(2B)]F_1
XWC14-134-17	2ES-2BS·2BL + 2E	42	[♀ (♀ CS DS 2E(2B) × ♂ CS *ph1b* mutant) BC_1F_1 × ♂ CS DS 2E(2B)]F_1
XWC14-134-19	2ES·2EL-2BL + 2E	42	[♀ (♀ CS DS 2E(2B) × ♂ CS *ph1b* mutant) BC_1F_1 × ♂ CS DS 2E(2B)]F_1
XWC14-134-26	2ES·2EL-2BL + 2E	42	[♀ (♀ CS DS 2E(2B) × ♂ CS *ph1b* mutant) BC_1F_1 × ♂ CS DS 2E(2B)]F_1
XWC14-134-31	2ES·2BL + 2E	42	[♀ (♀ CS DS 2E(2B) × ♂ CS *ph1b* mutant) BC_1F_1 × ♂ CS DS 2E(2B)]F_1
XWC14-134-55	2ES-2BS·2BL + 2E	42	[♀ (♀ CS DS 2E(2B) × ♂ CS *ph1b* mutant) BC_1F_1 × ♂ CS DS 2E(2B)]F_1
XWC14-134-74	T2ES + 2E	42	[♀ (♀ CS DS 2E(2B) × ♂ CS *ph1b* mutant) BC_1F_1 × ♂ CS DS 2E(2B)]F_1
XWC14-134-81	2ES-2BS·2BL + 2E	42	[♀ (♀ CS DS 2E(2B) × ♂ CS *ph1b* mutant) BC_1F_1 × ♂ CS DS 2E(2B)]F_1
XWC14-134-82	2ES·2EL-2BL + 2E	42	[♀ (♀ CS DS 2E(2B) × ♂ CS *ph1b* mutant) BC_1F_1 × ♂ CS DS 2E(2B)]F_1
XWC14-134-87	T2ES + 2E	42	[♀ (♀ CS DS 2E(2B) × ♂ CS *ph1b* mutant) BC_1F_1 × ♂ CS DS 2E(2B)]F_1

Recombinants	Chromosome constitution	Chromosome number	Pedigree
XWC14-134-96	2ES·2EL-2BL + 2E	42	[♀ (♀ CS DS 2E(2B) × ♂ CS *ph1b* mutant) BC_1F_1 × ♂ CS DS 2E(2B)]F_1
XWC14-134-103	2ES-2BS·2BL + 2E	42	[♀ (♀ CS DS 2E(2B) × ♂ CS *ph1b* mutant) BC_1F_1 × ♂ CS DS 2E(2B)]F_1
XWC14-134-106	T2ES + 2E	42	[♀ (♀ CS DS 2E(2B) × ♂ CS *ph1b* mutant) BC_1F_1 × ♂ CS DS 2E(2B)]F_1
XWC14-136-36	2ES-2BS·2BL + 2E	42	[♀ (♀ CS DS 2E(2B) × ♂ CS *ph1b* mutant) BC_1F_1 × ♂ CS DS 2E(2B)]F_1
XWC14-139-40	2ES·2BL + 2E	42	[♀ (♀ CS DS 2E(2B) × ♂ CS *ph1b* mutant) BC_1F_1 × ♂ CS DS 2E(2B)]F_1
XWC14-139-48	T2ES + 2E	42	[♀ (♀ CS DS 2E(2B) × ♂ CS *ph1b* mutant) BC_1F_1 × ♂ CS DS 2E(2B)]F_1
XWC14-139-49	2ES·2EL-2BL + 2E	42	[♀ (♀ CS DS 2E(2B) × ♂ CS *ph1b* mutant) BC_1F_1 × ♂ CS DS 2E(2B)]F_1
XWC14-130-3	2ES-2BS·2BL + 2E	42	[♀ (♀ CS DS 2E(2B) × ♂ CS *ph1b* mutant) BC_1F_1 × ♂ CS DS 2E(2B)]F_1
XWC14-141-57	2ES-2BS·2BL + 2E	42	[♀ (♀ CS DS 2E(2B) × ♂ CS *ph1b* mutant) BC_1F_1 × ♂ CS DS 2E(2B)]F_1
XWC14-142-8	2BS·2BL-2EL + 2E	42	[♀ (♀ CS DS 2E(2B) × ♂ CS *ph1b* mutant) BC_1F_1 × ♂ CS DS 2E(2B)]F_1
XWC14-142-28	2ES-2BS·2BL + 2E	42	[♀ (♀ CS DS 2E(2B) × ♂ CS *ph1b* mutant) BC_1F_1 × ♂ CS DS 2E(2B)]F_1
XWC14-142-30	2ES·2EL-2BL + 2E	42	[♀ (♀ CS DS 2E(2B) × ♂ CS *ph1b* mutant) BC_1F_1 × ♂ CS DS 2E(2B)]F_1
XWC14-142-36	2ES-2BS·2BL + 2E	42	[♀ (♀ CS DS 2E(2B) × ♂ CS *ph1b* mutant) BC_1F_1 × ♂ CS DS 2E(2B)]F_1
XWC14-143-50	2ES-2BS·2BL-2EL + 2E	42	[♀ (♀ CS DS 2E(2B) × ♂ CS *ph1b* mutant) BC_1F_1 × ♂ CS DS 2E(2B)]F_1
XWC14-143-56	2ES-2BS·2BL + 2E	42	[♀ (♀ CS DS 2E(2B) × ♂ CS *ph1b* mutant) BC_1F_1 × ♂ CS DS 2E(2B)]F_1
XWC14-143-59	2BS·2BL-2EL + 2E	42	[♀ (♀ CS DS 2E(2B) × ♂ CS *ph1b* mutant) BC_1F_1 × ♂ CS DS 2E(2B)]F_1
XWC14-143-77	2BS-2ES·2EL-2BL + 2E	42	[♀ (♀ CS DS 2E(2B) × ♂ CS *ph1b* mutant) BC_1F_1 × ♂ CS DS 2E(2B)]F_1
XWC14-143-87	2ES-2BS·2BL + 2E	42	[♀ (♀ CS DS 2E(2B) × ♂ CS *ph1b* mutant) BC_1F_1 × ♂ CS DS 2E(2B)]F_1
XWC14-715-2	2BS-2ES·2EL + 2E	42	[♀ (♀ CS DS 2E(2B) × ♂ CS *ph1b* mutant) BC_1F_1 × ♂ CS DS 2E(2B)]F_1
XWC14-715-47	2ES-2BS·2BL + 2BS·2BL-2EL + 2E	43	[♀ (♀ CS DS 2E(2B) × ♂ CS *ph1b* mutant) BC_1F_1 × ♂ CS DS 2E(2B)]F_1
XWC14-715-78	2ES-2BS·2BL + 2E	42	[♀ (♀ CS DS 2E(2B) × ♂ CS *ph1b* mutant) BC_1F_1 × ♂ CS DS 2E(2B)]F_1
XWC14-715-85	2BS·2BL-2EL + 2E	42	[♀ (♀ CS DS 2E(2B) × ♂ CS *ph1b* mutant) BC_1F_1 × ♂ CS DS 2E(2B)]F_1
XWC14-716-5	2ES-2BS·2BL + 2E	42	[♀ (♀ CS DS 2E(2B) × ♂ CS *ph1b* mutant) BC_1F_1 × ♂ CS DS 2E(2B)]F_1
XWC14-716-19	2BS-2ES·2EL + 2E	42	[♀ (♀ CS DS 2E(2B) × ♂ CS *ph1b* mutant) BC_1F_1 × ♂ CS DS 2E(2B)]F_1
XWC14-716-72	2ES-2BS·2BL + 2E	42	[♀ (♀ CS DS 2E(2B) × ♂ CS *ph1b* mutant) BC_1F_1 × ♂ CS DS 2E(2B)]F_1
XWC14-716-84	2ES-2BS·2BL + 2E	42	[♀ (♀ CS DS 2E(2B) × ♂ CS *ph1b* mutant) BC_1F_1 × ♂ CS DS 2E(2B)]F_1
XWC14-716-85	2BS·2BL-2EL + 2E	42	[♀ (♀ CS DS 2E(2B) × ♂ CS *ph1b* mutant) BC_1F_1 × ♂ CS DS 2E(2B)]F_1
XWC14-717-27	2BS-2ES·2EL + 2E	42	[♀ (♀ CS DS 2E(2B) × ♂ CS *ph1b* mutant) BC_1F_1 × ♂ CS DS 2E(2B)]F_1

Recombinants	Chromosome constitution	Chromosome number	Pedigree
XWC14-717-48	2ES-2BS·2BL + 2E	42	[♀ (♀ CS DS 2E(2B) × ♂ CS *ph1b* mutant) BC_1F_1 × ♂ CS DS 2E(2B)]F_1
XWC14-717-56	2BS·2BL-2EL + 2E	42	[♀ (♀ CS DS 2E(2B) × ♂ CS *ph1b* mutant) BC_1F_1 × ♂ CS DS 2E(2B)]F_1

APPENDIX D. SCREENING OF HOMOZYGOUS 2B-2S AND 2B-2E RECOMBINANT LINES WITH Ph1 ALLELE FROM THE BC_2F_2 GENERATION

146

Plants	Genotype	Pedigree	Chromosome constitution	Identification by markers	Validation by FGISH	*Ph1*allele
ZW14-001-3	Homozygous	(XWC14-034-5)⊗F_1	2BS·2BL-2SL		+	*Ph1*_
ZW14-001-15	Homozygous	(XWC14-034-5)⊗F_1	2BS·2BL-2SL		+	-
ZW14-002-1	Heterozygous	(XWC14-034-21)⊗F_1	2SS·2SL-2BL	+	+	*Ph1*_
ZW14-002-2	Homozygous	(XWC14-034-21)⊗F_1	2SS·2SL-2BL	+	+	-
ZW14-002-5	Homozygous	(XWC14-034-21)⊗F_1	2SS·2SL-2BL	+		*Ph1*_
ZW14-003-2	Homozygous	(XWC14-034-27)⊗F_1	2BS·2BL-2SL	+		-
ZW14-003-4	Homozygous	(XWC14-034-27)⊗F_1	2BS·2BL-2SL	+	+	*Ph1*_
ZW14-004-1	Homozygous	(XWC14-034-30)⊗F_1	2SS·2SL-2BL	+	+	*Ph1*_
ZW14-004-4	Homozygous	(XWC14-034-30)⊗F_1	2SS·2SL-2BL	+		-
ZW14-005-8	Homozygous	(XWC14-034-34)⊗F_1	2SS·2SL-2BL	+	+	*Ph1*_
ZW14-006-1	Homozygous	(XWC14-034-45)⊗F_1	2SS·2SL-2BL	+		*Ph1*_
ZW14-006-7	Homozygous	(XWC14-034-45)⊗F_1	2SS·2SL-2BL	+	+	-
ZW14-007-1	Heterozygous	(XWC14-034-52)⊗F_1	2BS-2SS·2SL	+	+	*Ph1*_
ZW14-007-7	Homozygous	(XWC14-034-52)⊗F_1	2BS-2SS·2SL	+	+	-
ZW14-007-8	Homozygous	(XWC14-034-52)⊗F_1	2BS-2SS·2SL	+	+	*Ph1*_
ZW14-008-5	Heterozygous	(XWC14-034-70)⊗F_1	2BS-2SS·2SL + 2SS-2BS·2BL	+	+	*Ph1*_
ZW14-008-6	Heterozygous	(XWC14-034-70)⊗F_1	2BS-2SS·2SL	+		-
ZW14-009-1	Heterozygous	(XWC14-034-74)⊗F_1	2BS·2BL-2SL	+	+	*Ph1*_
ZW14-009-3	Heterozygous	(XWC14-034-74)⊗F_1	2BS·2BL-2SL	+	+	*Ph1*_
ZW14-010-2	Heterozygous	(XWC14-034-76)⊗F_1	2SS-2BS·2BL	+	+	-
ZW14-010-3	Heterozygous	(XWC14-034-76)⊗F_1	2SS-2BS·2BL	+		*Ph1*_
ZW14-011-1	Homozygous	(XWC14-034-79)⊗F_1	2SS·2SL-2BL	+	+	*Ph1*_
ZW14-013-2	Heterozygous	(XWC14-035-9)⊗F_1	2SS·2SL-2BL	+		*Ph1*_
ZW14-013-4	Homozygous	(XWC14-035-9)⊗F_1	2SS·2SL-2BL	+	+	*Ph1*_
ZW14-014-2	Homozygous	(XWC14-035-10)⊗F_1	2BS·2BL-2SL	+	+	*Ph1*_

Plants	Genotype	Pedigree	Chromosome constitution	Identification by markers	Validation by FGISH	*Ph1*allele
ZW14-014-6	Homozygous	(XWC14-035-10)⊗F_1	2BS·2BL-2SL	+		*Ph1*_
ZW14-014-7	Homozygous	(XWC14-035-10)⊗F_1	2BS·2BL-2SL	+		*Ph1*_
ZW14-016-7	Homozygous	(XWC14-035-19)⊗F_1	2BS-2SS·2SL	+	+	-
ZW14-017-1	Homozygous	(XWC14-035-20)⊗F_1	2SS·2SL-2BL	+	+	*Ph1*_
ZW14-017-4	Homozygous	(XWC14-035-20)⊗F_1	2SS·2SL-2BL	+		*Ph1*_
ZW14-070-1	Homozygous	(XWC14-035-21)⊗F_1	2SS·2SL-2BL	+	+	*Ph1*_
ZW14-070-4	Homozygous	(XWC14-035-21)⊗F_1	2SS·2SL-2BL	+		*Ph1*_
ZW14-070-5	Homozygous	(XWC14-035-21)⊗F_1	2SS·2SL-2BL	+		-
ZW14-070-8	Homozygous	(XWC14-035-21)⊗F_1	2SS·2SL-2BL	+		*Ph1*_
ZW14-071-2	Homozygous	(XWC14-035-26)⊗F_1	2BS-2SS·2SL	+	+	*Ph1*_
ZW14-071-3	Homozygous	(XWC14-035-26)⊗F_1	2BS-2SS·2SL	+		*Ph1*_
ZW14-071-6	Homozygous	(XWC14-035-26)⊗F_1	2BS-2SS·2SL	+		*Ph1*_
ZW14-071-8	Homozygous	(XWC14-035-26)⊗F_1	2BS-2SS·2SL	+		-
ZW14-072-5	Homozygous	(XWC14-035-31)⊗F_1	2SS·2SL-2BL	+	+	*Ph1*_
ZW14-072-6	Homozygous	(XWC14-035-31)⊗F_1	2SS·2SL-2BL	+		*Ph1*_
ZW14-073-1	Homozygous	(XWC14-035-35)⊗F_1	2SS·2SL-2BL	+		*Ph1*_
ZW14-074-2	Homozygous	(XWC14-035-36)⊗F_1	2BS·2BL-2SL	+	+	-
ZW14-077-8-1	New recombinant	(XWC14-036-12)⊗F_1	2SS·2SL-2BL-2SL	+	+	*Ph1*_
ZW14-077-8-2	New telosome	(XWC14-036-12)⊗F_1	2BS·2BL-2SL + T2SS	+	+	*Ph1*_
ZW14-084-8-2	New telosome	(XWC14-037-80)⊗F_1	2BS·2BL-2SL + T2SL	+	+	*Ph1*_
ZW14-089-7-1	New isochromosme	(XWC14-036-40)⊗F_1	2SL·2SL + T2SL + T2SS	+	+	*Ph1*_
ZW14-093-8-1	Homozygous	(XWC14-036-51)⊗F_1	2BS-2SS·2SL	+	+	*Ph1*_
ZW14-095-3	Heterozygous	(XWC14-037-14)⊗F_1	2SS-2BS·2BL	+		-
ZW14-095-6	Heterozygous	(XWC14-037-14)⊗F_1	2SS-2BS·2BL	+	+	*Ph1*_
ZW14-100-1	Heterozygous	(XWC14-037-38)⊗F_1	2SS·2SL-T2BL	+	+	*Ph1*_
ZW14-106-1	Heterozygous	(XWC14-037-54)⊗F_1	T2SS	+	+	*Ph1*_

Plants	Genotype	Pedigree	Chromosome constitution	Identification by markers	Validation by FGISH	*Ph1*allele
ZW14-108-6	Homozygous	(XWC14-037-61)⊗F_1	2SS-2BS·2BL	+	+	-
ZW14-111-3	Homozygous	(XWC14-037-67)⊗F_1	2SS·2SL-2BL	+	+	*Ph1_*
ZW14-111-5	Homozygous	(XWC14-037-67)⊗F_1	2SS·2SL-2BL	+	+	*Ph1_*
ZW14-115-7	Homozygous	(XWC14-037-75)⊗F_1	2BS-2SS·2SL	+	+	*Ph1_*
ZW14-116-5	Homozygous	(XWC14-037-79)⊗F_1	2BS·2BL-2SL	+	+	*Ph1_*
ZW14-117-15	Heterozygous	(XWC14-037-81)⊗F_1	2BS·2BL-2SL + 2SS-2BS·2BL	+	+	*Ph1_*
ZW14-117-6	Heterozygous	(XWC14-037-81)⊗F_1	2BS·2BL-2SL + 2SS-2BS·2BL	+	+	-
ZW14-118-1	Homozygous	(XWC14-037-82)⊗F_1	2BS·2BL-2SL	+	+	*Ph1_*
ZW14-121-3	new telosome	(XWC14-037-87)⊗F_1	T2SL	+	+	*Ph1_*
ZW14-121-8	Heterozygous	(XWC14-038-5)⊗F_1	2BS·2BL-2SL	+	+	-
ZW14-127-8-1	Homozygous	(XWC14-037-96)⊗F_1	2BS-2SL·2SL	+	+	*Ph1_*
ZW14-127-8-2	New recombinant	(XWC14-037-96)⊗F_1	2BS·2BL-2SL	+	+	-
ZW14-128-1	Homozygous	(XWC14-038-5)⊗F_1	2BS·2BL-2SL	+	+	*Ph1_*
ZW14-134-3-1	Homozygous	(XWC14-038-13)⊗F_1	2BS-2SS·2SL	+	+	*Ph1_*
ZW14-135-6-2	Homozygous	(XWC14-038-14)⊗F_1	2BS·2BL-2SL	+	+	*Ph1_*
ZW14-137-7-1	Homozygous	(XWC14-038-17)⊗F_1	2SS-2BS·2BL	+	+	*Ph1_*
ZW14-139-1-1	Homozygous	(XWC14-038-21)⊗F_1	2SS-2BS·2BL	+	+	*Ph1_*
ZW14-139-6-1	Homozygous	(XWC14-038-21)⊗F_1	2SS-2BS·2BL	+	+	*Ph1_*
ZW14-139-7-2	Homozygous	(XWC14-038-21)⊗F_1	2SS-2BS·2BL	+	+	-
ZW14-141-7-2	Homozygous	(XWC14-038-28)⊗F_1	2BS-2SS·2SL	+	+	*Ph1_*
ZW14-141-8-2	Homozygous	(XWC14-038-28)⊗F_1	2BS-2SS·2SL	+	+	*Ph1_*
ZW14-141-8-3	Homozygous	(XWC14-038-28)⊗F_1	2BS-2SS·2SL	+	+	*Ph1_*
ZW14-142-3-1	Homozygous	(XWC14-038-32)⊗F_1	2BS-2SS·2SL	+	+	*Ph1_*
ZW14-142-4-1	Homozygous	(XWC14-038-32)⊗F_1	2BS-2SS·2SL	+	+	*Ph1_*
ZW14-142-4-2	Homozygous	(XWC14-038-32)⊗F_1	2BS-2SS·2SL	+	+	-
ZW14-147-4-1	Homozygous	(XWC14-038-38)⊗F_1	2SS·2SL-2BL	+	+	*Ph1_*

Plants	Genotype	Pedigree	Chromosome constitution	Identification by markers	Validation by FGISH	*Ph1*allele
ZW14-147-4-2	Homozygous	(XWC14-038-38)⊗F_1	2SS·2SL-2BL	+	+	*Ph1*_
ZW14-149-1-2	Homozygous	(XWC14-038-41)⊗F_1	2BS-2SS·2SL	+	+	*Ph1*_
ZW14-149-2-2	Homozygous	(XWC14-038-41)⊗F_1	2BS-2SS·2SL	+	+	-
ZW14-149-5-2	Homozygous	(XWC14-038-41)⊗F_1	2BS-2SS·2SL	+	+	*Ph1*_
ZW14-154-3-2	Homozygous	(XWC14-038-53)⊗F_1	2SS-2BS·2BL	+	+	*Ph1*_
ZW14-155-2-1	Homozygous	(XWC14-038-54)⊗F_1	2SS-2BS·2BL-2SL	+	+	*Ph1*_
ZW14-155-2-1	Homozygous	(XWC14-038-54)⊗F_1	2SS-2BS·2BL-2SL	+	+	-
ZW14-162-4	New recombinant	(XWC14-038-68)⊗F_1	2SS·2SL-2BL + 2BS·2BL-2SL-2SL	+	+	*Ph1*_
ZW14-166-3-2	Homozygous	(XWC14-038-74)⊗F_1	2SS-2BS·2BL-2SL	+	+	-
ZW14-167-1-1	Homozygous	(XWC14-038-76)⊗F_1	2SS-2BS·2BL	+	+	*Ph1*_
ZW14-167-1-2	Homozygous	(XWC14-038-76)⊗F_1	2SS-2BS·2BL	+	+	*Ph1*_
ZW14-167-2-2	Homozygous	(XWC14-038-76)⊗F_1	2SS-2BS·2BL	+	+	*Ph1*_
ZW14-167-4-2	Homozygous	(XWC14-038-76)⊗F_1	2SS-2BS·2BL	+	+	*Ph1*_
ZW14-167-8-2	Homozygous	(XWC14-038-76)⊗F_1	2SS-2BS·2BL	+	+	*Ph1*_
ZW14-169-3-1	Homozygous	(XWC14-038-80)⊗F_1	2BS·2BL-2SL	+	+	*Ph1*_
ZW14-169-3-2	Homozygous	(XWC14-038-80)⊗F_1	2BS·2BL-2SL	+	+	-
ZW14-169-5-2	Homozygous	(XWC14-038-80)⊗F_1	2BS·2BL-2SL	+	+	*Ph1*_
ZW14-171-4-2	Homozygous	(XWC14-038-86)⊗F_1	2BS·2BL-2SL + 2SS-2BS·2BL	+	+	*Ph1*_
ZW14-171-6-2	Homozygous	(XWC14-038-86)⊗F_1	2BS·2BL-2SL + 2SS-2BS·2BL	+	+	*Ph1*_
ZW14-173-7-2	Homozygous	(XWC14-038-89)⊗F_1	2SS-2BS·2BL	+	+	*Ph1*_
ZW14-174-2-2	Homozygous	(XWC14-038-92)⊗F_1	2SS-2BS·2BL	+	+	*Ph1*_
ZW14-175-7-1	Heterozygous	(XWC14-038-93)⊗F_1	2BS-2SS·D2SL	+	+	-
ZW14-180-2-2	Homozygous	(XWC14-038-100)⊗F_1	2SS-2BS-2SS·2SL	+	+	*Ph1*_
ZW14-180-5	New recombinant	(XWC14-038-100)⊗F_1	2SS-2BS-2SS·2SL-2BL	+	+	*Ph1*_
ZW14-181-3	Homozygous	(XWC14-039-1)⊗F_1	2SS-2BS·2BL-2SL	+	+	*Ph1*_
ZW14-184-6	Homozygous	(XWC14-039-6)⊗F_1	2SS-2BS·2BL	+	+	*Ph1*_

Plants	Genotype	Pedigree	Chromosome constitution	Identification by markers	Validation by FGISH	*Ph1*allele
ZW14-185-2	Homozygous	(XWC14-039-7)⊗F_1	2SS·2SL-2BL	+	+	*Ph1*_
ZW14-185-6	Homozygous	(XWC14-039-7)⊗F_1	2SS·2SL-2BL	+		-
ZW14-185-8	Homozygous	(XWC14-039-7)⊗F_1	2SS·2SL-2BL	+		*Ph1*_
ZW14-186-1-2	Homozygous	(XWC14-039-9)⊗F_1	2BS-2SS·2SL	+	+	-
ZW14-188-4-2	Homozygous	(XWC14-039-16)⊗F_1	2SS-2BS·2BL	+	+	*Ph1*_
ZW14-191-2	Homozygous	(XWC14-039-24)⊗F_1	2SS-2BS·2BL	+		*Ph1*_
ZW14-191-5	Homozygous	(XWC14-039-24)⊗F_1	2SS-2BS·2BL	+		*Ph1*_
ZW14-194-7	New recombinant	(XWC14-039-32)⊗F_1	2BS·2BL-2SL + 2SS-2BS·2BL	+	+	*Ph1*_
ZW14-197-2	New recombinant	(XWC14-039-36)⊗F_1	2BS-2SS·2SL	+		*Ph1*_
ZW14-197-6	Homozygous	(XWC14-039-36)⊗F_1	2SS-2BS·2BL-2SL	+		*Ph1*_
ZW14-201-2	Heterozygous	(XWC14-039-45)⊗F_1	2BS·2BL-2SL	+	+	*Ph1*_
ZW14-201-6	Heterozygous	(XWC14-039-45)⊗F_1	2BS·2BL-2SL	+		-
ZW14-203-3	Heterozygous	(XWC14-039-60)⊗F_1	2SS-2BS·2BL	+	+	*Ph1*_
ZW14-203-7	Heterozygous	(XWC14-039-60)⊗F_1	2SS-2BS·2BL	+		-
ZW14-204-4	Homozygous	(XWC14-039-61)⊗F_1	2BS·2BL-2SL	+		*Ph1*_
ZW14-205-7-1	new telosome	(XWC14-039-63)⊗F_1	2SS-2BS·2BL + T2SS	+	+	*Ph1*_
ZW14-205-7-2	Homozygous	(XWC14-039-63)⊗F_1	2SS-2BS·2BL	+	+	*Ph1*_
ZW14-206-2	Heterozygous	(XWC14-039-64)⊗F_1	T2SL	+	+	*Ph1*_
ZW14-206-7	Heterozygous	(XWC14-039-64)⊗F_1	T2SL	+		*Ph1*_
ZW14-207-2-1	New recombinant	(XWC14-038-75)⊗F_1	2BS-2SS·2SL-2BL-2SS	+	+	*Ph1*_
ZW14-207-2-2	Heterozygous	(XWC14-038-75)⊗F_1	2BS-2SS·2SL	+	+	*Ph1*_
ZW14-501-1	Homozygous	(XWC14-041-6)⊗F_1	2SS·2SL-2BL	+	+	-
ZW14-501-2	Homozygous	(XWC14-041-6)⊗F_1	2SS·2SL-2BL	+		*Ph1*_
ZW14-501-6	Homozygous	(XWC14-041-6)⊗F_1	2SS·2SL-2BL	+	+	*Ph1*_
ZW14-502-2	Homozygous	(XWC14-041-10)⊗F_1	2SS-2BS·2BL	+	+	*Ph1*_
ZW14-503-2	Homozygous	(XWC14-041-12)⊗F_1	2SS-2BS·2BL	+	+	*Ph1*_

Plants	Genotype	Pedigree	Chromosome constitution	Identification by markers	Validation by FGISH	*Ph1*allele
ZW14-503-4	Homozygous	(XWC14-041-12)⊗F_1	2SS-2BS·2BL	+		-
ZW14-504-5	Homozygous	(XWC14-041-13)⊗F_1	2SS-2BS·2BL	+	+	*Ph1_*
ZW14-505-1	Homozygous	(XWC14-041-15)⊗F_1	2SS-2BS·2BL	+	+	*Ph1_*
ZW14-505-2	Homozygous	(XWC14-041-15)⊗F_1	2SS-2BS·2BL	+	+	-
ZW14-506-1	Homozygous	(XWC14-041-18)⊗F_1	2SS-2BS·2BL	+	+	*Ph1_*
ZW14-507-4	Homozygous	(XWC14-041-19)⊗F_1	2SS-2BS·2BL	+		*Ph1_*
ZW14-507-5	Homozygous	(XWC14-041-19)⊗F_1	2SS-2BS·2BL	+	+	*Ph1_*
ZW14-508-4	Homozygous	(XWC14-041-37)⊗F_1	2SS·2SL-2BL	+	+	*Ph1_*
ZW14-508-6	Homozygous	(XWC14-041-37)⊗F_1	2SS·2SL-2BL	+		*Ph1_*
ZW14-510-7	Homozygous	(XWC14-041-46)⊗F_1	2SS-2BS·2BL	+	+	*Ph1_*
ZW14-511-5	New recombinant	(XWC14-041-49)⊗F_1	2SS·2SL-2BL	+	+	*Ph1_*
ZW14-511-7	Heterozygous	(XWC14-041-49)⊗F_1	2BS-2SS·2SL-2BL	+	+	*Ph1_*
ZW14-512-1	Heterozygous	(XWC14-041-63)⊗F_1	2SS·2SL-2BL + 2BS·2BL-2SL	+	+	-
ZW14-512-2	Heterozygous	(XWC14-041-63)⊗F_1	2SS·2SL-2BL + 2BS·2BL-2SL	+	+	-
ZW14-512-8	New recombinant	(XWC14-041-63)⊗F_1	2SS·2SL-2BL + 2BS·2BL-2SL	+	+	*Ph1_*
ZW14-513-6	Heterozygous	(XWC14-041-66)⊗F_1	2BS·2BL-2SL + 2SS·2SL-2BL	+	+	-
ZW14-514-6	Homozygous	(XWC14-041-78)⊗F_1	2SS·2SL-2BL	+	+	*Ph1_*
ZW14-515-3	Heterozygous	(XWC14-041-83)⊗F_1	2SS-2BS-2SS·2SL	+	+	*Ph1_*
ZW14-515-8	Heterozygous	(XWC14-041-83)⊗F_1	2SS-2BS-2SS·2SL	+	+	*Ph1_*
ZW14-516-4	Homozygous	(XWC14-041-84)⊗F_1	2SS·2SL-2BL	+	+	*Ph1_*
ZW14-516-5	Homozygous	(XWC14-041-84)⊗F_1	2SS·2SL-2BL	+		*Ph1_*
ZW14-517-5	Homozygous	(XWC14-041-85)⊗F_1	2SS·2SL-2BL	+		*Ph1_*
ZW14-517-6	Homozygous	(XWC14-041-85)⊗F_1	2SS·2SL-2BL	+	+	*Ph1_*
ZW14-518-8	Homozygous	(XWC14-041-87)⊗F_1	2SS·2SL-2BL-2SL	+	+	*Ph1_*
ZW14-519-2	Homozygous	(XWC14-043-16)⊗F_1	2BS-2SS·2SL	+		-
ZW14-519-3	New recombinant	(XWC14-043-16)⊗F_1	2BS-2SS·2SL-2BL	+	+	*Ph1_*

Plants	Genotype	Pedigree	Chromosome constitution	Identification by markers	Validation by FGISH	*Ph1*allele
ZW14-520-3	Homozygous	(XWC14-043-32)⊗F_1	2BS-2SS-2BS·2BL	+		*Ph1*_
ZW14-520-4	Homozygous	(XWC14-043-32)⊗F_1	2BS-2SS-2BS·2BL	+		-
ZW14-521-3	Heterozygous	(XWC14-043-47)⊗F_1	2BS-2SS·2SL-2BL	+	+	*Ph1*_
ZW14-522-3	Homozygous	(XWC14-043-61)⊗F_1	2SS·2SL-2BL	+		*Ph1*_
ZW14-522-4	Homozygous	(XWC14-043-61)⊗F_1	2SS·2SL-2BL	+	+	*Ph1*_
ZW14-523-7	Homozygous	(XWC14-043-87)⊗F_1	2SS·2SL-2BL-2SL	+	+	-
ZW14-524-4	Homozygous	(XWC14-043-89)⊗F_1	2SS·2SL-2BL	+	+	*Ph1*_
ZW14-524-8	Homozygous	(XWC14-043-89)⊗F_1	2SS·2SL-2BL	+		*Ph1*_
ZW14-525-3	Heterozygous	(XWC14-043-95)⊗F_1	2BS-2SS·2SL-2BL-2SL	+	+	*Ph1*_
ZW14-525-8	New telosome	(XWC14-043-95)⊗F_1	T2SL	+	+	*Ph1*_
ZW14-526-1	Homozygous	(XWC14-043-96)⊗F_1	2BS·2BL-2SL	+	+	*Ph1*_
ZW14-526-3	Homozygous	(XWC14-043-96)⊗F_1	2BS·2BL-2SL	+		-
ZW14-526-5	Homozygous	(XWC14-043-96)⊗F_1	2BS·2BL-2SL	+		*Ph1*_
ZW14-526-8	Homozygous	(XWC14-043-96)⊗F_1	2BS·2BL-2SL	+		*Ph1*_
ZW14-527-3	New recombinants	(XWC14-043-97)⊗F_1	2BS·2BL-2SL + 2BS-2SS·2SL-2BL	+	+	-
ZW14-527-6	Homozygous	(XWC14-043-97)⊗F_1	2SS·2SL-2BL-2SL	+	+	*Ph1*_
ZW14-528-5	Homozygous	(XWC14-043-98)⊗F_1	2BS·2BL-2SL	+		*Ph1*_
ZW14-217-2	Heterozygous	(XWC14-130-38)⊗F_1	T2ES	+	+	*Ph1*_
ZW14-217-8	Heterozygous	(XWC14-130-38)⊗F_1	T2ES	+		-
ZW14-220-2	Homozygous	(XWC14-131-4)⊗F_1	2ES·2BL	+		*Ph1*_
ZW14-221-1	Homozygous	(XWC14-131-8)⊗F_1	2ES·2BL	+	+	*Ph1*_
ZW14-222-4	Homozygous	(XWC14-131-11)⊗F_1	2ES·2BL	+		*Ph1*_
ZW14-224-1	Homozygous	(XWC14-131-13)⊗F_1	2ES·2BL	+	+	-
ZW14-224-4	Homozygous	(XWC14-131-13)⊗F_1	2ES·2BL	+		*Ph1*_
ZW14-225-1	Homozygous	(XWC14-131-17)⊗F_1	2ES·2BL	+		-
ZW14-225-7	Homozygous	(XWC14-131-17)⊗F_1	2ES·2BL	+		*Ph1*_

Plants	Genotype	Pedigree	Chromosome constitution	Identification by markers	Validation by FGISH	*Ph1*allele
ZW14-226-8	Homozygous	(XWC14-131-18)⊗F_1	2ES·2BL	+	+	*Ph1*_
ZW14-227-2	Homozygous	(XWC14-131-19)⊗F_1	2ES·2BL	+		*Ph1*_
ZW14-228-2	Homozygous	(XWC14-131-20)⊗F_1	2ES·2BL	+	+	*Ph1*_
ZW14-228-5	Homozygous	(XWC14-131-20)⊗F_1	2ES·2BL	+		-
ZW14-228-8	Homozygous	(XWC14-131-20)⊗F_1	2ES·2BL	+		*Ph1*_
ZW14-229-2	New recombinant	(XWC14-131-23)⊗F_1	2ES·2BL + 2ES-2BS·2BL	+	+	*Ph1*_
ZW14-230-8	Homozygous	(XWC14-131-25)⊗F_1	2ES·2BL	+		*Ph1*_
ZW14-231-7	Homozygous	(XWC14-131-26)⊗F_1	2ES·2BL	+		*Ph1*_
ZW14-232-2	Homozygous	(XWC14-131-28)⊗F_1	2ES·2BL	+	+	-
ZW14-232-3	Homozygous	(XWC14-131-28)⊗F_1	2ES·2BL	+		*Ph1*_
ZW14-233-2	Homozygous	(XWC14-131-29)⊗F_1	2ES·2BL	+		*Ph1*_
ZW14-234-2	Homozygous	(XWC14-131-31)⊗F_1	2ES·2BL	+		*Ph1*_
ZW14-234-3	Homozygous	(XWC14-131-31)⊗F_1	2ES·2BL	+	+	-
ZW14-235-4	Homozygous	(XWC14-131-32)⊗F_1	2ES·2BL	+	+	*Ph1*_
ZW14-235-8	Homozygous	(XWC14-131-32)⊗F_1	2ES·2BL	+		*Ph1*_
ZW14-236-2	Homozygous	(XWC14-131-33)⊗F_1	2ES-2BS·2BL	+	+	-
ZW14-236-4	Homozygous	(XWC14-131-33)⊗F_1	2ES-2BS·2BL	+		*Ph1*_
ZW14-236-7	Homozygous	(XWC14-131-33)⊗F_1	2ES-2BS·2BL	+		*Ph1*_
ZW14-236-8	Homozygous	(XWC14-131-33)⊗F_1	2ES-2BS·2BL	+		*Ph1*_
ZW14-237-2	Homozygous	(XWC14-131-35)⊗F_1	2ES·2BL	+	+	*Ph1*_
ZW14-238-3	Homozygous	(XWC14-131-36)⊗F_1	2ES·2BL	+	+	*Ph1*_
ZW14-239-2	Homozygous	(XWC14-131-38)⊗F_1	2ES·2BL	+	+	-
ZW14-239-6	Homozygous	(XWC14-131-38)⊗F_1	2ES·2BL	+		*Ph1*_
ZW14-241-3	Homozygous	(XWC14-132-3)⊗F_1	2BS-2ES·2EL	+	+	*Ph1*_
ZW14-241-7	Homozygous	(XWC14-132-3)⊗F_1	2BS-2ES·2EL	+		*Ph1*_
ZW14-242-2	New recombinant	(XWC14-132-15)⊗F_1	2BS-2ES·2EL-2BL + T2ES	+	+	*Ph1*_

Plants	Genotype	Pedigree	Chromosome constitution	Identification by markers	Validation by FGISH	*Ph1*allele
ZW14-242-3	Monosomic	(XWC14-132-15)⊗F_1	2BS-2ES·2EL-2BL	+	+	*Ph1*_
ZW14-243-7	Homozygous	(XWC14-132-20)⊗F_1	2ES·2EL-2BL	+		*Ph1*_
ZW14-245-1	Homozygous	(XWC14-132-36)⊗F_1	2ES-2BS·2BL	+	+	*Ph1*_
ZW14-245-8	Homozygous	(XWC14-132-36)⊗F_1	2ES-2BS·2BL	+		*Ph1*_
ZW14-246-4	Homozygous	(XWC14-132-54)⊗F_1	2ES·2EL-2BL	+	+	*Ph1*_
ZW14-253-4	Heterozygous	(XWC14-132-71)⊗F_1	2ES·2EL-2BL	+	+	*Ph1*_
ZW14-253-8	Homozygous	(XWC14-132-71)⊗F_1	2ES·2EL-2BL	+	+	*Ph1*_
ZW14-255-1	Monosomic	(XWC14-132-73)⊗F_1	T2ES	+	+	-
ZW14-257-3	Homozygous	(XWC14-132-75)⊗F_1	2BS-2ES·2EL	+	+	*Ph1*_
ZW14-257-6	Homozygous	(XWC14-132-75)⊗F_1	2BS-2ES·2EL	+	+	*Ph1*_
ZW14-258-4	Heterozygous	(XWC14-132-80)⊗F_1	2BS-2ES·2EL	+	+	*Ph1*_
ZW14-258-7	Homozygous	(XWC14-132-80)⊗F_1	2BS-2ES·2EL	+	+	*Ph1*_
ZW14-261-4	Homozygous	(XWC14-132-87)⊗F_1	2BS-2ES·2EL	+	+	*Ph1*_
ZW14-261-5	Homozygous	(XWC14-132-87)⊗F_1	2BS-2ES·2EL	+	+	-
ZW14-261-6	Homozygous	(XWC14-132-87)⊗F_1	2BS-2ES·2EL	+	+	*Ph1*_
ZW14-266-3	Heterozygous	(XWC14-132-99)⊗F_1	2ES-2BS·2BL	+	+	-
ZW14-266-6	Homozygous	(XWC14-132-99)⊗F_1	2ES-2BS·2BL	+	+	*Ph1*_
ZW14-266-8	Homozygous	(XWC14-132-99)⊗F_1	2ES-2BS·2BL	+	+	*Ph1*_
ZW14-267-3	Heterozygous	(XWC14-132-101)⊗F_1	2ES-2BS·2BL	+	+	*Ph1*_
ZW14-267-7	Heterozygous	(XWC14-132-101)⊗F_1	2ES-2BS·2BL	+	+	*Ph1*_
ZW14-269-7	Heterozygous	(XWC14-132-105)⊗F_1	2ES·2EL-2BL	+	+	*Ph1*_
ZW14-270-3	Homozygous	(XWC14-132-108)⊗F_1	2BS-2ES·2EL	+	+	*Ph1*_
ZW14-270-5	Heterozygous	(XWC14-132-108)⊗F_1	2BS-2ES·2EL	+	+	-
ZW14-272-2	Homozygous	(XWC14-132-111)⊗F_1	2ES·2EL-2BL	+	+	*Ph1*_
ZW14-273-6	Homozygous	(XWC14-132-114)⊗F_1	2ES·2EL-2BL	+	+	*Ph1*_
ZW14-273-7	Homozygous	(XWC14-132-114)⊗F_1	2ES·2EL-2BL	+	+	*Ph1*_

Plants	Genotype	Pedigree	Chromosome constitution	Identification by markers	Validation by FGISH	*Ph1*allele
ZW14-280-1	Homozygous	(XWC14-132-127)⊗F_1	2ES-2BS·2BL	+	+	*Ph1*_
ZW14-280-2	Heterozygous	(XWC14-132-127)⊗F_1	2ES-2BS·2BL	+	+	*Ph1*_
ZW14-280-3	Homozygous	(XWC14-132-127)⊗F_1	2ES-2BS·2BL	+	+	*Ph1*_
ZW14-280-5	Homozygous	(XWC14-132-127)⊗F_1	2ES-2BS·2BL	+	+	*Ph1*_
ZW14-280-8	Homozygous	(XWC14-132-127)⊗F_1	2ES-2BS·2BL	+	+	*Ph1*_
ZW14-284-1	Homozygous	(XWC14-132-127)⊗F_1	2ES-2BS·2BL	+	+	*Ph1*_
ZW14-289-3	Homozygous	(XWC14-133-35)⊗F_1	2BS-2ES·2EL	+	+	*Ph1*_
ZW14-293-4	Homozygous	(XWC14-133-49)⊗F_1	2ES-2BS·2BL	+	+	*Ph1*_
ZW14-293-6	Homozygous	(XWC14-133-49)⊗F_1	2ES-2BS·2BL	+	+	*Ph1*_
ZW14-293-7	Homozygous	(XWC14-133-49)⊗F_1	2ES-2BS·2BL	+	+	-
ZW14-297-2	Homozygous	(XWC14-133-55)⊗F_1	2ES-2BS·2BL	+	+	*Ph1*_
ZW14-297-6	Homozygous	(XWC14-133-55)⊗F_1	2ES-2BS·2BL	+	+	*Ph1*_
ZW14-299-3	Homozygous	(XWC14-133-58)⊗F_1	2ES·2EL-2BL	+	+	*Ph1*_
ZW14-299-5	Homozygous	(XWC14-133-58)⊗F_1	2ES·2EL-2BL	+	+	*Ph1*_
ZW14-299-7	Heterozygous	(XWC14-133-58)⊗F_1	2ES·2EL-2BL	+	+	*Ph1*_
ZW14-300-6	Homozygous	(XWC14-133-59)⊗F_1	2ES-2BS·2BL	+	+	*Ph1*_
ZW14-301-5	New telosome	(XWC14-133-60)⊗F_1	T2ES	+	+	*Ph1*_
ZW14-306-2	New recombinant	(XWC14-134-6)⊗F_1	2BS-2ES·2EL	+	+	*Ph1*_
ZW14-306-6	Heterozygous	(XWC14-134-6)⊗F_1	2BS-2ES·2EL-2BL	+	+	-
ZW14-306-8	Heterozygous	(XWC14-134-6)⊗F_1	2BS-2ES·2EL	+	+	*Ph1*_
ZW14-308-2	Homozygous	(XWC14-134-10)⊗F_1	2ES·2EL-2BL	+	+	*Ph1*_
ZW14-310-4	Homozygous	(XWC14-134-13)⊗F_1	2ES-2BS·2BL	+	+	*Ph1*_
ZW14-311-3	Homozygous	(XWC14-134-15)⊗F_1	2ES-2BS·2BL	+	+	*Ph1*_
ZW14-311-6	Homozygous	(XWC14-134-15)⊗F_1	2ES-2BS·2BL	+	+	-
ZW14-311-8	Homozygous	(XWC14-134-15)⊗F_1	2ES-2BS·2BL	+	+	*Ph1*_
ZW14-313-4	Heterozygous	(XWC14-134-17)⊗F_1	2ES-2BS·2BL	+	+	*Ph1*_

Plants	Genotype	Pedigree	Chromosome constitution	Identification by markers	Validation by FGISH	*Ph1*allele
ZW14-313-8	Homozygous	(XWC14-134-17)⊗F_1	2ES-2BS·2BL	+	+	-
ZW14-315-1	Heterozygous	(XWC14-134-19)⊗F_1	2ES·2EL-2BL	+	+	*Ph1_*
ZW14-320-6	Heterozygous	(XWC14-134-26)⊗F_1	2ES·2EL-2BL	+	+	*Ph1_*
ZW14-323-2	Heterozygous	(XWC14-134-31)⊗F_1	2ES·2BL	+	+	*Ph1_*
ZW14-323-3	Heterozygous	(XWC14-134-55)⊗F_1	2ES-2BS·2BL	+	+	-
ZW14-328-4	New recombinant	(XWC14-134-55)⊗F_1	2ES-2BS·2BL	+	+	*Ph1_*
ZW14-331-1	Homozygous	(XWC14-134-74)⊗F_1	T2ES	+	+	*Ph1_*
ZW14-334-4	Homozygous	(XWC14-134-81)⊗F_1	2ES-2BS·2BL	+	+	*Ph1_*
ZW14-335-2	Homozygous	(XWC14-134-82)⊗F_1	2ES·2EL-2BL	+	+	*Ph1_*
ZW14-338-1	Monosomic	(XWC14-134-74)⊗F_1	T2ES	+	+	*Ph1_*
ZW14-343-2	Homozygous	(XWC14-134-96)⊗F_1	2ES·2EL-2BL	+	+	*Ph1_*
ZW14-343-7	Homozygous	(XWC14-134-96)⊗F_1	2ES·2EL-2BL	+		*Ph1_*
ZW14-347-2	Homozygous	(XWC14-134-103)⊗F_1	2ES-2BS·2BL	+	+	*Ph1_*
ZW14-347-4	Homozygous	(XWC14-134-103)⊗F_1	2ES-2BS·2BL	+	+	-
ZW14-349-6	Monosomic	(XWC14-134-106)⊗F_1	T2ES	+	+	*Ph1_*
ZW14-357-1	Homozygous	(XWC14-136-36)⊗F_1	2ES-2BS·2BL	+	+	*Ph1_*
ZW14-357-3	Homozygous	(XWC14-136-36)⊗F_1	2ES-2BS·2BL	+	+	*Ph1_*
ZW14-357-8	Homozygous	(XWC14-136-36)⊗F_1	2ES-2BS·2BL	+	+	*Ph1_*
ZW14-380-2	Monosomic	(XWC14-139-40)⊗F_1	2ES·2BL	+	+	-
ZW14-381-7	Homozygous	(XWC14-139-48)⊗F_1	T2ES	+	+	*Ph1_*
ZW14-382-5	Homozygous	(XWC14-139-49)⊗F_1	2ES·2EL-2BL	+	+	*Ph1_*
ZW14-382-6	Homozygous	(XWC14-139-49)⊗F_1	2ES·2EL-2BL	+		*Ph1_*
ZW14-382-7	Homozygous	(XWC14-139-49)⊗F_1	2ES·2EL-2BL	+		*Ph1_*
ZW14-387-5	Homozygous	(XWC14-130-3)⊗F_1	2ES-2BS·2BL	+	+	-
ZW14-390-1	Homozygous	(XWC14-141-57)⊗F_1	2ES-2BS·2BL	+		*Ph1_*
ZW14-390-2	Homozygous	(XWC14-141-57)⊗F_1	2ES-2BS·2BL	+	+	-

Plants	Genotype	Pedigree	Chromosome constitution	Identification by markers	Validation by FGISH	*Ph1*allele
ZW14-390-3	Homozygous	(XWC14-141-57)⊗F_1	2ES-2BS·2BL	+		-
ZW14-390-8	Homozygous	(XWC14-141-57)⊗F_1	2ES-2BS·2BL	+		*Ph1_*
ZW14-391-2	Homozygous	(XWC14-142-8)⊗F_1	2BS·2BL-2EL	+		*Ph1_*
ZW14-391-7	Homozygous	(XWC14-142-8)⊗F_1	2BS·2BL-2EL	+	+	*Ph1_*
ZW14-392-1	Homozygous	(XWC14-142-28)⊗F_1	2ES-2BS·2BL	+	+	*Ph1_*
ZW14-392-3	Homozygous	(XWC14-142-28)⊗F_1	2ES-2BS·2BL	+		*Ph1_*
ZW14-392-5	Homozygous	(XWC14-142-28)⊗F_1	2ES-2BS·2BL	+		*Ph1_*
ZW14-392-6	Homozygous	(XWC14-142-28)⊗F_1	2ES-2BS·2BL	+	+	*Ph1_*
ZW14-393-1	Homozygous	(XWC14-142-30)⊗F_1	2ES·2EL-2BL	+	+	-
ZW14-393-7	Homozygous	(XWC14-142-30)⊗F_1	2ES·2EL-2BL	+		*Ph1_*
ZW14-394-4	Homozygous	(XWC14-142-36)⊗F_1	2ES-2BS·2BL	+	+	*Ph1_*
ZW14-395-1	Homozygous	(XWC14-143-50)⊗F_1	2ES-2BS·2BL-2EL	+		*Ph1_*
ZW14-395-4	Homozygous	(XWC14-143-50)⊗F_1	2ES-2BS·2BL-2EL	+	+	*Ph1_*
ZW14-396-3	Homozygous	(XWC14-143-56)⊗F_1	2ES-2BS·2BL	+	+	*Ph1_*
ZW14-396-7	Homozygous	(XWC14-143-56)⊗F_1	2ES-2BS·2BL	+	+	*Ph1_*
ZW14-397-5	Homozygous	(XWC14-143-59)⊗F_1	2BS·2BL-2EL	+	+	*Ph1_*
ZW14-398-1	Heterozygous	(XWC14-143-77)⊗F_1	2BS-2ES·2EL-2BL	+		-
ZW14-398-4	New recombinant	(XWC14-143-77)⊗F_1	2BS-2ES·2EL-2BL + 2BS-2ES·2EL	+	+	-
ZW14-398-5	Heterozygous	(XWC14-143-77)⊗F_1	2BS-2ES·2EL-2BL	+	+	*Ph1_*
ZW14-398-7	Heterozygous	(XWC14-143-77)⊗F_1	2BS-2ES·2EL-2BL + 2ES·2EL-2BL	+		*Ph1_*
ZW14-399-5	Homozygous	(XWC14-143-87)⊗F_1	2ES-2BS·2BL	+	+	*Ph1_*
ZW14-399-8	Homozygous	(XWC14-143-87)⊗F_1	2ES-2BS·2BL	+	+	*Ph1_*
ZW14-400-5	Homozygous	(XWC14-715-2)⊗F_1	2BS-2ES·2EL	+	+	*Ph1_*
ZW14-400-6	Homozygous	(XWC14-715-2)⊗F_1	2BS-2ES·2EL	+	+	*Ph1_*
ZW14-401-1	Homozygous	(XWC14-715-47)⊗F_1	2ES-2BS·2BL + 2BS·2BL-2EL	+		-
ZW14-401-11	Homozygous	(XWC14-715-47)⊗F_1	2ES-2BS·2BL + 2BS·2BL-2EL	+		*Ph1_*

Plants	Genotype	Pedigree	Chromosome constitution	Identification by markers	Validation by FGISH	*Ph1*allele
ZW14-401-13	Homozygous	(XWC14-715-47)⊗F_1	2ES-2BS·2BL + 2BS·2BL-2EL	+		-
ZW14-401-14	Homozygous	(XWC14-715-47)⊗F_1	2ES-2BS·2BL + 2BS·2BL-2EL	+		*Ph1_*
ZW14-401-4	Homozygous	(XWC14-715-47)⊗F_1	2ES-2BS·2BL + 2BS·2BL-2EL	+	+	*Ph1_*
ZW14-402-6	Homozygous	(XWC14-715-78)⊗F_1	2ES-2BS·2BL	+	+	*Ph1_*
ZW14-403-6	Homozygous	(XWC14-715-85)⊗F_1	2BS·2BL-2EL	+	+	*Ph1_*
ZW14-404-7	Homozygous	(XWC14-716-5)⊗F_1	2ES-2BS·2BL	+	+	*Ph1_*
ZW14-405-5	Homozygous	(XWC14-716-19)⊗F_1	2BS-2ES·2EL	+		*Ph1_*
ZW14-405-7	Homozygous	(XWC14-716-19)⊗F_1	2BS-2ES·2EL	+	+	-
ZW14-406-4	Homozygous	(XWC14-716-72)⊗F_1	2ES-2BS·2BL	+	+	*Ph1_*
ZW14-406-7	Homozygous	(XWC14-716-72)⊗F_1	2ES-2BS·2BL	+		*Ph1_*
ZW14-407-3	Homozygous	(XWC14-716-84)⊗F_1	2ES-2BS·2BL	+		*Ph1_*
ZW14-407-4	Homozygous	(XWC14-716-84)⊗F_1	2ES-2BS·2BL	+	+	-
ZW14-407-5	Homozygous	(XWC14-716-84)⊗F_1	2ES-2BS·2BL	+		*Ph1_*
ZW14-407-6	Homozygous	(XWC14-716-84)⊗F_1	2ES-2BS·2BL	+	+	*Ph1_*
ZW14-408-4	Heterozygous	(XWC14-716-85)⊗F_1	2BS·2BL-2EL	+	+	*Ph1_*
ZW14-409-6	Homozygous	(XWC14-717-27)⊗F_1	2BS-2ES·2EL	+	+	*Ph1_*
ZW14-410-2	Homozygous	(XWC14-717-48)⊗F_1	2ES-2BS·2BL	+	+	-
ZW14-410-6	Homozygous	(XWC14-717-48)⊗F_1	2ES-2BS·2BL	+		*Ph1_*
ZW14-412-4	Homozygous	(XWC14-717-56)⊗F_1	2BS·2BL-2EL	+	+	*Ph1_*

APPENDIX E. MEASUREMENT AND SIZE CALCULATION OF ALIEN CHROMOSOME SEGMENTS IN THE 2B-2S AND 2B-2E RECOBMINANTS

Recombinants	Chromosome constitution	Length (μm)				Proportion (%)a
		Alien segment on short arm	Short arm	Alien segment on long arm	Long arm	
XWC14-034-27	2BS·2BL-2SL	0	4.9	2.3	6.47	20.2
XWC14-034-40	2SS-2BS·2BL	0.97	3.99	0	4.5	11.4
XWC14-034-40	2BS-2SS·2SL	4.18	5.09	5.56	5.56	91.5
XWC14-034-45	2SS·2SL-2BL	7.73	7.73	7.42	9.97	85.6
XWC14-035-17	2SS·2SL-2BL	7.98	7.98	8.02	9.35	92.3
XWC14-035-20	2SS·2SL-2BL	5.97	5.97	6.33	7.97	88.2
XWC14-035-31	2SS·2SL-2BL	5.69	5.69	6.24	7.25	92.2
XWC14-039-24	2SS-2BS·2BL	0.54	4.73	0	5.21	5.4
XWC14-039-27	2SS·2SL-2BL	5.25	5.25	5.04	6.41	88.3
XWC14-039-61	2BS·2BL-2SL	0	4.52	2.11	5.17	21.8
ZW14-001-15	2BS·2BL-2SL	0	5.06	2.33	6.24	20.6
ZW14-002-1	2SS·2SL-2BL	6.09	6.09	5.59	7.73	84.5
ZW14-004-1	2SS·2SL-2BL	7.73	7.73	6.25	8.85	84.3
ZW14-005-8	2SS·2SL-2BL	5.56	5.56	5.04	7.67	80.1
ZW14-007-7	2BS-2SS·2SL	3.41	4.4	6.5	6.5	90.9
ZW14-008-5	2SS-2BS·2BL	1.68	4.5	0	5.6	16.6
ZW14-008-5	2BS-2SS·2SL	5.07	6.27	7.04	7.04	91.0
ZW14-009-3	2BS·2BL-2SL	0	5.59	2.98	7.16	23.4
ZW14-010-2	2SS-2BS·2BL	1.09	4.78	0	5.87	10.2
ZW14-011-1	2SS·2SL-2BL	5.59	5.59	4.4	6.18	84.9
ZW14-013-4	2SS·2SL-2BL	5.61	5.61	5.49	6.63	90.7
ZW14-014-2	2BS·2BL-2SL	0	5.74	2.05	6.64	16.6
ZW14-016-6	2BS-2SS·2SL	2.7	4.73	6.1	6.1	81.3
ZW14-070-1	2SS·2SL-2BL	6.65	6.65	7.18	8.8	89.5
ZW14-071-2	2BS-2SS·2SL	3.04	4.03	4.22	4.22	88.0
ZW14-073-1	2SS·2SL-2BL	6.64	6.64	5.84	8.08	84.8
ZW14-074-2	2BS·2BL-2SL	0	6.76	2.7	8.77	17.4
ZW14-077_8_1	2SS·2SL-2BL-2SL	4.88	4.88	3.41 + 0.88	5.77	86.1
ZW14-077-8-2	2BS·2BL-2SL	0	6.44	5.4	11.32	30.4
ZW14-084	2BS·2BL-2SL	0	4.62	4.69	6.83	41.0
ZW14-093-8-1	2BS-2SS·2SL	3.01	3.87	4.94	4.94	90.2
ZW14-095-6	2SS-2BS·2BL	1.57	5.3	0	7.37	12.4
ZW14-100-1	2SS·2SL-D2BL	6.66	6.66	4.44	5.77	89.3
ZW14-108-6-2	2SS-2BS·2BL	1.27	5.12	0	5.51	11.9
ZW14-111-3-2	2SS·2SL-2BL	6.13	6.13	5.05	7.97	79.3
ZW14-115-7-2	2BS-2SS·2SL	4.07	5.06	6.34	6.34	91.3

Recombinants	Chromosome constitution	Length (μm)				Proportion (%)a
		Alien segment on short arm	Short arm	Alien segment on long arm	Long arm	
ZW14-116-5	2BS·2BL-2SL	0	6.65	0.97	7.68	6.8
ZW14-117-15	2BS·2BL-2SL	0	4.51	2.05	6.33	18.9
ZW14-117-15	2SS-2BS·2BL	1.24	7.45	0	10.48	6.9
ZW14-118-1	2BS·2BL-2SL	0	5.84	2.46	7.01	19.1
ZW14-121-3	2BS·2BL-2SL	0	4.51	2.01	5.97	19.2
ZW14-127_8_2	2BS·2BL-2SL	4.05	5.85	6.8	6.8	85.8
ZW14-127-8-2	2BS-2SL·2SL	0	7.62	3.69	11.99	18.8
ZW14-128-1	2BS·2BL-2SL	0	6.16	2.8	8.47	19.1
ZW14-134-3-1	2BS-2SS·2SL	7.05	7.88	9.67	9.67	95.3
ZW14-135-6-2	2BS·2BL-2SL	5.1	5.1	4.31	5.8	86.3
ZW14-137-7-1	2SS-2BS·2BL	1.55	6.52	0	7.24	11.3
ZW14-139-7-1	2SS-2BS·2BL	2.08	8.08	0	11.48	10.6
ZW14-141-8-2	2BS-2SS·2SL	7.6	8.71	11.01	11.01	94.4
ZW14-142-4-2	2BS-2SS·2SL	5.04	5.94	7.35	7.35	93.2
ZW14-147-4-1	2SS·2SL-2BL	4.98	4.98	4.47	6.79	80.3
ZW14-149-1-2	2BS-2SS·2SL	4.98	5.63	7.37	7.37	95.0
ZW14-154-3-2	2SS-2BS·2BL	1.83	5.11	0	4.46	19.1
ZW14-155-2-1	2SS-2BS·2BL-2SL	0.4	5.38	0.2	6.95	4.9
ZW14-162_4	2BS·2BL-2SL-2BL	0	5.42	3.42 + 2.6	8.32	16.7
ZW14-162-4-2	2SS·2SL-2BL	6.4	6.4	4.69	7.07	82.3
ZW14-166-3-2	2SS-2BS·2BL-2SL	1.48	6.94	1.02	7.32	17.5
ZW14-167-1-2	2SS-2BS·2BL	1.69	7.88	0	8.95	10.0
ZW14-169-5-2	2BS·2BL-2SL	0	4.9	1.46	6.64	12.7
ZW14-171-4-2	2SS-2BS·2BL	1.61	6.9	0	7.99	10.8
ZW14-171-4-2	2BS·2BL-2SL	0	7.33	5.59	9.53	33.2
ZW14-173-7-2	2SS-2BS·2BL	1.48	6.73	0	9.32	9.2
ZW14-174-2-2	2SS-2BS·2BL	1.63	6.24	0	8.31	11.2
ZW14-175-7-1	2BS-2SS·T2SL	5.24	6.68	0	0	78.4
ZW14-180-2-1	2SS-2BS-2SS·2SL	0.68 + 4.58	6.26	6.98	6.98	92.4
ZW14-180-5-1	2SS-2BS-2SS·2SL-2BL	0.64 + 4.55	6.16	5.2	6.61	81.4
ZW14-181-3	2SS-2BS·2BL-2SL	1.61	9.86	1.84	10.65	16.8
ZW14-184-6	2SS-2BS·2BL	1.3	4.12	0	5.07	14.1
ZW14-185-2	2SS·2SL-2BL	5.57	5.57	4.37	6.15	84.8
ZW14-186-1-2	2BS-2SS·2SL	4.42	5.92	7.03	7.03	88.4
ZW14-188-4-2	2SS-2BS·2BL	1.21	6.03	0	7.02	9.3
ZW14-194-7	2BS·2BL-2SL	0	5.13	2.14	6.43	18.5
ZW14-194-7	2SS-2BS·2BL	1.21	6.69	0	8.85	7.8

Recombinants	Chromosome constitution	Length (μm)				Proportion (%)a
		Alien segment on short arm	Short arm	Alien segment on long arm	Long arm	
ZW14-197-6	2SS-2BS·2BL-2SL	1.41	6.15	1.54	7.53	21.6
ZW14-201-2	2BS·2BL-2SL	0	7.99	7.74	9.91	43.2
ZW14-203-3	2SS-2BS·2BL	0.64	7.96	0	8.75	3.8
ZW14-205_7_1	2SS-2BS·2BL	0.46	5.24	0	5.76	4.2
ZW14-207-2-1	2SS-2BS·2BL	2.62	3.97	3.87 + 0.45	5.15	76.1
ZW14-207-2-1	2BS-2SS·2SL-2BL-2BS	4.68	6.12	4.99 + 0.51	6.72	79.3
ZW14-501-1	2SS·2SL-2BL	6.44	6.44	4.21	6.33	83.4
ZW14-502-2	2SS-2BS·2BL	1.93	6.66	0	8.95	12.4
ZW14-503-2	2SS-2BS·2BL	1.17	6.92	0	7.46	8.1
ZW14-504-5	2SS-2BS·2BL	1.45	4.88	0	6.49	12.8
ZW14-505-1	2SS-2BS·2BL	1.04	5.48	0	6.63	8.6
ZW14-506-1	2SS-2BS·2BL	1.57	5.12	0	6.26	13.8
ZW14-507-5	2SS-2BS·2BL	0.92	4.69	0	5.48	9.0
ZW14-508-4	2SS·2SL-2BL	5.96	5.96	3.42	6.32	76.4
ZW14-510-7	2SS-2BS·2BL	1.02	5.59	0	7.17	8.0
ZW14-511-5	2SS·2SL-2BL	5.7	6.52	6.16	7.86	82.5
ZW14-511-7	2BS-2SS·2SL-2BL	5.11	5.11	5.61	6.75	90.4
ZW14-512-1	2BS·2BL-2SL	0	6.01	1.2	8.09	8.5
ZW14-512-2	2SS·2SL-2BL	5.63	5.63	4.89	6.66	85.6
ZW14-513-6	2SS·2SL-2BL	9.32	9.32	7.79	10.56	86.1
ZW14-513-6	2BS·2BL-2SL	0	5.47	1.47	6.42	12.4
ZW14-514-6	2SS·2SL-2BL	9.33	9.33	8.71	11.72	85.7
ZW14-515-8	2SS-2BS-2SS·2SL	0.5 + 3.58	5.12	6.41	6.41	91.1
ZW14-516-4	2SS·2SL-2BL	7.43	7.43	7.51	9.01	90.9
ZW14-517-6	2SS·2SL-2BL	6.76	6.76	5.51	7.56	85.7
ZW14-518-8	2SS·2SL-2BL-2SL	4.36	4.36	2.81 + 0.47	4.51	86.1
ZW14-519-2	2BS-2SS·2SL	7.83	7.83	6.93	9.09	87.2
ZW14-520-3	2SS-2BS·2BL	1.71	7.23	0	10.16	9.8
ZW14-521-3	2SS·2SL-2BL	5.13	5.13	3.94	6.17	80.3
ZW14-522-4	2SS·2SL-2BL	4.69	4.69	2.82	5.11	76.6
ZW14-523-7	2SS·2SL-2BL-2SL	7.13	7.13	5.33 + 0.66	7.94	87.1
ZW14-524-4	2SS·2SL-2BL	5.77	5.77	5.56	6.64	91.3
ZW14-525-5	2BS-2SS·2SL-2BL-2SL	6.91	8.091	8.02 + 0.75	10.11	86.1
ZW14-526-1	2BS·2BL-2SL	0	8.4	2.67	10.77	13.9
ZW14-527_3	2BS·2BL-2BS	0	7.38	5.14	9.82	29.9
ZW14-527_3	2BS-2SS·2SL-2BL	0.33 + 5.20	6.72	3.62	6.76	67.9
ZW14-527_3	2BS·2BL-2SL	0	8.3	1.41	10.43	7.5

Recombinants	Chromosome constitution	Length (μm)				Proportion (%)a
		Alien segment on short arm	Short arm	Alien segment on long arm	Long arm	
ZW14-527-3	2SS·2SL-2BL-2SS	7.37	7.37	4.69 + 0.43	8.5	78.7
ZW14-528-5	2BS·2BL-2SL	0	6.02	2.11	5.17	18.9
XWC14-130-3	2ES-2BS·2BL	2.95	5.84	0	8.84	20.1
ZW14-229-2	2ES-2BS·2BL	1.55	7.78	0	10.08	8.7
ZW14-234-3	2ES·2BL	10.15	10.15	0	13.19	43.5
XWC14-131-33	2ES-2BS·2BL	3.43	7.83	0	8.93	20.5
ZW14-267-1	2ES-2BS·2BL	17.89	25.12	30.5	30.5	87.0
ZW14-269-7	2ES·2EL-2BL	6.28	6.28	6.64	6.93	97.8
ZW14-270-3	2BS-2ES·2EL	4.71	5.32	6.77	6.77	95.0
ZW14-272-2	2ES·2EL-2BL	5.15	5.15	5.01	5.7	93.6
ZW14-273-6	2ES·2EL-2BL	4.89	4.89	3.79	5.11	86.8
ZW14-280-5	2ES-2BS·2BL	0.69	5.12	0	6.91	5.7
XWC14-132-15	2BS-2ES·2EL-2BL	3.59	5.8	6.72	8.93	70.0
ZW14-243-7	2ES·2EL-2BL	5.89	5.89	5.6	7.17	88.0
XWC14-132-3	2BS-2ES·2EL	3.43	5.67	6.7	6.7	81.9
ZW14-245-1	2ES-2BS·2BL	2.7	4.43	0	5.67	26.7
ZW14-246-4	2ES·2EL-2BL	8.18	8.18	10.03	10.98	95.0
ZW14-253-8	2ES·2EL-2BL	5.27	5.27	4.34	6.15	84.2
ZW14-257-6	2BS-2ES·2EL	4.67	5.66	6.94	6.94	92.1
ZW14-258-7	2BS-2ES·2EL	3.32	6.06	7.18	7.18	79.3
ZW14-261-4	2BS-2ES·2EL	3.67	5.16	6.48	6.48	87.2
ZW14-266-8	2ES-2BS·2BL	2.7	6.36	0	7.16	20.0
ZW14-289-3	2BS-2ES·2EL	4.37	4.86	5.71	5.71	95.4
ZW14-293-4	2ES-2BS·2BL	1.02	6.65	0	7.57	7.2
ZW14-297-2	2ES-2BS·2BL	1.25	5.24	0	6.28	10.9
ZW14-299-5	2ES·2EL-2BL	5.57	5.57	5.45	6.82	88.9
ZW14-300-6	2ES-2BS·2BL	2.42	6.04	0	7.12	18.4
ZW14-308-2	2ES·2EL-2BL	6.71	6.71	7.82	8.52	95.4
ZW14-347-4	2ES-2BS·2BL	2.1	6.16	0	7.46	15.4
ZW14-310-4	2ES-2BS·2BL	1.9	5.44	0	7.67	14.5
ZW14-311-8	2ES-2BS·2BL	2.18	7.07	0	6.69	15.8
ZW14-313-8	2ES-2BS·2BL	2.16	7.75	0	9.97	12.2
ZW14-315-1	2ES·2EL-2BL	5.67	5.67	6.71	7.17	96.4
ZW14-320-6	2ES·2EL-2BL	5.89	5.89	4.75	7.16	81.5
ZW14-328-8	2ES-2BS·2BL	1.4	5.83	0	6.98	10.9
ZW14-306-2	2BS-2ES·2EL-2BL	4.12	5.03	5.2	5.54	88.2
ZW14-306-2	2BS-2ES·2EL	4.08	5.53	6.95	6.95	88.4

Recombinants	Chromosome constitution	Length (μm)				Proportion (%)a
		Alien segment on short arm	Short arm	Alien segment on long arm	Long arm	
ZW14-334-4	2ES-2BS·2BL	1.22	6.69	0	8.52	8.0
ZW14-335-2	2ES·2EL-2BL	6.23	6.23	6.38	7.29	93.3
ZW14-343-2	2ES·2EL-2BL	7.3	7.3	8.46	9.46	94.0
ZW14-357-8	2ES-2BS·2BL	1.33	5.94	0	7.13	10.2
ZW14-382-5	2ES·2EL-2BL	9.47	9.47	7.78	10.41	86.8
ZW14-390-2	2ES-2BS·2BL	1.55	6.38	0	11.6	8.6
ZW14-392-6	2ES-2BS·2BL	2.19	8.48	0	11.05	11.2
ZW14-393-1	2ES·2EL-2BL	4.98	4.98	1.71	5.8	62.1
ZW14-394-4	2ES-2BS·2BL	5.42	5.8	9	9	97.4
ZW14-391-7	2BS·2BL-2EL	0	7.43	2.74	10.07	15.7
ZW14-395-4	2ES-2BS·2BL-2EL	1.3	7.26	1.61	8.05	19.0
ZW14-396-7	2ES-2BS·2BL	2	7.1	0	8.13	13.1
XWC14-143-59	2BS·2BL-2EL	0	6.58	3.09	10.14	18.5
ZW14-398-4	2BS-2ES·2EL-2BL	4.17	4.83	4.5	5.31	85.5
ZW14-398-4	2BS-2ES·2EL	4.17	5.11	6.83	6.83	92.1
ZW14-399-5	2ES-2BS·2BL	1.68	8.72	0	11.09	8.5
XWC14-715-2	2BS-2ES·2EL	3.98	6.26	7.08	7.08	82.9
ZW14-401-4	2ES-2BS·2BL	3.56	11.33	0	13.16	14.5
ZW14-402-6	2ES-2BS·2BL	4.97	7.01	7.56	7.56	86.0
ZW14-403-6	2BS·2BL-2EL	0	6.59	1.38	8.93	8.9
ZW14-405-7	2BS-2ES·2EL	5.46	5.98	7.61	7.61	96.2
ZW14-404-7	2ES-2BS·2BL	0.99	6.73	0	8.69	6.4
ZW14-406-4	2ES-2BS·2BL	2.54	7	0	7.95	17.0
ZW14-407-4	2ES-2BS·2BL	1.55	9.07	0	13.68	6.8
ZW14-408-4	2ES-2BS·2BL	1.23	7.74	0	8.93	7.4
ZW14-409-6	2BS-2ES·2EL	2.65	4.34	6.43	6.43	84.3
ZW14-410-2	2ES-2BS·2BL	1.47	9.86	0	7.45	8.5
ZW14-412-4	2BS·2BL-2EL	1.23	10.22	0	8.99	6.4

[a] Percentage of length of alien chromosome/total length of the translocation chromosome.

APPENDIX F. SNPS ON THE COMPOSITE BIN MAP OF CHROMOSOME 2B

Bins	SNPs	Genetic postion (cM)	Physical position (bp)	e value	Bins	SNPs	Genetic position (cM)	Physical position (bp)	e value
1	IWB59140	20.20997	1,272,430	9E-44	7	IWB59257	18.86909	7,909,473	4E-46
2	IWB11378	20.606	1,832,804	4E-46	7	IWA1413	16.87959	8,250,178	1E-105
2	IWB11379	20.20997	1,832,808	4E-46	7	IWB10720	16.87959	8,567,347	4E-46
3	IWB17368	23.50918	2,236,593	4E-69	7	IWB2289	16.87959	8,593,101	4E-46
3	IWB7407	20.606	3,300,107	4E-46	7	IWB8416	17.93047	8,598,285	5E-24
3	IWB15924	20.20997	3,402,462	2E-89	8	IWB75048	17.93047	9,740,995	1E-24
3	IWB32317	20.20997	3,404,583	1E-19	8	IWB47291	16.87959	9,871,592	6E-39
4	IWA4808	20.20997	4,185,932	5E-66	9	IWB12069	16.87959	10,781,807	4E-46
4	IWA4723	20.86483	4,637,555	1E-105	9	IWB46236	17.93047	10,784,126	4E-38
4	IWB45010	20.86483	4,663,284	9E-44	9	IWB217	16.87959	10,784,233	4E-46
4	IWB43909	20.86483	4,664,248	2E-41	9	IWB991	17.93047	11,077,398	2E-41
5	IWB25535	20.16008	4,988,304	4E-46	9	IWB66352	16.87959	11,077,610	2E-41
6	IWB50555	19.15598	6,210,157	4E-46	9	IWB66351	16.87959	11,077,615	2E-41
6	IWB26054	19.84513	6,210,321	4E-46	10	IWB54334	18.18617	11,083,846	4E-46
6	IWB7669	19.15598	6,253,562	2E-32	11	IWB48525	23.89897	11,389,793	7E-43
6	IWA6262	19.15598	6,263,338	1E-104	11	IWB3937	25.10889	11,390,405	4E-46
6	IWB22941	19.15598	6,263,842	1E-27	11	IWB5503	25.10889	11,390,603	6E-39
6	IWB74531	16.87959	6,313,904	4E-46	11	IWB11217	23.50918	12,076,610	4E-46
6	IWB32486	19.15598	6,337,736	4E-46	11	IWB6918	26.47784	12,076,714	4E-46
6	IWA7633	19.15598	6,338,185	1E-104	11	IWB1326	23.89897	12,881,061	4E-46
6	IWB51150	19.15598	6,338,608	9E-44	12	IWB59943	26.47784	13,166,109	4E-46
6	IWB20867	16.87959	6,338,782	4E-46	12	IWB59945	23.50918	13,166,174	9E-44
6	IWB26313	16.87959	6,712,802	4E-46	12	IWB48463	25.10889	13,238,095	3E-45
6	IWB34938	16.87959	6,712,858	2E-86	12	IWB10931	26.47784	13,757,972	4E-46
6	IWB35642	16.87959	6,712,917	6E-55	12	IWB10853	26.47784	13,767,909	4E-46
6	IWB26314	16.87959	6,715,741	2E-26	12	IWB42660	26.47784	14,047,162	4E-46
6	IWB23866	16.87959	6,986,006	4E-46	12	IWB32344	26.47784	14,047,446	3E-33
6	IWB21872	16.87959	6,986,157	4E-46	12	IWB55108	26.47784	14,047,615	4E-46
6	IWB55770	18.86909	7,067,706	6E-39	12	IWB27344	26.47784	14,047,866	4E-46
6	IWB36390	16.87959	7,108,761	1E-105	12	IWB24314	26.47784	14,047,984	2E-41
6	IWB24835	16.87959	7,429,447	4E-46	13	IWB542	26.99237	16,813,662	2E-35
6	IWB24834	16.87959	7,429,546	4E-46	14	IWB7915	32.16258	16,857,574	4E-46
6	IWB58123	16.87959	7,429,616	2E-45	14	IWB72375	26.10676	16,871,376	8E-29
6	IWB24457	16.87959	7,430,956	4E-46	14	IWA2304	26.10676	16,895,902	1E-100
6	IWB47038	16.87959	7,436,667	3E-34	14	IWB8328	26.10676	16,990,776	4E-46
6	IWB8754	16.87959	7,436,732	4E-46	15	IWB73884	27.19818	17,388,834	2E-41
6	IWB11320	16.87959	7,443,043	4E-46	15	IWB11557	27.19818	17,388,974	4E-46
6	IWB11321	16.87959	7,443,155	4E-46	15	IWB41644	27.19818	17,389,177	4E-46
6	IWB36143	16.87959	7,579,493	3E-19	15	IWB72156	27.19818	17,390,831	2E-41

Bins	SNPs	Genetic postion (cM)	Physical position (bp)	e value	Bins	SNPs	Genetic position (cM)	Physical position (bp)	e value
15	IWB29097	26.10676	17,390,904	2E-41	25	IWB9111	42.91462	26,581,598	4E-46
15	IWB7674	27.19818	17,394,435	4E-46	25	IWB9433	42.91462	26,581,603	4E-46
15	IWB9583	27.19818	17,456,915	4E-46	25	IWB6410	46.76266	26,588,861	1E-36
15	IWB26388	27.19818	17,564,545	4E-46	25	IWB61616	42.46558	26,752,991	4E-46
15	IWB59719	32.16258	17,564,807	4E-46	25	IWB8489	42.46558	26,856,145	8E-32
15	IWB46573	27.19818	17,570,893	4E-46	25	IWB9006	47.49858	26,987,132	4E-46
15	IWB12617	27.19818	17,572,453	4E-46	25	IWB32593	48.06924	28,293,629	3E-35
15	IWB7013	27.19818	17,572,454	4E-46	25	IWB69830	46.76266	28,339,781	4E-46
15	IWB71519	27.19818	17,778,990	4E-46	25	IWB26149	48.54011	28,368,571	1E-30
15	IWB46230	27.19818	17,780,657	9E-44	25	IWB69976	48.54011	28,415,944	4E-46
15	IWB24938	27.19818	17,781,604	9E-38	25	IWB12972	48.54011	28,416,207	4E-46
15	IWB32197	32.16258	17,783,253	1E-41	25	IWB2368	48.54011	28,451,656	9E-44
15	IWB62118	28.49541	17,787,186	2E-32	26	IWA2275	48.54011	29,032,035	1E-105
15	IWB43468	28.49541	17,787,292	1E-33	26	IWB22739	48.54011	29,032,619	4E-46
16	IWB60877	27.19818	18,176,463	9E-44	26	IWA7106	48.54011	29,032,622	7E-99
17	IWB26232	27.19818	18,263,048	1E-24	26	IWB48989	48.54011	29,156,051	4E-46
17	IWB26233	27.19818	18,263,074	9E-41	26	IWB12154	48.54011	29,991,153	4E-46
18	IWB26231	27.19818	18,263,358	4E-46	26	IWB26791	48.54011	29,993,208	4E-46
19	IWB70698	32.16258	19,375,278	9E-44	26	IWB22874	51.86738	30,465,951	9E-44
19	IWB9739	32.16258	19,441,391	4E-46	26	IWB36282	51.86738	30,499,259	6E-90
19	IWB65752	32.16258	20,076,011	8E-21	26	IWB65439	49.64712	30,543,512	2E-55
19	IWB8850	32.16258	20,077,125	4E-46	27	IWB46375	53.73527	31,622,742	6E-45
19	IWB57508	16.87959	20,347,638	1E-27	27	IWB12400	53.73527	32,064,898	4E-46
20	IWB3039	34.25187	23,364,288	7E-43	27	IWB10910	53.73527	32,871,698	4E-46
21	IWB32606	34.25187	23,543,329	6E-39	27	IWB65469	53.73527	32,963,759	7E-12
22	IWB10435	32.16258	24,091,993	4E-46	27	IWB2317	56.27048	33,839,794	4E-46
22	IWB10616	32.16258	24,091,994	4E-46	27	IWB22495	56.27048	33,840,506	2E-41
22	IWB12404	38.66744	24,264,503	4E-46	28	IWB31989	56.86609	35,284,423	3E-35
22	IWB10512	39.01358	24,510,176	4E-46	28	IWB31988	56.86609	35,284,488	3E-35
22	IWA7936	41.35857	24,861,141	2E-74	28	IWB31987	56.86609	35,284,620	1E-41
23	IWA2407	38.66744	25,017,740	2E-97	28	IWB31986	56.86609	35,284,630	1E-41
23	IWB47095	40.96878	25,021,435	2E-35	28	IWB62184	56.86609	35,367,964	4E-46
23	IWB5813	40.96878	25,185,961	5E-24	29	IWA2441	66.19617	40,068,242	1E-105
23	IWB8132	42.46558	25,236,589	1E-33	29	IWA7120	66.19617	40,448,045	3E-61
24	IWB6356	42.46558	25,594,756	4E-46	29	IWB21536	66.19617	40,510,393	2E-26
24	IWB30434	42.46558	26,297,600	2E-32	30	IWA1931	65.44464	41,957,387	1E-105
24	IWB61608	42.46558	26,298,110	1E-30	30	IWA1929	65.2669	41,960,988	1E-105
24	IWA8430	42.46558	26,298,110	3E-28	30	IWB10974	65.2669	42,281,570	4E-46
24	IWA6768	42.46558	26,314,314	3E-38	30	IWB54956	65.2669	42,943,582	6E-45
24	IWB6033	46.76266	26,564,156	2E-35	30	IWB48927	65.2669	42,953,626	9E-38

Bins	SNPs	Genetic postion (cM)	Physical position (bp)	e value	Bins	SNPs	Genetic position (cM)	Physical position (bp)	e value
30	IWA6048	67.07242	43,629,666	1E-105	34	IWB44373	74.46912	58,675,215	4E-46
30	IWB14167	67.07242	44,310,967	4E-46	34	IWA2571	74.89946	58,978,467	1E-105
30	IWB7336	67.07242	44,404,954	4E-46	34	IWA2572	74.89946	58,978,827	1E-105
30	IWB11823	67.1036	44,424,337	4E-46	34	IWB70191	74.46912	58,993,930	4E-46
30	IWB39393	67.1036	45,537,580	4E-46	35	IWB54881	76.70186	63,292,068	1E-42
30	IWB65494	67.54017	45,788,663	3E-20	35	IWB23929	76.70186	64,205,007	4E-46
30	IWA4284	67.54017	45,788,714	1E-104	35	IWB10193	76.70186	65,100,057	6E-42
30	IWB27391	67.54017	45,793,984	6E-39	35	IWB55936	76.70186	65,100,755	8E-29
30	IWB43573	69.08375	46,090,281	4E-46	35	IWB29319	76.70186	65,113,586	3E-25
30	IWB67043	69.08375	46,090,703	4E-46	35	IWB11952	78.99384	65,370,483	4E-46
30	IWB23418	69.08375	46,091,136	9E-44	35	IWB56961	76.70186	65,375,510	9E-44
30	IWB32470	69.08375	46,880,123	6E-42	36	IWB24280	77.20703	66,214,720	4E-46
30	IWB53473	69.08375	46,886,731	3E-24	36	IWB256	77.93672	66,544,152	4E-46
30	IWB24908	67.92061	46,887,237	2E-23	36	IWB21237	76.70186	66,544,374	3E-22
30	IWB31710	69.08375	47,140,460	9E-31	37	IWB73973	78.99384	68,219,192	4E-46
30	IWB31706	69.08375	47,140,524	2E-38	37	IWB73971	78.99384	68,220,786	4E-46
30	IWB31707	69.08375	47,140,606	4E-24	37	IWB39654	78.11446	68,363,434	4E-46
30	IWB43754	69.08375	47,168,997	9E-44	38	IWB32008	80.77441	69,043,295	8E-32
30	IWB49164	69.08375	47,169,549	5E-33	38	IWB21394	79.49277	69,344,059	4E-46
30	IWB43753	69.08375	47,169,593	3E-45	38	IWB61142	80.77441	69,370,567	4E-46
30	IWB54529	70.72088	47,181,366	4E-46	38	IWB40809	79.49277	69,414,716	4E-46
30	IWB54530	70.36539	47,181,430	4E-46	38	IWB9450	81.75045	69,648,893	4E-46
30	IWB54531	69.7729	47,181,499	4E-46	38	IWB72086	79.14976	69,650,681	4E-46
30	IWB8281	70.36539	47,425,734	4E-46	38	IWB73904	79.49277	71,292,516	4E-46
30	IWB8280	69.7729	47,426,940	6E-45	38	IWB55384	79.49277	72,577,255	4E-46
30	IWB34527	69.7729	47,427,272	1E-105	38	IWB48595	79.49277	72,580,227	4E-46
30	IWB19719	69.7729	47,427,955	4E-46	38	IWA4652	79.49277	72,580,310	1E-105
30	IWB53589	69.7729	47,430,632	4E-46	38	IWB72776	79.74848	73,989,699	4E-46
30	IWB34849	69.7729	47,430,633	1E-105	38	IWB43682	79.74848	75,693,582	4E-46
31	IWB9207	71.9994	50,290,471	4E-46	38	IWB43459	79.74848	75,969,835	2E-41
31	IWB32171	71.9994	51,083,638	7E-35	38	IWB23422	81.75045	76,817,110	4E-46
31	IWB46832	71.9994	51,890,777	2E-23	38	IWA6739	79.74848	76,817,723	2E-99
32	IWB6117	71.9994	52,669,992	4E-40	38	IWA6740	79.74848	76,818,180	5E-38
32	IWB34673	71.9994	52,670,346	1E-93	38	IWB36769	79.74848	76,916,706	4E-46
32	IWB44675	71.9994	52,700,856	4E-46	38	IWB27355	79.74848	76,918,651	9E-44
32	IWB35959	71.9994	52,872,937	1E-47	38	IWB27354	79.74848	76,918,671	9E-44
33	IWA7916	71.9994	53,464,964	1E-105	38	IWB41771	79.74848	76,922,118	6E-39
34	IWB43273	74.46912	56,784,859	4E-46	38	IWB60907	79.74848	76,929,459	4E-46
34	IWB2702	73.74879	57,651,518	3E-22	38	IWB29747	79.74848	77,172,620	4E-46
34	IWB72380	73.74879	58,325,009	4E-46	38	IWB69854	79.74848	77,172,889	9E-44

Bins	SNPs	Genetic postion (cM)	Physical position (bp)	e value	Bins	SNPs	Genetic position (cM)	Physical position (bp)	e value
38	IWB69853	79.74848	77,172,967	4E-46	43	IWA5392	85.25235	104,237,306	7E-85
38	IWB73250	79.74848	77,290,852	1E-33	43	IWB73495	84.69105	104,237,413	4E-46
38	IWB73252	79.74848	77,291,044	4E-46	43	IWB11072	83.79609	104,237,414	4E-46
39	IWB49878	80.37215	87,350,805	4E-46	43	IWB53367	86.4498	104,240,017	3E-37
39	IWB62513	80.85549	87,351,775	4E-46	43	IWB40265	86.4498	104,242,552	2E-23
40	IWB63381	80.37215	89,305,600	4E-46	43	IWB47284	86.4498	104,242,982	4E-46
40	IWB60107	81.95315	89,308,426	2E-23	43	IWB22995	86.4498	104,243,134	4E-46
40	IWB45402	81.95315	89,313,010	4E-46	43	IWB64716	86.4498	104,816,448	4E-46
41	IWB46988	80.85549	89,315,221	4E-46	43	IWB10568	81.95315	105,375,881	4E-46
41	IWB7072	80.77441	89,491,656	4E-46	43	IWB6075	87.12024	105,696,297	5E-27
41	IWB11187	80.77441	89,491,846	4E-46	43	IWB58252	87.12024	105,696,297	8E-35
41	IWB23644	80.77441	89,558,483	4E-46	44	IWB73598	86.4498	105,909,245	4E-46
41	IWB65391	80.77441	90,014,074	3E-20	44	IWB70370	87.18572	105,909,301	8E-32
41	IWB72307	82.46767	91,044,210	4E-46	44	IWB47379	86.4498	105,909,328	4E-46
41	IWB70041	83.95824	91,259,384	3E-19	44	IWB47380	86.4498	105,909,355	4E-46
41	IWB7781	82.29305	91,547,952	4E-46	44	IWB45822	87.18572	105,913,021	4E-46
41	IWB31001	82.12466	91,836,588	4E-46	44	IWB50438	86.4498	105,991,619	4E-46
41	IWB71775	82.43337	91,837,797	4E-46	45	IWB45048	87.43519	108,238,044	4E-46
41	IWB31002	82.43337	91,837,798	4E-46	45	IWB55365	88.4393	110,480,414	4E-46
41	IWB36919	82.43337	91,837,869	9E-44	46	IWA608	88.92888	115,381,191	6E-58
41	IWB7346	82.46767	92,996,903	4E-46	46	IWA607	88.92888	115,381,728	6E-58
41	IWB36124	82.12466	93,409,767	8E-41	46	IWB71005	88.4393	116,157,770	4E-46
41	IWB72894	82.46767	94,033,158	9E-44	46	IWB18439	88.92888	116,272,037	5E-84
41	IWB72760	83.39382	94,192,783	4E-46	46	IWB59396	88.70124	116,323,292	3E-45
41	IWB36550	84.17964	94,927,862	2E-32	46	IWB42992	88.92888	116,324,736	6E-42
41	IWB35850	83.39382	95,797,358	2E-57	46	IWA3329	88.92888	117,618,445	2E-49
41	IWB10024	81.95315	97,188,903	4E-46	46	IWA7030	88.92888	118,285,365	1E-69
42	IWB3877	81.75669	97,952,873	4E-46	46	IWA7029	88.92888	118,286,601	1E-105
42	IWB55924	83.79609	98,298,288	7E-26	46	IWB39369	88.92888	118,286,953	4E-46
42	IWB41316	81.95315	98,299,577	9E-44	46	IWB39370	88.92888	118,287,555	4E-46
42	IWA5818	83.79609	99,759,678	1E-105	46	IWA2887	88.8634	120,590,348	4E-60
42	IWA4673	83.79609	99,760,903	2E-34	46	IWB36727	88.70124	120,590,700	5E-24
42	IWB74841	83.79609	99,760,904	3E-34	46	IWB49035	88.8634	121,357,812	1E-27
42	IWB74844	87.18572	99,765,448	7E-26	46	IWA295	88.8634	121,364,887	4E-57
42	IWB7738	83.79609	99,773,057	4E-46	46	IWB35350	88.8634	121,367,430	2E-46
42	IWB26449	83.79609	100,088,852	4E-46	46	IWB4951	88.8634	121,367,431	3E-34
42	IWB68550	83.79609	100,095,144	4E-46	46	IWB5826	88.8634	121,370,808	4E-46
42	IWB24889	87.18572	100,101,507	2E-45	46	IWA762	88.8634	121,370,809	1E-105
42	IWA4135	84.69105	102,977,549	1E-105	46	IWB10430	88.8634	122,010,450	4E-46
43	IWB30853	87.12024	104,236,762	6E-45	46	IWB42880	88.70124	122,265,599	4E-46

Bins	SNPs	Genetic postion (cM)	Physical position (bp)	e value	Bins	SNPs	Genetic position (cM)	Physical position (bp)	e value
46	IWB37019	88.8634	122,265,753	4E-46	46	IWB12063	90.97139	140,850,078	4E-46
46	IWB38875	88.70124	122,265,756	4E-46	46	IWB63625	90.97139	141,559,397	4E-46
46	IWB6599	88.8634	122,267,554	9E-44	46	IWB63624	90.97139	141,564,720	4E-46
46	IWB42289	89.10662	122,697,195	4E-46	46	IWB54123	90.97139	142,374,592	2E-23
46	IWB35614	89.10662	122,697,196	1E-100	46	IWB11184	90.97139	142,446,105	4E-46
46	IWB51653	89.10662	122,701,236	4E-46	47	IWB62466	92.19378	143,773,951	4E-46
46	IWB32	89.63674	122,756,813	4E-46	47	IWB35283	92.19378	144,431,599	1E-105
46	IWA3824	89.33738	122,756,814	1E-101	47	IWB33921	92.19378	144,432,958	3E-37
46	IWB7348	89.63674	123,062,358	4E-46	47	IWA429	92.5711	146,636,945	6E-58
46	IWB6607	88.8634	126,731,282	4E-46	47	IWB26224	92.5711	146,717,449	4E-46
46	IWB34697	90.97139	126,731,442	2E-61	47	IWB48352	92.5711	146,717,673	4E-46
46	IWB58852	90.97139	126,948,190	1E-36	47	IWB48351	92.5711	146,717,933	9E-44
46	IWB58853	88.8634	126,949,324	3E-34	47	IWB51418	92.5711	146,732,976	4E-46
46	IWB58854	88.8634	126,949,416	8E-32	47	IWB51419	92.5711	146,735,843	4E-46
46	IWB11285	89.63674	131,130,470	4E-46	47	IWB35158	92.5711	148,239,847	1E-105
46	IWA4532	89.63674	131,572,333	1E-105	47	IWB63570	92.2811	148,589,582	4E-46
46	IWA1114	89.63674	131,573,925	1E-105	47	IWB63569	92.2811	148,589,796	4E-46
46	IWA8046	89.63674	131,574,747	1E-105	47	IWB56514	88.08381	149,841,690	4E-46
46	IWB9085	89.77707	132,518,532	4E-46	47	IWB38081	92.20625	149,842,993	4E-46
46	IWB32005	88.4393	135,000,501	2E-40	47	IWB66885	92.2811	150,607,851	4E-46
46	IWB32007	88.4393	135,000,544	2E-40	47	IWB34871	92.20625	151,643,468	1E-105
46	IWB22202	88.4393	135,002,104	4E-46	47	IWB73197	93.01079	152,175,265	9E-44
46	IWB11568	88.4393	135,003,886	4E-46	47	IWB68715	93.01079	152,712,540	4E-46
46	IWB60585	90.2417	135,007,974	4E-46	47	IWB11527	93.01079	153,223,664	4E-46
46	IWB22257	88.8634	136,150,897	1E-27	47	IWB73834	93.01079	153,223,758	4E-46
46	IWB3455	88.8634	136,154,643	5E-24	47	IWA6509	93.01079	153,223,759	1E-104
46	IWB36600	88.4393	136,430,582	4E-46	47	IWB74443	92.20625	153,227,087	5E-36
46	IWB24397	88.4393	138,117,670	4E-46	47	IWB7825	93.01079	153,610,499	4E-46
46	IWB8772	88.4393	138,536,902	4E-46	48	IWB8214	93.28208	154,911,183	2E-35
46	IWB22543	88.4393	139,068,437	4E-46	48	IWB32260	90.97139	157,639,992	1E-33
46	IWB34545	88.4393	139,068,438	1E-105	48	IWB21988	93.46606	157,688,842	2E-44
46	IWA328	91.29258	139,814,569	6E-58	48	IWB53512	93.46606	157,693,584	4E-46
46	IWB45082	90.97139	140,765,055	4E-46	48	IWB52095	93.46606	157,694,646	3E-34
46	IWB53499	90.97139	140,772,477	2E-32	49	IWA10	93.46606	158,432,170	6E-58
46	IWB12056	90.97139	140,775,160	4E-46	49	IWA4894	93.46606	158,618,930	1E-102
46	IWB44515	93.01079	140,776,053	4E-46	49	IWB11750	93.46606	158,622,283	3E-34
46	IWB61587	88.4393	140,776,871	7E-23	49	IWB11751	93.46606	158,624,762	4E-46
46	IWB47399	90.97139	140,777,084	2E-44	49	IWB35747	93.46606	159,205,820	5E-38
46	IWB44975	90.97139	140,845,993	4E-46	49	IWB32441	93.46606	159,207,016	4E-46
46	IWB7335	90.97139	140,850,052	4E-46	49	IWB32439	93.46606	159,207,101	5E-36

Bins	SNPs	Genetic postion (cM)	Physical position (bp)	e value	Bins	SNPs	Genetic position (cM)	Physical position (bp)	e value
49	IWB30179	93.46606	159,207,419	4E-46	49	IWB53627	96.98667	199,021,553	4E-46
49	IWB42613	93.46606	159,208,094	1E-21	49	IWB57218	96.98667	200,904,871	8E-35
49	IWB32069	93.46606	160,904,115	2E-37	49	IWB22676	96.98667	202,740,572	4E-46
49	IWB65998	93.46606	161,406,230	3E-20	49	IWA7821	96.37236	202,917,364	1E-105
49	IWB24026	93.46606	161,409,260	4E-46	49	IWB54447	97.69453	202,917,823	9E-44
49	IWB60513	93.46606	161,468,676	2E-29	49	IWB58691	97.5355	206,113,217	4E-46
49	IWA50	93.84026	164,089,285	6E-58	49	IWB59317	96.98667	206,373,685	4E-46
49	IWB8031	95.14685	164,107,335	4E-46	49	IWB39776	97.5355	206,752,113	4E-46
49	IWB31804	93.46606	164,896,491	1E-24	49	IWA169	96.98667	209,097,111	4E-57
49	IWB74209	96.98667	164,938,839	4E-46	49	IWA170	96.98667	209,097,178	4E-57
49	IWA6554	96.98667	164,938,840	1E-104	49	IWB57293	97.69453	210,262,587	5E-33
49	IWB44316	95.14685	165,506,841	4E-46	49	IWB9584	97.69453	210,455,800	4E-46
49	IWB48765	96.98667	171,024,930	4E-46	49	IWB14239	96.98667	210,652,110	8E-25
49	IWB40886	96.98667	172,215,534	4E-46	49	IWB14712	96.98667	210,652,110	1E-26
49	IWA4388	96.98667	172,890,859	4E-51	49	IWA776	96.98667	210,652,110	1E-52
49	IWB54344	96.98667	174,394,262	3E-37	49	IWA771	96.98667	210,652,215	6E-82
49	IWB47155	96.13537	179,397,163	4E-46	49	IWA777	96.98667	210,652,216	4E-74
49	IWB54789	96.98667	179,399,008	2E-35	49	IWA1130	96.98667	210,652,216	6E-79
49	IWB6357	95.82353	180,568,905	4E-46	49	IWA1237	96.98667	210,652,243	3E-45
49	IWB6330	95.82353	180,569,211	1E-30	49	IWA1229	96.98667	210,652,282	4E-46
49	IWB65377	96.13537	181,614,629	8E-21	50	IWB4546	97.37334	211,535,314	9E-44
49	IWB13596	96.98667	183,315,454	9E-44	50	IWB65990	96.37236	212,297,743	3E-20
49	IWB35916	95.82353	183,315,492	2E-57	50	IWB64392	98.75789	212,943,615	4E-46
49	IWB5784	95.82353	183,315,493	9E-44	50	IWA7520	98.52713	213,254,278	1E-105
49	IWB7451	96.98667	184,874,623	5E-30	50	IWB31492	98.52713	214,283,245	4E-46
49	IWB48313	96.13537	185,761,574	4E-46	50	IWB55026	98.52713	214,587,429	2E-41
49	IWB62369	96.98667	185,806,940	3E-37	50	IWB32222	98.52713	214,588,281	9E-44
49	IWB7715	98.52713	187,197,406	5E-27	50	IWB48168	99.73081	214,596,658	4E-46
49	IWA5149	97.26421	189,594,755	1E-105	50	IWB52411	98.52713	215,204,347	4E-46
49	IWA4984	95.14685	189,603,420	1E-105	50	IWA1981	96.98667	215,204,441	1E-104
49	IWB7968	95.14685	189,603,683	4E-46	50	IWB49756	96.98667	216,463,275	4E-46
49	IWA2977	95.14685	189,603,983	1E-105	50	IWB72081	96.98667	216,467,653	2E-45
49	IWB20601	95.14685	189,612,751	9E-44	50	IWB56541	96.98667	234,634,297	4E-46
49	IWB58207	95.14685	189,619,966	4E-46	50	IWB56542	96.98667	234,634,390	4E-46
49	IWA5059	95.14685	189,619,967	3E-64	50	IWB4008	96.98667	234,636,794	4E-46
49	IWB30276	97.26421	190,018,049	2E-41	50	IWB23131	98.52713	236,806,649	3E-37
49	IWA3213	95.14685	190,018,049	1E-105	50	IWB12643	98.52713	237,177,073	4E-46
49	IWB40922	96.98667	191,752,685	4E-46	50	IWB12642	98.52713	237,177,079	4E-46
49	IWA3656	96.98667	192,364,853	1E-105	50	IWB59746	98.92316	239,646,060	4E-46
49	IWB36818	96.98667	195,664,018	1E-29	50	IWB27246	97.6041	239,647,340	7E-28

Bins	SNPs	Genetic postion (cM)	Physical position (bp)	e value	Bins	SNPs	Genetic position (cM)	Physical position (bp)	e value
50	IWB74681	99.15704	240,318,305	4E-46	52	IWA4420	99.15704	393,468,425	1E-105
50	IWB23529	99.15704	242,825,134	4E-46	52	IWA1935	99.80254	393,469,968	2E-92
50	IWB59779	99.73081	244,572,477	3E-34	52	IWA6505	99.80254	393,470,565	1E-105
50	IWB8174	98.52713	245,008,366	4E-46	52	IWA6438	99.15704	395,541,132	1E-105
50	IWB43295	99.15704	245,790,743	4E-43	52	IWB31020	99.5593	396,338,354	4E-46
50	IWB27810	99.15704	245,888,170	4E-46	52	IWA5575	99.5593	396,338,513	1E-105
50	IWB7755	99.15704	245,888,698	4E-46	52	IWB50192	99.5593	396,338,514	4E-46
50	IWB22058	100.2048	246,068,689	3E-39	52	IWA4224	99.5593	397,244,839	1E-75
50	IWB10611	99.73081	249,198,748	4E-46	52	IWA4399	99.5593	397,446,866	4E-92
50	IWB28408	99.16016	249,370,504	4E-46	52	IWB46574	99.80254	397,920,069	4E-46
50	IWB59321	99.16016	249,374,614	4E-46	52	IWB2914	99.80254	398,707,071	4E-43
50	IWB25870	99.73081	250,257,043	9E-44	52	IWB54991	99.80254	399,339,149	9E-44
50	IWB1699	99.15704	251,770,161	4E-46	52	IWB13970	99.80254	403,084,898	4E-42
50	IWB64603	99.15704	275,326,925	2E-23	52	IWB44851	99.80254	403,698,727	4E-46
51	IWB56551	98.27766	359,861,257	1E-27	52	IWA7959	99.16016	403,700,745	2E-37
51	IWA3817	99.16016	363,979,244	1E-105	52	IWA2625	99.73081	404,427,500	1E-102
51	IWB10875	99.73081	381,795,129	4E-46	52	IWA3554	99.73081	404,427,892	1E-105
51	IWB65593	99.73081	381,917,350	3E-20	52	IWA4014	99.80254	405,646,463	1E-104
51	IWB8863	99.16016	382,083,911	4E-43	52	IWB61966	99.73081	405,752,165	4E-46
51	IWB63504	99.16016	382,597,848	4E-46	52	IWB55096	99.80254	406,110,848	4E-46
51	IWA4751	99.80254	383,279,937	1E-104	52	IWB25934	99.78383	407,237,657	4E-46
51	IWB64	99.80254	384,319,875	2E-23	52	IWA1309	99.80254	407,239,208	1E-105
51	IWB12709	99.73081	384,397,739	2E-26	52	IWA5248	99.5593	409,344,508	1E-105
51	IWB22197	99.73081	384,749,502	4E-46	52	IWB5084	99.5593	409,344,545	2E-41
51	IWB56047	99.15704	385,193,677	1E-33	52	IWB64311	99.80254	411,143,395	4E-46
52	IWB27089	99.73081	385,201,729	4E-46	52	IWB1207	99.5593	412,659,517	6E-45
52	IWA3258	99.73081	385,201,730	1E-105	52	IWB57571	99.5593	412,663,741	4E-46
52	IWB38467	99.80254	385,202,019	9E-44	52	IWB47236	99.5593	412,664,657	9E-44
52	IWB35625	99.80254	385,564,300	6E-58	52	IWB55932	99.5593	412,665,218	4E-46
52	IWA5723	99.5593	385,564,890	1E-75	52	IWB57577	97.26421	412,717,124	4E-46
52	IWA3210	99.73081	385,573,169	1E-105	52	IWB57574	99.5593	412,718,879	4E-46
52	IWB509	99.80254	387,103,786	4E-46	52	IWB29821	99.73081	412,990,278	4E-46
52	IWA2739	99.80254	388,950,114	1E-87	52	IWA3948	99.5593	412,991,606	1E-105
52	IWA2025	99.27242	389,410,479	2E-99	52	IWB26389	99.86802	413,063,885	5E-33
52	IWA6723	99.16016	389,462,211	4E-92	52	IWA6009	99.5593	413,864,793	1E-105
52	IWA4881	99.73081	389,471,745	1E-100	52	IWB43065	99.5593	413,865,666	4E-46
52	IWA4880	99.5593	389,472,491	4E-57	52	IWA5259	99.5593	413,865,667	1E-103
52	IWB64782	99.5593	390,116,879	4E-46	52	IWB21075	99.5593	413,865,723	4E-46
52	IWA5678	99.73081	390,944,064	1E-105	52	IWB43068	99.79318	413,865,888	4E-46
52	IWB57964	99.15704	390,976,224	4E-46	52	IWB21074	99.80254	413,866,250	4E-46

Bins	SNPs	Genetic postion (cM)	Physical position (bp)	e value	Bins	SNPs	Genetic position (cM)	Physical position (bp)	e value
52	IWA5261	99.5593	413,866,312	1E-104	52	IWA837	99.73081	448,080,536	3E-78
52	IWB43066	99.5593	413,866,468	4E-46	52	IWA6966	99.86802	449,842,050	1E-105
52	IWA5263	99.86802	413,866,719	1E-58	52	IWB42378	99.86802	450,184,271	4E-46
52	IWB43799	99.90544	414,072,483	9E-44	52	IWA2972	99.16016	450,184,272	1E-105
52	IWB64297	99.5593	415,055,295	2E-44	52	IWB9833	99.80254	452,811,221	4E-46
52	IWA4696	99.5593	415,058,500	8E-57	52	IWA587	99.73081	453,267,263	6E-58
52	IWA3696	99.5593	416,874,849	1E-105	52	IWA586	99.73081	453,267,358	6E-58
52	IWA310	99.5593	417,080,910	6E-58	52	IWB2679	99.73081	453,272,781	3E-34
52	IWA2050	99.5593	417,793,523	5E-47	52	IWA1661	99.80254	453,752,054	2E-71
52	IWA3453	99.79318	420,610,461	1E-105	52	IWB48057	99.16016	453,752,055	6E-42
52	IWA3452	99.79318	420,610,708	3E-68	52	IWB23106	99.73081	454,326,756	1E-24
52	IWB45225	99.79318	422,732,184	9E-44	52	IWB51413	99.73081	456,025,530	4E-46
52	IWB30548	99.79318	423,661,778	3E-45	52	IWB3491	99.73081	456,053,339	2E-26
52	IWA5090	99.79318	423,661,779	1E-104	52	IWB30844	99.73081	456,173,891	3E-33
52	IWA5091	99.79318	423,661,851	1E-104	52	IWB29666	99.86802	456,176,919	2E-44
52	IWA2544	99.73081	423,663,219	1E-105	52	IWB2458	99.73081	457,343,204	4E-46
52	IWA742	99.79318	423,904,697	1E-105	52	IWB43188	99.73081	457,348,618	2E-23
52	IWA4136	99.16016	424,332,372	1E-105	52	IWA5794	99.73081	457,680,600	3E-66
52	IWA2465	99.80254	429,145,485	1E-105	52	IWA3840	99.73081	458,622,067	1E-105
52	IWB61024	99.79318	429,147,181	9E-44	52	IWB57693	99.73081	461,523,481	9E-44
52	IWA4822	99.79318	433,540,162	1E-105	52	IWA7684	99.73081	461,980,866	1E-87
52	IWB57846	99.5593	438,932,738	4E-46	52	IWB3118	99.73081	462,936,077	9E-44
52	IWA2184	99.79318	439,225,260	1E-105	52	IWB46692	99.73081	462,947,184	4E-46
52	IWB34438	99.79318	439,225,262	1E-103	52	IWB28450	99.73081	462,949,436	4E-46
52	IWA389	99.5593	439,770,415	6E-58	52	IWB685	99.73081	463,771,117	4E-46
52	IWB52349	99.73081	440,214,910	4E-46	52	IWB52240	99.73081	467,476,357	4E-46
52	IWB59508	99.80254	440,825,282	7E-23	52	IWA326	99.73081	476,408,035	6E-58
52	IWB41831	99.80254	442,338,782	4E-46	52	IWB67903	99.90544	476,415,666	4E-46
52	IWB62931	99.80254	442,518,430	7E-24	52	IWB66959	99.90544	476,563,279	4E-46
52	IWA5290	99.80254	442,518,432	3E-48	52	IWB1518	99.41586	494,374,288	3E-25
52	IWB34687	99.80254	442,522,682	2E-31	52	IWB1520	99.41586	494,375,520	4E-46
52	IWB49222	99.80254	442,524,073	4E-33	52	IWB72999	99.41586	494,375,521	2E-41
52	IWB75295	99.80254	442,524,144	9E-44	52	IWB4602	101.5363	522,835,671	4E-46
52	IWB952	99.73081	442,569,637	6E-39	52	IWB21339	102.2754	529,102,584	4E-46
52	IWB55149	99.86802	442,792,857	4E-46	52	IWB52801	102.2754	529,103,765	8E-32
52	IWB25961	99.86802	442,793,207	9E-44	52	IWA1690	102.2754	529,108,090	1E-105
52	IWB55148	99.80254	442,794,504	4E-46	52	IWB30234	102.2255	529,539,008	9E-41
52	IWB396	99.16016	442,794,540	2E-41	52	IWB72986	102.2255	530,046,504	7E-26
52	IWA6216	99.73081	442,796,872	1E-104	52	IWB69362	102.2255	530,098,933	4E-46
52	IWA2081	99.73081	445,683,704	1E-44	52	IWB36462	102.2255	530,730,830	1E-36

Bins	SNPs	Genetic postion (cM)	Physical position (bp)	e value	Bins	SNPs	Genetic position (cM)	Physical position (bp)	e value
52	IWA5008	102.2255	539,811,500	2E-86	53	IWB36041	105.322	599,813,155	2E-48
52	IWB24879	102.2255	539,961,921	6E-32	54	IWB32126	105.9082	604,999,310	3E-37
52	IWA4853	104.3896	540,424,987	1E-105	54	IWB50067	106.5631	606,038,284	2E-41
52	IWA5525	104.3896	540,428,618	1E-87	54	IWA3035	105.9082	606,038,609	1E-105
52	IWA6969	104.3896	540,429,044	1E-105	54	IWA3037	105.9082	606,040,685	1E-81
52	IWA2253	102.2255	541,106,633	7E-68	54	IWA2189	105.9082	607,244,845	2E-58
53	IWB22298	104.4146	542,355,044	4E-46	54	IWA1304	105.9082	608,201,426	1E-104
53	IWA2955	102.2255	542,759,443	1E-105	54	IWB26404	105.9082	608,201,459	9E-44
53	IWB12692	102.2255	543,704,834	4E-46	54	IWA1305	105.9082	608,201,977	1E-105
53	IWA3786	103.3356	544,765,714	1E-104	54	IWB52361	105.9082	608,231,168	4E-46
53	IWA5846	103.3356	544,766,186	1E-101	54	IWB43954	105.9082	608,942,339	4E-46
53	IWB46339	103.3356	544,767,315	1E-27	54	IWA6453	106.5631	611,065,528	1E-100
53	IWB50897	103.0893	546,201,967	4E-46	54	IWB13303	106.5631	611,282,850	2E-41
53	IWB32588	102.9832	546,424,815	4E-46	54	IWB8535	106.5631	612,213,302	2E-41
53	IWB26325	102.9832	546,588,955	4E-46	54	IWB55736	106.5631	612,684,670	4E-46
53	IWB36708	102.9832	547,058,576	4E-46	54	IWA2237	107.0059	612,686,935	1E-103
53	IWB64779	103.6163	553,623,475	4E-46	54	IWB22798	106.5631	615,877,735	4E-43
53	IWB69271	103.6163	554,292,532	3E-19	54	IWB60374	107.0059	616,928,762	2E-23
53	IWB63790	104.3896	555,840,835	4E-46	54	IWA4256	107.0059	616,928,763	6E-53
53	IWB67168	103.8252	556,200,749	4E-46	54	IWB60039	107.0059	616,956,509	9E-44
53	IWB67169	103.8252	556,201,004	6E-45	54	IWB28486	107.0059	616,962,562	4E-46
53	IWB67170	104.2493	556,201,226	3E-37	54	IWB21140	107.0059	616,966,109	2E-29
53	IWB42742	103.8252	556,202,628	6E-39	54	IWB49862	107.0059	616,969,770	4E-46
53	IWB69109	106.5631	556,677,220	4E-46	54	IWB49783	107.0059	616,969,938	4E-46
53	IWB56173	106.5631	556,685,803	4E-46	54	IWB27165	107.0059	617,140,983	9E-44
53	IWB63896	104.3896	559,427,945	3E-28	54	IWB48279	107.0059	617,141,017	9E-44
53	IWB63900	104.4146	559,429,762	4E-46	54	IWB27166	107.0059	617,141,464	6E-39
53	IWB63897	104.3896	559,430,384	4E-46	54	IWB48278	107.0059	617,142,634	9E-44
53	IWB874	104.3896	561,283,604	4E-46	54	IWB21199	107.0059	617,142,917	9E-44
53	IWB5039	106.5631	563,043,722	4E-46	54	IWB59086	107.0059	619,044,539	4E-46
53	IWB2052	104.3896	563,045,881	4E-46	54	IWB73040	107.4861	621,185,388	2E-45
53	IWB46098	104.3896	564,233,222	4E-46	54	IWB73022	106.5631	622,918,546	4E-46
53	IWB68043	104.3896	564,234,672	5E-36	54	IWB39865	107.1494	635,199,129	2E-38
53	IWB21895	104.9104	564,921,623	4E-46	54	IWB73198	108.0381	635,206,667	4E-46
53	IWB28529	109.5255	573,200,421	4E-46	54	IWB73199	108.0381	635,207,022	9E-44
53	IWB64817	109.2449	586,120,536	4E-46	54	IWB71648	107.3895	636,209,105	4E-46
53	IWB35013	109.2449	592,584,191	1E-105	54	IWB72411	108.0381	637,574,237	4E-46
53	IWA5411	108.0381	593,675,130	6E-62	54	IWB64321	108.0381	637,574,238	4E-46
53	IWB43186	108.0381	594,849,586	4E-46	54	IWB72407	107.3895	637,574,450	4E-46
53	IWB7263	108.0381	595,126,655	2E-41	54	IWB65589	108.3468	638,630,217	3E-98

Bins	SNPs	Genetic postion (cM)	Physical position (bp)	e value	Bins	SNPs	Genetic position (cM)	Physical position (bp)	e value
54	IWB9310	108.3468	638,955,436	9E-44	56	IWB32487	109.5255	657,844,054	2E-38
54	IWB14419	108.0381	640,103,065	1E-36	56	IWB32488	109.5255	657,844,107	2E-28
54	IWB39785	108.0381	640,691,822	3E-40	56	IWB35244	108.4528	657,844,969	1E-105
54	IWB10411	108.0381	640,794,808	4E-46	57	IWB45932	109.5255	658,615,066	9E-44
55	IWB63105	108.3468	641,665,079	7E-26	57	IWA4948	109.5255	660,156,482	1E-105
55	IWB7979	108.0381	641,665,199	4E-46	57	IWB47664	109.5255	662,684,808	6E-45
55	IWB12239	108.4528	641,877,283	4E-46	57	IWA3395	109.5255	664,213,676	2E-92
55	IWB7018	108.0381	643,297,994	4E-46	57	IWB49572	109.5255	664,213,677	4E-46
55	IWB48486	108.4528	643,682,925	3E-31	57	IWB45933	109.4756	664,219,546	4E-46
55	IWB63172	108.4528	643,684,175	4E-46	57	IWB6433	109.4756	664,219,708	4E-46
55	IWB48482	108.4528	643,684,582	5E-33	57	IWB6031	109.4756	664,219,712	4E-46
55	IWB21477	108.4528	643,684,950	9E-44	57	IWB6438	109.4756	664,219,796	2E-29
55	IWB28694	108.4528	644,146,980	1E-27	57	IWB3891	109.5255	664,934,844	4E-46
55	IWB28695	108.4528	644,147,034	6E-42	57	IWB1556	109.5255	665,189,392	4E-46
55	IWB35071	108.4528	644,151,368	9E-86	57	IWB72651	109.5255	665,189,393	4E-46
55	IWB41234	108.4528	644,151,555	4E-46	57	IWB72650	109.5255	665,189,654	4E-46
55	IWB35072	108.4528	645,309,795	1E-105	57	IWB53839	109.5255	665,668,955	4E-46
55	IWB6515	108.4528	646,215,600	4E-46	57	IWA4357	109.5255	665,669,514	1E-105
55	IWB67744	108.4528	647,104,612	1E-21	58	IWB13870	109.5255	666,532,057	4E-46
55	IWB52433	108.4528	647,108,830	4E-46	58	IWB5492	109.5255	666,650,025	4E-46
55	IWB65443	107.3957	648,481,740	3E-20	59	IWB72542	109.5255	668,570,063	4E-46
55	IWB28591	107.3957	648,482,735	4E-46	59	IWB13160	109.5255	669,359,723	4E-46
55	IWB45296	109.5255	648,920,753	4E-46	59	IWB51807	109.1357	669,436,096	4E-46
55	IWA2261	109.1357	650,285,278	7E-34	59	IWA7850	109.5255	669,436,308	1E-87
55	IWB66494	107.4861	651,358,139	5E-36	59	IWB11159	109.1357	669,436,309	4E-46
55	IWB68993	107.4861	651,363,846	9E-44	59	IWB28479	109.5255	670,752,004	4E-46
55	IWB67609	107.4861	651,932,274	4E-46	59	IWB7131	109.1357	670,837,338	4E-46
55	IWB67608	108.4528	651,932,447	4E-46	59	IWB48291	109.5255	671,740,152	4E-46
55	IWB73241	109.5255	652,613,164	4E-46	59	IWB40768	109.5255	672,021,082	2E-44
56	IWB36229	107.3895	653,607,971	8E-80	59	IWB73172	109.5255	672,746,059	9E-44
56	IWB73669	114.0939	653,620,437	9E-44	60	IWB28337	109.4756	675,345,868	4E-46
56	IWB49833	108.4528	655,005,661	5E-35	60	IWB11652	109.5255	680,409,129	4E-46
56	IWB25841	108.3374	655,602,876	8E-29	60	IWB7226	109.0734	680,573,507	4E-46
56	IWB28850	107.4861	655,605,853	4E-46	61	IWB56161	110.8228	681,539,900	4E-46
56	IWB28849	107.4861	655,606,117	4E-46	61	IWB66021	110.8228	681,540,018	3E-20
56	IWB24309	108.6119	656,228,477	4E-46	61	IWB56162	109.5255	681,540,452	4E-46
56	IWB35393	109.2449	657,790,878	1E-105	61	IWB36307	110.8228	681,542,496	1E-103
56	IWB6098	109.2449	657,793,077	4E-46	61	IWB6480	110.8228	681,542,509	6E-39
56	IWB47695	109.5255	657,816,061	9E-44	61	IWB30356	110.8228	682,039,430	4E-46
56	IWB47694	109.5255	657,818,379	2E-41	61	IWB1188	119.0708	682,848,605	4E-46

Bins	SNPs	Genetic postion (cM)	Physical position (bp)	e value	Bins	SNPs	Genetic position (cM)	Physical position (bp)	e value
62	IWB6631	109.2449	683,029,170	4E-46	72	IWB26416	114.9109	708,436,453	3E-34
62	IWB34949	109.2449	683,029,171	6E-74	72	IWB56400	114.9109	708,436,564	4E-46
62	IWB36062	109.2449	683,029,237	8E-48	72	IWB10282	114.3215	710,053,041	2E-41
62	IWA3742	110.8727	683,029,261	2E-93	72	IWB36072	115.1105	712,600,543	1E-31
62	IWB63030	109.2449	683,029,265	2E-41	72	IWB74201	115.3319	713,675,759	4E-46
62	IWB12298	110.8727	683,046,802	4E-46	72	IWB28963	115.3319	713,675,815	9E-44
62	IWB11177	109.2449	683,758,793	4E-46	72	IWB28962	115.3319	713,676,041	4E-46
62	IWB9247	110.8727	686,049,366	9E-44	73	IWB32020	114.8174	714,499,621	9E-38
62	IWB4443	109.2449	686,818,449	7E-26	73	IWB32017	114.8174	714,500,027	6E-30
62	IWB32165	109.2449	686,836,489	2E-36	73	IWB8450	114.9109	714,779,769	4E-46
62	IWB6150	109.2449	687,248,647	3E-25	73	IWB8449	114.8174	714,779,852	4E-46
62	IWB6270	109.2449	687,248,675	4E-46	73	IWB34664	115.7279	715,028,611	9E-86
63	IWB12230	114.0939	690,218,326	2E-41	73	IWA3176	115.7279	715,029,294	1E-105
64	IWB6147	114.3215	691,780,794	4E-46	73	IWA2873	115.7279	715,030,099	1E-105
64	IWB36270	112.4505	691,780,864	1E-105	73	IWA6561	115.0076	715,031,654	1E-103
65	IWB64008	113.1584	692,461,536	4E-46	73	IWB2286	115.0076	715,601,570	9E-44
66	IWB46242	113.5295	693,314,968	2E-26	73	IWB8386	115.7279	716,553,673	6E-39
67	IWB54520	114.0939	693,845,390	9E-44	73	IWB22526	115.0076	716,782,389	4E-46
67	IWB28722	113.358	694,051,080	2E-45	73	IWB67729	126.5298	718,968,246	6E-39
68	IWB34588	114.0939	695,689,202	5E-74	73	IWB67728	115.862	718,968,354	1E-42
68	IWB34719	114.5679	695,693,403	2E-71	73	IWB60671	115.7965	719,800,817	6E-39
69	IWA4096	113.8569	696,677,569	1E-105	73	IWB70765	115.7965	719,800,817	2E-41
69	IWA7371	113.8569	696,679,754	1E-105	73	IWA2459	115.7965	719,965,246	1E-105
69	IWB8419	113.8507	697,510,374	4E-46	73	IWA7955	115.7965	720,480,288	1E-105
69	IWB34633	113.8507	697,511,636	9E-76	73	IWB73441	115.7965	720,807,493	4E-46
69	IWB25695	113.8507	697,512,105	4E-46	73	IWA5024	115.7965	721,113,551	2E-76
70	IWB6711	114.3683	698,212,115	4E-46	73	IWB9044	114.8174	721,922,229	4E-46
70	IWB52991	114.1874	698,303,835	4E-46	73	IWB27775	115.7965	722,085,721	3E-34
70	IWB24676	114.3683	698,963,683	8E-35	73	IWB53685	115.7965	722,620,506	4E-46
70	IWB3588	114.3215	698,968,758	4E-46	73	IWB19785	116.8193	723,333,631	4E-46
70	IWB1888	114.3215	699,106,310	4E-46	74	IWB49827	119.2017	730,188,295	2E-29
70	IWB58060	114.3683	699,108,737	4E-46	74	IWB69431	119.2017	730,189,918	3E-31
70	IWA2678	114.3215	699,109,205	1E-105	74	IWB7223	119.2017	730,191,782	9E-44
70	IWB54945	114.3215	699,109,351	2E-45	74	IWB73567	119.0708	730,562,762	2E-41
70	IWB3648	114.3215	699,109,783	9E-44	74	IWB5957	119.0708	730,563,020	2E-38
70	IWB34658	114.1874	699,173,435	4E-38	74	IWB22381	119.0708	730,563,982	2E-23
70	IWB19972	114.5679	699,827,018	4E-46	74	IWB9560	119.0708	731,536,217	4E-46
70	IWB63996	114.5679	700,456,554	3E-22	74	IWB48386	119.0708	733,743,362	4E-46
71	IWB11942	114.5679	702,714,575	4E-46	75	IWB7010	119.0708	734,050,376	4E-46
71	IWB38318	114.3683	703,976,259	4E-46	75	IWB25546	118.4315	734,495,342	4E-46

Bins	SNPs	Genetic postion (cM)	Physical position (bp)	e value	Bins	SNPs	Genetic position (cM)	Physical position (bp)	e value
75	IWB25313	119.5198	736,408,809	4E-46	84	IWB10455	134.4598	763,091,422	4E-46
76	IWB73196	119.6134	738,410,414	4E-46	85	IWA1324	134.65	763,631,139	1E-105
76	IWA8406	119.6134	740,805,226	9E-44	85	IWB11366	134.4598	763,633,070	4E-46
77	IWB23010	126.1432	743,694,001	4E-46	85	IWB56627	133.9234	763,842,415	2E-41
77	IWB69628	126.3116	743,746,441	4E-46	85	IWB36334	134.4598	763,862,057	1E-103
77	IWB7265	129.0806	745,719,283	4E-46	85	IWB23797	134.4598	763,862,485	9E-44
78	IWB60041	130.618	746,037,361	4E-46	85	IWB36286	133.9234	764,074,057	2E-61
78	IWB8338	129.0806	747,125,491	9E-44	85	IWB1092	134.4598	764,117,343	9E-44
78	IWB57069	129.0806	747,602,868	4E-46	85	IWB51555	134.4598	765,050,153	4E-46
78	IWB45063	129.0806	747,821,277	3E-45	85	IWB2534	134.4598	765,069,673	1E-21
78	IWB6028	129.4704	747,821,526	4E-46	85	IWB36753	134.4598	765,072,212	4E-46
78	IWB36805	126.5298	748,079,417	2E-41	85	IWB5864	134.4598	765,278,515	8E-29
78	IWB57292	126.3116	748,305,423	4E-46	85	IWB6334	134.4598	765,278,696	4E-46
79	IWB23232	130.2906	748,979,803	5E-33	85	IWB28564	138.3889	767,016,806	4E-46
79	IWB57313	130.2906	748,982,329	1E-30	85	IWB28565	138.3889	767,016,859	4E-46
79	IWB14677	130.2906	748,985,683	4E-46	85	IWB43464	138.3889	767,018,160	4E-46
80	IWB6888	130.2906	749,972,454	4E-46	85	IWB12294	134.4598	767,171,588	4E-46
80	IWB7767	130.618	750,013,549	4E-46	85	IWB8430	134.4598	767,375,356	4E-46
80	IWB11280	130.6991	750,016,338	4E-46	85	IWB6130	134.4598	767,651,618	9E-44
81	IWB10845	130.618	751,322,544	4E-46	85	IWB55806	134.4598	768,105,301	9E-44
81	IWB26300	130.618	752,485,079	4E-40	85	IWB43052	134.4598	768,292,034	4E-46
81	IWB26301	130.618	752,485,223	7E-26	85	IWB6223	134.4598	768,292,420	4E-46
81	IWB7626	130.618	752,486,039	4E-46	85	IWB36243	134.4598	768,548,010	1E-66
81	IWB7514	129.3488	752,491,717	4E-46	85	IWB23209	134.4598	768,548,795	1E-27
81	IWB10162	134.4598	754,661,080	4E-46	85	IWB28375	134.4598	769,072,216	6E-42
81	IWB25863	134.4598	754,864,431	1E-36	85	IWB36009	185.6661	769,428,475	5E-55
82	IWB64472	134.4598	758,592,619	4E-46	85	IWB61112	134.4598	769,911,883	4E-46
82	IWB47343	134.4598	758,592,725	9E-44	85	IWB61339	141.4823	770,680,644	3E-22
82	IWB31944	134.4598	758,594,502	4E-46	85	IWB40501	141.4823	770,684,874	1E-39
82	IWB7671	134.7124	759,172,999	4E-46	85	IWB54701	141.4823	770,685,939	1E-42
83	IWA571	134.4598	760,882,831	6E-58	85	IWB48923	134.3475	771,191,267	3E-37
83	IWB3249	134.4598	760,930,887	1E-33	85	IWB64675	141.317	772,026,789	1E-24
83	IWA8589	134.4598	760,950,622	9E-28	85	IWB47254	142.9916	773,141,220	2E-45
83	IWB40702	134.4598	760,950,702	2E-41	85	IWB45108	142.9916	773,144,939	1E-42
83	IWB29590	134.4598	760,950,906	4E-46	85	IWB45109	142.9916	773,146,976	4E-46
83	IWB21063	173.3517	761,279,407	6E-42	85	IWB27625	142.9916	773,147,179	4E-46
84	IWB52447	134.4598	761,280,190	4E-46	85	IWB45110	142.9916	773,147,390	2E-44
84	IWB37216	134.4598	761,283,203	3E-16	85	IWB60544	142.9916	773,151,605	3E-45
84	IWB22835	132.4734	762,503,266	4E-46	85	IWB54383	142.9916	773,348,787	4E-46
84	IWB14219	133.9234	762,505,270	9E-38	85	IWB23686	142.9916	773,349,577	4E-46

Bins	SNPs	Genetic postion (cM)	Physical position (bp)	e value	Bins	SNPs	Genetic position (cM)	Physical position (bp)	e value
86	IWB63210	144.1641	775,053,185	4E-46	90	IWB7569	153.1761	787,742,839	9E-44
86	IWB40456	145.1276	775,169,349	2E-41	90	IWB12415	157.2143	787,819,631	4E-46
86	IWB5439	144.136	775,336,420	4E-46	90	IWB22132	173.3517	788,656,076	7E-23
86	IWB9919	144.136	775,337,394	4E-46	90	IWA1667	147.4695	788,656,859	2E-68
86	IWB71	144.1641	775,371,494	7E-38	91	IWA2551	173.3517	788,804,816	2E-49
86	IWB50532	147.4695	777,335,355	6E-39	91	IWB21954	157.2143	789,133,597	4E-46
86	IWB13829	145.1276	777,385,087	2E-41	91	IWB40427	153.1418	789,436,641	9E-44
86	IWA3474	145.5361	777,514,134	1E-105	91	IWB29266	157.2143	789,437,155	4E-46
86	IWB70683	173.3517	777,650,293	3E-22	91	IWB63563	161.4147	789,601,632	4E-40
87	IWB66207	145.7513	779,341,273	4E-46	91	IWB10623	161.4147	789,605,639	4E-46
87	IWB32211	145.1276	779,341,458	1E-41	91	IWB44797	161.4147	789,609,076	8E-35
87	IWB4319	145.7513	779,344,648	9E-38	91	IWB36702	181.9178	789,684,959	5E-36
87	IWB72278	145.7513	779,345,376	3E-34	91	IWA3315	158.7298	789,867,245	8E-83
88	IWB61940	148.1119	779,855,057	4E-46	91	IWB13362	161.4147	789,965,438	3E-45
89	IWB429	146.7959	780,590,447	2E-41	91	IWB50794	159.656	790,753,464	4E-46
89	IWB3073	146.1629	780,779,176	4E-43	91	IWA2094	161.4147	791,704,244	1E-105
89	IWB74780	146.1629	780,786,186	4E-46	91	IWB54548	159.656	791,704,600	4E-46
89	IWB4585	152.5898	781,181,186	1E-30	91	IWB8699	161.4147	793,148,681	4E-46
89	IWB58205	152.5898	781,183,001	5E-27	91	IWB7606	159.656	793,151,179	4E-46
89	IWB54751	152.5898	781,579,033	4E-46	91	IWB7605	163.1329	793,151,451	4E-46
89	IWB12724	153.0825	782,534,065	4E-46	92	IWB54766	169.3041	796,803,336	4E-46
89	IWB38530	152.5898	782,534,075	4E-46	92	IWB48017	157.2143	796,803,717	9E-44
89	IWA692	152.5898	782,534,076	8E-72	92	IWB668	173.3517	797,126,794	8E-42
89	IWB41547	157.2143	782,534,298	4E-46	92	IWA5694	157.2143	797,327,211	6E-62
89	IWB65625	157.2143	782,833,434	8E-21	92	IWB51417	173.3517	797,335,315	3E-34
89	IWB7106	153.1761	783,226,978	4E-46	92	IWB166	157.2143	797,625,996	9E-38
89	IWB32143	157.2143	783,446,588	4E-32	92	IWB13403	157.2143	797,627,020	4E-46
89	IWA2377	152.5898	784,297,022	4E-38	92	IWB24806	161.4147	798,190,597	4E-46
89	IWB4592	152.5898	784,553,492	7E-26	92	IWB41613	158.9918	798,213,263	2E-35
90	IWA3252	154.4733	785,138,741	4E-94	92	IWB54507	169.3041	798,224,942	2E-41
90	IWB32245	157.2143	786,034,208	2E-38	92	IWB44889	157.2143	798,306,090	5E-27
90	IWB1354	157.2143	786,035,733	4E-46	92	IWB42373	157.2143	798,308,359	2E-35
90	IWB36409	154.1147	786,105,458	9E-44	93	IWB26304	157.2143	799,920,373	2E-41
90	IWB54389	154.1147	786,105,954	4E-46	93	IWB35539	173.3517	799,971,389	8E-77
90	IWB69343	157.2143	786,225,768	9E-44	93	IWB46023	169.3041	800,031,403	4E-40
90	IWB53581	157.2143	786,229,394	4E-46	93	IWB27000	161.4054	800,123,089	2E-41
90	IWB46858	157.2143	786,232,090	4E-46	93	IWB23911	157.2143	801,217,526	9E-44
90	IWB7625	155.4088	787,140,804	5E-36	93	IWB32031	157.2143	801,222,223	3E-35
90	IWB7624	155.4088	787,140,808	3E-37					

APPENDIX G. MORPHOLOGICAL PHENOTYPES OF 2B-2S RECOMBINANTS

Line	Chromosomes 2B and 2S	Phenotype
CS	2B	Normal
RL6082	2BS-2SS·2SL	Normal
XWC11-003	DS 2S(2B)	Stunted
ZW14-001-15	2BS·2BL-2SL	Normal
ZW14-002-2	2SS·2SL-2BL	Stunted
ZW14-003-4	2BS·2BL-2SL	Normal
ZW14-004-1	2SS·2SL-2BL	Stunted
ZW14-005-8	2SS·2SL-2BL	Stunted
ZW14-006-1	2SS·2SL-2BL	Stunted
ZW14-008-5	2BS-2SS·2SL	Stunted
ZW14-009-3	2BS·2BL-2SL	Stunted
ZW14-010-2	2SS-2BS·2BL	Normal
ZW14-011-1	2SS·2SL-2BL	Stunted
ZW14-013-4	2SS·2SL-2BL	Stunted
ZW14-014-2	2BS·2BL-2SL	Normal
ZW14-015-8	2SS·2SL-2BL	Stunted
ZW14-016-7	2BS-2SS·2SL	Normal
ZW14-017-4	2SS·2SL-2BL	Stunted
ZW14-070-1	2SS·2SL-2BL	Stunted
ZW14-071-2	2BS-2SS·2SL	Normal
ZW14-072-6	2SS·2SL-2BL	Stunted
ZW14-073-1	2SS·2SL-2BL	Stunted
ZW14-074-2	2BS·2BL-2SL	Normal
ZW14-077-8-1	2SS·2SL-2BL-2SL	Stunted
ZW14-077-8-2	2BS·2BL-2SL + T2SS	Normal
ZW14-084-8-2	2BS·2BL-2SL + T2SL	Normal
ZW14-089-7-1	2SS-2BS·2BL	Normal
ZW14-093-4-2	2BS-2SS·2SL	Normal
ZW14-093-8-1	2BS-2SS·2SL	Normal
ZW14-095-6	2SS-2BS·2BL	Normal
ZW14-097-5	2SS-2BS·2BL	Stunted
ZW14-100-1	2SS·2SL-T2BL	Normal
ZW14-108-6-1	2SS-2BS·2BL	Stunted
ZW14-111-5-2	2SS·2SL-2BL	Stunted
ZW14-115-7-2	2BS-2SS·2SL	Normal

Line	Chromosomes 2B and 2S	Phenotype
ZW14-116-5	2BS·2BL-2SL	Normal
ZW14-118-1	2BS·2BL-2SL	Normal
ZW14-121-3	2BS·2BL-2SL	Normal
ZW14-121-8-1	2BS·2BL-2SL	Normal
ZW14-121-8-2	2BS·2BL-2SL	Normal
ZW14-128-1	2BS·2BL-2SL	Normal
ZW14-135-6-2	2BS·2BL-2SL	Stunted
ZW14-139-7-2	2SS-2BS·2BL	Stunted
ZW14-141-7-2	2BS-2SS·2SL	Normal
ZW14-142-4-2	2BS-2SS·2SL	Normal
ZW14-147-4-2	2SS·2SL-2BL	Stunted
ZW14-149-1-2	2BS-2SS·2SL	Normal
ZW14-154-3-2	2SS-2BS·2BL	Stunted
ZW14-155-2-1	2SS-2BS·2BL-2SL	Stunted
ZW14-162-4-2	2SS·2SL-2BL	Stunted
ZW14-166-3-2	2SS-2BS·2BL-2SL	Stunted
ZW14-167-8-2	2SS-2BS·2BL	Stunted
ZW14-169-5-2	2BS·2BL-2SL	Normal
ZW14-171-4-2	2BS·2BL-2SL + 2SS-2BS·2BL	Stunted
ZW14-171-6-2	2BS·2BL-2SL + 2SS-2BS·2BL	Stunted
ZW14-173-7-2	2SS-2BS·2BL	Stunted
ZW14-174-2-2	2SS-2BS·2BL	Stunted
ZW14-175-7-1	2BS-2SS·D2SL	Normal
ZW14-180-2-1	2SS-2BS-2SS·2SL	Normal
ZW14-180-5-2	2SS-2BS-2SS·2SL	Normal
ZW14-181-3	2SS-2BS·2BL-2SL	Stunted
ZW14-184-6	2SS-2BS·2BL	Stunted
ZW14-185-2	2SS·2SL-2BL	Stunted
ZW14-186-1-2	2BS-2SS·2SL	Normal
ZW14-188-4-2	2SS-2BS·2BL	Stunted
ZW14-191-2	2SS-2BS·2BL	Stunted
ZW14-194-7	2BS·2BL-2SL	Normal
ZW14-197-2	2SS-2BS·2BL-2SL	Stunted
ZW14-201-2	2BS·2BL-2SL	Normal
ZW14-203-3	2SS-2BS·2BL	Stunted
ZW14-204-4	2BS·2BL-2SL	Normal

Line	Chromosomes 2B and 2S	Phenotype
ZW14-205-7-2	2SS-2BS·2BL	Stunted
ZW14-206-2	T2SL	Normal
ZW14-207-2-1	2SS-2BS·2BL	Normal
ZW14-501-1	2SS·2SL-2BL	Stunted
ZW14-502-2	2SS-2BS·2BL	Stunted
ZW14-504-5	2SS-2BS·2BL	Stunted
ZW14-505-2	2SS-2BS·2BL	Stunted
ZW14-506-1	2SS-2BS·2BL	Normal
ZW14-507-4	2SS-2BS·2BL	Stunted
ZW14-508-4	2SS·2SL-2BL	Stunted
ZW14-510-7	2SS-2BS·2BL	Stunted
ZW14-511-6	2BS-2SS·2SL-2BL	Normal
ZW14-512-8	2SS·2SL-2BL + 2BS·2BL-2SL	Stunted
ZW14-513-6	2BS·2BL-2SL + 2SS·2SL-2BL	Stunted
ZW14-514-6	2SS·2SL-2BL	Stunted
ZW14-515-3	2SS-2BS-2SS·2SL	Stunted
ZW14-515-8	2SS-2BS-2SS·2SL	Stunted
ZW14-516-4	2SS·2SL-2BL	Stunted
ZW14-517-6	2SS·2SL-2BL	Stunted
ZW14-518-8	2SS·2SL-2BL	Stunted
ZW14-519-2	2BS-2SS·2SL	Normal
ZW14-520-3	2SS-2BS·2BL	Normal
ZW14-521-3	2SS·2SL-2BL	Normal
ZW14-522-4	2SS·2SL-2BL	Normal
ZW14-523-7	2SS·2SL-2BL-2SS	Stunted
ZW14-524-4	2SS·2SL-2BL	Stunted
ZW14-525-3	2BS-2SS·2SL-2BL	Normal
ZW14-526-1	2BS·2BL-2SL	Normal
ZW14-527-3	2SS·2SL-2BL-2SS	Normal
ZW14-528-5	2BS·2BL-2SL-2SS	Normal